



Universidade do Minho
Escola de Engenharia

Bruno Henriques
Bond strength enhancement of
metal-ceramic dental restorations by FGM design

Bruno Alexandre Pacheco de Castro Henriques

Bond strength enhancement of metal-ceramic
dental restorations by FGM design



Universidade do Minho
Escola de Engenharia

Bruno Alexandre Pacheco de Castro Henriques

Bond strength enhancement of metal-ceramic
dental restorations by FGM design

Tese de Doutoramento
Engenharia Mecânica

Trabalho efectuado sob a orientação do
Professor Doutor Filipe Samuel Correia Pereira Silva

e co-orientação do
Professor Doutor Delfim Fernandes Soares

This thesis is dedicated to my parents...

ACKNOWLEDGMENTS

The road that brought me to this thesis was made of challenges and obstacles that were successfully transposed with the help of many people to whom I would like to acknowledge.

Firstly I wish to express my sincere gratitude to my supervisors, Professors Filipe Samuel Silva and Delfim Soares. I thank the opportunity they gave me to research under their guidance as well as for all their encouragements, patience, understanding and respect for me. I will forever remember the intensive and fructuous discussions about the work and about a broad range of interesting subjects.

I would like to address a special thank to my old friend and work colleague Paulo Pinto for his help and friendship during this research period.

I want to extend my gratitude to all present and past members of the Interdisciplinary Laboratory of Functionalized Materials and Materials Testing Laboratory, who have given me all kinds of assistance, encouragement, and friendship. Special thanks must be given to Nuno Costa, Oscar Carvalho, Georgina Miranda, João Vilaça, Mr. Fernando Araújo, Vítor Neto, Miguel Abreu and Mr. Leite for their sincere friendship, warm-hearted and unlimited help given to me, and technical and moral support throughout the research.

I want to especially thank to Dr. Francisco Castro, owner of the prosthetic laboratory “DentalCastro”, for all the support he gave to this research.

I also owe a word of acknowledgement to Professor Michael Gasik, for having given me the opportunity to research under his guidance and supervision at Aalto University, Finland. His constant availability in sharing his wisdom and experience made this stay a very enriching experience at a personal and professional level.

I also want to thank to my close family and to friends (STAFF) for their support. Finally, deep in my heart, I want to thank my girlfriend, who shared with me the good times and supported me through the bad times with her love, encouragement, incredible understanding, great tolerance, and sacrifices.

Finally, I gratefully acknowledge the FCT - Fundação para a Ciência e a Tecnologia for its financial support throughout the BD - Bolsa de Doutorado (PhD Grant) with the reference SFRH/BD/ 41584 / 2007.

ABSTRACT

Bond strength enhancement of metal-ceramic dental restorations by FGM design

Metal ceramic dental restorations are widely used in dental prosthetics due to their good esthetic properties but mainly because of their higher survival rates when compared to other restorative systems. Nevertheless, they still encompass some medium to long term clinical failures, which puts patients back to the dentists' chair, causing uncomfortable interventions and undesired money expenditures. This work is concerned with the development of FGM's (Functionally Graded Material) based solution that enhances metal-ceramic bond strength aiming at increasing of long term survival rates of metal-ceramic dental restorations and with the study of the variables that affect metal-ceramic bond strength. The variables that were subjected to study were the hot pressing, the surface treatment, the type of processing used to produce metal substructures, and the preoxidation heat treatment.

The hot pressing technique revealed to have significant ($p < 0.05$) influence on the metal-ceramic bond strength, resulting in composites with significantly ($p < 0.05$) higher bond strength values when compared to those obtained by conventional Porcelain-Fused-to-Metal technique for high gold dental alloys and for CoCrMo dental alloys. In the same way, the hot pressing technique also produced a significant enhancement on porcelain shear strength relative to the conventional vacuum sintered porcelain. The flawless metal-ceramic interfaces and the absence of pores within ceramics thus produced were regarded for the bond strength and cohesion improvements, respectively. The metal-ceramic adhesion was also assessed for different surface treatments of the metal substructure, namely polished and rough surfaces. Porcelain exhibited higher adhesion to rough metal substrates than to polished ones. The mechanical interlocking and the higher surface area for chemical bonding caused the bond strength improvements seen in rough surfaces.

The CoCrMo alloy obtained by casting and hot pressing was assessed in terms of microstructure, corrosion resistance, hardness and metal-ceramic bond strength. The casted alloy exhibited a dendritic microstructure whereas the hot pressed alloy exhibited a globular microstructure. The hot pressed alloy revealed higher hardness due to a finer microstructure. The finer microstructure was also regarded for the enhanced corrosion resistance of hot pressed alloys over casted alloy. No significant differences were found in metal-ceramic bond strength between the two types of processing techniques.

The preoxidation heat treatment, performed in CoCrMoSi dental alloy, significantly ($p < 0.05$) affected the metal-ceramic bond strength. Non-preoxidized specimens exhibited higher metal-ceramic bond strength than preoxidized/ground ones. The lower bond strength results observed in preoxidized/ground specimens were originated by the presence of oxide remnants on their metal surface after grinding and by the higher oxide thickness formed at the metal-ceramic interface. All preoxidized specimens exhibited adhesive failure type while non-preoxidized presented both adhesive and mixed failure types. Preoxidation heat treatment revealed a detrimental effect on the adhesion of CoCrMoSi-porcelain composites for dental restorations.

Several metal/ceramic composites were used as interlayers aiming at the improvement of the bond strength between metal and ceramic, following a FGM approach. Two types of alloys were tested, namely a high-noble alloy and a CoCrMo alloy. Both alloys showed significant ($p < 0.05$) improvements in the metal-ceramic bond strength when using a graded transition provided by the metal/ceramic composite interlayer. The metal particles of the composite interlayer acted as a reinforcing phase that increased the fracture strength of the composite interlayer and improved the strength of the metal-interlayer-ceramic system. The bond strength improvements, relative to conventional PFM technique, proved to be in excess of 140%.

The newly developed FGM approach for dental metal-ceramic dental restorations was also evaluated in terms of its performance under thermo-mechanical fatigue conditions. These new functionally graded restorations showed significantly ($p < 0.05$)

higher performance under fatigue conditions relative to conventional PFM restorations. The bond strength results showed that the presence of a composite interlayer at the interface significantly ($p < 0.05$) improves the adhesion between the two materials under fatigue conditions, relative to those found in conventional PFM technique. The reduction of the properties mismatch at the metal-ceramic interface of the functionally graded restorations was considered to be the main cause for the bond strength improvements after fatigue tests. Improvements in the range of 210% were observed for the most severe testing conditions.

In the end of this work, a preliminary test comprising the manufacture of a graded metal-ceramic dental restorations in real crowns were conducted. The restorations were fabricated using the hot pressing technology currently available in dental prosthetic laboratories. This process produced crowns with a good quality of the bond between metal and ceramic. Moreover, no geometric restraints or others were observed to the restorations' proceedings.

RESUMO

Melhoria da resistência mecânica da ligação metal-cerâmico para restauros dentários recorrendo aos materiais com gradiente funcional de propriedades (FGMs).

Os restauros dentários metalocerâmicos são muito usados em prótese dentária devido às suas boas propriedades estéticas, mas sobretudo devido às suas elevadas taxas de sucesso clínico comparativamente com outros sistemas de restauro. Contudo, apesar de menos frequentes, também eles apresentam falhas clínicas a médio e longo prazo que fazem com que o paciente regresse à cadeira do dentista, causando intervenções desconfortáveis e gastos desnecessários de dinheiro. Assim, esta tese prende-se com o desenvolvimento de novos sistemas metal-cerâmico para restauro dentário recorrendo ao conceito dos materiais com gradiente funcional de propriedades (FGMs) tendo em vista o aumento da durabilidade e da taxa de sucesso clínico deste tipo de restauro. Esta tese também se debruçou sobre o estudo de variáveis que afetam o resistência da ligação metal-cerâmico. As variáveis alvo de estudo foram: a prensagem a quente, o tratamento superficial, o tipo de processamento das subestruturas metálicas e o tratamento de pré-oxidação.

A técnica de prensagem a quente revelou uma influência significativa ($p < 0.05$) na resistência mecânica da ligação metal-cerâmico, dando origem a compósitos com resistências de ligação significativamente ($p < 0.05$) maiores do que os mesmos obtidos pelo processo convencional de porcelana fundida sobre o metal, para ligas de ouro e de CoCrMo. A prensagem a quente também introduziu uma melhoria significativa ($p < 0.05$) na resistência ao corte da porcelana, relativamente ao processo convencional de cozimento da porcelana em vácuo. A quase completa ausência de defeitos, como poros, na interface metal-cerâmico e na própria porcelana estiveram na base das melhorias da ligação metal-cerâmico e da coesão da porcelana, respetivamente. A adesão entre o metal e o cerâmico foi também avaliada para diferentes tratamentos

superficiais da subestrutura metálica, nomeadamente em superfícies polidas e superfícies rugosas. A porcelana apresentou maior adesão às superfícies rugosas do que às superfícies polidas, dado que as superfícies rugosas permitiram uma maior retenção mecânica e também uma maior área superficial para promoção das ligações químicas.

Neste trabalho foi feita a avaliação de uma liga de CoCrMo, obtida por fundição e por prensagem a quente, em termos da sua microestrutura, resistência à corrosão, dureza e resistência da ligação metal-cerâmico. A liga fundida apresentou uma microestrutura dendríticas enquanto a liga prensada a quente apresentou uma microestrutura globular. A maior dureza exibida pela liga prensada a quente está associada a uma microestrutura mais fina. Também as melhores propriedades de corrosão apresentadas pela liga prensada a quente, em relação à liga fundida, estão relacionadas com o seu tipo de microestrutura. Não foram encontradas diferenças significativas nos valores da resistência mecânica da ligação metal-cerâmico quando se usou a liga prensada a quente ou a liga fundida.

O tratamento de pré-oxidação afetou significativamente ($p < 0.05$) a resistência da ligação metal-cerâmico, num estudo em que se usou uma liga dentária de CoCrMoSi. Os provetes não pré-oxidados apresentaram maiores valores de ligação metal-cerâmico que os provetes pré-oxidados/lixados. A presença de resíduos da camada de óxido na superfície do metal, após a sua remoção com lixa, bem como a formação de uma camada de óxido espessa na interface metal-cerâmico aquando do cozimento da porcelana, foram os fatores que estiveram na base da perda de resistência da ligação dos provetes pré-oxidados. Todos os provetes pré-oxidados revelaram falhas adesivas ao passo que os provetes não pré-oxidados apresentaram falhas adesivas e mistas. O tratamento de pré-oxidação revelou um efeito prejudicial na adesão entre a liga de CoCrMoSi e a porcelana dentária.

Vários compósitos metal/cerâmico foram testados como intercamadas com o objetivo de melhorar a resistência da ligação entre o metal e o cerâmico, seguindo uma abordagem dos materiais com gradiente funcional propriedades. Foram testados dois

tipos de ligas metálicas, uma liga de alto teor de ouro e uma liga de CoCrMo. Ambas as ligas mostraram melhorias significativas ($p < 0.05$) na resistência da ligação metal-cerâmico com o uso de uma transição gradual entre o metal e o cerâmico, por meio de uma intercamada de compósito metal/cerâmico. As partículas metálicas da intercamada atuaram como uma fase de reforço da matriz cerâmica, aumentando a resistência à fratura do compósito da intercamada e aumentando a resistência do sistemas metal-intercamada-cerâmico. A melhoria da resistência da ligação conseguida com o uso de uma intercamada, relativamente à ligação metal-cerâmico convencional, ascendeu a 140%.

Os novos restauros dentários desenvolvidos com base no conceito de materiais com gradiente funcional de propriedades foram avaliados em termos do seu desempenho em condições de fadiga termo-mecânica, simulando as condições clínicas. A resistência da ligação destes novos restauros após fadiga térmica e mecânica foi significativamente ($p < 0.05$) maior que a verificada para os restauros convencionais. A transição gradual de propriedades entre o metal e o cerâmico por via da introdução da intercamada de compósito na interface metal-cerâmico foi responsável pela melhoria do desempenho dos novos restauros dentários nos testes de fadiga. Com este novo sistema foram observadas melhorias na resistência da ligação metal-cerâmico, após fadiga, da ordem dos 210%.

No final do trabalho foi feito um teste preliminar de execução de um restauro dentário metalocerâmico em coroas reais, aplicando o conceito da intercamada de compósito na interface entre o metal e o cerâmico. O processo foi executado com recurso à tecnologia atual de prensagem da cerâmica a quente e resultou numa boa qualidade da ligação metal-cerâmico. Não se verificou nenhuma restrição geométrica ou outras ao procedimento de restauro.

TABLE OF CONTENTS

Aknowledgments	iii
Abstract	v
Resumo	ix
Table of contents	xii
List of abbreviations	xviii
List of figures	xx
List of tables	xxviii
Scope and Structure of the thesis	xxx

Chapter 1 - Introduction

1. Teeth - Function and Structure	1
2. Dental Materials	5
2.1. Dental alloys.....	7
2.1.1. Noble and Precious alloys	7
2.1.2. Base metal alloys.....	10
2.2. Dental ceramics	15
2.2.1. Classification of dental porcelains.....	15
2.2.2. Composition	16
2.2.3. Processing.....	18
2.3. Properties of dental porcelain	21
2.4. High-strength core ceramics.....	23
3. Metal-ceramic systems.....	28
3.1. Metal-ceramic bonding.....	29
3.2. Bond strength tests.....	32
3.3. Ceramics for metal-ceramic restorations	37
3.4. Alloys for metal-ceramic restorations	39
3.5. Preparation of metal-ceramic restorations	44
4. Functionally graded materials for dental applications.....	46

5. Motivation of this study.....	51
6. References	52

Chapter 2 - Shear bond strength of a hot pressed Au-Pd-Pt alloy-porcelain dental composite

Abstract	61
1. Introduction.....	62
2. Materials and Methods	64
2.1. Shear tests.....	66
2.2. Analysis of the metal-porcelain interface and failure mode	68
2.3. Statistical analysis	68
3. Results.....	69
4. Discussion	73
4.1. Materials	73
4.2. Shear bond strength test	74
4.3. Hot pressing	75
4.4. Fracture type analysis	78
4.6. EDS analysis.....	79
5. Conclusions.....	81
6. Acknowledgements	81
7. References	82

Chapter 3 - Optimization of bond strength between gold alloy and porcelain through a composite interlayer obtained by powder metallurgy

Abstract	87
1. Introduction.....	88
2. Materials and Methods	90
2.1. Materials	90
2.2. Processing	91
3. Results.....	94
4. Discussion	97

4.1. Materials	97
4.2. Metal-ceramic sharp transition vs. smooth transition	97
4.3. Toughening mechanisms of the metal-ceramic composite interlayer.....	100
4.4. Practical application.....	103
5. Conclusions	104
6. References	104

Chapter 4 - Influence of preoxidation cycle on the bond strength of CoCrMoSi-porcelain dental composites

Abstract	109
1. Introduction	110
2. Materials and methods.....	113
2.1. Specimens composition and preparation	113
2.2. Shear bond strength tests.....	115
2.3. Analysis of the metal-porcelain interface	116
2.4. Metal surface characterization	117
2.5. Statistical analysis	117
3. Results.....	118
4. Discussion	123
4.1. Preoxidation heat treatment	123
4.2. Analysis of CoCrMoSi alumina-blasted surface	124
4.3. Reaction zone EDS analysis.....	127
4.4. Fracture type analysis	128
5. Conclusions	129
6. Acknowledgements	130
7. References	130

Chapter 5 - Microstructure, hardness, corrosion resistance and porcelain shear bond strength comparison between cast and hot pressed CoCrMo alloy for metal-ceramic dental restorations

Abstract	135
----------------	-----

1. Introduction.....	136
2. Materials and Methods	138
2.1. Electrochemical tests	141
2.2. Shear tests.....	142
2.3. Statistical analysis	142
2.4. Analysis of the metal-porcelain interface.....	142
3. Results.....	143
4. Discussion	148
4.1. Metals substrates.....	148
4.2. Metal-ceramic composites	153
5. Conclusions.....	155
6. References	156

Chapter 6 - Hot pressing effect on the shear bond strength of dental porcelain to CoCrMoSi alloy substrates with different surface treatments

Abstract.....	161
1. Introduction	162
2. Material and Methods	164
2.1. Shear tests.....	167
2.2. Analysis of the metal-porcelain interface and failure mode	167
2.3. Statistical analysis	168
2.4. Metal surface characterization.....	168
3. Results.....	169
4. Discussion	172
4.1. Materials	172
4.2. Shear bond strength test	173
4.3. Hot Pressing	174
4.4. Fracture type analysis	177
4.5. EDS analysis.....	177
5. Conclusions.....	178
6. Acknowledgements	179

7. References	179
---------------------	-----

Chapter 7 - Experimental evaluation of the bond strength between a CoCrMo dental alloy and porcelain through a composite metal-ceramic graded transition interlayer

Abstract	183
1. Introduction	184
2. Materials and Methods	187
2.1. Materials	187
2.2. Processing	188
2.3. Shear tests.....	190
2.4. Analysis of the metal-porcelain interface and failure mode	191
3. Results.....	191
4. Discussion	198
4.1. Sharp vs. graded metal-ceramic transition.....	198
4.2 – Bond strength and Fracture Analysis	199
4.3 – Fracture strength of the composites used as interlayers	201
5. Conclusions	202
6. Acknowledgements	202
7. References	202

Chapter 8 - Shear bond strength comparison between conventional porcelain fused to metal and new functionally graded dental restorations after thermo-mechanical cycling

Abstract	205
1. Introduction	207
2. Materials and Methods	209
2.1. Materials	209
2.2. Specimens Manufacturing	210
2.3. Thermal and mechanical cycling.....	212
2.4. Shear Test.....	214
2.5. Analysis of the metal-ceramic interface and failure mode	214

2.6. Statistic Analysis.....	215
3. Results.....	216
3.1. Shear bond strength	216
3.2. SEM observation	217
4. Discussion	223
4.1. Shear test	223
4.2. Fatigue tests.....	223
4.3. Shear bond strength after fatigue tests.....	225
5. Conclusions.....	228
6. References	229

Chapter 9 - Fabrication of functionally graded metal-ceramic crowns

9.1. Fabrication of functionally graded metal-ceramic crowns.....	236
9.2. References	243

Chapter 10 - General discussion

10.1. Hot pressing effect and surface treatment	245
10.2. Cast vs. hot pressed metal substructures.....	247
10.3. Influence of preoxidation heat treatment.....	249
10.4. Bio-inspired FGM restorations.....	250
10.4.1. Evaluation of m/c composite interlayers for graded metal-ceramic systems 250	
10.4.2. Evaluation of functionally graded metal-ceramic systems under fatigue conditions.....	252
10.5. References	253
Main conclusions and future perspectives	255

LIST OF ABBREVIATIONS

ANOVA	Analysis of Variance
ANSI/ADA	American National Standard Institute/American Dental Association
BE	Backscattering electron
CMC	Ceramic Matrix Composites
CAD	Computer Aided Design
CAM	Computer Aided Manufacturing
CTE	Coefficient of Thermal Expansion
CoCrMo	Cobalt Chromium Molybdenum alloy
DEJ	Dentin Enamel Junction
EDS	Energy Dispersive Spectroscopy
E_{corr}	Corrosion Potential
FGM	Functionally Graded Materials
FGMR	Functionally Graded Restorations
FPD	Fixed Partial Dentures
GB	Grit Blasted
GPa	Gigapascal
HIP	Hot Isostatic Pressing
HP	Hot Pressing
HV	Hardness Vickers
Hz	Hertz
i_{corr}	Current density
ISO	International Organization for Standardization
kN	kilonewton
MMCp	Metal Matrix Composites
MPa	Megapascal
N	Newton
P	Polished

PFM	Porcelain Fused to Metal
PJC	Porcelain Jacket crown
PM	Powder Metallurgy
PMCC	Pressed Metal Ceramic Composites
PPPS	Porcelain Pressed onto Porcelain Surface
PPMP	Porcelain Pressed to Metal Powders
PPRS	Porcelain Pressed onto Rough Surface
Ra	Arithmetic average of roughness profile
rpm	revolutions per minute
SCE	Standard calomel electrode
SE	Secondary electrons
SEM	Scanning Electronic Microscopy
SiC	Silicon Carbides
σ_y	Yield strength
OCP	Open circuit potential
UTS	Ultimate tensile strength
VS	Vacuum Sintered
wt.%	weight percent
YM	Young's Modulus

LIST OF FIGURES

Figure 1.1. Maxillary and mandibular permanent dentition (Scheid and Weiss, 2012).	2
Figure 1.2. A mandibular posterior tooth sectioned longitudinally through the middle to show the distribution of the tooth tissues and the shape of the pulp cavity (made up of pulp chamber and root canal).	3
Figure 1.3. Radiograph (x-rays) showing tooth teeth structure, crowns and roots. The former are covered with enamel, and the latter are embedded within the alveolar bone. The whiter outer enamel shape is also distinguished from the darker inner dentin, and the darkest pulp chamber in the middle of the tooth. Between the root and the bone it is visible the very thin, dark periodontal ligament, but the cementum cannot be seen (Scheid and Weiss, 2012).	4
Figure 1.4. Dental restorative systems: 1 – Full-metallic crown; 2 - ceramic onlay; 3 - metal-ceramic crown; 4 - implant; 5 – Teeth cleaning; 6 – Bridge; 7 – All-ceramic crown; 8 - Metallic inlay.	6
Figure 1.5. Cobalt-chromium partial denture.	10
Figure 1.6. Relative composition of ceramic products based on feldspar, kaolin and quartz (van Noort, 2007).	17
Figure 1.7. Micrographs of the polished surfaces of six porcelains etched with 2% hydrofluoric acid (HF) for 15 s. A: Ceramco I (Dentsply), B: Ceramco II (Dentsply), C: Finesse (Dentsply), D: d.Sign (Ivoclar), Cb: Cerabien (Noritake), and V: Vitadur-Alpha (Vita) (Cesar et al.,2005).	19
Figure 1.8. Porcelains used in the build-up of a jacket crown (van Noort, 2007).	20
Figure 1.9. Porcelain jacket crown failure due to internal surface flaw (van Noort, 2007).	22
Figure 1.10. Micrograph of an alumina-reinforced core material showing the dispersed alumina particles embedded in a glassy matrix composed by feldspar (van Noort, 2007).	24
Figure 1.11. Alumina particles acting as crack stoppers and thus preventing crack propagation (van Noort, 2007).	24
Figure 1.12. Zirconia porous structure obtained by slip-casting and after a 10 hours sintering stage at 1120°C. After it should be infiltrated by a low viscosity lanthanum glass for 4-6 hours at 1100°C to produce a dense ceramic structure (In-Ceram-	25

Zirconia).

Figure 1.13. CEREC CAD-CAM system, which constructs ceramic partial dentures from machined dry-pressed ceramic blocks.	25
Figure 1.14. Cross section of a metal-ceramic dental restoration.	28
Figure 1.15. Micrograph showing the metal-ceramic interface with mechanical interlocking between the two materials.	30
Figure 0.1. Grit blasted surface of a CoCrMo alloys.	31
Figure 1.17. Three point bending of a metal–ceramic specimen according to ISO 9693:2000. A) Shape and dimensions of metal-ceramic specimen; B) Cross-section dimensions of specimen; C) Transverse load application; D) Separation of ceramic from metal. (Vázquez et al., 2008).	33
Figure 1.18. Shear bond strength test (Henriques et al., 2011).	35
Figure 1.19. Diagram showing three types of bond failure in metal-ceramic systems. A – metal-metal oxide; B – metal oxide-metal-oxide; and C – ceramic-ceramic. Note: the dimensions of the layers are not to scale.	36
Figure 1.20. Porcelain veneering steps in a metal-ceramic crown obtained by the porcelain-fused-to metal technique (Ceramco3 Instructions Guide, Dentsly).	45
Figure 1.21. Microstructure of a graded W/Cu composite produced by electrochemical gradation (Kieback et al.,2003)	46
Figure 1.22. Characteristics of functionally graded material (Kawasaki and Watanable, 1995)	47
Figure 1.23. Femoral bone structure (German Institute for Quality and Efficiency in Health Care, 2012).	48
Figure 1.24. Functionally Graded Integrated Implant being developed at AMMG, University of North Texas, USA.	48
Figure 1.25. Schematic view of an FGM dental implant with graded materials composition (Sadollah and Bahreininejad, 2011)	49
Figure 1.26. Elastic modulus distribution in dentin-enamel-junction (DEJ) (Marshall et al., 2001).	50
Figure 1.27. Schematic of the conventional sharp restoration and the new graded approach.	50
Figure 2.1. Hot pressing apparatus. (a) Temperature and pressure conditions during	66

the hot pressing cycle. (b) Hot pressing schematic. (c) Processing a specimen in the vacuum chamber.

Figure 2.2. Test apparatus. (a) Cross-section schematic of the shear test device (b) stainless steel shear test device. (c) Metal–ceramic specimen. 67

Figure 2.3. Shear bond strength comparative results for traditional method (PFM) and the two new proposed approaches PPRS and PPPS. The values represent means \pm SD. a, p < 0.05 vs. PFM. 69

Figure 2.4. Fracture surface of specimens. a) PFM – mixed failure mode; b) PPPS – adhesive failure; c) PPRS – adhesive failure. 70

Figure 2.5. EDS line analysis of metal-porcelain interface processed by the PPRS technique. 71

Figure 2.6. Fracture Element line distribution (wt. %) of metal/ceramic interface for PPPS and PPRS specimens. 72

Figure 2.7. Interface appearance for (a) PFM (50x), (b) PPPS (50x) and (c) PPRS (50x) specimens, respectively. High porosity in the ceramic side and interface at PFM technique a). 77

Figure 3.1. Hot pressing apparatus. (a) Hot pressing schematic (b) Processing a specimen in the vacuum chamber (c) Hot pressing cycle. 92

Figure 3.2. Shear test apparatus. (a) Metal-composite and ceramic-composite specimens (b) Cross-section schematic of the shear test device. 93

Figure 3.3. Shear bond strength results for the metal and ceramic bonding to different pressed metal-ceramic composites (PMCC) and comparison to alternative processing methods (Davidson, 1991). 94

Figure 3.4. Cross section view of metal-ceramic specimen's with 50Met50Cer composite interlayer. a) Fracture zone showing remnants of the composite interlayer in the metal surface. b) Schematic of the specimen's cross-section. 95

Figure 3.5. EDS line analysis of metal/ceramic interface. a) Inter-diffusion of metal alloy elements in ceramic. b) Inter-diffusion of ceramic elements in metal. 96

Figure 3.6. Optical microscope view of a 50Met-50Cer composite interlayer 200x. 98

Figure 3.7. Schematic of shear stresses in metal-ceramic interface. (a) conventional PFM restoration – sharp interface; (b) Hot pressed metal-ceramic restoration with a composite interlayer – smooth transition. 100

Figure 3.8. Different energy absorption mechanisms in metal matrix composites with discontinuous reinforcements (Davidson, 1991).	102
Figure 4.1. Plot of the shear bond strength results of CoCrMoSi-porcelain composites with different metal surface treatments: non-preoxidized, preoxidized/ground and preoxidized, respectively.	118
Figure 4.2. Fracture surface of preoxidized/ground specimen – mixed failure type.	119
Figure 4.3. EDS line analysis of metal/ceramic interface. (a) Inter-diffusion elements in non-preoxidized specimens. (b) Inter-diffusion elements in preoxidized/ground specimens.	120
Figure 4.4. SEM micrographs (x500) of two CoCrMoSi surface conditions: (A) alumina-blasted surface; (B) transition zone between alumina-blasted and non-blasted oxidized surface; (C) finely ground surface after preoxidation.	122
Figure 4.5. SEM micrograph: detailed view (5000x) of oxide layer remnants present on metal's surface, after fine grinding (2400-grit SiC).	122
Figure 4.6. SEM micrograph (x15000) of (a) non-preoxidized and (b) preoxidized metal-porcelain interaction zone showing some lenticular pockets accumulation at the metal-oxide interface.	125
Figure 4.7. SEM micrograph showing the topography of an alumina-blasted CoCrMoSi surface after preoxidation heat treatment.	127
Figure 4.8. (a) EDS analysis of the CoCrMoSi alloy surface before Al ₂ O ₃ -blasting --- no Al peak detected. (b) EDS analysis of the CoCrMoSi alloy surface after Al ₂ O ₃ -blasting -- - an Al peak detected (see arrow).	127
Figure 5.1. SEM micrographs of (A) CoCrMo alloy powders and (B) opaque porcelain powders (Ceramco3)	139
Figure 5.2. Microstructure of cast (A, B) and hot pressed (C, D) CoCrMo alloy metal substrates	144
Figure 5.3. Hardness (HV/1) of cast and hot pressed metal substrates.	145
Figure 5.4. Metal-ceramic shear bond strength results for cast and hot pressed metal substrates.	145
Figure 5.5. Fracture surface of cast CoCrMo alloy-ceramic specimen.	146
Figure 5.6. EDS line analysis of metal/ceramic interface showing the inter-diffusion of	147

elements in (a) cast and (b) hot pressed specimens.

Figure 5.7. Electrochemical curves for CoCrMo substrates: a) Open Circuit Potential (OCP) curves; b) Potentiodynamic polarization curves. 148

Figure 5.8. Micrographs of metal surfaces after potentiodynamic polarization tests: a) cast (100x); b) hot pressed (500x). 152

Figure 6.1. Hot pressing procedure: 1 – Painting die’s cavity with zirconium oxide; 2 – Place the metal substrate in die’s cavity; 3 – Place the porcelain powders in die’s cavity; 4 – Hot pressing (pressure+temperature) metal-porcelain set. 166

Figure 6.2. Cross-section schematic of the shear test device (A: external part; B internal part). The specimens’ dimensions are also shown. 167

Figure 6.3. Metal-ceramic shear bond strength results for each combination of Processing type (PFM – Porcelain-Fused-to-Metal; HP – Hot Pressing) and Surface treatment (P – Polished; GB - Grit-Blasted). 169

Figure 6.4. Porcelain shear strength results for different processing conditions (VS – conventional Vacuum Sintering technique; HP – Hot Pressing). 169

Figure 6.5. EDS line analysis of metal/ceramic interface showing the inter-diffusion of elements in (a) Porcelain-Fused-to-Metal and (b) Hot Pressed specimens 172

Figure 6.6. Metal-ceramic interface micrographs of Porcelain-Fused-to-Metal (A- Polished; B-Grit-Blasted) and Hot Pressed (C- Polished; D-Grit-blasted). The arrows indicate processing defects at the interface. 176

Figure 7.1. HSMP specimens’ manufacturing procedure: 1 – Die’s cavity painting with zirconium paint followed by metal substrate’s placement; 2 – Placement of metal/ceramic composite powders in the die’s cavity; 3 – Porcelain powders placement; 4 - Hot pressing (pressure+temperature) the metal-interlayer-porcelain specimen. 189

Figure 7.2. Cross-section schematic of the shear test device (A: external part; B internal part). The specimens’ dimensions are also shown. 191

Figure 7.3. Plot of the shear bond strength results for metal-ceramic restorations with interlayers of different compositions, and for PFM specimens, the control group. 192

Figure 7.4. Micrographs of the ceramic-interlayer-metal region for specimens having interlayers with different metal/ceramic contents. 193

Figure 7.5. SEM micrographs showing the microstructure of monolithic base materials- ceramic (porcelain and metal (CoCrMo alloy).	194
Figure 7.6. Comparison between the designed and the experimental volume fractions in different composites.	194
Figure 7.7. Micrographs showing a cross-section view of the fracture zones for specimens with different interlayers (20M; 40M; 60M; 80M). After bond strength tests, fractured specimens were embedded in resin and ground until reaching the longitudinal mid-plane, to allow the analysis of fracture zone in cross-section.	195
Figure 7.8. Normalized Fracture Strength of the different homogeneous composites used as interlayers (20M; 40M; 60MC; 80M) and their respective monolithic base materials (100C; 100M). Normalization method consisted in dividing the Fracture Strength data by the minimum value.	196
Figure 7.9. Young's Moduli plot of the metal-ceramic composites and monolithic base materials, obtained experimentally by DMA. It is also shown the Voigt- and Reuss-models based on the rule of mixtures, and Gasik's micromechanical model (Gasik, 2009).	197
Figure 7.10. Normalized Young's Moduli schematic plot of the metal-ceramic interface for a sharp transition (A) and for a smooth transition provided by different interlayers (B). Normalization method consisted in dividing the Young's modulus data by the minimum value.	198
Figure 8.1. FGMR specimens manufacturing procedure: 1 – Painting the cavity of the die with zirconium oxide followed, and metal substrates placement; 2 – Placement of the composite mixture in the die's cavity; 3 – Porcelain powders placement; 4 - Hot pressing (pressure+temperature) the metal-interlayer-porcelain specimen	212
Figure 8.2. Mechanical cycling device used for dynamic loading of metal-ceramic specimens	213
Figure 8.3. Cross-section schematic of the shear test device (A: external part; B internal part). The specimens' dimensions are also shown.	214
Figure 8.4. Mean \pm standard deviation (SD) of the shear bond strength results for conventional porcelain fused to metal specimens (PFM) and for functionally graded specimens (FGMR), after thermal and mechanical cycling.	216
Figure 8.5. Representative SEM micrographs of PFM (A,B) and FGMR (C,D) metal-	218

ceramic interfaces, before fatigue tests (A,C) and after fatigue tests (12000 thermal cycles + 100000 mechanical cycles) (B,D), respectively. Figures 4B and 4D show cracks within porcelain formed during fatigue tests.

Figure 8.6. SEM micrograph showing a detailed view of the ceramic-interlayer-metal region of the new functionally graded specimens. 219

Figure 8.7. SEM micrographs of PFM and FGMR specimens' fracture surfaces, after fatigue tests (*condition 3*- 12000 thermal cycles + 100000 mechanical cycles). **PFM** specimens: **A**-topography; **B**-chemical composition. **FGMR** specimens: **C**- topography; **D**- chemical composition. 220

Figure 8.8. SEM/EDS analysis of salts found on fracture surface of PFM cycled specimens after *condition 3* fatigue tests. A- The spectrum reveals traces of P and Ca with probable origin in artificial saliva; B- Chemical composition; C- Topography. 221

Figure 8.9. Fracture micrograph of the new functionally graded specimens showing remnants of metal particles from the interlayer retained at the metal surface. 221

Figure 8.10. Fractography of the composite interlayer, showing no traces of liquid ingress. It is also shown the metal particles embedded in the ceramic matrix after fracture. 222

Figure 8.11. Mechanical properties (Young's modulus and hardness) measured at the metal-ceramic interface for a sharp (PFM) and a graded transition (FGMR). 222

Figure 9.1. Master model and metal copings. 236

Figure 9.2. Application of the metal-ceramic composite interlayer with a brush. 237

Figure 9.3. A and B - Wax-up on the metal coping; **C** – waxed restoration on attached to the plunger with a sprue. 237

Figure 9.4. Investing the restoration with IPS PressVEST. 238

Figure 9.5. Investment ring in the heating oven towards the rear wall, tipped with the opening facing down. The IPS InLine PoM ceramic ingot and the IPS plunger were not preheated. 238

Figure 9.6. A - Insertion of the IPS InLine PoM ingot and the IPS Alox Plunger into the hot investment ring. Placing of the hot and completed investment ring in the centre of the hot press furnace and starting the program. **B** - Programat EP5000 press furnace. 239

Figure 9.7. Separation of the investment ring using a separating disk and alumina 240

sandblasting.

Figure 9.8. Separation of the sprue using a diamond disk. 241

Figure 9.9. Application of the glaze material using a brush. 241

Figure 9.10. Final aspect of functionally graded metal-ceramic restorations fitted to the master model. 242

Figure 9.11. Cross section of a functionally graded restoration obtained by hot pressing. The micrographs show the metal-interlayer-ceramic transition zone in several locations of the restoration. 243

LIST OF TABLES

Table 1.1. Composition of high-gold alloys (wt.%) (van Noort, 2007).	9
Table 1.2. Range of mechanical properties of high-gold alloys (van Noort, 2007).	9
Table 1.3. Comparison of some properties of base metal casting alloys (Van Noort, 2007).	14
Table 1.4. Classification of dental porcelains according to their fusion temperature (Craig and Powers, 2002).	16
Table 1.5. Composition of household and dental porcelain (wt.%) (van Noort, 2007).	17
Table 1.6. Comparison ranges of the main constituents in ceramics for metal-ceramic restorations (Craig and Powers, 2002).	37
Table 1.7. Composition ranges and color of noble-alloys for metal-ceramic restorations (wt.%) (Craig and Powers, 2002).	40
Table 1.8. Composition Ranges of base metals for metal-ceramic restorations (wt.%) (Craig and Powers, 2002).	40
Table 1.9. Properties of the alloys used in metal-ceramic restorations (Craig and Powers, 2002).	40
Table 2.1. Gold alloy chemical composition (wt.%).	64
Table 2.2. Ceramic chemical composition (wt.%).	64
Table 3.3. Base materials properties.	64
Table 2.4. Results of one-way ANOVA for tested conditions according to shear bond strength data.	70
Table 2.5. Elemental composition (wt.%) of different phases present in metal and porcelain.	72
Table 3.1. Gold alloy chemical composition (wt.%).	91
Table 3.2. Ceramic chemical composition (wt.%).	91
Table 0.1. Base materials properties.	91
Table 4.1. Base alloy composition (wt.%) (according to manufacturer).	113
Table 4.2. Ceramic chemical composition (wt.%).	114
Table 4.3. Typical oxide layer element content (wt.%), after porcelain firing, obtained by EDS.	120

Table 4.4. Elemental analysis of four types of surface conditions (wt.%).	121
Table 5.1. Chemical composition of CoCrMo alloy according to manufacturer (wt.%).	139
Table 5.2. Chemical composition of porcelain according to manufacturer (wt.%).	140
Table 5.3. EDS analysis of the different phases found in cast and hot pressed substrates.	144
Table 5.4. Corrosion parameters of cast and hot pressed CoCrMo substrates measured in saline solution (8g NaCl/L).	148
Table 6.1. Base alloy composition (wt.%) (according to manufacturer).	165
Table 6.2. Ceramic chemical composition (wt.%).	165
Table 6.3 – Two-way ANOVA results according to metal-ceramic shear bond strength data.	170
Table 6.4 – Mean \pm standard deviation (SD) of the shear strength of porcelain processed by two routes, hot pressing and vacuum sintering (MPa).	170
Table 6.5 – Mean \pm standard deviation (SD) of the shear bond strength results (MPa).	171
Table 7.1. Base alloy composition (wt.%) (according to manufacturer).	187
Table 7.2. Ceramic chemical composition (wt.%).	188
Table 8.1. Base alloy composition (wt.%) (according to manufacturer).	209
Table 8.2. Ceramic chemical composition (wt.%).	210
Table 8.3. Relevant materials' properties.	210
Table 8.4. Chemical composition of Fusayama's artificial saliva.	212
Table 0.2. Fatigue tests conditions based on the thermal and mechanical number of cycles.	213
Table 8.6. Two-way ANOVA results according to metal-ceramic shear bond strength data.	217
Table 9.1. Investment materials mixing ratio.	238
Table 9.2. Manufacturer's instructions of the burnout cycle of the IPS Press Vest.	239
Table 9.3. Firing parameters of ceramic for furnace Programat EP 5000.	240

SCOPE AND STRUCTURE OF THE THESIS

This thesis is concerned with the development of a FGM's (Functionally Graded Material) based solution for metal-ceramic bond strength enhancement in dental restorations, and also with the study of variables affecting the metal-ceramic bond strength. The goal is ultimately to produce more reliable and durable dental restorations provided with greater long term survival rates than those found today.

This thesis is elaborated in 10 chapters. Chapter 1 deals with a general introduction including a literature review on the aspects related to the prosthetic dentistry in general and to metal-ceramic systems in particular. This chapter is designed to bring readers with different backgrounds to a common level of knowledge. The topics dealt with are: a) function and structure of teeth; b) dental materials; c) dental ceramics; d) metal-ceramic systems; and e) functionally graded materials for biomedical applications. The motivation of this study is given in the end of this chapter.

The following chapters encompass 7 research reports that comprise Introduction, Methods and materials, Results, Discussion and Conclusions of the experimental work held during the research program. Chapter 2 deals with the study of the hot pressing effect on the shear bond strength of a gold dental alloy to porcelain. Metal-ceramic composites obtained by conventional PFM technique are compared with hot pressed ones with different surface roughness. The interfaces are analyzed by the means of different techniques. This paper is published in the Journal of Mechanical Behavior of Biomedical Materials (from Elsevier with an Impact factor of 2.814, Q1).

Chapter 3 is devoted to the optimization of the metal-ceramic bond strength by the means of a graded interface between gold dental alloy and porcelain. The bond strength of several composites with different metal/ceramic volume fractions to metal and ceramic frameworks is assessed. Bond strength results are compared with conventionally obtained PFM composites. This paper is published in the journal Materials Science and Engineering A (from Elsevier with an Impact factor of 2.003, Q1).

Chapter 4 is concerned with the influence of preoxidation cycle on the bond strength of CoCrMo-porcelain dental composites. Besides the metal-ceramic bond strength assessment for non-oxidized and preoxidized metal substrates, the analysis of non-oxidized, preoxidized and alumina-blasted preoxidized CoCrMo surfaces prior to porcelain firing was also conducted. This paper is published in the journal *Materials Science and Engineering C* (from Elsevier with an Impact factor of 2.686, Q1).

Chapter 5 reports on the comparison between cast and hot pressed CoCrMo alloy for metal-ceramic dental restorations. The comparison is made in terms of microstructure, hardness, corrosion resistance and porcelain bond strength. This paper is published in the *Journal of Mechanical Behavior of Biomedical Materials* (from Elsevier with an Impact factor of 2.814, Q1).

Chapter 6 deals with the effect of Hot Pressing on the bond strength of a CoCrMoSi alloy to a low-fusing feldspathic porcelain, for two types of surface treatments. The hot pressed metal-ceramic specimens are compared to conventional porcelain fused to metal specimens. The study was performed with polished and sandblasted metal substrates. This paper is submitted for publication in the journal *Materials Science and Engineering C* (from Elsevier with an Impact factor of 2.686, Q1).

In Chapter 7 is reported the experimental evaluation of the bond strength between a CoCrMo dental alloy and porcelain through a composite metal-ceramic graded transition interlayer. Several metal/ceramic composites were produced and tested as interlayers aiming at the improvement of metal-ceramic adhesion. This paper is published in *Journal of the Mechanical Behavior of Biomedical Materials* (from Elsevier with an Impact factor of 2.814, Q1).

In Chapter 8 is studied the effect of thermo-mechanical cycling on the metal-ceramic bond strength of conventional porcelain fused to metal restorations (PFM) and new high strength metal-porcelain restorations characterized by a metal-ceramic graded transition. This paper is currently submitted for publication in *Journal of the Mechanical Behavior of Biomedical Materials* (from Elsevier with an Impact factor of 2.814, Q1).

Chapter 9 presents the experimental procedure for the fabrication of functionally graded dental restorations, using real crown geometries, making use of current technology yet employed in the fabrication of conventional restorations

Finally, Chapter 10 encompasses a general discussion and the main conclusions are drawn. Here is also presented an outlook for future works.

Chapter 1

Introduction

1. Teeth - Function and Structure

Teeth are small, calcified, whitish structures found in the mouths of many vertebrates. In humans, their main function is helping digestion through mastication, which is the process by which food is crushed and ground. Teeth are also of extreme importance in helping correct sound pronunciation and speech articulation. Furthermore, teeth are regarded for keeping the facial profile and healthy teeth will traduce a good appearance.

The complete permanent dentition present in a human adult is composed of 32 teeth: 16 in the upper maxillary arch and 16 in the lower mandibular arch (Figure 1.1). The permanent dentition has eight teeth in each quadrant, which are divided into four classes: incisors, canines, premolars and molars. Based on location, the two permanent front teeth in each quadrant are incisors (**I**), followed by one canine (**C**), then two premolars (**PM**), and finally three molars (**M**).

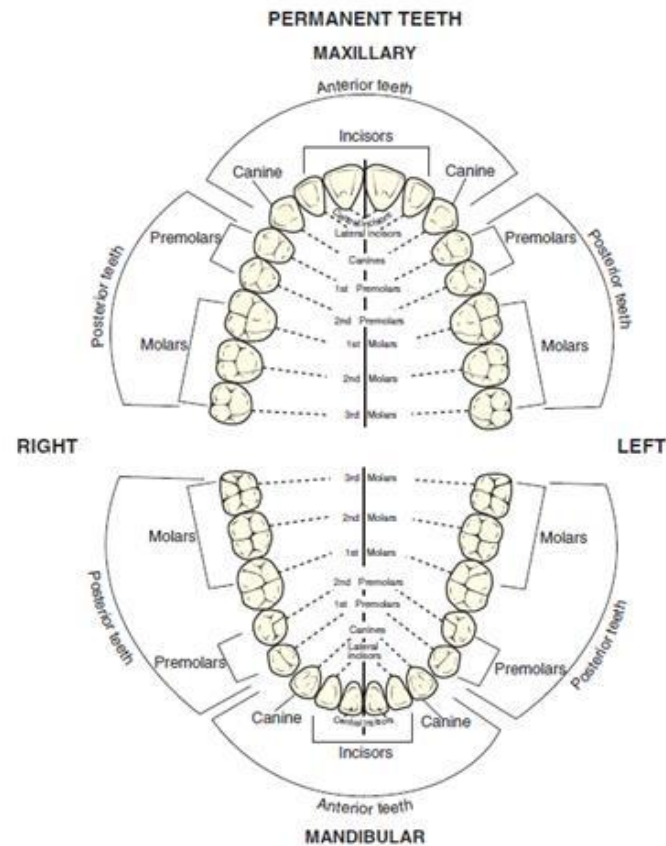
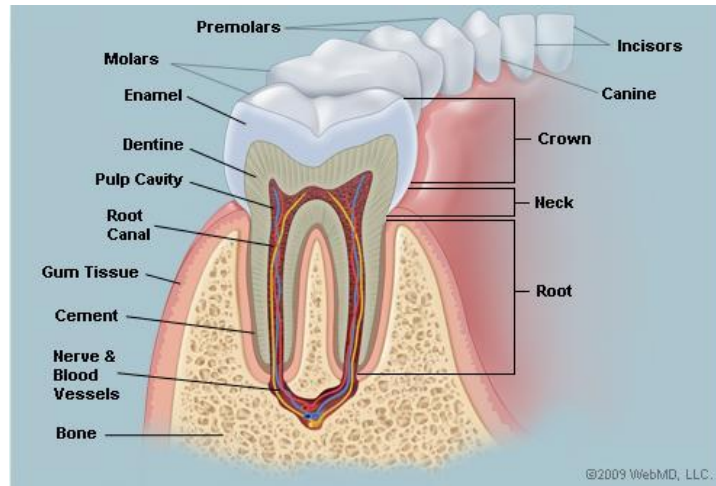


Figure 1.1. Maxillary and mandibular permanent dentition (Scheid and Weiss, 2012).

Teeth can be categorized or distinguished in groups according to their location: **anterior** and **posterior** teeth. **Anterior** teeth are those teeth in the front of the mouth, specifically, the incisors and the canines. **Posterior** teeth are those in the back of the mouth, specifically, the premolars and the molars.

The tooth is composed of four tissues: enamel, dentin, cementum, and pulp (Figure 2). The first three of these (enamel, dentine, and cement) are relatively hard since they contain considerable mineral content, especially calcium. Within these tissues only enamel and cement are visible in an intact extracted tooth. The other two tissues (dentin and pulp) are usually not visible on an intact tooth.



<http://www.webmd.com/oral-health/picture-of-the-teeth>

Figure 1.2. A mandibular posterior tooth sectioned longitudinally through the middle to show the distribution of the **tooth tissues** and the shape of the pulp cavity (made up of pulp chamber and root canal).

Scheid and Weiss (2012) describe the four dental tissues as follows:

Enamel is the white, protective external surface layer of the anatomic crown. It is highly calcified or mineralized, and is the hardest substance in the body. Its mineral content is 95% calcium hydroxyapatite (which is calcified). The remaining substances include 5% water and enamel matrix.

Cementum is the dull yellow external layer of the tooth root. The cementum is very thin, especially next to the cervical line, similar in thickness to a page in this text (only 50-100 μm thick where one μm is one millionth of a meter). It is composed of 65% calcium hydroxyapatite (mineralized and calcified), 35% organic matter (collagen fibers), and 12% water (Melfi (2000), states that the mineral content of cementum is about 50%). Cement is about as hard as bone but considerably softer than enamel.

Dentin is the hard yellowish tissue underlying the enamel and cementum, and makes up the major bulk of the inner portion of each tooth crown and root. It extends from the pulp cavity in the center of the tooth outward to the inner surface of the enamel

(on the crown) or cementum (on the root). Dentin is not normally visible except on a dental radiograph, or when the enamel or cementum have been worn away, or cut away when preparing a tooth with a bur, or destroyed by decay. Mature dentin is composed of about 70% calcium hydroxyapatite, 18% organic matter (collagen fibers), and 12% water, making it harder than cementum but softer and less brittle than enamel. The **dentinoenamel junction (DEJ)** is the inner surface of the enamel cap where enamel joins dentin. This junction can be best seen on a radiograph (Figure 1.3).

Pulp is the soft (not calcified or mineralized) tissue in the cavity or space in the center of the crown and root called the **pulp cavity**. The pulp cavity has a coronal portion (**pulp chamber**) and a root portion (**pulp canal** or **root canal**). The pulp cavity is surrounded by dentin, except at a hole (or holes) near the root tip (apex) called an **apical foramen** (plural foramina). Nerves and blood vessels enter the pulp through apical foramina. Like dentin, the pulp is normally not visible, except on a dental radiograph (x-ray) or sectioned tooth (Figure 1.3).

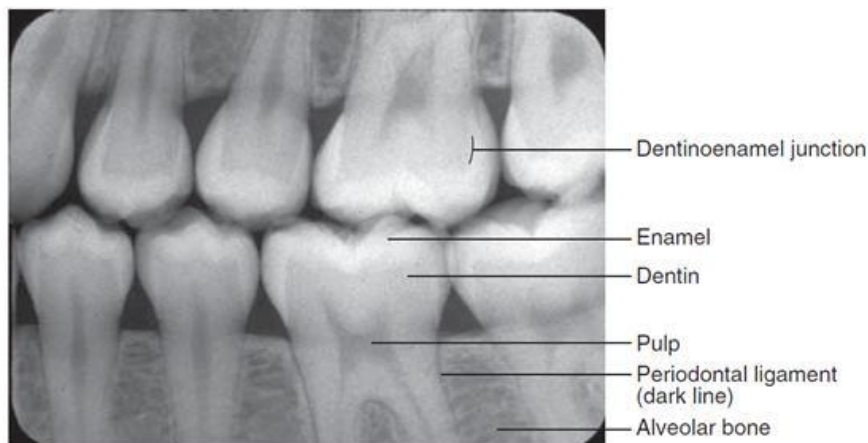


Figure 1.3. Radiograph (x-rays) showing tooth teeth structure, crowns and roots. The former are covered with enamel, and the latter are embedded within the alveolar bone. The whiter outer enamel shape is also distinguished from the darker inner dentin, and the darkest pulp chamber in the middle of the tooth. Between the root and the bone it is visible the very thin, dark periodontal ligament, but the cementum cannot be seen (Scheid and Weiss, 2012).

2. Dental Materials

Dental materials are materials used in the replacement or alteration of the tooth structure for aesthetic or functional purposes. The development and selection of biocompatible, long-lasting, direct-filling tooth restoratives and indirectly prosthetic materials capable of withstand the aggressive environment of the oral cavity, have been a challenge for practitioners of dentistry since the beginning of dental practice.

Historically, the materials used to replace missing teeth included animal teeth, bone, human teeth, ivory, seashells, ceramics and metals. Today, the materials used for restorative dentistry are divided in four groups: metals, ceramics, polymers and composites. A great endeavor has been made by dentists and materials scientists in searching for the ideal material that would be: biocompatible; bond permanently to the tooth structure or bone; match the natural appearance of tooth structure and other visible tissues, exhibit properties similar to those of tooth enamel, dentin and other tissues; and be capable of initiating tissue repair or regeneration of missing or damaged tissues (Anusavice, 2003).

According to Anusavice (2003), dental materials can be classified as preventive materials, restorative materials, or auxiliary materials. Regarding **preventive materials**, these include pit and fissure sealants; sealing agents that prevent leakage; materials that are used in primarily for their antibacterial effects; and liners, bases, cements and restorative materials that are used primarily because they release fluoride, chlorhexidine, or other therapeutic agents used to prevent or inhibit the progression of tooth decay, such as dental caries.

Restorative dental materials comprises all synthetic components that can be used to repair or replace tooth structure, including primers, bonding agents, liners, cement bases, amalgams, resin-based composites, compomers, hybrid ionomers, cast metals, metal-ceramics, ceramics and denture polymers. These materials may be used for temporary, short-term purposes (e.g. temporary cements and temporary crown and bridge resins), or for long-term applications (dentin bonding agents, inlays, onlays,

crowns, removable dentures, fixed dentures, and orthodontic appliances). Figure 1.4 shows some of the dental restorative systems yet described.



<http://revistageo.uol.com.br/cultura-expedicoes/15/artigo178043-8.asp>

Figure 1.4. Dental restorative systems: **1** – Full-metallic crown; **2**- ceramic onlay; **3**- metal-ceramic crown; **4** - implant; **5** – Teeth cleaning; **6** – Bridge; **7** – All-ceramic crown; **8**- Metallic inlay.

Restorative materials may further be classified as **direct restorative materials** and **indirect restorative materials**. Hence, the former materials are used intraoral to fabricate restorations or prosthetic devices directly on the teeth or tissues. The latter materials are used extraorally and are formed indirectly on casts or other replicas of the teeth or other tissues. Another type of materials are the auxiliary dental materials which are substances used in the fabrication of dental prostheses and appliances but that do not become part of these devices (e.g. impression materials, casting investments, gypsum cast and model materials, etc.)

Finally, the restorative materials which comprises products used for dental restorations and appliances that are not intended for moderate-term or long-term applications belong to the subcategory of **temporary restorative materials** (e.g. temporary cements, resins for feelings, orthodontic wires and brackets, acrylic resins for temporary inlays, onlays, crowns and fixed partial dentures.

This thesis deals with indirect restorative materials since the object of the study are metal-ceramic composites for dental-restorations. The materials involved in these restorations, namely dental alloys and dental porcelains, are presented in the following sections of this chapter.

2.1. Dental alloys

Most of the metallic components for dental restorations, such as crowns, bridges, inlays, cast posts and cores and partial dentures are produced by the lost wax technique. Dental restorations produced with computer assistance are becoming more common in recent years and these systems rely in production techniques like Powder-metallurgy laser sintering and CNC-milling (Beuer et al, 2008; Dewidar et al, 2006; Ucar et al. 2009). Nevertheless, the lost wax casting is still the most employed technique used in prosthetic laboratories and, although its history can be traced back beyond 3000 BC, its use in dentistry reports to 1890s. The first alloys used in this technique were gold alloys, being gradually replaced by cobalt-chromium (CoCr) alloys during the 1950s for the construction of removable partial dentures. Titanium started to be used as fixed and removable partial denture-casting alloy in the latter part of the 20th century. The factors that govern the choice of the alloy to be employed in a dental prosthesis are: the biocompatibility, cost, mechanical properties, ease of casting and density (van Noort, 2007).

The metal alloys used in dentistry are divided in two groups: 1) the noble and precious metal alloys; and 2) the base metal alloys.

2.1.1. Noble and Precious alloys

The noble and precious metals are regarded to be noble due to their high corrosion resistance and are precious because of their high price. The noble alloys are considered to be made up of gold, platinum, rhodium, ruthenium, iridium and osmium,

whereas silver and palladium are generally referred as the precious metals (van Noort, 2007). Within this group it should be highlighted the high-gold alloys; medium and low-gold and; silver palladium alloys.

The **high-gold alloys** can be distinguished from other alloys used in dentistry by their high precious metal content, which must not be less than 75% and a gold content in excess of 60%. The precious metal content in these alloys is usually made up of gold, silver, platinum and palladium. These alloys can be classified into four groups (Table 1.1) and, depending on the alloy composition, different mechanical properties are expected (Table 1.2). The alloys used in metal-ceramic prostheses are the Type III and Type IV alloys (see Table 1.1) because of their greater strength compared with the Type I and Type II alloys (Knosp et al, 2003). These alloys can be generally described as easy to cast and easy to polish, producing well-fitting castings with good quality, excellent corrosion and tarnish resistance, as is their biocompatibility (Roberts et al. 2007; Knosp et al, 2003).

The **medium- and low-gold alloys** were introduced in the early 1970s due to the sharp increase of noble metals. Manufacturers were then encouraged to produce new alloys with reduced gold contents (varying from 40% to 60%) and increased contents of palladium and silver – **medium gold-alloys**.

There are also available **low-gold alloys**, in which the gold content is of the order of 10-20% and the rest of the elements are silver (40-60%) and palladium (up to 40%).

The **medium gold-alloys** are recommended for the same applications of Type III and Type IV alloys, but exhibit lower ductility and they are difficult to burnish.

The **low-gold content** alloys are recommended for the same applications of Type III alloys although they tend to have lower mechanical properties than medium-gold alloys. These alloys when containing indium can present an additional difficulty in casting. Also, the properties variability within low-gold alloys and medium-gold alloys are higher than the verified for each of the four types of high-gold alloys. Nevertheless, they both exhibit excellent biocompatibility and good corrosion resistance.

Table 1.1. Composition of high-gold alloys (wt.%) (van Noort, 2007).

Type	Description	Au	Ag	Cu	Pt	Pd	Zn
I	Soft	80-90	3-12	2-5	-	-	-
II	Medium	75-78	12-15	7-10	2	1-4	0-1
III	Hard	62-78	8-26	8-11	5	2-4	0-1
IV	Extra Hard	60-70	4-20	11-16	10	0-5	1-2

Table 1.2. Range of mechanical properties of high-gold alloys (van Noort, 2007).

Type	Condition	σ_y (MPa)	UTS (MPa)	Elongation (%)	HV
I	As cast	60-140	200-310	20-35	40-70
II	As cast	140-250	310-380	20-35	70-100
III	As cast	180-260	330-390	20-25	90-130
	Hardened	280-350	410-560	6-20	115-170
IV	As cast	300-390	410-520	4-25	130-160
	Hardened	550-680	690-830	1-6	200-240

Silver-palladium alloys (Ag-Pd) are mainly composed by silver and presents significant amounts of palladium (Roberts et al., 2007). These alloys, also designated as “white golds”, were introduced in dentistry in the 1960s as an alternative to high-gold alloys. The presence of palladium has a dual effect in these alloys which is the improvement of the resistance to corrosion and the prevention of tarnishing that is usually associated with silver. These alloys get improved properties when they are submitted to a careful controlled hardening heat treatment. Depending on the composition, these alloys can present a wide range of properties which makes that the selection of the alloy must take into account the type of application. Despite the Ag-Pd alloys high biocompatibility, these alloys present some drawbacks such as the tendency for tarnishing and the tendency to work-harden rapidly, which precludes excessive adjustments and any burnishing. For these reasons, these alloys are considerably less popular than medium and low-gold alloys.

2.1.2. Base metal alloys

Cobalt-chromium (Co-Cr) alloys have a successful track record in prosthetic dentistry since they were first introduced in 1930s in the profession (Roberts et al., 2007). Their low cost and excellent mechanical properties made this alloy a good substitute for Type IV gold alloys in large castings as partial denture frameworks, for instance (**Figure 1.5**) (van Noort, 2007).



http://www.d-group-cn.com/en/about.asp?big_id=40&pageid=67

Figure 1.5. Cobalt-chromium partial denture.

The alloy is formed by cobalt (55-65%, in wt.%) with up to 30% chromium. Other major alloying elements are molybdenum (4-5%), carbon, beryllium, tungsten, carbon, aluminum and níquel. Chromium is responsible for the tarnish and corrosion resistance (Saji and Choe, 2009) of these alloys and when its content is greater than 30% the alloy is difficult to cast. Beyond this value of Cr content in the alloy, a detrimental brittle second phase (sigma) forms because it was reached the limit of solubility of Cr in Co (Gupta, 2005). Molybdenum is present in order to refine the alloy grain size by providing more sites for crystal nucleation during the solidification process (Craig and Powers, 2002).

Carbon is an extremely important constituent of the alloy, although it is present only in small quantities. The typical carbon contents for Co-Cr alloys are: 0.25 wt.% for cast

alloys; 0.04-0.05 wt.% for wrought alloys; and 0.20-0.25 wt.% for high carbon wrought alloys (Disegi et al., 1999). Small variations of carbon content can significantly influence the strength, hardness and ductility of the alloy, in such an extent that the alloy would no longer be usable in dentistry. Carbon contents of 0.2% above or below the desired amount would result in an alloy excessively hard and brittle, or with low yield and ultimate tensile strengths, respectively. Furthermore, carbon can combine with any of the alloying elements in these alloys, such as cobalt, chromium, molybdenum, silicon, níquel, forming carbides. Their distribution also depends upon the casting temperature and the cooling rate (Mineta et al., 2010; Lee et al., 2008). Discontinuous carbides formation at the grain boundaries are preferable to continuous carbide formation (Shi et al. 1993).

Co-Cr alloys present considerably higher melting temperatures (1300-1400°C) and associated casting shrinkage (2.0%) than the gold alloys, which make them more difficult to handle. As they present high hardness, they are also more difficult to polish. The lack of ductility, resulting from carbon contamination can be a problem, especially as these alloys are also prone to casting porosity. These limitations combine to give rise to a common problem with partial dentures: clasp fractures. Nevertheless, these alloys present some features that make them suited for to the construction of partial denture frameworks. The Young's modulus of a Co-Cr alloy is substantially higher than those of the alloys previously discussed, e.g. 230GPa vs. 70-100GPa (Roberts et al, 2009). Using alloys with high Young's modulus allows the design of restorations with slightly reduced dimensions, maintaining the adequate rigidity. This fact, combined with a density of about half that of the gold alloys, produce considerably lighter restorations with great benefit to the comfort of the patient.

The addition of chromium makes this a highly corrosion-resistant alloy (Saji and Choe, 2009), which has at the same time an excellent history of biocompatibility (Roberts et al., 2007; Pilliar, 2009). Some alloys also contain níquel, which is added in order to increase ductility and reduce hardness (Hiromoto et al., 2005; Matković et al., 2003) Because nickel is a well-known allergen and its use in the mouth may trigger an allergic

reaction, patients known to have a propensity for allergic reactions are advised to use a nickel-free Co-Cr alloy.

Titanium-based alloys are very attractive for use in dentistry because of several factors: resistance to electrochemical degradation, benign biological response elicited, low density, low modulus, and high strength (Roberts et al., 2007). Titanium forms a very stable oxide layer with a few angstroms thickness which is in the basis for its corrosion resistance and biocompatibility (Roach, 2007). Titanium has therefore been considered the "material of choice" in dentistry. Commercially pure titanium (Cp Ti) is used for dental implants, surface coatings, and, more recently, for crowns, partial and complete dentures, and orthodontic wires (Roach et al., 2007). Within the available titanium alloys, Ti-6Al-4V is the most widely used. The term *titanium* is often used to include all types of pure and alloyed titanium. However, it should be noted that the processing, composition, structure, and properties of the various titanium alloys are quite different, and also that differences exist between the wrought and cast forms of a given type of titanium (Niinomi, 1998).

Commercially Pure Titanium

Titanium is allotropic, with a hexagonal close-packed (HCP) structure (α) at low temperatures and a body-centered cubic (BCC) structure (β) above 882°C (Roach, 2007). Commercially pure titanium (cpTi) is in fact an alloy of titanium with up to 0.5% oxygen (wt.%). The oxygen is in solution so that the metal is single phase. Elements such as oxygen, nitrogen and carbon have a greater solubility in the HCP structure of the α -phase than in the cubic form of the β -phase. These elements form interstitial solid solutions with titanium and help to stabilize the α -phase. Transition elements such as molybdenum, niobium and vanadium act as β stabilizers.

Titanium - 6% Aluminum - 4% Vanadium

The addition of small quantities of aluminum and vanadium to titanium produce a significant increase in the alloy's strength, over that of cpTi (Niinomi, 1998). Aluminum is considered to be an α -stabiliser with vanadium acting as a β -stabiliser. When these are added to titanium the temperature at which the α - β transition occurs is depressed such that both the α and β forms can exist at room temperature. Thus, Ti- 6% Al-4% V has a two-phase structure of α and β grains (Roach, 2007).

Pure titanium is a white, lustrous metal that is characterized by a low density, good strength and an excellent corrosion resistance. It is ductile and constitutes an important alloying element with many other metals. Alloys of titanium are widely used in the aircraft industry and military applications where the low density, the high-tensile strength ($\sim 500\text{MPa}$) and the ability to withstand high temperatures are important features in such high demanding industries (Boyer, 1996). The elastic modulus of cpTi is 110 GPa, which is half that of stainless steel or Co-Cr alloy (van Noort, 2007).

The tensile properties of cpTi depend significantly on the oxygen content and although the ultimate tensile strength, proof stress and hardness increase with increased oxygen concentration, this is at the expense of the ductility.

By alloying titanium with aluminium and vanadium a wide range of mechanical properties superior to the cpTi are possible (Niinomi, 1998). Such alloys of titanium are a mixture of the α and β phase, where the α phase is relatively soft and ductile while the β phase is harder and stronger but also less ductile. Thus by changing the relative proportions of α and β a wide variety of mechanical properties can be achieved.

Due to the considerably higher tensile properties ($\sim 1030\text{MPa}$) of the Ti-6% Al-4% V alloy relatively to pure titanium, the former alloy is more suited for use in high-stress-bearing situations such as partial dentures.

Other important features of titanium and titanium alloys are the fatigue and the corrosion resistance. In fact, titanium has become popular because it is one of the most corrosion-resistant metals known to man and this applies equally to the alloys.

The corrosion resistance of titanium is provided by the oxide formed on its surface (TiO_2) which is extremely stable and thus has a passivating effect on the metal.

The high melting point of titanium ($\sim 1670^\circ\text{C}$), put technicians faced with problems arising from casting in such high temperatures, like the compensation of the cooling contraction. Moreover, because the metal is very reactive, all castings need to be carried out in a vacuum or an inert atmosphere, which requires special casting equipment (Roach, 2007). Thus only few dental laboratories will be set up for the casting of titanium alloys. Another point to consider is the fact that the molten alloy has a propensity to react with the refractory investment mould, leaving behind a surface scale, which can compromise the quality of fit of the restoration. Internal porosity is also often observed with titanium castings. Hence, other forms of processing titanium for dental prostheses are also used such as CAD/CAM combined with milling and spark erosion (Roach, 2007). In Table 1.3 are presented some of the properties of the base metal alloys discussed above for comparison.

Table 1.3. Comparison of some properties of base metal casting alloys (Van Noort, 2007).

Property	Co-Cr alloy	Titanium	Ti-6% Al-4% V
Density (g/cm^3)	8.9	4.5	4.5
Casting temperature ($^\circ\text{C}$)	~ 1500	~ 1700	~ 1700
Casting shrinkage (%)	2.3	3.5	3.5
Tensile Strength (MPa)	850	520	1000
Proportional limit (MPa)	550-650	350	920
Elastic modulus (GPa)	190-230	110	85-115
Hardness (Vickers)	360-430	200	--
Ductility (%)	2-8	20	14

2.2 Dental ceramics

Craig and Powers (2002) define ceramic and porcelain in the following way: the term ceramic is defined as any product made essentially from a nonmetallic material by firing at a high temperature to achieve desirable properties. The term porcelain refers to a family of ceramic materials composed essentially of kaolin, quartz, and feldspar, also fired at high temperature (Barreiro et al., 1989). Dental ceramics for ceramic-metal restorations belong to this family and are commonly referred to as dental porcelains.

Dental ceramics are used in dentistry since the late 1700s but they suffered significant improvements since then. In the 1900s, porcelain jacket crowns were developed but their use was limited to anterior teeth due to the porcelain's low strength. The 1960's were considered the turning point in porcelains' use with the development of the leucite containing feldspathic porcelains. These porcelains solved the problem of the poor match in thermal expansion (and contraction) between framework alloys and veneering porcelains which often caused restoration's fracture and failure upon cooling. The coefficient of thermal expansion (CTE) adjustment between that of metal and porcelain was made by mixing controlled amounts of high expansion leucite with feldspar glass at the manufacturing stage.

2.2.1. Classification of dental porcelains

Dental porcelains can be classified according several aspects, such as: fusion temperature, application, fabrication technique or crystalline phase.

In Table 1.4 is presented the porcelain classification with regard to their fusing temperatures.

Table 1.4. Classification of dental porcelains according to their fusion temperature (Craig and Powers, 2002).

Porcelain type	Fusing temperature
High-fusing	1315-1370°C
Medium-fusing	1090-1260°C
Low-fusing	870-1065°C
Ultra-low-fusing	<870°C

The medium- and high- fusing ceramics are used for denture teeth while the low- or medium- fusing ones are used for ceramic-metal or all-ceramic fixed restorations.

Some of the ultra-low fusing porcelains are used for titanium and titanium alloys because of their low contraction coefficients that closely match those of the alloy.

The three major applications of ceramics in dentistry are: (1) metal crowns and partial dentures; (2) all-ceramic crowns, inlays, onlays and veneers; and (3) ceramic denture teeth.

The most common processing technique of dental ceramics is sintering, which consists of the ceramic densification at high temperature. Ceramics employed in metal-ceramic prostheses are sintered whereas those used in all-ceramic can also be processed by other techniques like heat-pressing, machining and slip casting (Craig and Powers, 2002; Qualtrough and Piddock, 1997; Kelly et al., 1996).

2.2.2. Composition

The dental porcelains differ from the earthenware, stoneware and domestic porcelain in the content of kaolin, feldspar and quartz (Figure 1.6). The compositions of domestic and dental porcelain are exhibited in Table 1.5 and Figure 1.6.

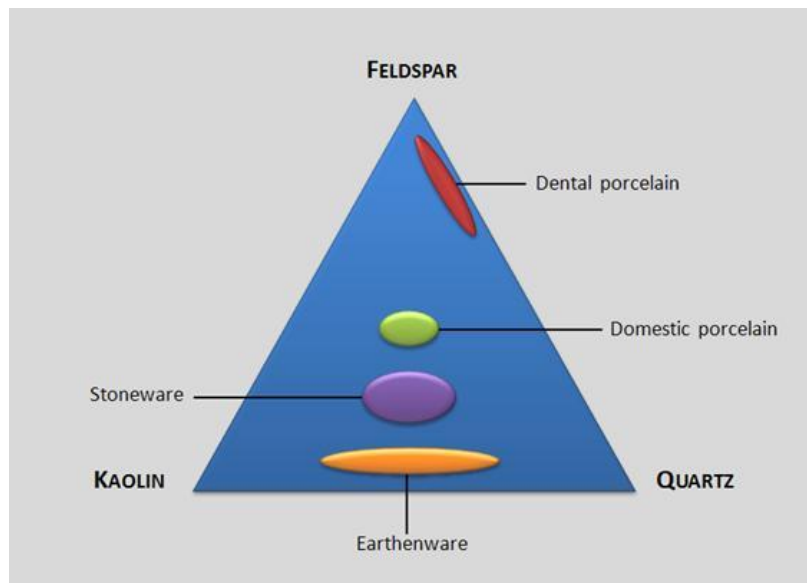


Figure 1.6. Relative composition of ceramic products based on feldspar, kaolin and quartz (van Noort, 2007).

Table 1.5. Composition of household and dental porcelain (wt.%) (van Noort, 2007).

Porcelain	Kaolin	Quartz	Feldspar
Household	50	20-25	25-30
Dental	0	25	65

Although Kaolin ($\text{Al}_2\text{O}_3 \cdot 2\text{SiO}_2 \cdot 2\text{H}_2\text{O}$) can act as a binder and improve the ability to mould the unfired porcelain, it is opaque and that compromises the translucency required for dental porcelains. Therefore, dental porcelains do not contain kaolin in their composition.

Quartz (SiO_2), which is one of the crystalline forms of silica, act as a strengthening agent. It is spread throughout the glassy phase that is produced by the melting of feldspar.

The feldspars are mixtures of potassium alumino-silicate ($K_2O \cdot Al_2O_3 \cdot 6SiO_2$) and sodium alumino-silicate ($Na_2O \cdot Al_2O_3 \cdot 6SiO_2$). The properties of feldspars are influenced by the different proportion of potash (K_2O) and soda (Na_2O), in that the former increases the viscosity of the molten glass and the latter tends to lower the fusion temperature. In order to obtain a full range of shades necessary to mimic the natural teeth, coloring pigments are added to dental porcelains in small quantities (e.g. titanium oxide, manganese oxide, iron oxide, cobalt oxide, copper and níquel oxide). Tin, titanium and zirconium oxides are used as opacifiers.

Feldspathic dental porcelains are composed by two phases: a glassy phase surrounding a crystalline phase. The glass phase has properties typical of glass such as brittleness, non-directional fracture pattern, translucency and high surface tension in the fluid state. The crystalline phase is leucite, a potassium alumino-silicate ($KAlSi_2O_6$), with high thermal expansion ($>20 \times 10^{-6}/^{\circ}C$), which presence (10% to 20%) controls the coefficient of thermal expansion and the strength of the porcelain. Figure 1.7 shows the leucite crystals in six different commercial dental porcelains.

2.2.3. Processing

The production of a porcelain restoration (porcelain jacket crown) comprises several steps, each of them with its own specificities. Steps are the following: Porcelain application and condensation; Drying; Firing/sintering; Glazing and Cooling.

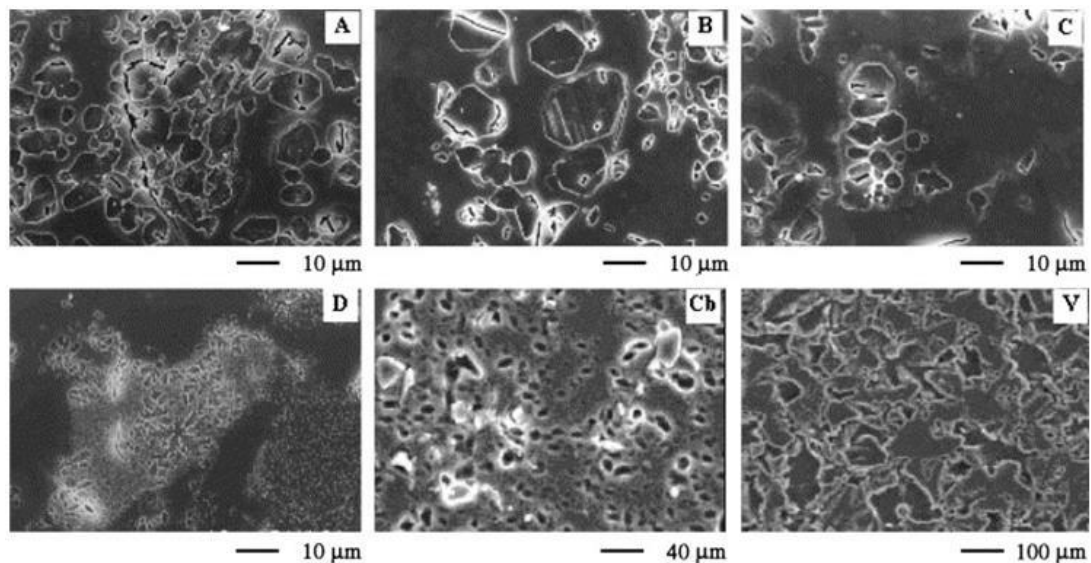


Figure 1.7. Micrographs of the polished surfaces of six porcelains etched with 2% hydrofluoric acid (HF) for 15 s. A: Ceramco I (Dentsply), B: Ceramco II (Dentsply), C: Finesse (Dentsply), D: d.Sign (Ivoclar), Cb: Cerabien (Noritake), and V: Vitadur-Alpha (Vita) (Cesar et al.,2005).

2.2.3.1. Porcelain application and condensation (Compaction)

In the construction of a porcelain jacket crown (PJC) the die, previously coated with a platinum metal foil, is veneered with a past of ceramic powder mixed with water. The platinum foil is necessary to assure the separation from the die and the transport to the furnace. To recreate all the aesthetic features of a tooth are necessary several porcelain types, namely, the opaque shade, the dentin and the enamel. The opaque porcelain is used to mask the underlying structure while the others are used to provide the restoration with the natural tooth aspect. The PJC construction is shown in Figure 1.8.

The powder compaction is performed by several possible routes (spatulation, brush application, whipping or vibration) and results in a high density of particles that minimizes the firing shrinkage.

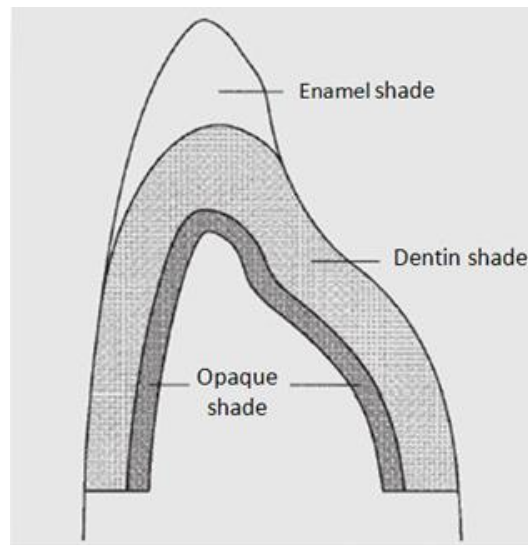


Figure 1.8. Porcelains used in the build-up of a jacket crown (van Noort, 2007).

2.2.3.2. Firing

The firing process is initiated with a slow heating of the crown in the furnace entrance. This step is regarded to remove the excess water in the restoration before it can form steam and its escape to surface could cause the fragile powder-compact to crack. After it, the porcelain sintering takes place and it is accompanied by a large volume contraction (~20%) caused by the fusion of particles during this stage, as the powder particles are brought into close contact.

The firing of the porcelain must strictly follow the manufacturers' schedule and excessive firing cycles should be avoided to prevent pyroplastic flow (flow of the molten glass) and excessive glaze.

A slow cooling should therefore be performed to avoid the possibility of crazing or cracking. The porcelain firing can occur in air or vacuum, depending on the type of furnace. Vacuum-firing removes the air during firing cycle thus producing denser porcelain than air-firing. The lack of voids within porcelain resultant from vacuum-firing accounts for higher strength and aesthetics (Cheung and Darvel, 2002). Pores are stress concentration sites that can cause premature failure of the crowns and can also alter its translucency (Cheung and Darvel, 2002).

2.2.3.3. Glazing

Despite all efforts to avoid or minimize the porosity within the porcelain, there will always be some voids being exposed at the surface that allows the ingress of bacteria and oral fluids, thus acting as potential sites for the build-up of plaque (Bollen et al., 1997). The glazing of the surface helps to avoid this since it produces a smooth, shiny and impervious outer layer in restoration. This final treatment can be achieved either by fusing glasses, at low temperature, after the construction of the crown or, by a controlled final firing of the crown that allows only the fusing of the superficial layer.

2.3. Properties of dental porcelain

Dental porcelain provides excellent aesthetics that do not deteriorate with time due to its chemical stability. The thermal conductivity and the coefficient of thermal expansion are similar to those of dentin and enamel, which means that, a good marginal sealing would prevent percolation related problems.

As dental porcelains are primarily glasses, they exhibit properties similar to them. Hence, they show high compressive strength (350-550MPa), very low tensile strength (20-60MPa) and very low fracture toughness (<0.1% strain). Glasses are characterized for being extremely sensitive to the presence of surface microcracks, and this represents a major drawback. On cooling, thermal gradients form on the crown due to the rapid cooling of the outer surface and the slower cooling of the inner part of the restoration. These thermal gradients derives in contraction gradients, i.e., as the outside surface contracts more than the inside initially, it leads to the formation of a compressive load on the outside and a residual tensile stress on the inside as the interior is being prevented from shrinkage by the outside layer. When the dimensional change is excessive, some microcracks can arise in the inner surface of the crown that was under tension. The internal surface layer rupture occurs as a means of stress relief. Microcracks at the fit surface of the crown can ultimately cause the crown to fracture catastrophically (Figure 1.9).

The presence of any cracks on the outside layer of the porcelain can be solved by the application of a glaze with a slightly lower coefficient of thermal expansion that will fill the cracks and let the surface under compression. However, this is not applicable to the fitting surface of the crown (where the majority of cracks occur) as it may result in a misfitting of the crown. Porcelains showed that they weren't strong enough to be used in multi-unit bridges and, even anterior porcelain jacket crowns cracked in situations of heavy occlusion.

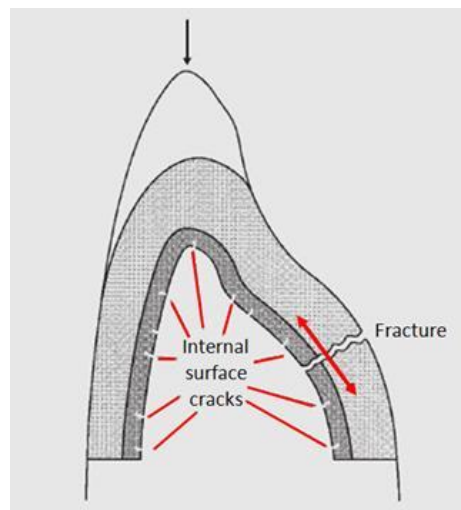


Figure 1.9. Porcelain jacket crown failure due to internal surface flaw (van Noort, 2007).

Therefore, to overcome the problem related to the lack of strength and toughness of dental porcelains, two types of solutions were developed. One solution consists in providing the dental porcelain with support from a stronger substructure and the other solution is regarded with the production of stronger and tougher ceramics. Based on this, it is possible to categorize the dental ceramics based on the nature of the supporting substructure in three categories: metal-ceramics, reinforced ceramic core systems and resin-bonded ceramics. In the first case, metal-ceramics, is a metal substructure that provides the necessary support to the aesthetic ceramic. This type of system is treated separately in Section 4 of this chapter. The reinforced ceramic core systems, as the name refers, the support for aesthetic ceramics is provided by a strong

and tough ceramic that may lack the desired aesthetic. Regarding the resin-bonded ceramic, the aesthetic ceramic is directly bonded to the enamel and dentine of the tooth to repair, and the support is provided by the tooth itself.

2.4. High-strength core ceramics

The high-strength core ceramics systems were first introduced in the mid 1960s by McLean and Hughes who developed a core material based on the reinforcement of a feldspathic glass with alumina, also known as alumina-reinforced porcelain. Later, in 1980s, the glass-infiltrated high strength ceramic cores were developed (In-Ceram, Vita) and in 1990s appeared the all-alumina cores (Techceram, Techceram Lta: Procera AllCeram, Nobel Biocare). Lately, the introduction of yttria stabilized zirconia has been seen for the fabrication of cores for crown and bridge frameworks.

Alumina-reinforced feldspathic cores consist of a feldspathic glass containing 40-50 vol% of alumina (Figure 1.10). The alumina particles are very strong and thus very effective in preventing crack propagation (Figure 1.11), making that flexural strength rise from the 60MPa (at best) of feldspathic porcelain to 120-150MPa from the aluminous core porcelains. However, the very strong core still needs to be veneered by the weaker feldspathic porcelains (dentin and enamel) because it is not possible to produce aluminous porcelains with the required translucency as that of feldspathic porcelains. This type of PJC is restricted to anterior teeth applications because, despite the considerable improvement in its strength, it is still insufficient to allow its application posteriorly or even in multi-unit bridges.

Glass infiltrated high strength ceramic core systems differs from the above described alumina-reinforced feldspathic cores in the amount of the alumina incorporation. This new system called In-Ceram (Vita Zahnfabrik, Bad Säckingen, Germany) has an alumina content of ~85 vol.% instead of the 40-50 vol% verified in the alumina-reinforced feldspathic cores. The ceramic cores are formed by slip casting and sintered for 10 hours at 1120°C. After this sintering stage, it has been formed a porous structure with

low strength (6-10 MPa) which is then infiltrated by a low viscosity lanthanum glass for 4-6 hours at 1100°C, producing a dense ceramic. From this process results a very strong ceramic cores (400-500MPa of flexural strength) which might be suitable for anterior and posterior crowns. The final functional and aesthetic form is provided by veneering the ceramic core with conventional feldspathic porcelain.

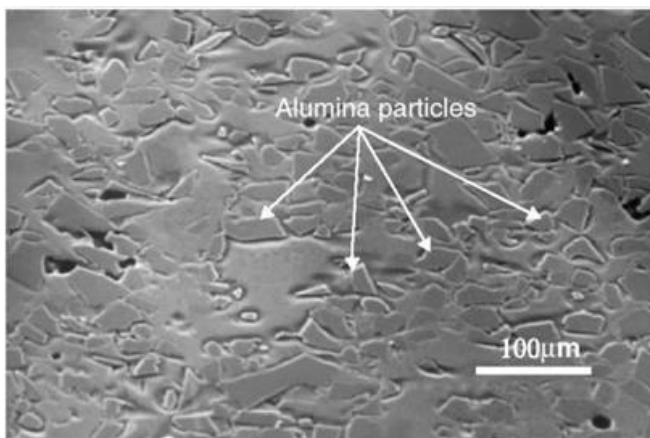


Figure 1.10. Micrograph of an alumina-reinforced core material showing the dispersed alumina particles embedded in a glassy matrix composed by feldspar (van Noort, 2007).

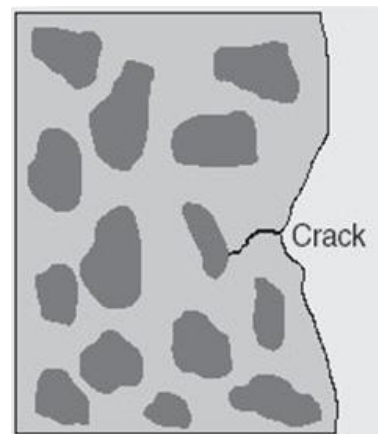


Figure 1.11. Alumina particles acting as crack stoppers and thus preventing crack propagation (van Noort, 2007).

The same systems have been used with spinel (In-Ceram-Spinel) and zirconia (In-Ceram-Zirconia) replacing alumina. The In-Ceram-Spinel has a slightly lower flexural strength (~350MPa) but better aesthetics than In-Ceram-Alumina. The In-Ceram-Zirconia has higher flexural strength (~700MPa) but has slightly poor aesthetics. The reason is that it is formed by glass, alumina and 33wt.% zirconia, which turns the material very opaque.

Besides slip casting route, it is also available new CAD-CAM systems, namely CEREC (Siemens) (Figure 1.13) and Celay (Vident), which allow the machining of dry-pressed ceramic blocks (In-Ceram/Spinel/Alumina/Zirconia) with a denser and a more homogeneous open-pore structure that results in a yet higher flexural strength after glass infiltration.



www.infinident.com

Figure 1.12. Zirconia porous structure obtained by slip-casting and after a 10 hours sintering stage at 1120°C. After it should be infiltrated by a low viscosity lanthanum glass for 4-6 hours at 1100°C to produce a dense ceramic structure (In-Ceram-Zirconia).



www.jamesklim.com/single-visit-crowns.html

Figure 1.13. CEREC CAD-CAM system, which constructs ceramic partial dentures from machined dry-pressed ceramic blocks.

Pure alumina cores have increased strength and superior translucency when compared to glass-infiltrated glass-ceramics. The flexural strength is in the region of 700MPa, which is comparable to that achieved in In-Ceram-Zirconia. There are at least two systems on the market that offer pure alumina cores, the Procera AllCeram (Nobel Biocare AB, Gotenburg, Sweeden) and the Techceram system (Techceram Ltd, Shipley, UK). In both systems, the coping is produced in one of the companies' laboratories and then returned to the dental laboratory for building on the crown's aesthetics using compatible feldspathic glasses. This is so, as it requires a complex process of sintering of 99.5% pure alumina at temperatures of 1600-1700°C for densification.

Zirconia core systems are known for their high translucency and outstanding strength (in excess of 1000MPa). The actual material used is yttria-stabilized zirconia and the yttria, despite it is there in a small amount (~3.0 mol%), plays a very important role in the zirconia toughness. Zirconia cores and bridge frameworks are produced by CAD-CAM systems existent in dental laboratories' facilities. The manufacturing process encloses the following steps: taking an impression; digitalizing the model; designing a 3D model of the restoration on the computer and then machining the restoration. The restoration is machined from a porous blank ("Soft" machining) which is much easier to machine than a full-dense one. Then, the restoration is fired in the furnace to allow the material to densify. During this stage, typically occurs a significant shrinkage of the material that was previously accounted during the CAD-aided design process, thus producing either a very close-fitting core or bridge framework.

Resin-bonded ceramics, as the name implies, consists in bonding a ceramic veneer permanently to the teeth with a resin-based composite. In this case, the underlying tooth structure provides the necessary support for the thin ceramic veneering.

The advantages of ceramic veneers over composites are superior aesthetics, color stability, surface finish, abrasion resistance, tissue compatibility, chemical stability and thermal compatibility with enamel (Hengchang et al., 1989).

The typical materials of choice used in the construction of veneers are simple feldspathic glasses or leucite containing feldspathic glasses due to their excellent aesthetics, mainly color and translucency, which is hardly matched by any other ceramic. However, because these ceramics lack of strength to be used in posterior crowns and all-ceramic bridges, a new class of ceramics suitable for use as resin-bonded all-ceramic restoration, has been developed and are known as glass-ceramics.

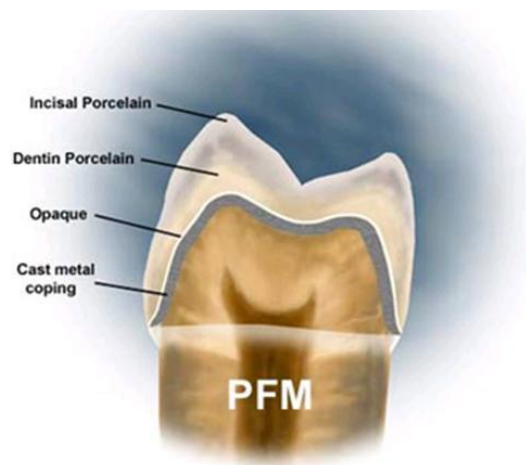
In glass-ceramics, the restoration is formed while liquid and a metastable glass results from cooling. Then, it is subjected to a heat treatment where controlled crystallization occurs, with the nucleation and growth of internal crystals. This conversion process from a glass to a partially crystalline glass is called *ceraming*. The high strength of the glass-ceramics results from numerous crystals uniformly distributed throughout the glassy phase (Quinn et al, 2003; Cesar et al., 2005). The crystalline phase grows during ceraming and can occupy from 50% to 100% of the material volume.

Examples from glass-ceramics are Leucite-Reinforced Feldspar Glass-Ceramics, Fluormica Glass-Ceramics, and Lithium Disilicate and Apatite Glass-Ceramics (van Noort, 2007).

Some of the available methods for producing glass-ceramics items include sintering on a refractory die, hot pressing and CAD-CAM machining from block (Beuer et al., 2008).

3. Metal-ceramic systems

The success of metal-ceramic restorations relies on the aesthetic qualities of ceramic materials combined with the strength and toughness of metals (van Noort, 2007). A cross-section of a metal-ceramic anterior crown is shown in Figure 1.14. The metal coping provides a substructure on which the ceramic coating is fused. The ceramic used in these restorations are porcelains, hence the name used for this type of restorations – porcelain-fused-to-metal (PFM) restorations. The metal-ceramic dental restorations are very popular restorations and are used for most of the crown and bridge restorations made today (McLaren, 2006).



<http://www.worldlabusa.com/porcelain.aspx>

Figure 1.14. Cross section of a metal-ceramic dental restoration.

It is of extreme importance that a good bond is created between the metal and ceramic as one of the most likely modes of failure with this system is the separation of the ceramic from the metal due to an interfacial breakdown of the metal-ceramic bond (van Noort, 2007). Another important aspect is to assure the correct mismatch between the coefficient of thermal expansion of the metal and the ceramic (Lopes et al., 2009). A great mismatch will produce stresses during cooling process after firing. Such stresses can result in crazing or cracking of the ceramic.

3.2. Metal-ceramic bonding

The bond strength between the ceramic and metal is perhaps the most important requirement. It is also a subject strongly linked with the scope of this thesis and thus will be given special attention. The bond between metal and ceramic results from chemisorption by elements diffusion between oxides formed on the metal surface and from the ceramic (Mackert et al., 1984; Shell and Nielsen, 1962). These metal surface oxides are formed during the wetting of the alloy by the porcelain and during the firing of the porcelain. As stated before, the ceramic debonding from the metal is the most common mechanical failure of these restorations. The nature of the bond between the metal substructure and the ceramic is agreed to be controlled by the following factors: the formation of strong chemical bonding, mechanical interlocking between the two materials and compressive residual stresses (Shell and Nielsen, 1962; Wagner et al., 1993). Additionally, the ceramic must wet and fuse to the metal surface to form a uniform interface without voids.

The formation of oxides on the metal surface has been proven to contribute for the formation of strong bonding (Wagner et al., 1984; Mackert et al., 1984; Mackert et al., 1988). These bonds are formed at the ceramic firing process where ceramic is taken above its glass transition temperature such that it can flow and fuse with the oxides at the metal surface by migration of the oxides into the ceramic. In the case of noble alloys which are resistant to oxidizing, easy oxidizing elements such as indium and tin are added to the alloy to form surface oxides (Anusavice et al., 1977; Hautaniemi, 1995). This results in bond strength increasing between metal and ceramic, thus showing the importance of the presence of the surface oxides.

Base metal alloys, however, due to their content in easily oxidized elements such as nickel, chromium and beryllium, forms oxides easily during degassing¹ and care must be taken to avoid too thick oxide layers (Rokni and Baradaran, 2007). Usually, manufacturers provide information about the conditions to form the optimal oxide

¹ Heat treatment applied to the metal coping before porcelain firing, which burns off any remaining impurities and reduces the formation of bubbles due to trapped gasses at the interface.

and which color it should take. Oxides rich in NiO tend to be dark gray whereas those rich in Cr₂O₃ are greenish.

The mechanical failure of the restoration can take place at the oxide-alloy interface because oxides are not completely dissolved during the fusion of the ceramic. This situation gets critical especially in the case of alloys that form layers rich in Cr₂O₃, which do not exhibit a good adhesion to the alloy (Mackert et al, 1984). Conversely, the oxides formed by Be containing alloys exhibit a good adhesion to its metal. The BeO, particularly, is a slow-growing oxide that does not delaminate from the surface of the alloy.

The roughness of a metal-ceramic interface plays a very important role in the ceramic adhesion. The mechanical retention occurs as the ceramic flows into the rough metal surface, creating a Velcro-like effect (Figure 1.15), and thus improving the adhesion (Wagner et al., 1993).

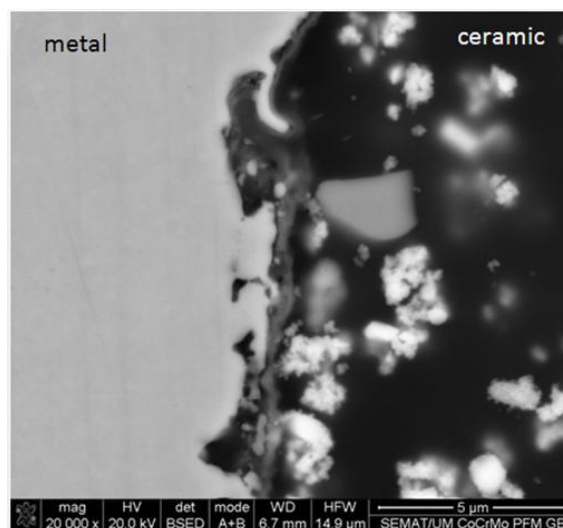


Figure 1.15. Micrograph showing the metal-ceramic interface with mechanical interlocking between the two materials.

A rough interface also corresponds to a greater surface area where chemical bonds can be established. Though, rough surfaces can also reduce adhesion in cases where the ceramic does not penetrate into the surface and voids are formed at the interface. This may occur when metals are poorly wetted by the porcelain or when the porcelain is not properly fired. The roughness of the surface is often promoted by alumina-air abrasive or by grinding. Figure 1.16 shows an alumina-blasted surface of a CoCrMo alloy. Sandblasting has the added benefit of removing the excess oxide, thus creating a clean surface that aids the wetting of the ceramic onto the metal.

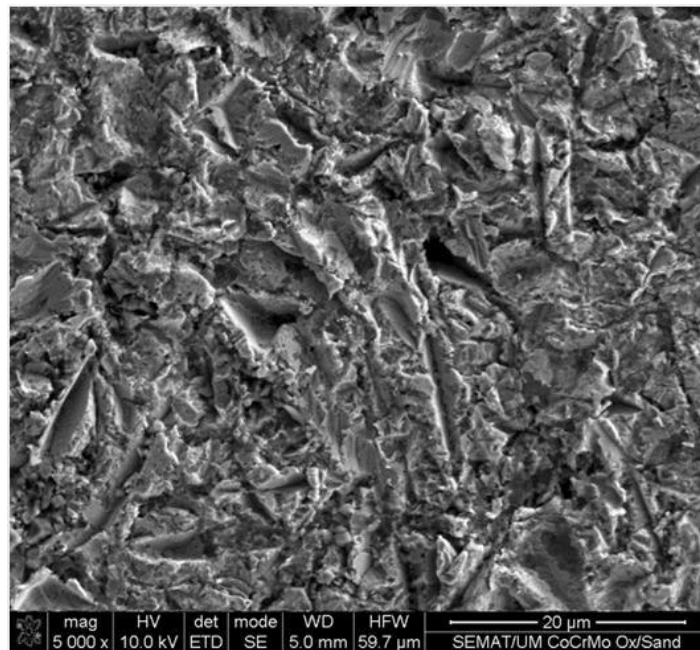


Figure 1.16. Grit blasted surface of a CoCrMo alloys.

Wetting is important to the formation of a good metal-ceramic bonding. The ceramic must wet the metal in order to form a good bond. A good wetting indicates the interaction between surface atoms in the metal with the ceramic. Low contact angles indicate good wetting, i.e. $\theta < 90^\circ$ (Shell and Nielsen, 1962). The contact angle of ceramic on a gold alloy is about 60° (Craig and Powers, 2002).

High residual stresses at the metal-ceramic system can lead to failure. Metal and ceramics have different thermal expansion coefficients and therefore they will contract

at different rates when cooling from porcelain's firing temperature. This will make that, at the interface, residual stresses are formed. Depending on their magnitude, these stresses can cause the crack of the porcelain or its separation from the metal. Therefore, the ceramics and the alloys are formulated to have closely matched thermal expansion coefficients. The porcelain's CTE is usually within the range of $13.0 - 14.0 \times 10^{-6}/^{\circ}\text{C}$, while for metals are between $13.5 - 14.5 \times 10^{-6}/^{\circ}\text{C}$. The difference of 0.5×10^{-6} in thermal expansion between the metal and ceramic (intentionally used) puts ceramic under slightly compression during cooling and turns it less sensitive to applied tensile stresses.

3.3. Bond strength tests

Various tests have been designed and selected by researchers to evaluate metal-ceramic bond strengths. These tests can be classified according to the nature of stresses created such as shear, tension, combination of shear and tension, flexure, and torsion test designs (Hammad and Tallic, 1996). Within these tests, the most commonly used configurations are the flexural tests (Figure 1.17) and the shear tests (Figure 1.18).

The flexural test configuration can assume the form of three- or four- point loading (Lavine and Custer, 1966; Caputo et al., 1977; O'Brien and Craig, 1977). It consists in a flat strip of metal with porcelain fused on the tensile face, which is then tested for transverse strength. The metal-ceramic strip is supported by two knife edges and the specimen is loaded in the center with the ceramic surface down until failure of the ceramic occurs (Figure 1.17). The ISO 9693/2000 recommends the 3-point-bending test and sets a minimum value of 25MPa for bond strength, although some metal-ceramic systems commonly yield values of 40-60MPa (Korkmaz and Asar, 2009). Finite element stress analysis demonstrated higher tensile stresses compared with shear stresses, creating a greater probability of tensile failures. Tensile stresses could

be either perpendicular or parallel to a metal-ceramic interface. The four-point loading test reduces the possibility of tensile failures occurring in three-point loading test and develops relatively greater interfacial shear stresses (Caputo et al., 1977). Four-point loading tests are also easy to fabricate, require no special equipment for testing, and thicknesses of porcelain and metal simulates clinical conditions (Caputo et al. 1977).

Bend tests has been subjected to criticism because maximum tensile stresses are created at the surface of porcelain, thus resulting in predictable tensile failures (Anusavice et al. 1980; McLean, 1980). Moreover, this test is might not be appropriate to evaluate different alloys since the ceramic breakage depends on the Young's modulus of the metal tested. An alloy with an elevated modulus of elasticity would resist bending to a greater extent, creating a higher bond (Hammad et al., 1987). It remains therefore the doubt whether the bond or the Young's modulus of the metal is the characteristic actually tested (Lopes et al., 2009).

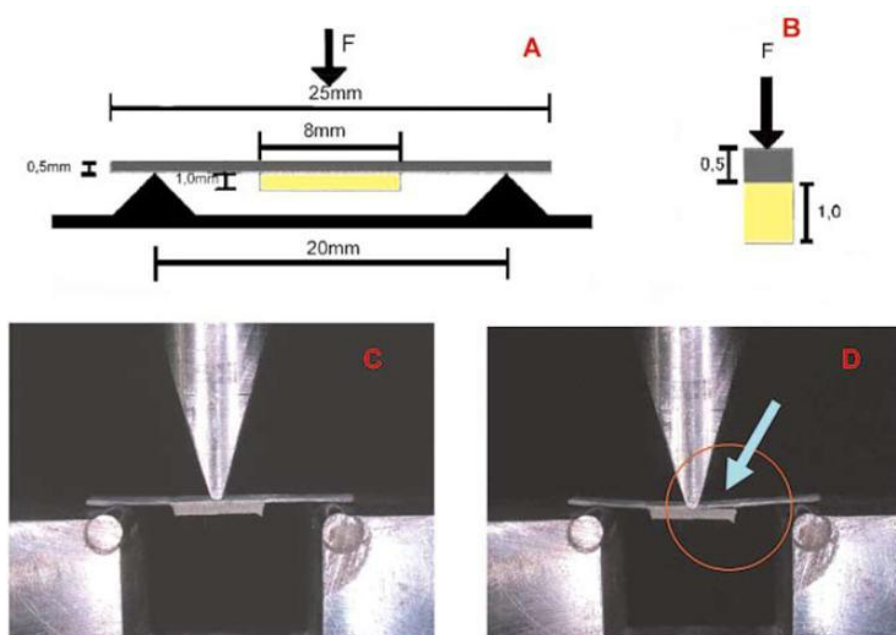


Figure 1.17. Three point bending of a metal–ceramic specimen according to ISO 9693:2000. A) Shape and dimensions of metal-ceramic specimen; B) Cross-section dimensions of specimen; C) Transverse load application; D) Separation of ceramic from metal (Vázquez et al., 2008).

The tests intended to measure shear bond strength include the pull-shear test (Shell and Nielsen, 1962) and the push-shear test (Asgar and Giday, 1978), (each with a cylindrical interface), the planar interface shear test (Civjanet et al., 1974), the conical-interface shear test (Seed and McLean, 1972), and the lap shear test (Wight et al., 1976). In general, the configuration of choice for this test has been the planar interface shear bond test (DeHoff et al., 1995). The planar interface shear bond tests are bond tests with porcelain applied to a flat metal surface. The metal-ceramic bond sites can be either circular or rectangular. The most used specimens' geometry is circular. The samples are mounted in a testing machine for application of the shearing load (P) to separate porcelain from metal substrate (Figure 1.18).

These tests are also uncomplicated and easy to fabricate. The planar interface tests directed stresses mainly at the interface and modulus of elasticity are not as critical as pull through and flexural tests.

The analysis of published literature on metal-ceramic bond strength using different tests reveals great variability in mean bond strength values with large standard deviations for the same metal-ceramic systems. This variability in results may be related with the known variation of specimen preparation and design. Therefore, these tests should only be used as screening tests to compare one system with another using the same test configuration or to determine the effect of changing some variable for the same system (DeHoff et al., 1995).

Knowing what each type of test is actually measuring is extremely helpful in the correct interpretation of the results. Anusavice et al. (1980) calculated stresses in the porcelain at the metal-porcelain interface using a finite element computer code to analyze the stress distributions. It was concluded that tensile stresses were the most probable cause of failure in most of the test geometries and that the presence of stress concentrations reduced the calculated shear bond strength below the true failure stress levels. Van Noort et al. (1989) reached a similar conclusion and found little relationship between the bond strengths based on average stress values and the actual stress states at the interface.

Dental materials should be tested in conditions similar to those found in the oral cavity. Hence, one important variable in testing dental materials is their fatigue behavior, since most clinical fractures occur after many load cycles rather than after a single static load. Therefore, the prediction of service performance should be based on fracture mechanics concepts and cyclic loading parameters that account for the variability and time dependency inherent in the failure of brittle materials (DeHoff et al., 1995). This allows testing the dental materials in more realistic conditions and generates information that is useful to better predict clinical reliability of metal-ceramic dental systems.

According to DeHoff et al. (1995), the use of traditional bond strength data based on static load-to-failure tests should be restricted to comparisons of relative effects of material properties, material microstructure and treatment conditions that may enhance the resistance to fracture. They should not be used to make clinical inferences on the susceptibility to fracture.

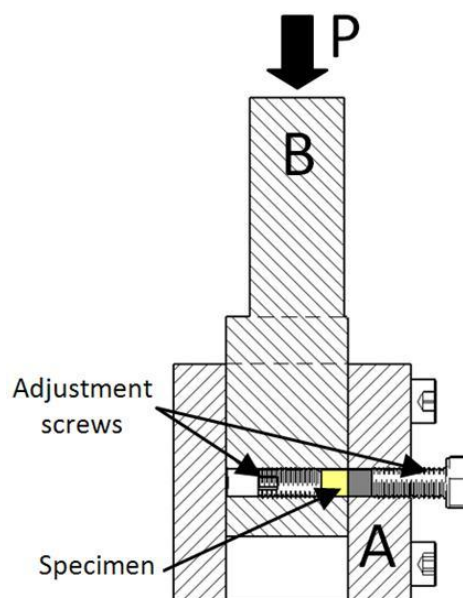


Figure 1.18. Shear bond strength test device (Henriques et al., 2011).

There are three possible locations where a metal-ceramic bond can fail: A) at the metal-metal oxide; B) at the metal oxide-metal-oxide; and C) ceramic-ceramic. (Figure

1.19). The fracture location can provide useful information about the bond strength in some cases. Fractures within the ceramic (C) are usually related with high strength metal-ceramic bonding whereas fractures within metal oxide (B) or metal-metal oxide (A) can reveal poor bonding between the two materials. Base metal alloys commonly fracture through the oxide layer if an excessively thick oxide layer is present. Conversely, metals that are resistant to forming surface oxides, such as gold and platinum, tend to present interfacial fractures.

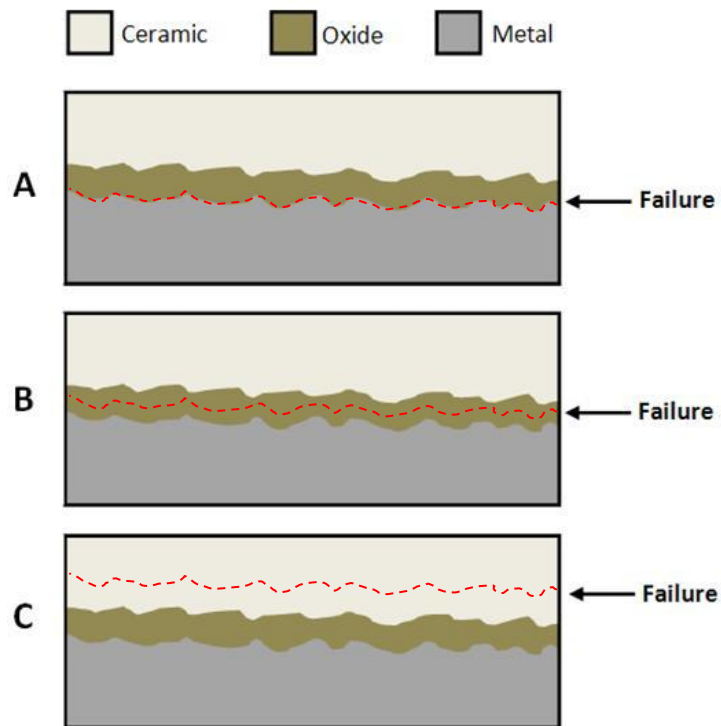


Figure 1.19. Diagram showing three types of bond failure in metal-ceramic systems. **A** – metal-metal oxide; **B** – metal oxide-metal-oxide; and **C** – ceramic-ceramic. **Note:** the dimensions of the layers are not to scale (Craig and Powers, 2002).

3.4. Ceramics for metal-ceramic restorations

There are five requirements that ceramics used for porcelain-fused-to-metal restorations must fulfill (Craig and Powers, 2002):

- 1) They must simulate the appearance of natural teeth;
- 2) They must fuse at relatively low temperatures;
- 3) They must have thermal coefficient expansions compatible with the metal alloys that are used in metal-ceramic restorations;
- 4) They must withstand the oral environment;
- 5) They must do not unduly abrade the opposite teeth.

They are composed by a crystalline phase surrounded by an amorphous and glassy matrix. Table 1.6 presents the main constituents of ceramics used in metal-ceramic dental restorations. The ceramic are mainly constituted by the following oxides SiO_2 , Al_2O_3 , Na_2O and K_2O . They also comprise TiO_2 , ZrO_2 and SnO_2 , which are opacifiers, and various heat stable pigments (e.g. CeO_2).

Table 1.6. Comparison ranges of the main constituents in ceramics for metal-ceramic restorations (Craig and Powers, 2002).

Component	Opaque Powder (%)	Dentin (Body) Powder (%)
SiO_2	50-59	57-62
Al_2O_3	9-15	11-16
Na_2O	5-7	4-9
K_2O	9-11	10-14
TiO_2	0-3	0-0.6
ZnO_2	0-5	0.1-1.5
SnO_2	5-15	0-0.5
Rb_2O	0-0.1	0-0.1
CeO_2	---	0-3
Pigments	---	Trace

The thermal expansion compatibility between the ceramic and the alloy is achieved by the presence of leucite crystals, which is a high-expansion phase ($22-24 \times 10^{-6} \text{ 1/}^\circ\text{C}$). The amount of leucite in the porcelain is carefully controlled to provide a ceramic with a correct coefficient of expansion for a particular alloy (Piché et al., 1994), and can represent 30-40% of the volume of the material. This is, therefore, the reason why the composition of the ceramic for metal-ceramic restorations is different from that of the ceramic used for all-ceramic restorations. The ceramics used in porcelain jacket crowns have CTEs of $\sim 7-8 \times 10^{-6} \text{ 1/}^\circ\text{C}$ whereas for metal-ceramic applications it should be in the range of $14-16 \times 10^{-6} \text{ 1/}^\circ\text{C}$.

Because these ceramics contain leucite crystals, they also belong to the group of leucite-reinforced glass ceramic previously described in Section 3.5 of this chapter. However, they differ in the leucite content, as the leucite content in ceramics for metal-ceramic restorations has the purpose to increase the CTE of the ceramic and not to obtain the highest possible strength. In fact, the ceramics used in metal-ceramic restorations have flexure strengths of the order of 60MPa when compared with up to 120MPa of that of the leucite-reinforced glass-ceramics. Leucite content and crystal size in ceramic is dependent on temperature, and its increase can occur during firing the ceramic onto metal (Mackert and Evans, 1991). Excessive multi firing and slow cooling are thus contraindicated as it can compromise the thermal compatibility between metal and ceramic. The temperature should be raised and lowered as fast as possible without imparting thermal shocks to the ceramic.

The ceramic fusing temperature is a very important issue in metal-ceramic restorations as lower fusing temperatures lessen the potential of distorting of the metal copings. Sodium and potassium oxides in the glassy matrix play an important role in lowering the fusing temperatures to the range of 930°C to 980°C . Low fusing ceramics, which are usually coupled with Ti alloys, have hydroxyl groups and more Na_2O to lower fusing temperatures to as low as 660°C . These are ceramics with an excellent corrosion resistance and show great resistance to the fluids present in the oral cavity. Their high hardness can, however, constitute a problem as they can be abrasive to the opposing

teeth, especially when its surface is rough due to improper processing (surface containing porosity) or by the action of the oral environment.

3.5. Alloys for metal-ceramic restorations

The requirements for alloys used in metal-ceramic dental restorations are different from that of the alloys used in all-metal constructions, especially in what concerns to melting temperatures and mechanical properties. The alloy's melting temperature must be well above the sintering temperature of the ceramic to prevent distortions or localized melting of thin sections of the metal coping. The alloy must also have high elastic modulus and yield strength, especially in the construction of long-span bridges. These structures are sensitive to excessive strains upon occlusion loadings, as ceramic cannot withstand them without failing and, therefore, stiffer alloys perform better in this situation. In addition, stiffer metal substructures can also cope better with the differential contraction stresses that are generated on cooling after ceramic firing.

The first alloys to be used in prosthetic dentistry were the high-gold alloys. However, due to the sharp price increase of this metal, other alloys were introduced in the dental profession, such as gold-palladium, high palladium, palladium-silver, nickel-chromium alloys, cobalt-chromium alloys, commercially pure titanium and titanium alloys. The composition and mechanical properties of some of the alloys used in metal-ceramic dental restorations are shown in Table 1.7, Table 1.8 and Table 1.9.

Table 1.7. Composition ranges and color of noble-alloys for metal-ceramic restorations (wt.%) (Craig and Powers, 2002).

Type	Au	Pt	Pd	Ag	Cu	Other	Total noble metal content	Color
Au-Pt-Pd	84-86	4-10	5-7	0-2	---	Fe, In, Re, Sn 2-5	96-98	Yellow
Au-Pd	45-52	---	38-45	0	---	Ru, Re, In 8.5, Ga 1.5	89-90	White
Au-Pd-Ag	51-52	---	26-31	14-16	---	Ru, Re, In 1.5, Sn 3-7	78-83	White
Pd-Ag	---	---	53-88	30-37	---	Ru, In 1-5, Sn 4-8	49-62	White
Pd-Cu	0-2	---	74-79	---	10-15	In, Ga 9	76-81	White

Table 1.8. Composition Ranges of base metals for metal-ceramic restorations (wt.%) (Craig and Powers, 2002).

Type	Ni	Cr	Co	Ti	Mo	Al	V	Fe	Be	Ga	Mn	Nb	W	B	Ru
Ni-Cr	69-77	13-16	---	---	4-14	0-4	---	0-1	0-2	0-2	0-1	---	---	---	---
Co-Cr	---	15-25	55-58	---	0-4	0-2	---	0-1	---	0-7	---	0-3	0-5	0-1	0-6
Ti	---	---	---	90-100	---	0-6	0-4	0-0.3	---	---	---	---	---	---	---

Table 1.9. Properties of the alloys used in metal-ceramic restorations (Craig and Powers, 2002).

Type	Ultimate Tensile Strength (MPa)	0.2% Yield Strength (MPa)	Elastic Modulus (GPa)	Elongation (%)	Hardness (DPH, kg/mm ²)	Density (g/cm ³)	Casting temperature (°C)
Au-Pt-Pd	4800-500	400-420	81-96	3-10	175-180	17.4-18.6	1150
Au-Pd	700-730	550-575	100-117	8-16	210-230	13.5-13.7	1320-1330
Au-Pd-Ag	650-680	475-525	100-113	8-18	210-230	13.6-13.8	1320-1350
Pd-Ag	550-730	400-525	95-117	10-14	185-235	10.7-11.1	1310-1350
Pd-Cu	690-1300	550-1100	94-97	8-15	350-400	10.6-10.7	1170-1190
Ni-Cr	400-1000	255-730	150-210	8-20	210-380	7.5-7.7	1300-1450
CoCr	520-820	460-640	145-220	6-15	330-465	7.5-7.6	1350-1450
Ti	240-890	170-830	103-114	10-20	125-350	4.4-4.5	1760-1860

High-gold alloys

Pure gold has relatively low melting temperature ($\sim 1064^{\circ}\text{C}$) and, therefore, it is raised by the means of platinum and palladium addition, both of which have a high melting temperature. On the other hand, these alloys don't have copper in their constitution as it reduces the melting temperature and tends to react with the ceramic producing a green discoloration. Due to their high noble content, they are provided of good corrosion resistance. Indium, tin and iron are usually added to form oxides that will be important in bonding to ceramic (Hautaniemi, 1995; Ohno et al., 1992; Anusavice et al., 1977). Rhenium is added as a grain refiner. The hardening mechanism of these alloys results from solid solution hardening and the formation of a FePt_3 precipitate.

These alloys are known to exhibit a very strong and reliable bond to ceramics. Their low melting temperature relatively to others alloys, together with their susceptibility to creep at high temperatures arises as a drawback. They also have low elastic modulus, which implies the design of relatively thicker copings in order to achieve the necessary stiffness (minimum thickness of 0.5 mm required for these alloys).

Gold-palladium alloys

These alloys have less gold but increased palladium content, making them also very corrosion resistant. They contain no platinum or iron and thus, their hardening mechanism is from solid solution rather than precipitation. They contain Indium, rhenium for grain refinement and ruthenium for castability. The color they present is white due to the high palladium content.

These alloys have better mechanical properties (stronger, stiffer, harder and more ductile) and higher melting temperatures than high gold alloys. Their lower density, though, makes casting a more delicate operation as the force with which the molten alloy enters in the mold cavity decreases. But generally, these alloys are considered easy to cast.

High-Palladium alloys

These alloys contain very high palladium content with 10% to 15% Cu, Indium and Gallium, and have become very popular in the last years. They reveal high strength and hardness, moderate stiffness and elongation, and low density. These alloys, however, have low sag resistance and form dark oxides that can be difficult to mask. Their color is white.

Palladium-silver alloys

These alloys are gold free and have high silver content which makes it as the “less noble” within the five nobles alloys. They also contain Indium and Tin for bonding improvement and Ruthenium for castability. The palladium-silver alloys have a high elastic modulus and reduced tendency to sag on porcelain firing. The high presence of silver in the alloy puts some ceramic discoloration problems, which can be lessened by the careful selection of the metal-porcelain combination. They present lower density than the gold palladium alloys.

Nickel-Chromium-Molybdenum alloys

The Ni-Cr-Mo alloys are harder than noble alloys but usually have lower yield strengths. They also have a Young’s Modulus that can be 2.5 times higher than that of the latter alloys. The high rigidity of these alloys allows the reduction of copings thickness from an average of 0.5 mm to 0.3 mm, which lessens the problem of over-contouring. The high rigidity of these alloys is also important in the construction of long-span bridges. Their high melting temperature reduces the sag potential during porcelain firing.

These alloys are more difficult to cast and the higher casting shrinkage can put some problems of fitting. Literature also refers these alloys as having lower metal-ceramic bond strength than other alternative alloys. Their low price arises as an advantage for

these alloys but there are some biocompatible concerns about them, as níquel is a recognized allergen. Beryllium (Be) is also a source of concern in these alloys. It is added to the alloy to decrease the melting temperature and to enhance bond strength to porcelain. However it is a known carcinogen and its release in mechanical grinding and polishing processes can be a potential problem to the technician.

Cobalt-Chromium-Molybdenum alloys

Co-Cr-Mo alloys are very corrosion resistance and presents good biocompatibility. The presence of Cr in the alloys provides tarnish and corrosion resistance. Molybdenum helps lower the coefficient of expansion. The Co-Cr alloys for metal-ceramic restorations have solution hardening strength mechanisms rather than carbide formation typical of the Co-Cr partial denture alloys. They are stronger and harder than noble and Ni-Cr alloys, although they have approximately the same densities and casting temperatures of the latter ones.

Pure Titanium and Titanium alloys

There are several aspects that have made the cp-Ti and Ti-alloys (particularly Ti-6Al-4V) popular alloys for metal-ceramic restorations. They are: high corrosion resistance, excellent biocompatibility, low density and low cost when compared to the metal noble alloys.

The reaction layer formed on the surface of titanium castings due to the reaction of the molten metal with the refractory investment can present a problem for ceramic bonding. Therefore, this layer should be removed to avoid and for that purpose, several operations can be used, such as sandblasting or immersion dissolution, for instance. Casting problems can also be avoided by using alternative techniques like spark-erosion and copy-milling. Another point of extreme importance for porcelain bonding is the fact that Ti has a high chemical reactivity and when taken above 800°C

its forms a thick oxide coating which can jeopardize its bond to porcelain. Due to the lower CTE of Ti alloys ($9.6 \times 10^{-6} \text{ 1/}^\circ\text{C}$) relatively to the other alloys used in metal-ceramic dental restorations, it cannot be used leucite-containing porcelains developed to the latter. Therefore, specially designed porcelains should be used in these cases. The bond strength between Ti-alloys and porcelain is commonly reported as being inferior to that observed for the other alloys (Oyafuso et al., 2008; Zinelis et al. 2010; Vásquez et al., 2009).

3.6. Preparation of metal-ceramic restorations

The production of a metal-ceramic restoration comprises several intermediate steps from the point of metal coping obtaining until the finalized crown. The main steps are: 1) metal coping manufacturing; 2) surface heat treatment; 3) surface sandblasting; 4) porcelain application; 5) porcelain firing.

The metal coping for metal-ceramic restorations can be obtained by the traditional lost-wax casting technique or by alternative processes like spark-erosion, CNC-milling or powder sintering (Anusavice, 2006).

The surface treatment of the copings is required before porcelain bonding in order to achieve the appropriate chemical and mechanical bonding. In that way, these treatments aim to produce a surface roughness and the formation of surface oxides. The surface sandblasting is often performed by fine abrasive particles (25 to $110\mu\text{m}$) that can be alumina particles, silica particles, etc. These treatments often yield substantial increases in metal-ceramic bond strength (Wagner et al., 1993; Shell and Nielsen, 1962; Lombardo et al., 2010). Most of the alloys need a surface heat treatment either in air or in partial vacuum, to produce a surface oxide for bonding enhancement. Some palladium alloys exhibit an internal oxidation that penetrates the metal from the surface, resulting in roughness and increasing the bond strength. In the case of base metal alloys, an excessively thick oxide layer is formed on the surface

after the heat-treatment, and subsequent sandblasting is required to remove the oxides in excess (Lombardo et al., 2010).

Ceramic is applied in several layers to provide the restoration with the teeth-like aspect (Figure 1.20). The first ceramic layer applied has the function to hide the metal and it is called the opaque ceramic. After the opaque ceramic has been applied and fired, the dentin (or body) ceramic is then applied and fired. Dentin has less opaque oxides (e.g. SnO_2 and ZnO_2), pigments and fluorescing oxides than the opaque ceramic. Finally, after the final contour has been established, an essentially transparent glaze layer is applied and fired.

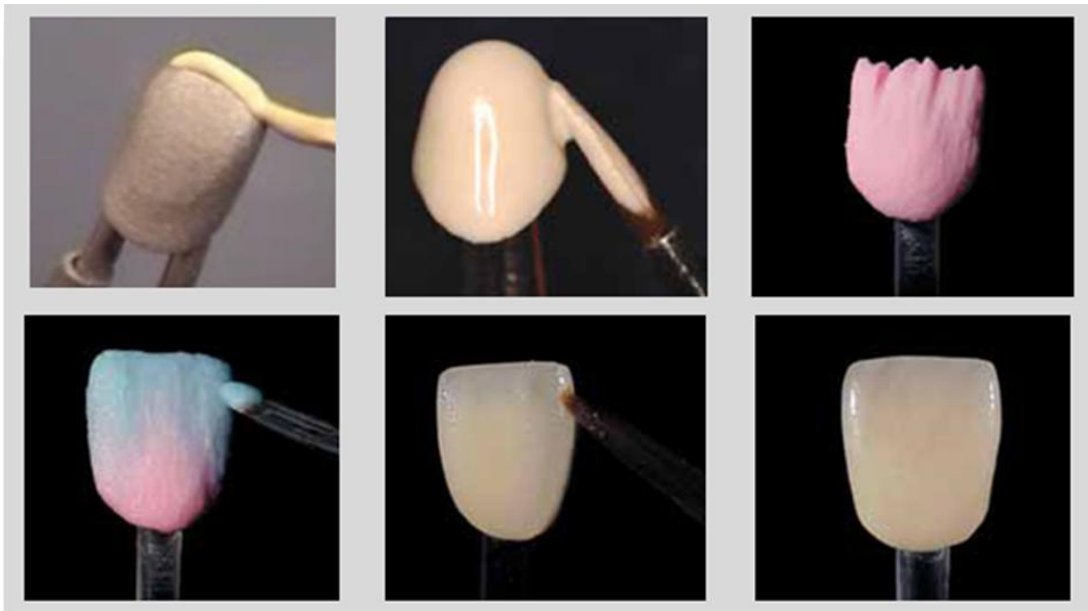


Figure 1.20. Porcelain veneering steps in a metal-ceramic crown obtained by the porcelain-fused-to metal technique (Ceramco3 Instructions Guide, Dentsly).

4. Functionally graded materials for dental applications

A **Functionally graded material (FGM)** may be characterized by the variation in composition and structure gradually over volume, resulting in corresponding changes in properties of the material. It can be said that these are types of materials that are designed to have innovative properties and perform functions that cannot be achieved by conventional homogeneous materials (Kawasaki and Watanable, 1997). A simple approach of an FGM structure can be described as a smooth transition between two dissimilar materials, performed by an intermediate layer whose structure, composition and morphology vary smoothly from one material to the other at a micron level (Figure 1.21) (Kawasaki and Watanable, 1997). The transition profile between the two materials must be designed in order to achieve the desired function. This makes the FGM a new class of materials, diverse from conventional homogeneous composite materials (Figure 1.22).

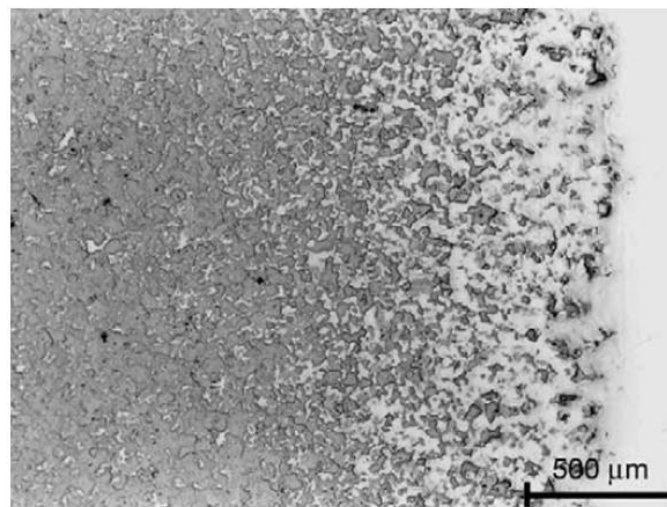


Figure 1.21. Microstructure of a graded W/Cu composite produced by electrochemical gradation (Kieback et al.,2003).

The FGM concept was developed in 1987, in Japan, during the national space plane project, which aimed to develop superheat-resistant materials for the propulsion system and air-frame of the shuttle (Kawasaki and Watanable, 1988). This was a thermal barrier material that should withstand a surface temperature of 1726°C and a

temperature gradient of 727°C across a section of <10mm. Since then, FGMs has received increasing interest in the electrical, chemical, optical, nuclear and biomedical areas (Sánchez-Herencia et al., 2000; Seifried et al., 2001; Wang et al., 2000; Sengupta et al., 2011; Pompe et al., 2003).

The use of gradients in surface composition of materials has long been proved to improve the mechanical performance of the material (Suresh and Mortensen, 1998). Going back in time, the early examples of FGMs in synthetic materials can be traced back to the blades of Japanese steel swords, which used a graded transition from a softer and tougher core to a hardened edge (Smith, 1960). Carburizing and nitriding are also two surface treatments that are commonly given to steel surfaces to impart hardness, which in the case of transmission gear teeth also improves the fatigue and wear resistance.

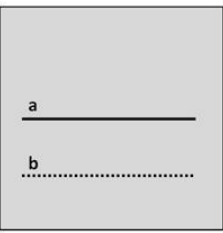
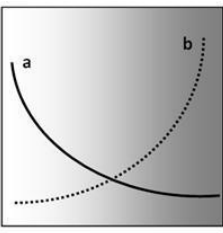
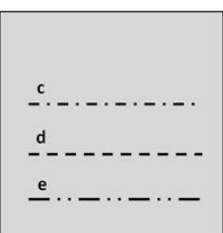
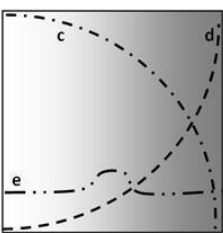
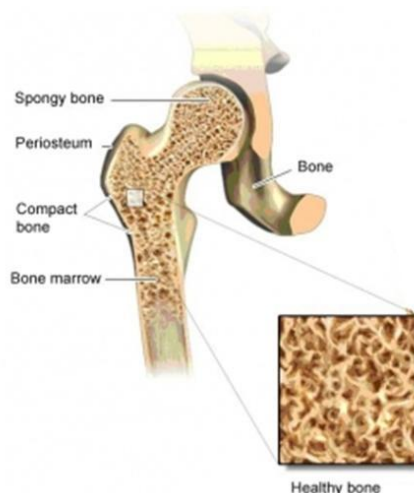
	HOMOGENEOUS MATERIAL	FUNCTIONALLY GRADED MATERIAL
FUNCTION/PROPERTY a) Heat resistance b) Fracture toughness		
STRUCTURE/TEXTURE c) Ceramics d) Metal e) Pore, fiber		

Figure 1.22. Characteristics of functionally graded material (Kawasaki and Watanable, 1995).

Graded transitions in composition, either continuous or in fine, discrete steps, across an interface between two dissimilar materials (such as a metal and a ceramic), can be used to redistribute thermal and mechanical stresses (Hirano and Wakashima, 1995; Koizumi, 1992), thereby limiting the stresses at critical locations and thus suppressing

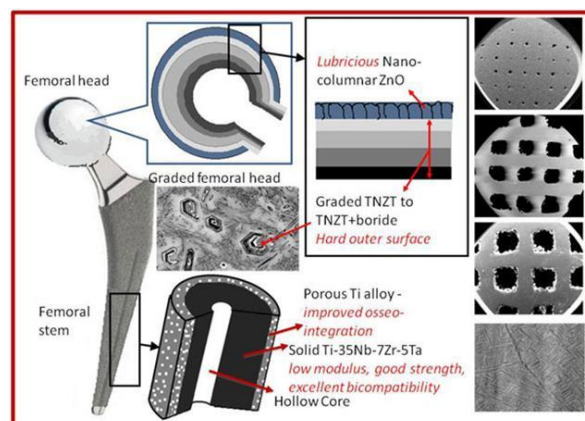
the onset of permanent (plastic) deformation, damage, or cracking (Williamson et al, 1993; Giannakopoulos, 1995). Moreover, smooth transitions in composition across an interface also improve interfacial bonding between dissimilar materials (Suresh and Mortensen, 1998).

The development of FGM concept had its origin in the sophisticated properties which arise from materials in nature, such as shells, bamboo (Tan et al., 2011), teeth (He and Swain, 2009) and bones (Pompe et al, 2003). These outstanding properties are traced to inhomogeneity of chemical composition, structure and morphology in the components of these materials (Kawasaki and Watanabe, 1995). For instance, the design of a bone with a change from dense, stiff external structure (the cortical bone) to a porous internal one (the cancelous bone) demonstrates that functional gradation has been utilized by biological adaptation (Pompe et al, 2003) (Figure 1.22). This bone's structure reflects a biologic evolution and optimizes the material's response to external loading. Thus, optimized structure for an artificial implant should show similar gradation. In that way, there are several studies being conducted with the aim of replicate the same graded structures as observed in real bones (Figure 1.23).



<http://www.ncbi.nlm.nih.gov/pubmedhealth/PMH0004996>

Figure 1.23. Femoral bone structure (German Institute for Quality and Efficiency in Health Care, 2012).



<http://research.unt.edu/ises/research%20prof>

Figure 1.24. Functionally Graded Integrated Implant being developed at AMMG, University of North Texas, USA.

The same trend has been observed in the development of functionally graded dental implants with the introduction of surface coatings, porosity gradients and composite materials made essentially of metal and ceramics (e.g. hydroxyapatite), which aimed to improve the implant performance in terms of biocompatibility and stress distribution (Figure 1.24) (Sadollah and Bahreininejad, 2011; Lin et al., 2009).



Figure 1.25. Schematic view of an FGM dental implant with graded materials composition (Sadollah and Bahreininejad, 2011).

Natural teeth are composed by layered structures, dentin and enamel, that are bonded by a functionally graded dentin-enamel-junction (DEJ) layer that is about 10-100 micrometers thick (Francis et al., 1995; Lin and Douglas, 1993; Lin and Douglas, 1994). The DEJ acts as a bridge between the hard brittle enamel ($E \sim 70\text{GPa}$) and the softer durable dentin layer ($E \sim 20\text{GPa}$), allowing a smooth Young modulus transition between the two structures (Figure 1.25) (Marshall et al., 2001).

In metal-ceramic restorations, the Young's modulus of the veneering porcelain is 60-80 GPa (Rizcalla and Jones, 2003) while that of the metal core is in the range of 80-230GPa. In addition, the coefficients of thermal expansion (CTE) of the two materials are also different, with that of the metal being usually higher than that of porcelain. The mismatch in Young's moduli and CTE results in high stresses that can give rise to

cracks arising at the metal-ceramic interface and consequently to the failure of the system.

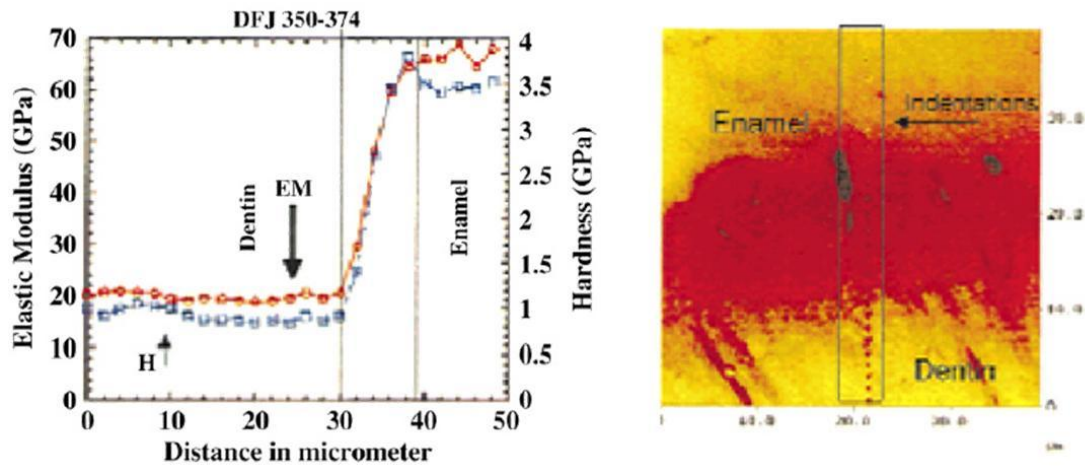


Figure 1.26. Elastic modulus distribution in dentin-enamel-junction (DEJ)
(Marshall et al., 2001).

Learning from nature, a bio-inspired functionally graded architecture of the metal-ceramic interface is proposed in this thesis (Chapters 7 and 8) in order to improve the clinical performance of dental restorations (Figure 1.26). It is shown in this work that a graded transition between metal and ceramic provides a huge increase in bond strength of the two materials even after fatigue conditions simulating the oral environment.

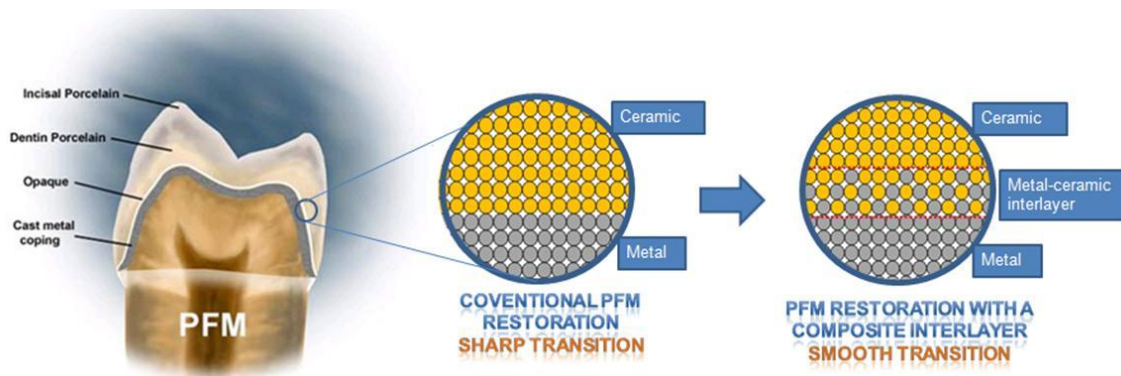


Figure 1.27. Schematic of the conventional sharp restoration and the new graded approach.

5. Motivation of this study

Metal-ceramic restorations are known to be very strong, aesthetic and reliable, owing the best clinical performance within the available alternatives used in fixed partial denture applications. Therefore, they had been the primary choice of dentists since their creation, back in 1950s. The success of PFM restorations strongly depends on the success of a strong bond between porcelain and the metal substructure. The quality of such bond is highly influenced by the correct selection of materials and the right handling of the manufacturing process of the prosthesis. In fact, despite all the efforts made to ensure the best metal to porcelain bond possible, failures still occur. Clinical studies indicated that the prevalence of ceramic fractures within PFM restoration ranged between 10 and 20% over 10 years of use (Kerschbaum et al., 1997; Coornaert et al., 1984) and the failure rate due to fracture and exfoliation of porcelain is 59.1% of the whole clinical failure (Özcan, 2003; Liu et al., 2008). Hence, one of the most likely modes of failure with this system is the separation of the ceramic from the metal due to an interfacial breakdown of the metal-ceramic bond. Therefore, this subject represents a problem which is still getting the researchers' attention in a way that there are a continuous seeking for processing methods that minimize or avoid metal-ceramic failures.

Based on the previously stated, this work intended to assess on several levels the influence of some processing parameters, like surface roughness, preoxidation heat treatment, metal substrate processing type and hot pressing, on the metal-ceramic bond strength for dental restorations.

It was also proposed a new bio-inspired functionally graded approach for the metal-ceramic bond strength improvement. Besides all the processing characterization and experimental validation of this new solution, is also important to assess it under physiologic-like conditions and compare its performance with the conventional metal-ceramic restorations with sharp transition. A comprehensive description of the strengthening mechanisms provided by this new solution is also required.

6. References

Anusavice KJ. Phillips' science of dental materials. 11th ed. Philadelphia:W.B. Saunders, 2006.

Anusavice KJ, Horner JA, Fairhurst CW. Adherence Controlling Elements in Ceramic-Metal Systems. I. Precious Alloys. J Dent Res, 1977; 56:1045.

Anusavice KJ, De Hoff PH, Fairhurst CW. Comparative evaluation of ceramic-metal bond tests using finite element stress analysis. J Dent Res, 1980; 59: 608-13.

Barreiro MM, Rlesgo O, Vicente EE. Phase identification in dental porcelains for ceramo-metallic restorations. Dent Mater, 1989; 5:51-57.

Beuer F, Schweiger J, Edelhoff D. Digital dentistry: an overview of recent developments for CAD/CAM generated restorations. Brit Dent J, 2008; 204(9) : 505-511

Bollen CML, Lambrechts P, Quirynen M. Comparison of surface roughness of oral hard materials to the threshold surface roughness for bacterial plaque retention: A review of the literature. Dent Mater, 1997; 13:258-269

Boyer RR. An overview on the use of titanium in the aerospace industry. Mater Sci Eng A, 1996; 213:103-114.

Caputo AA, Dunn B, Reisbick MH. A flexure method for evaluation of metal-ceramic bond strengths. J Dent Res 1977; 56:1501-1506.

Cesar PF, Yoshimura HN, Miranda Junior WG, Okada CY. Correlation between fracture toughness and leucite content in dental porcelains. J Dent , 2005; 33: 721–729.

Cheung KC, Darvell BW. Sintering of dental porcelain: effect of time and temperature on appearance and porosity. Dent Mater, 2002; 18: 163-173.

Craig RG, Powers JM. Restorative dental materials. 11th ed. Mosby. 2002, pp.480-492.

Coornaert J, Adriaens P, De Boever: Long-term clinical study of porcelain fused to gold restorations. J Prosthet Dent, 1984; 51(3):338-342.

DeHoff PH, Anusavice AJ, Wang Z. Three-dimensional finite element analysis of the shear bond test. Dent Mater, 1995; 11: 126-131.

- Dewidar MM, Yoon H, Lim JK. Mechanical Properties of Metals for Biomedical Applications Using Powder Metallurgy Process: A Review. *Met & Mater Inter*, 2006; 12(3): 193-206.
- Disegi JA, Kennedy RL, Pilliar R. Cobalt-base alloys for biomedical applications. *ASTM*, 1999, pp. 136-137
- Giannakopoulos AE, Suresh S, Finot M, Olsson M. Elastoplastic analysis of thermal cycling layered materials with compositional gradients. *Acta Metal Mater*, 1995; 43:1335-1354.
- Gupta KP. The Co-Cr-Mo (Cobalt-Chromium-Molybdenum) System. *J Phase Equilib Diffus*, 2005; 26: 87–95.
- Hammad IA, Goodkind RJ, Gerbrich WW. A shear test for the bond strength of ceramometals. *J Prostheh Dent* 1987; 58: 431-7.
- Hautaniemi JA. The effect of indium on porcelain bonding between porcelain and Au-Pd-In alloy. *J Mater Sci Mater Med*, 1995; 6:46-50.
- He LH, Swain MV. Enamel—A functionally graded natural coating. *J Dent*, 2009; 37: 596-603.
- Hengchang X, Wenyi L, Tong W. Measurement of thermal expansion coefficient of human teeth. *Aust Dent J*, 1989; 34(6): 530-535.
- Hirano T, Wakashima K. Mathematical modeling and design. *MRS Bull*, 1995; 20 (1): 40.
- Hiromoto S, Onodera E, Chiba A, Asami K, Hanawa T. Microstructure and corrosion behaviour in biological environments of the new forged low-Ni Co – Cr – Mo alloys. *Biomaterials*, 2005; 26:4912-4923.
- Kawasaki A, Watanabe R. In *Sintering '87Tokyo*, Vol. 2, ed. S. Somiya. M. Shimada, M. Yoshimura & R. Watanabe. Elsevier, London, 1988, pp. 1197-1202.
- Kerschbaum T, Seth M, Teeuwen U. Verweildauer von Kunststoff-und Metal-Keramisch verblendeten Kronen und Brucken. *Deutsche Zahnärztliche Zeitschriften*, 1997; 52: 404.

- Kelly JR, Nishimura I, Campbell SD. Ceramics in dentistry: Historical roots and current perspectives. *J Prosthet Dent*, 1996; 75: 18-32.
- Knosp H, Holliday RJ, Corti CW. Gold in dentistry: Alloys, Uses and Performance. *Gold Bulletin*, 2003; 36(3): 93-102.
- Koizumi M. Recent progress of Functionally Gradient Materials in Japan. *Ceram Eng Sci. Proc*, 1992; 13: 333-347.
- Korkmaz T , Asar V. Comparative evaluation of bond strength of various metal – ceramic restorations. *Mater and Design*, 2009; 30:445 – 451.
- Lavine MH, Custer RF. Variables affecting the strength of bond between porcelain and gold. *J Dent Res* 1966; 45: 32-36.
- Lee, S, Nomura, S, Chiba A. Significant Improvement in Mechanical Properties of Biomedical Co-Cr-Mo Alloys with Combination of N Addition and Cr-Enrichment . *Mater Trans*, 2008; 49(2): 260-264.
- Liu J, Qiu XM, Zhu S, Sun DQ. Microstructures and mechanical properties of interface between porcelain and Ni-Cr alloy. *Mat Sci Eng A*, 2008; 497: 421-425.
- Lin D, Li Q, Li W, Zhou S, Swain MV. Design optimization of functionally graded dental implant for bone remodeling. *Comp Part B*, 2009; 40:668-675.
- Lombardo GHL, Nishioka RS, Souza ROA, Michida SMA, Kojima AN, Mesquita AMM, Buso L. Influence of Surface Treatment on the Shear Bond Strength of Ceramics Fused to Cobalt–Chromium. *J Prosthodont*, 2010; 19: 103-111.
- Lopes SC, Pagnano VO, Rollo JM, Leal MB, Bezzon OL. Correlation between metal-ceramic bond strength and coefficient of linear thermal expansion difference. *J Appl Oral Sci*. 2009; 17(2):122-8.
- Marshall Jr GW, Balooch M, Gallagher RR, Gansky SA, Marshall SJ. Mechanical properties of the dentinoenamel junction: AFM studies of nanohardness, elastic modulus, and fracture. *J Biomed Mater Res A*, 2001; 54: 87-95.

Mackert JR, Evans AL. Effect of Cooling Rate on Leucite Volume Fraction in Dental Porcelains. *J Dent Res*, 1991; 70(2):137-139.

Mackert JR, Rindle RD, Parry EE, Evans AL, Fairhurst CW. The Relationship Between Oxide Adherence and Porcelain-Metal Bonding. *J Dent Res* 67(2):474-478.

Mackert JR, Parry EE, Hashinger DT, Fairhurst CW. Measurement of oxide adherence to PFM alloys. *J Dent Res*, 1984; 63(11):1335-1340.

Matković T, Matković P, Malina J. Effects of Ni and Mo on the microstructure and some other properties of Co–Cr dental alloys. *J Alloys Comp*, 2004; 366:293–297.

McLean JW. The science and art of dental ceramics. vol 1. Chicago: Quintessence Pub1 Co, Inc; 1980: 72-78.

Melfi RC. Oral embryology and microscopic anatomy, a textbook for students in dental hygiene. 10th ed. Philadelphia PA: Lippincott Williams & Wilkins, 2000.

Mineta S, Namba S, Yoneda T, Ueda K, Narushima T. Carbide Formation and Dissolution in Biomedical Co-Cr-Mo Alloys with Different Carbon Contents during Solution Treatment. *Met Mater Trans A*, 2010; 41A: 2010-2129.

McLaren. Modern Metal-Ceramic Restorations. Inside dentistry, 2006.

Niinomi M. Mechanical properties of biomedical titanium alloys. *Mater Sci Eng A*, 1998; 243:231-236 Ohno H, Araki Y, Endo K. ESCA Study on Dental Alloy Surfaces Modified by Ga-Sn Alloy. *J Dent Res*, 1992; 71: 1332.

O'Brien WJ, Craig RG, ed. Dental porcelains. Dental material review. Ann Arbor: Univ. of Michigan Press; 1977:123-35.

Oyafuso DK, Özcan M, Bottino MA, Itinoche MK. Influence of thermal and mechanical cycling on the flexural strength of ceramics with titanium or gold alloy frameworks. *Dent Mater*, 2008; 24: 351–356

Özcan M. Fracture reasons in ceramic-fused-to metal restorations. *J of Oral Rehab*, 2003; 30: 265-269.

Piché PW, O'Brien WJ, Groh CL, Boenke KM. Leucite content of selected dental porcelains. *J Biomed Mater Res*, 1994; 28: 603-609.

Pompe W, Worch H, Epple M, Friess W, Gelinsky M, Greil P. Functionally graded materials for biomedical applications. *Mater Sci Eng A*, 2003; 362:40–60.

Qualtrough AJE, Piddock V. Ceramics update. *J Dent*, 1997; 25(2):91-95

Quinn B, Sundar V, Lloyd IK. Influence of microstructure and chemistry on the fracture toughness of dental ceramics. *Dent Mater*, 2003; 19: 603–611
Roach M. Base Metal Alloys Used for Dental Restorations and Implants. *Dent Clin N Am*, 2007; 51: 603-627.

Rizkalla AS, Jones DW. Indentation fracture toughness and dynamic elastic moduli for commercial feldspathic dental porcelain materials. *Dent Mat*, 2004; 20: 198-206.

Rokni SR, Baradaran H. The effect of oxide layer thickness on the bond strength of porcelain to Ni-Cr alloy. *J Mashhad Dental School*, 2007; 31:17-21.

Sadollah A, Bahreininejad A. Optimum gradient material for a functionally graded dental implant using metaheuristic algorithms. *J Mech Behav Biomed Mater*, 2011; 4: 1384-1395.

Sánchez-Herencia AJ, Moreno R, Jurado JR. Electrical transport properties in zirconia/alumina functionally graded materials. *J Europ Cer Soc*, 2000; 20:1611-1620.

Saji VS, Choe HC. Electrochemical behavior of Co-Cr and Ni-Cr dental cast alloys. *Trans Nonferrous Met Soc China*, 2009; 19: 785-790.

Scheid C, Weiss G. *Woelfel's Dental Anatomy*, 8th ed. Lippincott Williams & Wilkins, 2012.

Seifried S, Winterer M, Hahn H. Nanocrystalline gradient films through chemical vapor synthesis. *Scripta Mater*, 2001; 44: 2165–2168.

Sengupta P, Rogalla D, Beckerd HW, Deya GK, Chakraborty S. Development of graded Ni – YSZ composite coating on Alloy 690 by Pulsed Laser Deposition technique to reduce hazardous metallic nuclear waste inventory. *J Hazard Mater*, 2011; 192:208-221.

- Shi L, Nortwood DO, Cao Z. Alloy design and microstructure of a biomedical Co-Cr alloy. *J Mater Sci*, 1993; 28: 1312-1316.
- Shell JS, Nielsen JP. Study of the Bond between Gold Alloys and Porcelain. *J Dent Res*, 1962; 41: 1424-1437.
- Smith CS. *A History of Metallography*. MIT Press, Cambridge, MA, 1960, pp. 3-5.
- Suresh S, Mortensen A. *Fundamentals of Functionally Graded Materials*. Institute of Materials, London, 1998, pp. 3-8.
- Tan T, Rahbar N, Allameh SM, Kwofie S, Dissmore D, Ghavami K, Soboyejo WO. Mechanical properties of functionally graded hierarchical bamboo structures. *Acta Biomater*, 2011; doi:10.1016/j.actbio.2011.06.008.
- Ucar Y, Akova T, Akyil MS, Brantley WA. Internal fit evaluation of crowns prepared using a new dental crown fabrication technique: Laser-sintered Co-Cr crowns. *J Prosthet Dent*, 2009; 102:253-259.
- Van Noort R. *Introduction to Dental Materials*. 3rd ed. Elsevier, 2007.
- Vásquez VZC, Özcan M, Kimpara ET. Evaluation of interface characterization and adhesion of glass ceramics to commercially pure titanium and gold alloys after thermal- and mechanical-loading. *Dent Mater*, 2009; 25: 221–31.
- Wagner WC, Asgar K, Bigelow WC, Flinn RA. Effect of interfacial variables on metal-porcelain bonding. *J Biomater Res*, 1993; 27:531-537.
- Wang Z, Cao J, Michette AG. Depth-graded multilayer X-ray optics with broad angular response. *Optics Communications*, 2000; 177: 25–32.
- Williamson RL, Rabin BH, Drake JT. Finite element analysis of thermal residual stresses at graded ceramic/metal interfaces, part I: model description and geometrical effects. *J Appl Phys*, 1993; 74: 1310-1320.
- Vázquez V, Özcan M, Nishioka R, Souza R, Mesquita A, Pavanelli C. Mechanical and Thermal Cycling Effects on the Flexural Strength of Glass Ceramics Fused to Titanium. *Dent Mater J*, 2008; 27(1): 7-15.

Chapter 2

Shear bond strength of a hot pressed Au-Pd-Pt alloy-porcelain dental composite

Published in Journal of Mechanical Behavior of Biomedical Materials 4(8) (2011) 1718-1726

B. Henriques, D. Soares, F.S. Silva

*Centre for Mechanical and Materials Technologies (CT2M) and Department of Mechanical Engineering,
University of Minho, Azurém, 4800-058 Guimarães, Portugal*

Abstract

Objectives: The purpose of this study was to evaluate the effect of hot pressing on the shear bond strength of a Au-Pt-Pd alloy-porcelain composite.

Methods: Several metal-porcelain composites specimens were produced by two different routes: conventional porcelain fused to metal (PFM) and hot pressing. In the latter case, porcelain was hot pressed onto a polished surface (PPPS) as well as a roughened one (PPRS). Bond strength of all metal-porcelain composites were assessed by the means of a shear test performed in a universal test machine (crosshead speed:

0.5mm/min) until fracture. Interfaces of fractured specimens as well as undestroyed interface specimens were examined with optical microscope, stereomicroscope, Scanning Electron Microscope (SEM) and Energy Dispersive X-Ray Spectroscopy (EDS). The data were analyzed using one-way ANOVA followed by Tuckey's test ($p < 0.05$).

Results: Shear bond strength of conventional PFM specimens were in line with the upper range of literature data (83 ± 14 MPa). Hot pressing proved to significantly increase bond strength between metal and porcelain ($p < 0.05$). For both polished and roughened surface the shear bond strength values for hot pressed specimens were 120 ± 16 MPa and 129 ± 5 MPa, respectively, which represents an improvement of more than 50% relatively to a conventional PFM. Roughened surface didn't have a significant effect on bond strength of hot pressed specimens ($p > 0.05$).

Significance: This study shows that it is possible to significantly improve metal-porcelain bond strength by applying an overpressure during porcelain firing.

1. Introduction

Metal-ceramic restorations are still the most reliable method in dental prosthetics, especially when a good adhesion of the ceramic to the metal substrate is achieved (Anusavice, 2006). The rising use of all ceramic restorations is not accompanied of the desired life span and premature clinical failure is often reported (Kelly, 1997; Donovan and Swift, 2009). Within the materials for all-ceramic restorations, zirconia is one of the most promising restorative materials because of its favorable mechanical and aesthetic properties. Several studies confirmed its suitability in particular for single crowns and short-span partial dentures (pre molars and anterior teeth), being registered higher failure rates on molars. The major problem associated with zirconia-cored restorations is the high incidence of ceramic veneer chipping from zirconia core (Donovan and Swift, 2009 and Zarone et al, 2011). A study about zirconia-porcelain bond strength performed by Guess et al (2008) showed significantly higher values for

non- and thermocycled gold alloy-porcelain specimens than in the case of all-ceramic ones (zirconia).

Many dental alloys are available for metal-ceramic dental restorations. Noble alloys, such as gold alloys of high and low gold content, palladium alloys, platinum alloys, etc. The common base metal alloys are Ni-Cr and Co-Cr which are used when economical concerns come into play. Their higher hardness and Young's module is also a criterion of selection. Despite its cost, a well-approved high gold alloy is still the best option in terms of longevity, functionality, aesthetics, and biocompatibility, together with ease of manufacture (Knosp et al., 2003). Therefore, according to Knosp et al. (2003) "it is no co-incidence that in all testing and development of competing materials, gold is always defined as the standard material to be judge against". For this study a high gold content dental alloy (Keramit 750, Nobilmetal, Villafranca d'Asti ,Italy) was used.

Metal-ceramic dental restorations strongly depend on the success of the bond between porcelain and the metal substrate (Shell and Nielsen, 1962; Drummond et al., 1984). This is achieved by attaining to the characteristics of compatibility of the materials involved, e.g. choose the metals and ceramics with the proper Coefficients of Thermal Expansion (CTEs). Despite the greater longevity of PFM restorations when compared to all-ceramic restorations, clinical failures can occur and the failure rate due to fracture and exfoliation of porcelain is 59.1% of the whole clinical failure (Liu et al., 2008; Özcan, 2003). So, there is still some work to do in the increasing of metal-porcelain bond strength. Hot pressing can be the answer to this challenge, since it promotes a full contact between metal and porcelain, enhancing the diffusion of the elements in the metal-porcelain interaction zone and contributing to a superior chemical bonding by the absence of residual porosity and cracks.

The purpose of this study was to evaluate the use of hot pressing on the shear bond strength of a gold dental alloy-porcelain composite when compared to a conventional Porcelain Fused to Metal (PFM) one. The null hypothesis was that hot pressing increase metal-porcelain bond strength.

2. Materials and Methods

For this work a dental gold alloy (KERAMIT 750, Nobilmetal, Villafranca d’Asti, Italy) and a dental opaque porcelain (Ceramco3, Dentsply, York, USA) (batch number:08004925) were used. The gold alloy was used both in powder (170 mesh) and cast form. The chemical compositions and mechanical properties of the gold alloy and opaque porcelain are presented in the Tables 1, 2 and 3, respectively.

Table 2.1. Gold alloy chemical composition (wt.%).

Au	Pt	Pd	Ag	In	Others
75	4.3	8.5	9	1.7	Fe, Ir

Table 2.2. Ceramic chemical composition (wt.%).

SiO ₂	Al ₂ O ₃	K ₂ O	SnO ₂	ZrO ₂	CaO	P ₂ O ₅	Na ₂ O	Others
41.3	14.5	14.0	11.9	5.8	4.1	4.1	3.0	MgO, SO ₃ , ZnO, Cr ₂ O ₃ , Fe ₂ O ₃ , CuO, Rb ₂ O

Table 2.3. Base materials properties.

	Density g/cm ³	Melting Range [°C]	CTE [25- 600°C]	E [GPa]	Hardness
Keramit750	16.2 [*]	1160-1230 [*]	14.8 [*]	100 [*]	HV200 (self-hardened) [*]
Ceramco3 Opaque	2.8 ^{**}		13.2 ^{***}	83 ^{**}	

*Keramit 750 supplier webpage; ** Rizkalla and Jones, 2004; *** Souza et al, 2010

Several metal-ceramic composites specimens were produced by two routes: hot pressing and conventional furnace firing. The specimens conventionally fired in the furnace (Porcelain Fused to Metal – PFM) (n=5) were used as standards to be compared with those processed by hot pressing. Hot pressed specimens were divided in two groups: in the first group porcelain was hot pressed onto a polished surface

(Porcelain Pressed to Polished Surface – PPPS) (n=4) and in the second group porcelain was hot pressed onto a roughened surface (Porcelain Pressed to Roughened Surface – PPRS) (n=4).

Metal substrates with the dimensions of $\varnothing 4 \times 4$ mm were obtained from a casted rod with approximately 30 mm in length and the same diameter. Substrates were then polished with 1200-grit SiC sand-paper, ultrasonically cleaned in an alcohol bath for 10 min and rinsed in distilled water for another 10 min to remove contaminants. After, they were dried with adsorbent paper towels. No initial oxidation step was performed on the substrates prior to porcelain application.

To produce porcelain fused to metal (PFM) specimens an acrylic template was used to ensure that the porcelain height was the same for all specimens (4mm). Porcelain was applied to metal substrates in the form of a creamy paste resulting from the addition of distilled water to porcelain powders in the ratio of 1:2 (water:porcelain). The excess of water was removed using an adsorbent paper and after the porcelain condensing, metal-porcelain sets were carefully moved to a furnace (Termolab, Braga, Portugal) and sintered under vacuum (1mBar) at 970°C and at a heat rate of approx. 10°C/min. Power was shut down after reaching 970°C and the vacuum was removed at the same time. Specimens cooled down inside the furnace.

To obtain specimens of PPPS (porcelain pressed to a polished surface), porcelain powders and metal substrate were hot pressed in a graphite die under vacuum (5x10⁻¹mbar) at a temperature of 970°C and a constant pressure of 20 MPa. Graphite die cavity was veneered by a zirconium paint to avoid carbon diffusion to specimens. The heat rate was 60°C/min and after reaching 970°C, the power of the induction heating furnace was shut down, letting the die to cool down naturally (Figure 2.1 a-c).

The surface roughness in PPRS (porcelain pressed to a roughened surface) specimens was produced by the means of metal powders that were placed in the metal-porcelain interface. This method intended to produce a relatively high level of well distributed roughness. Other options to produce surface roughness like alumina sandblasting or

sandpaper grinding were also considered. Nevertheless, metal powders (same alloy as metal substrates) were selected to better fulfill the initial requirements. The hot pressing procedure was the same as the one used for PPS specimens (Figure 2.1 a-c), but with the presence of metal powders in metal-porcelain interface.

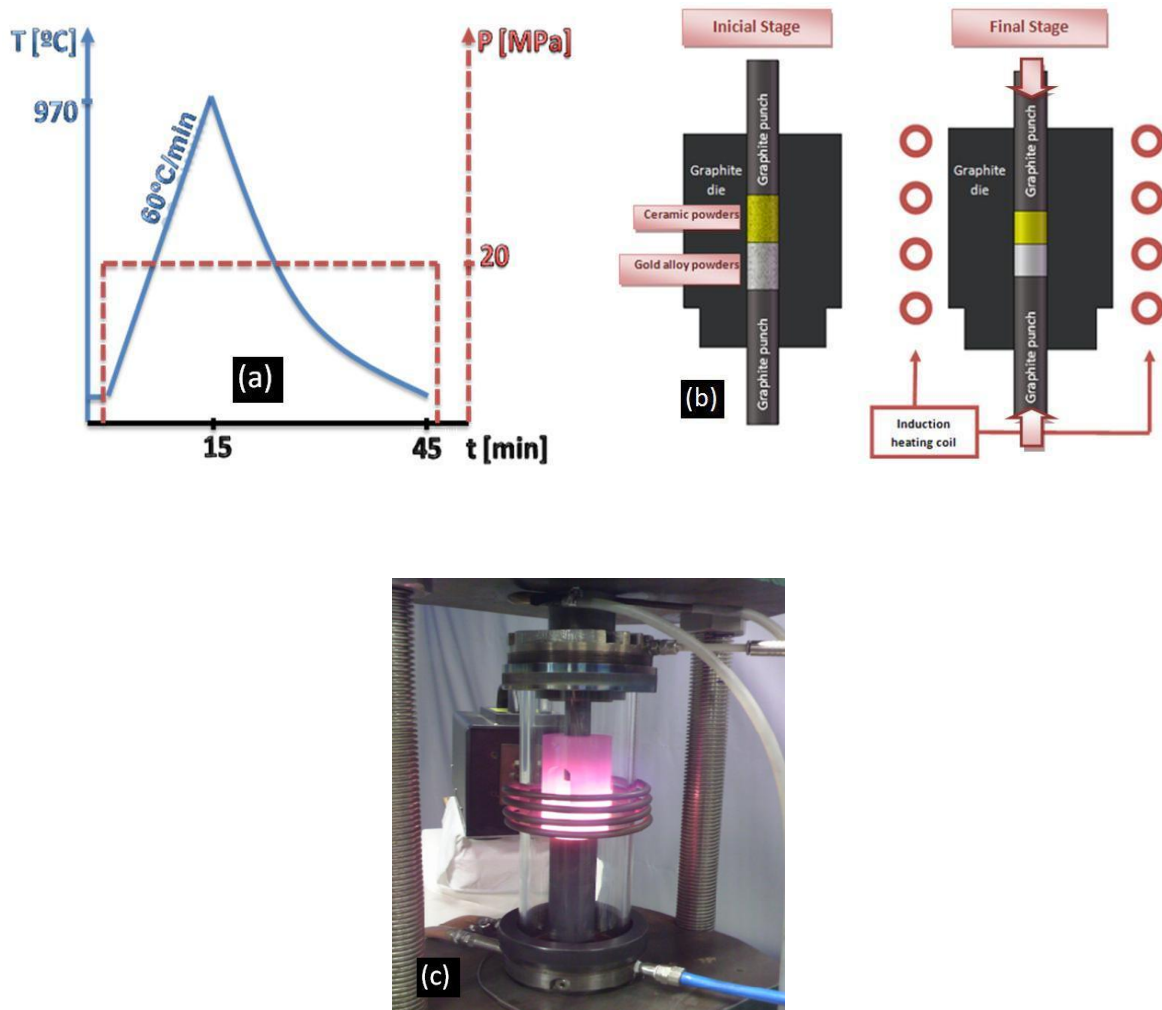


Figure 2.1. Hot pressing apparatus. (a) Temperature and pressure conditions during the hot pressing cycle. (b) Hot pressing schematic. (c) Processing a specimen in the vacuum chamber.

2.1. Shear tests

The shear bond strength tests were carried out at room temperature and performed in a universal testing machine (Instron 8874, MA, USA), with a load cell having 25 kN

capacity and under a crosshead speed of 0.5mm/s. Tests were performed in a custom-made stainless steel apparatus consisting in two sliding parts A and B (Figure 2.2 a) and b)), each one having a hole perfectly aligned to the other. After alignment of the holes, the specimens were placed in the jig letting the metal-porcelain interface aligned with the sliding plane of parts A and B. Then, a compressive load was applied in part B until fracture occurred. The shear bond strength (MPa) was calculated by dividing the highest recorded fracture force (N) for the area of adherent porcelain (mm^2).

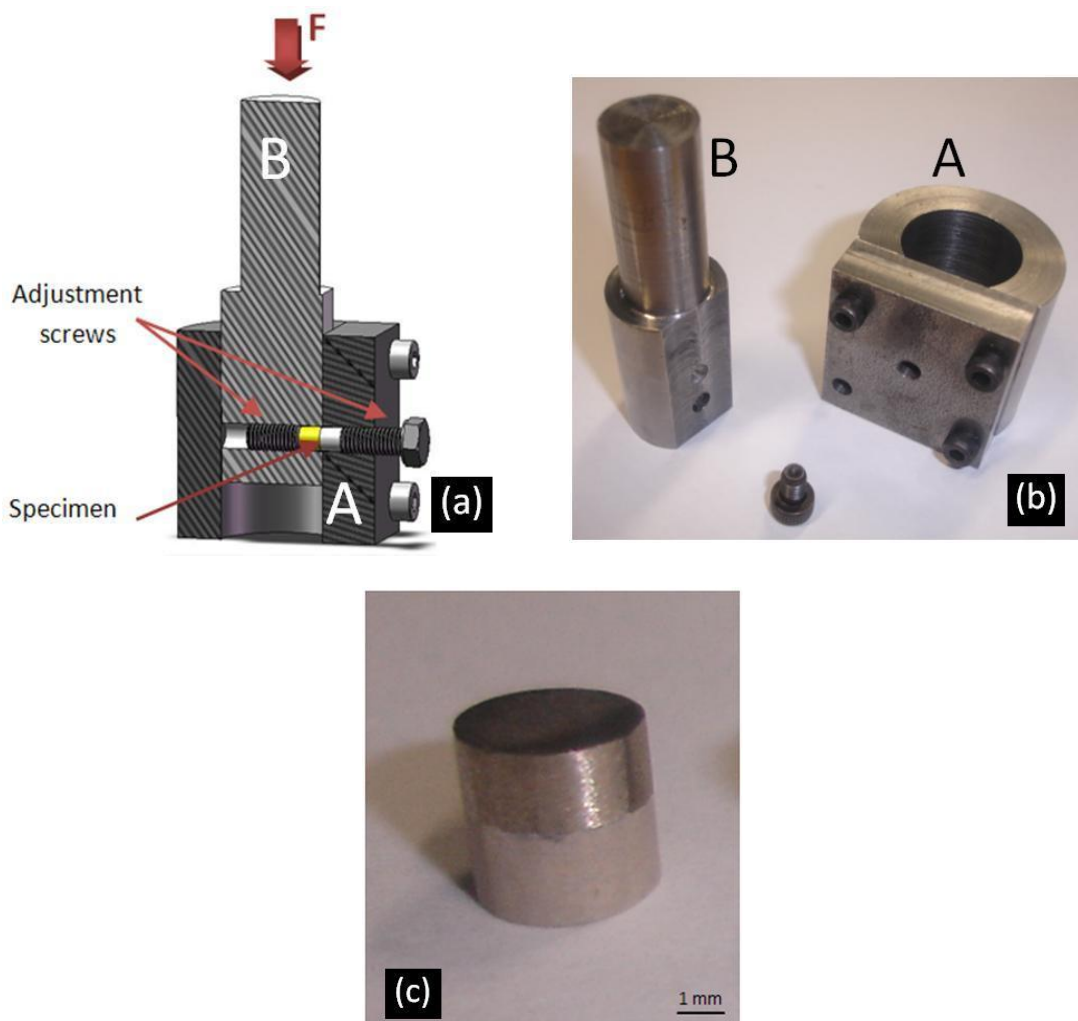


Figure 2.2. Test apparatus. (a) Cross-section schematic of the shear test device (b) stainless steel shear test device. (c) Metal–ceramic specimen.

2.2. Analysis of the metal-porcelain interface and failure mode

The metal-ceramic interface as well as representative fracture surfaces were evaluated by stereomicroscope (SMZ-2T, Nikon, Japan), optical microscope (Axiotech, Carl Zeiss, USA) and SEM/EDS (Nova 200, FEI, Oregon, USA). For interface analysis, the specimens were embedded in auto-polymerizing resin, ground finished to 1200 grit SiC sandpaper and polished with diamond paste first in 6 μ m and finally in 1 μ m felt disc. Morphology and chemical analysis were performed. The interface chemical analysis was made by the means of 20 perpendicular to the interface points allowing to obtain the chemical composition profile through the interface, comprising metal, interfacial zone and porcelain. Of these 20 aligned points, 10 were in the metal zone and 10 in the ceramic zone.

The specimens' failure modes were classified as: (1) if no remnants of ceramic were found in the metal surface; (2) adhesive, if fractures occurred within the ceramic side; (3) mixed, if remnants of ceramic were found in the metal surface.

The arithmetic roughness values (R_a) were obtained by in-situ measurements of 10 randomly chosen metal-ceramic interface micrographs of the two types of specimens' surfaces tested: polished (1200-grit) and roughened (metal powders). It was performed 10 measurements in each micrograph and calculated the average roughness following expression $R_a = \frac{1}{n} \sum_{i=1}^n |y_i|$.

2.3. Statistical analysis

Data was analyzed by using one-way ANOVA followed by Tukey's test for multiple comparisons. $P < 0.05$ or lower was considered statistically significant.

3. Results

Results of shear bond strength tests for different bonding conditions are presented in Figure 2.3. Conventional PFM results were in line with the upper range of literature data (83 ± 14 MPa) for gold alloys-porcelain composites (Drummond et al., 1984). Bond strength of hot pressed porcelain onto a polished surface (PPPS) and onto a roughened surface (PPRS) registered the values of 120 ± 16 MPa and 129 ± 5 MPa, respectively.

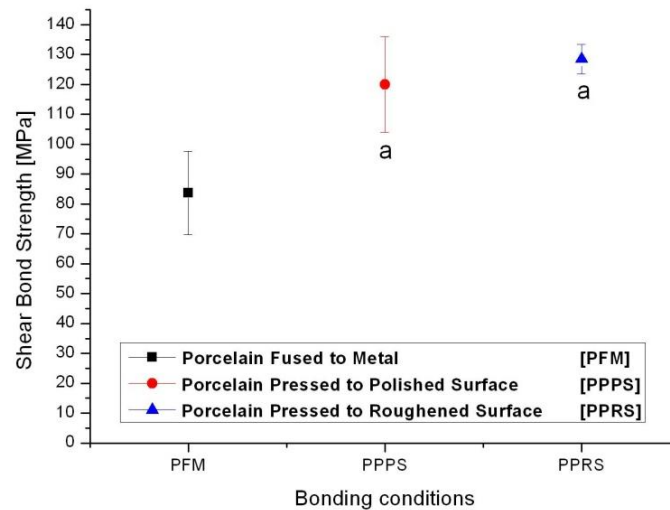


Figure 2.3. Shear bond strength comparative results for traditional method (PFM) and the two new proposed approaches PPRS and PPPS. The values represent means \pm SD. a, $p < 0.05$ vs. PFM.

The results for one-way ANOVA for experimental conditions are presented in Table 4 and shows that metal-porcelain bond strength for different bonding conditions are statistically different ($p < 0.05$). A Tuckey's HSD test indicated a significant difference between material PFM/PPPS and PFM/PPRS conditions, $p = 0.047$ and $p = 0.034$, respectively. No significant difference was found between PPPS and PPRS conditions ($p > 0.05$).

Table 2.4. Results of one-way ANOVA for tested conditions according to shear bond strength data.

Effect	df	SS	MS	F	p
Bonding conditions	2	5454.5	2727.3	16.9	6.2E-4
Error	10	1616.6	161.7		
Total	12	7071.1			

*Statistically significant at a level of $p < 0.05$. DF: Degrees of freedom; SS: Sum of squares; MS: Mean square; F: F-ratio; p: p-value

Specimens were classified under their failure types as adhesive, cohesive or mixed. The PFM specimens exhibited a mixed-failure mode. Some remnants of ceramic were present at the fracture surface of these specimens. All other specimens showed adhesive failure (Figure 2.4).

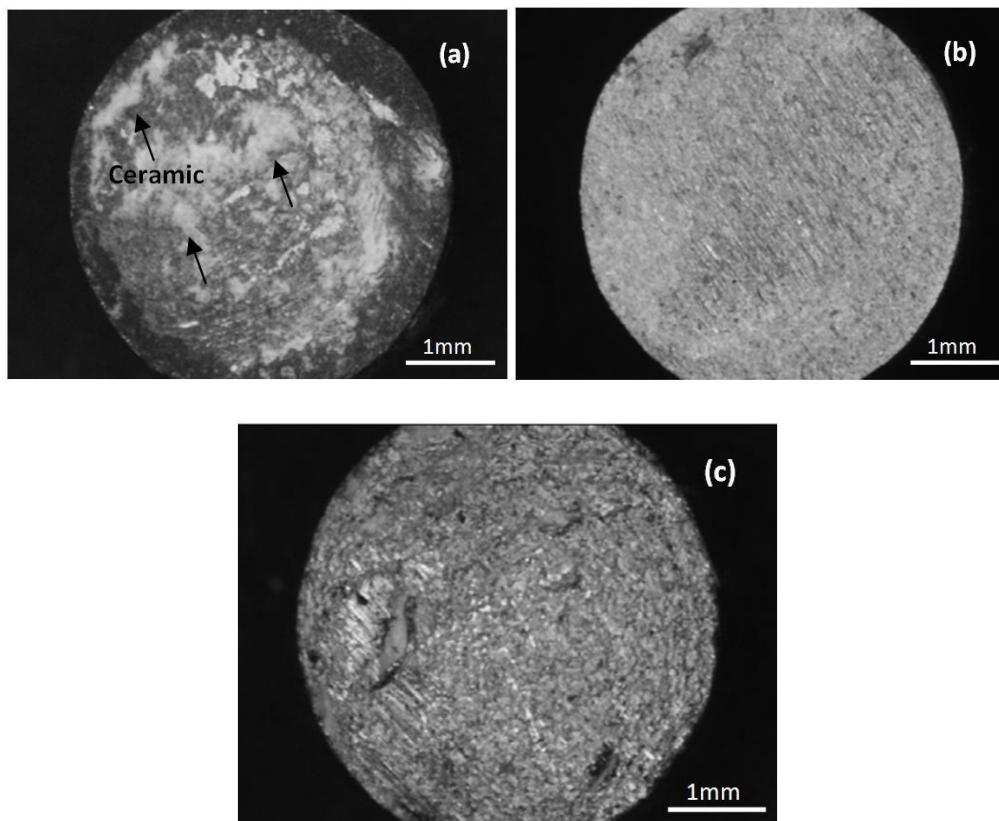


Figure 2.4. Fracture surface of specimens. a) PFM – mixed failure mode; b) PPPS – adhesive failure; c) PPRS – adhesive failure.

Figure 2.5 illustrates the metal/porcelain interface and line a-b through which the EDS analysis was made for a PPRS specimen. This picture reveals two phases in the metal side. The darker phase (zone 1) is rich in O, Pd, In, Sn and Pt while the lighter phase (zone 2) is rich in Au, Ag and Pd. In the porcelain side, the darker phase is composed mainly by SiO_2 , while the lighter one is composed mainly by SnO_2 and Al_2O_3 . These results are presented in Table 5.

The EDS analysis of line a-b is plotted in Figure 2.6. The results show the interdiffusion of atoms occurring during firing for some elements. Elements constituting the gold alloy (e.g. Au, Pt, Pd, Ag and In) barely diffuse into porcelain. On the other hand, an extensive diffusion of almost all elements constituting porcelain (e.g. O, Sn, Al, Si, Ca, Na and K) can be seen, with special relevance to the O_2 detected in a higher concentration.

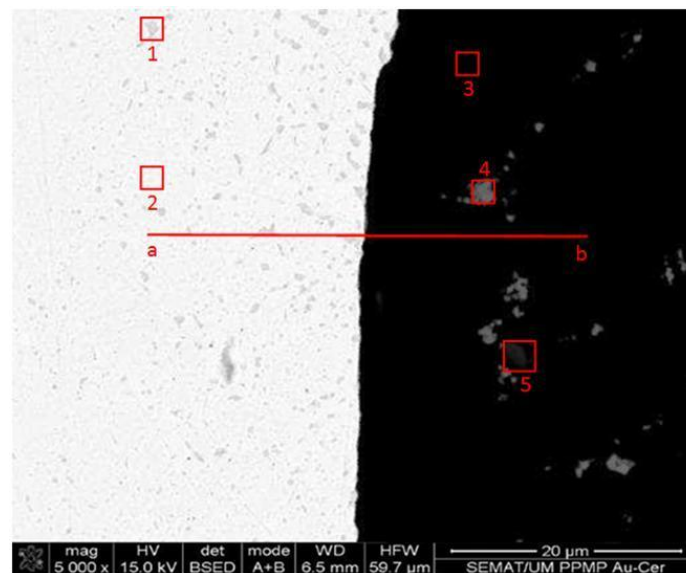
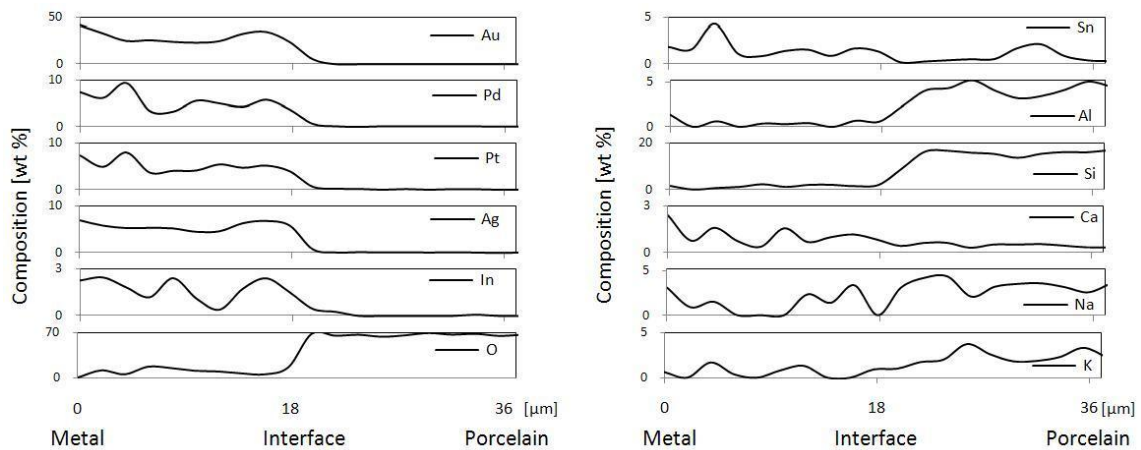


Figure 2.5. EDS line analysis of metal-porcelain interface processed by the PPRS technique.

Table 2.5. Elemental composition (wt.%) of different phases present in metal and porcelain.

Elem.	Points	Metal		Porcelain		
		1	2	3	4	5
Au		39.46	84.66	---	---	---
Pd		15.62	7.34	0.14	---	---
Pt		24.06	---	0.13	---	---
Ag		3.34	8.00	0.09	---	---
In		2.70	---	0.08	---	---
O		2.96	---	71.25	44.43	46.30
Si		---	---	16.82	8.00	15.74
Al		---	---	4.31	1.97	1.54
K		---	---	2.43	1.43	1.77
Sn		6.87	---	0.92	40.98	8.35
Zr		---	---	0.06	---	24.57
Ca		---	---	0.47	1.28	0.49
P		5.00	---	---	---	---
Na		---	---	1.94	1.91	1.24

**Figure 2.6.** Fracture Element line distribution (wt. %) of metal/ceramic interface for PPPS and PPRS specimens.

4. Discussion

4.1. Materials

This study evaluated the effect of hot pressing on the bond strength of metal-porcelain dental composites and made a comparison with conventionally obtained porcelain fused to metal specimens.

The gold alloy used in this study was Keramit 750 (Au-Pd-Pt; 18ct), a type 2 alloy according standard ISO 1562:1995. Every alloying element plays a specific role in this alloy. The significant presence of Pd and Pt contributes for a considerable solution hardening and leads to a widening of the separation between the solidus and the liquidus line of the solid solution phase diagram. These elements also increase the melting point and recrystallization temperature of gold alloys, a fact that is important for metaloceramic restorations. The presence of In is used to improve both the bonding strength between porcelain and metal and the mechanic properties of the metallic framework (Hautaniemi, 1995; Liu and Wang, 2007; Fisher, 2002). The rest of the elements such as Fe and Ir are used for grain refinement and also for mechanical strengthening, too. The bond strength between gold alloys and feldspatic porcelains are generally higher than those registered between base metal alloys and feldspatic porcelains (Vásquez et al., 2009; Donovan and Swift, 2009; Shell and Nielsen, 1962; Drummond et al., 1984; dos Santos et al. 2006; Haselton et al. 2001). Hence, a well-approved high gold alloy constitutes the best option for a durable, functional, aesthetic, biocompatible and easy manufactured metal-porcelain dental restoration (Knosp et al, 2003). Ceramco3 Opaque porcelain was selected to perform this study because of its recognized mechanical properties (Rizkalla and Jones, 2004) and its suitability for using with gold dental alloys (Vásquez et al., 2009; Shell and Nielsen, 1962; Drummond et al.1984; Lavine and Custer, 1966; Eames et al., 1997).

4.2. Shear bond strength test

Metal-porcelain adhesion strength can be assessed by several mechanical tests and there is no agreement about which one is the best. However, based on literature data, all of them show great variability in the mean bond strength values with large standard deviations. While some authors defend the shear test (Anusavice et al.,1980; Chong et al.1980) others point out the three-point-flexure test, four-point-flexure test or even the biaxial flexure test. In fact, there is not a consensual opinion about metal-ceramic bond strength testing. One of the drawbacks of shear test is that from point of high strength concentration, cohesive failure in ceramic can start and propagate through the interface. Bend tests have their drawbacks too, particularly the difficulty in analyzing the stress states present. Bond strength assessment in bend tests is influenced by the Young's modulus of the alloy, as the ceramic breakage depends on it. Therefore, an alloy with greater elastic modulus would resist bending to a greater extent, creating a higher bond. Therefore it is not clear as to whether the bond strength or the modulus of elasticity of the metal is the characteristic actually tested (Hammad et al, 1996).

For this study it was chosen the planar interface shear bond strength test because of its relatively uniform distribution of interface stresses and to be considered well-suited for evaluation of metal-ceramic bonds (Anusavice et al.,1980; Ihab and Yourself,1996), since the Young's modulus is not as critical as in bend tests (Hammad et al 1996). It should be referred that this test configuration has been used for many authors in metal-ceramic bond strength characterization (Akova et al, 2008; dos Santos et al, 2006; Shell et al, 1962; Vasquez et al, 2009; de Melo et al, 2005; M. Salazar et al., 2007).

The current standards that indicates the minimum acceptable bond strength for metal-ceramic composites are ANSI/ADA Specifications N°38 (2000) and ISO Standard 9693 (1999). Both employ the three-point-bending test and suggest a minimum value of 25 MPa for bond strength. Anusavice (2006) in his textbook suggests the minimum

of 51 MPa as a lower limit for bond strength, and points out that different values of bond strength are expected with different testing modes. Hence, due to geometrical differences of the specimens employed in the different bond strength tests, no direct comparison should be made of their results.

4.3. Hot pressing

As far as authors know, no published researches have been conducted using hot pressed conventional feldspathic porcelains to metals. Instead, we can find some studies involving low-fusing, leucite-based pressable ceramics to metals (Drumond et al., 2000; Schweitzer et al. 2005; Venkatachalam et al., 2009). These ceramics provide some advantages such as high compressive strengths and high flexural strength over traditional porcelains, due to an increased presence of uniformly distributed leucite phase (Kelly, 1997; Drumond et al., 2000). Venkatachalam et al. (2009) and Schweitzer et al. (2005) have compared the bond strength of ceramic pressed to metal versus feldspathic porcelain fused to metal for various noble and base alloys and found no significant differences ($p > 0.05$) between the two techniques. However they couldn't ascertain the effect that additional steps of divestment and sprue removal had on the debond strength values of pressed ceramic samples, which were characterized by larger standard deviations. Another important aspect to consider in their studies is the CTE mismatch between pressed ceramic and metal, which was greater than $3 \times 10^{-6} \text{ } 1/^{\circ}\text{C}$. It is recognized that CTEs differences of $1.7 \times 10^{-6} \text{ } 1/^{\circ}\text{C}$ or greater between metal and porcelain can generate shear stresses at the interface which can lead to a weak metal-ceramic bond or to its ultimate failure (Shillingburg et al., 1997). To assure that porcelain is under compression at the interface, the metal's CTE should be slightly higher than of the porcelain but ideally their difference should not be greater than $1 \times 10^{-6} \text{ } 1/^{\circ}\text{C}$ (Drumond et al., 2000).

The CTE mismatch is related with the CTE of porcelain and alloy, themselves, and not with the processing technique. PFM and Hot-pressing were not considered to originate

different pre-stresses states (at interface) due to CTE mismatch, once it was used the same heating/cooling rates for both cases.

Metallic specimen's dimension was chosen in accordance with the ones used in similar studies involving metal-porcelain shear bond strength tests (Akova et al, 2008; dos Santos et al., 2006; Vasquez et al., 2009; de Melo et al., 2005; M.Salazar et al., 2007). The fact of using the same metal substrates dimension's to produce specimens either from PFM or HP technique and, at the same time, the same heating/cooling cycle assures that thermal stresses generated at interface are of similar magnitude. Therefore, differences in metal-ceramic bond strength cannot be attributed to different specimen's geometry.

The present study reveals significant differences ($p < 0.05$) between hot pressed specimens and PFM ones. These results might be explained by several factors, as follows: hot pressing concurred to an intimate contact between metal and porcelain, producing an interface free of defects such as pores and cracks (Figure 2.7) where better chemical bonds can be established due to a perfect wetting of the metal's surface by the pressed fused porcelain. Despite chemical bonding is regarded to be the responsible for metal-ceramic adherence, mechanical interlocking plays also an important role in the bonding process. Mechanical interlocking is provided by the existence of an irregular surface, whether it is micro or macro-roughened. Wagner et al. (1993) found a direct correlation between roughness and bond strength, for a palladium alloy-porcelain couple, with greater roughness leading to higher bond strength. It happens that one of the limitations of using greater surface roughness relies on the possibility of air entrapment in the surface irregularities, thus reducing the effective bonding. Hot pressing appears to solve this problem by applying an external overpressure on porcelain contributing this way to an enhanced mechanical interlocking and to a greater area of adhesion surface. That seems to be the case of PPRS specimens, where no pores could be found in the metal-porcelain interface, even in the presence of a high level of surface roughness (see Figure 2.7c). In the case of

PPRS specimens, the rough surface was produced by the means of metal powders placed at the interface between metal and ceramic.

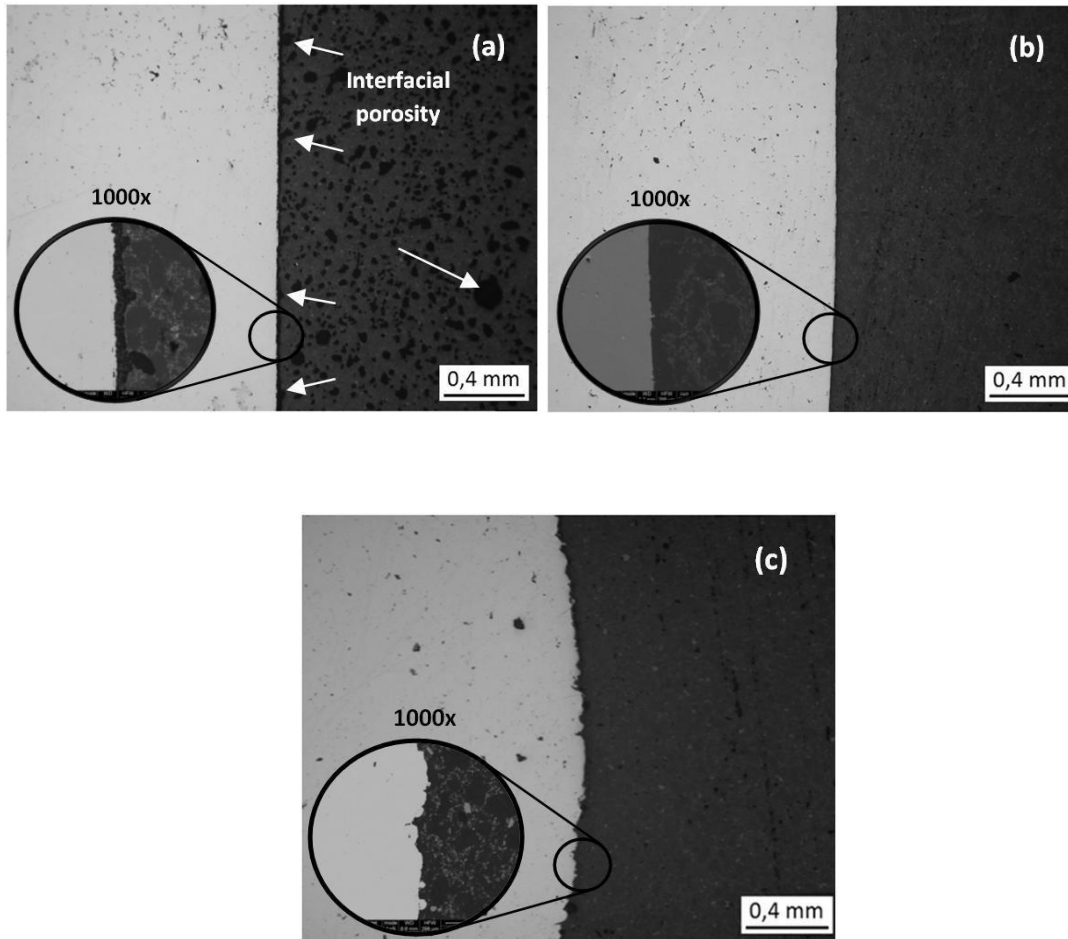


Figure 2.7. Interface appearance for (a) PFM (50x), (b) PPPS (50x) and (c) PPRS (50x) specimens, respectively. High porosity in the ceramic side and interface at PFM technique a).

By producing PPRS specimens, authors intended to investigate the influence of greater level of surface roughness (**PPRS**: $R_a = 6.8\mu\text{m}$) on bond strength of hot pressed specimens. It should be highlighted that general alumina sandblasting treatments can produce metal surface roughness until $1\mu\text{m}$ of arithmetic roughness (R_a) (Fisher, 2002). Even though PPRS specimens differed from PPPS ones for having a surface roughness approximately ten times greater (**PPPS**: $R_a = 0.7\mu\text{m}$; **PPRS**: $R_a = 6.8\mu\text{m}$), no significant

difference ($p > 0.05$) was found in the shear bond strength of both groups. However, it was noticed a reduction in the standard deviation of the latter specimens (PPSR), which might reflect greater reproducibility of results by this via.

As referred before, the surface roughness in PPRS specimens was created by the presence of metallic powder at the interface between metal and ceramic. As the sintering step was performed at a temperature of 970°C, which is 100°C below the alloy melting temperature (1160-1230°C), there were no fused particles besides porcelain powders. The bonding of metal powders to metal substrate occurred by solid state diffusion bonding and not by metal's fusion. On contrary, the bonding of porcelain to metal powders occurred by fusion of porcelain onto the solid metal powders.

4.4. Fracture type analysis

Based on the standards ISO 9693 (1991) and ANSI/ADA specification No. 38 (1991) for metal ceramic systems, some conclusions about the metal-ceramic adhesion can be drawn by the analysis of the fracture surface. Depending on the type of fracture, whether it is cohesive or adhesive, then the metal-ceramic bonding would be strong or weak, respectively. These standards follow the O'Brien (1977) nonspecific cohesive plateau theory that hypothesized that a metal-ceramic system under load will fail at the regions of weakest bonding. Hence, a 100% cohesive failure through the ceramic results from an optimum bonding between metal and porcelain. According to ISO 9693 and ANSI/ADA standards the characterization of the nature of the bond is made by the determining the percent of cohesive failure through the ceramic.

In this study, authors followed other published works of the same subject (Akova et al, 2008; dos Santos et al, 2006; Shell et al, 1962; Vasquez et al, 2009; de Melo et al, 2005; M. Salazar et al, 2007) and classified the failure types according to the presence or not of ceramic remnants on the metal substrate after shear tests (i.e. adhesive, cohesive or mixed).

Stereomicroscope observations of the fracture surfaces revealed two types of failure modes: mixed failure and adhesive failure. PFM specimens showed mixed failure mode, partly adhesive in the interface and partly cohesive with some remnants of porcelain at the fracture surface (Figure 2.4), suggesting a good metal-ceramic bond. PPPS and PPRS specimens exhibited adhesive failure, ie, no remnants of ceramic can be found in the metallic surface. Although this type of failure is described as a typical mechanism failure of ceramic bonded to noble alloy substrates (Eames et al., 1997; dos Santos et al., 2006; Haselton et al., 2001; Chang et al., 2002), perhaps it could suggest a weaker bond between metal and ceramic in hot pressed specimens. On the contrary, what we observed was a statistically significant increase ($p < 0.05$) of it. This means that the bonding between the metal and ceramic was not as effective as the cohesive strength of the ceramic which might result from improved strengthening mechanisms provided by the hot pressing (Kelly, 1997; Drumond et al., 2000).

In this study it was found no correlation between the type of failure and the bond strength and same thing was verified by other authors (de Melo et al. 2005; Akova et al. 2008). Moreover, the failure type could not be predicted although the origin of it might be pointed as the stresses generated at the metal-ceramic interface due to shear loading.

4.6. EDS analysis

The chemical analysis was performed only for polished surface specimens (PPPS). As referred above (chapter 4.3), porcelain powders were fused onto solid metal powders. Therefore, the interaction between fused porcelain and metal powders was the same as verified for fused porcelain onto the polished metal substrate. The important process variables are the same in both types of conditions (PPPS and PPRS): contact interface characteristics, temperature, pressure and contact time. What is different in the former case is the surface contact area that becomes higher for greater surface

roughness. Based on these facts, the chemical analysis was performed across the PPPS specimen's interface because this way it was minimized the side effect of the analysis (the interference of the volume analysis is minimized when the interface is well defined, as a straight line in the chosen configuration). Hence, the analysis of the interface with metal powders mixed with ceramic powders would be much less reliable.

The EDS line analysis of interaction zone concentration profiles in the present metal-porcelain system revealed an abrupt decrease in concentration of Au, Pd, Pt, Ag, In and O which is in accordance with other author's studies (Vásquez et al., 2009; Lautenschlager et al, 1969). All these elements revealed approximated sigmoidal profiles typical of diffusion, as obtained by Anusavice et al. (1977). It was also registered an accumulation of In and Sn at the interface region as Nally et al. (1968; 1970) observed in their study involving ceramic-precious alloys. Goeller et al. (1972) reported the same behavior of In in their study of the influence of metal coating agents on the bond strength of porcelain fused to gold alloys. The presence of O₂ on the metal side, suggests the formation of an oxide layer. The same finding is reported by Vasquez et al (2009). Si decrease towards the interface registering a low content on the metal side of the couple reflecting a behavior previously reported in analogue studies (Anusavice et al., 1977; Vázquez, 2009).

A low content of Sn was also registered at the interface which is not consistent with Anusavice et al. (1977) findings that revealed an accumulation of Sn atoms at the interface. This might be explained by the absence of Sn in the gold alloy in opposition with Sn containing alloys used in their study. It was also detected low traces of Al, Ca, Na and K on the metal side of the couple showing a diffusion of these elements with origin in porcelain.

This study shows the benefit of using pressure along with temperature in the enhancement of the bond strength between metal and porcelain for dental applications. However, further studies should be conducted involving other dental

alloys and porcelain types to determine whether the present study outputs are applicable to other materials.

Another question that remains open and should be investigated is the behavior of hot pressed metal-porcelain couples under thermal and/or mechanical fatigue since it best reproduces clinic conditions.

5. Conclusions

From this study, the following conclusions can be drawn:

1. Regardless of the bonding method (i.e. conventional porcelain fused to metal or hot pressing) Ceramco3 opaque presents a very good adhesion to Keramit750;
2. Hot pressed specimens (PPPS and PPRS) showed a significantly improvement (~50%) in metal-porcelain bond strength in metal-porcelain bond strength relatively to conventional porcelain fused to metal (PFM) specimens ($p < 0.05$).
3. Surface roughness (PPRS) did not contribute to a significant increase in metal-porcelain bond strength, relatively to the polished surface (PPPS), within hot pressed specimens ($p > 0.05$).

6. Acknowledgements

This work has been supported by PhD Grant of FCT (Portuguese Foundation for Science and Technology) with the reference SFRH / BD / 41584 / 2007.

7. References

- Akova, T., Ucar, Y., Tukay, A., Balkaya, M.C., Brantley, W.A., 2008. Comparison of the bond strength of laser-sintered and cast base metal dental alloys to porcelain. *Dent. Mater.* 24, 1400-1404.
- Anusavice, K.J., 2006. *Phillips' science of dental materials*. 11th ed. Philadelphia:W.B. Saunders. pp. 621-54.
- Anusavice, K.J., Horner, J.A., Fairhurst, C.W., 1977. Adherence controlling elements in ceramic-metal systems. I. Precious alloys. *J. Dent. Res.* 56, 1045.
- Anusavice, K.J., Dehoff, P.H., Fairhurst, C.W., 1980. Comparative evaluation of ceramic-metal bond tests using finite element stress analysis. *J. Dent. Res.* 59, 608-13.
- Chang, J.C., Koh, S.H., Powers, J.M., Duong, J.H., 2002. Tensile bond strengths of composites to a gold-palladium alloy after thermal cycling. *J. Prosthet. Dent.* 87, 271-6.
- Chong, M.P., Beech, D.R., Chem, M.R.I.C., 1980. A simple shear test to evaluate the bond strength of ceramic fused to metal. *Aust. Dent. J.* 25, 357-6.
- de Melo R.M., Travassos A.C., Neisser M.P., 2005. Shear bond strengths of a ceramic system to alternative alloys. *J. Prosthet. Dent.* 93, 64-69
- dos Santos, J.G., Fonseca, R.G., Adabo, L.G., Cruz, C.A.S., 2006. Shear bond strength of metal-ceramic repair systems. *J. Prosthet. Dent.* 165-73.
- Donovan, T.E., Swift, E.J.Jr., 2009. Porcelain-Fused-to-Metal (PFM) Alternatives. *J Comp.* 1, 4-6.
- Drummond, J.L., King, T.J., Bapna, M.S., Koperski, R.D., 2000. Mechanical property evaluation of pressable restorative ceramics. *Dent. Mater.*, 16, 226-233.
- Drummond, J.L., Randolph, R.G., Jekkals, V.J., Lenke, J.W., 1984. Shear Testing of the Porcelain-Metal Bond. *J. Dent. Res.* 63, 1400.
- Eames, W.B., Rogers, L.B., Feller, P.R., Price, W.R., 1997. Bonding agents for repairing porcelain and gold: an evaluation. *Oper. Dent.* 2, 118-2.

Fisher, J., 2002. Ceramic bonding to a dental gold-titanium alloy. *Biomaterials*. 23, 1303-1311.

Francis LF, Vaidya KJ, Huang HY, Wolf WD. Design and processing of ceramic-based analogs to the dental crown. *Materials Science and Engineering C: Biomimetic Materials, Sensors and Systems*, 1995; 3 (2): 63-74.

Goeller, I., Meyer, J.M., Nally, J.N., 1972. Comparative study of three coating agents and their influence on bond strength of porcelain-fused-to-gold alloys. *J. Prosthet. Dent.* 28, 504.

Guess P.C., Kulis A., Witkowski S., Wolkewitz M., Zhang Y., Strub J.R., 2008. Shear bond strengths between different zirconia cores and veneering ceramics and their susceptibility to thermocycling. *Dent. Mater.* 24, 1556-1567.

Hammad I.A., Talic Y.F., 1996. Designs of bond strength tests for metal-ceramic complexes: Review of the literature. *J. Prosthet. Dent.* 75, 602-608.

Haselton, D.R., Diaz-Arnold, A.M., Dunne, J.T Jr., 2001. Shear bond strengths of 2 intraoral porcelain repair systems to porcelain or metal substrates. *J. Prosthet. Dent.* 86, 526-31.

Hautaniemi, J.A., 1995. The effect of indium on porcelain bonding between porcelain and Au-Pd-In alloy. *J. Mater. Sci.: Mater. in Medicine*. 6, 46-50.

Ihab, A. H., Yourself, F. T., 1996. Designs of bond strength tests for metal-ceramic complexes: Review of literature. *J Prosthet. Dent.* 75, 602-8.

Kelly, J.R., 1997. Ceramics in restorative and prosthetic dentistry. *Annu. Rev. Mater. Sci.* 27, 443-36.

Keramit 750 Alloy data. Online. 2010. Available from URL: http://www.nobilmetal.it/english/pages/non_precious_alloys.html

Knosp, H., Holliday, .R.J., Corti, C.W., 2003. Gold in dentistry: Alloys, Uses and Performance. *Gold Bulletin*. 36/3, 93-102.

Lautenschlager, E.P., Greener, E.H., Elkingston, W.E., 1969. Microprobe analysis of Gold-porcelain bonding. *J. Dent. Res.* 48,1206.

Lavine, M.H., Custer, F., 1966. Variables affecting the strength of bond between porcelain and gold. *J. Dent. Res.* 45(1), 32-6.

Lin CP, Douglas WH, Erlandsen SL. Scanning electron microscopy of type I collagen at the dentin-enamel junction of human teeth. *The Journal of Histochemistry and Cytochemistry*, 1993; 41 (3): 381-388.

Lin CP, Douglas WH. Structure-property relations and crack resistance at the bovine dentin-enamel junction. *Journal of Dental Research*, 1994; 73 (5): 1072-1078.

Liu, J., Qiu, X.M., Zhu, S., Sun, D.Q., 2008. Microstructures and mechanical properties of interface between porcelain and Ni-Cr alloy. *Mat. Sce. and Eng. A.* 497, 421-425.

Liu, W.B., Wang, J.N., 2007. Strengthening of Pd-free high gold dental alloy for porcelain bonding by a pre-firing heat treatment. *Dent. Mater.* 23, 1136-1141.

M. Salazar S.M., Pereira S.M.B., V. Ccahuana V.Z., Passos S.P., Vanderlei A.D. Pavanelli C.A., Bottino M.A. 2007. Shear bond strength between metal alloy and a ceramic system, submitted to different thermocycling immersion times. *Acta Ontolog. Latinoam.* 20(2), 97-102

Nally, J.N., Monner, D., Meyer, J.M., 1968. Distribution topographique de certains elements de la porcelaine au niveau de la liaison céramo-métallique. *Schweiz Msch fur Zahnheilk.* 78, 868.

Nally, J.N., Monner, D., Meyer, J.M., 1970. Recherche experimentale sur la nature de la liasion Ceramo-Metallike. *Schweiz Msch fur Zahnheilk* 80, 250.

O' Brien, W.J., 1977. Cohesive plateau theory of porcelain-alloy bonding, in: *Dental porcelain: The state of the art*. Los Angeles: University of Southern California Press, pp. 137-141.

özcan, M., 2003. Fracture reasons in ceramic-fused-to metal restorations. *J. of Oral Rehabilitation.* 30, 265-269.

Rizkalla, A.S., Jones, D.W., 2004. Indentation fracture toughness and dynamic elastic moduli for commercial feldspathic dental porcelain materials. *Dent. Mater.* 20,198-206.

Schweitzer, D.M., Goldstein, G.R., Ricci, J.L., Silva, N.R., Hittelman, E.L., 2005. Comparison of bond strength of a pressed ceramic fused to metal versus feldspathic porcelain fused to metal. *J. Prosthodont.* 14, 239-247.

Shell, J.S., Nielsen, J.P., 1962. Study of the Bond between Gold Alloys and Porcelain. *J. Dent. Res.* 41, 1424-1437.

Shillingburg, T., Hobo, S., Whitsett, L.D. et al., 1997. *Fundamentals of Fixed Prosthodontics*, ed 3. Chicago: Quintessence pp. 456.

Souza, J.C.M., Nascimento, R.M., Martinelli A.E., 2010. Characterization of dental-ceramic interfaces immersed in artificial saliva after substructural mechanical metallization with titanium. *Surface & Coatings Technology* 205, 787-792.

Vásquez, V.Z.C., öscan, M., Kimpara, E.T., 2009. Evaluation of interface characterization and adhesion of glass ceramics to commercially pure titanium and gold alloys after thermal- and mechanical-loading. *Dent. Mater.* 25, 221–31.

Venkatachalam, B., Goldstein, R., Pines. M.S., Hittelman, E.L., 2009. Ceramic Pressed to Metal versus feldspathic porcelain fused to metal: a comparative study of bond strength. *Int. J. Prosthodont.* 22, 94-100.

Wargner, W.C., Asgar, K., Bigelow, W.C., Flinn, R.A., 1993. Effect of interfacial variables on metal-porcelain bonding. *J. Biom. Mater. Res.* 27, 531-537.

Zarone F., Russo S., Sorrentino R. From porcelain-fused-to-metal to zirconia: Clinical and experimental considerations. *Dent Mater* 2011, 27: 83-96.

Chapter 3

Optimization of bond strength between gold alloy and porcelain through a composite interlayer obtained by powder metallurgy

Published in Materials Science and Engineering A 528 (2011) 1415–1420

B. Henriques, D. Soares, F.S. Silva

*Centre for Mechanical and Materials Technologies (CT2M) and Department of Mechanical Engineering,
University of Minho, Azurém, 4800-058 Guimarães, Portugal*

Abstract

Objectives: The purpose of this study was to evaluate the influence of a composite interlayer (at the metal-ceramic interface) on the shear bond strength of a metal-ceramic composite when compared with a conventional Porcelain Fused to Metal (PFM).

Methods: Several metal-ceramic composites specimens were produced by hot pressing. To identify which was the best composition for the interlayer several

composites, with different relations of metal/ceramic volume fraction, were bonded to metal and to ceramic substrates. The bond strength of the composites to substrates were assessed by the means of a shear test performed in a universal test machine (crosshead speed: 0.5mm/min) until fracture. Some interfaces of fractured specimens as well as undestroyed interface specimens were examined with optical microscope and Scanning Electron Microscope (SEM/EDS).

Results: The shear bond strength results for all composites bonded to metal and to ceramic substrates were significantly higher (>150 MPa) than those registered in the upper range of conventional Porcelain Fused to Metal (PFM) techniques (~80MPa).

Significance: The use of a composite interlayer proved to enhance metal/ceramic adhesion in 160%.

1. Introduction

Metal-ceramic restoration, in the dentistry field, is still the most reliable method in dental prosthetics, especially when a good adhesion of the ceramic to the metal substrate is achieved (Vásquez et al., 2009). The recent trend for all ceramic restorations don't accomplish, yet, for the necessary longevity and clinical failure is often reported prematurely (Kelly, 1997; Donovan and Swift, 2009). Despite its cost, within the available metals used in PFM restorations, a well-approved high gold alloy is still the best option in terms of longevity, functionality, aesthetics, and biocompatibility, together with ease of manufacture (Knosp et al., 2003). Also, it is no coincidence that in all testing and development of competing materials, gold is always defined as standard material to be judge against. Therefore, for this study was used a high gold content dental alloy (KERAMIT 750, Nobilmetal, Villafranca d'Asti ,Italy). Nevertheless, with the recent increase in gold's price, reduced-gold content and palladium-based dental alloys are becoming very popular. Also, in some particular

economic contexts, base metal alloys constitutes the solutions for low cost dental restorations.

As referred above, metal-ceramic dental restorations strongly depend on the success of the bond between porcelain and the metal substrate (Shell and Nielsen, 1962; Drummond et al., 1984; Liu et al., 2008; Özcan et al., 2003; Lavine and Custer, 1966; Eames et al., 1977; dos Santos et al., 2006; Haselton et al., 2001; Chang et al., 2002; Anusavice et al., 2003). This is achieved by attaining to the characteristics of compatibility of the materials involved, e.g. choose the metals and ceramics with the proper CTEs (Coefficient of Thermal Expansion). Using metals and ceramics with different CTEs, means that when cooling down from processing (sintering) temperature, both materials will contract at different rates and strong residual stresses will form across the interface. Depending on their magnitude, these stresses can lead the ceramic to crack or even to separate from the metal substructure. Despite PFM restorations longevity, when compared to all-ceramic restorations, clinical failures sometimes occur and the failure rate, due to fracture and exfoliation of porcelain, represents 59.1% of the whole clinical failure (Liu et al., 2008; Özcan, 2003). In this study, it is proposed the presence of a composite interlayer in the metal-ceramic interfacial zone. This interlayer will eliminate the sharp transition between the materials and, consequently, of their properties. For instance, the Young Modulus of the gold alloy and Ceramco3 are different (100GPa and 83GPa, respectively) causing an elastic mismatch that can lead to the microcracks generation and finally to failure.

The specimens produced for this study were obtained through the Hot Pressing Powder Metallurgy (PM) technique. Powder Metallurgical (PM) processing was the chosen route in this study because of the ease in controlling the composition and microstructure, as well as shape forming of the specimens. Hot pressing allowed avoiding undesired residual porosity and small cracks, together with a better and quicker compaction and full densification. PM used in rapid manufacturing, in the dentistry field, is starting to grow and appears as a very promising technology (Liu et al., 2006; Strauss, 2009). There are already available commercial equipments that

produce precious metals dental copings using PM. Using laser assisted methods one can achieve fully-dense parts with good mechanical properties, as well as a dynamic and continuous transition in material composition when desired. This leads to a smooth transition in materials properties, e.g. Young Modulus, thus reducing or even avoiding critical stress concentrations in the component. Some work has been reported in multi-material dental restoration using laser assisted densification of powders (Liu et al., 2006), although no actual fabrication of dental prostheses has been reported yet.

The purpose of this study was to determine whether the use of a metal-ceramic graded interface would result in a more resistant one compared with the conventional sharp transition interface or not. So, studies were performed to find which was the best composition of the interlayer composite that simultaneously best adhered to ceramic and to the metal substrate, resulting in an enhanced mechanical strength metal-ceramic interface. Once the ideal composition for the interlayer was identified, some metal/interlayer/ceramic specimens were produced and tested with encouraging results.

2. Materials and Methods

2.1. Materials

The compositions of the dental gold alloy (Keramit 750, Nobilmetal, Villafranca d'Asti, Italy) and the dental opaque ceramic (Ceramco3, Dentsply, York, USA) (batch number: 08004925) used in this study are presented in Tables 1 and 2, respectively, as obtained from supplier catalogues. The gold alloy was used in irregular powder form, with dimensions of 170 mesh. The chemical compositions of the gold alloy and opaque ceramic are presented in the Tables 1 and 2, respectively, as well as their mechanical properties in Table 3.

Table 3.1. Gold alloy chemical composition (wt.%).

Au	Pt	Pd	Ag	In	Others
75	4.3	8.5	9	1.7	Fe, Ir

Table 3.2. Ceramic chemical composition (wt.%).

SiO ₂	Al ₂ O ₃	K ₂ O	SnO ₂	ZrO ₂	CaO	P ₂ O ₅	Na ₂ O	Others
41.3	14.5	14.0	11.9	5.8	4.1	4.1	3.0	MgO, SO ₃ , ZnO, Cr ₂ O ₃ , Fe ₂ O ₃ , CuO, Rb ₂ O

Table 3.3. Base materials properties.

	Density g/cm ³	Melting Range [°C]	CTE [25- 600°C]	E [GPa]	Hardness
Keramit750*	16.2	1160-1230	14.8	100	HV200 (self-hardened)
Ceramco3 Opaque	2.82**		13.2***	83**	

*Keramit750 alloy data (2010); **Rizkalla and Jones (2004); ***Souza (2006)

2.2. Processing

In order to obtain PMCC (Pressed Metal-Ceramic Composites), which is the designation for our obtained specimens, several different metal-ceramic composites were bonded by hot pressing them to a metal green compact and to a ceramic framework.

Tested composites had the following compositions [%Vol.]: 80Met20Cer; 60Met40Cer; 40Met60Cer; 20Met80Cer.

The processing of the metal-composites comprised three steps: first, a metal green compact was produced through the pressing of metal powders in a stainless steel die with 4.5 mm of diameter under a load of 3000 N; the second step consisted in producing the composites, blending the proper metal:ceramic powders ratio in a rotary machine at 40 rpm for 10 min.; the final step consisted in inserting both metal

green compact and composite powders in the graphite die for hot pressing (Figure 3.1a). A similar procedure was used in the manufacturing of ceramic-composite specimens, though with a slight difference. Instead of being pressed separately in a stainless steel die, like in metal powders, ceramic powders were initially stacked in the graphite die. After that, composite powders were also inserted into the graphite die and then the set was hot pressed (Figure 3.1a and b)). Hot pressing was performed in vacuum (5×10^{-2} mbar) till a temperature of 970°C (as suggested by the ceramic supplier technical data for the porcelain) and at a constant pressure of 20 MPa. The heat rate was approx. $60^{\circ}\text{C}/\text{min}$ and after reaching 970°C , the power of the induction heating furnace was shut down and the die was left to cool down naturally (Figure 3.1c).

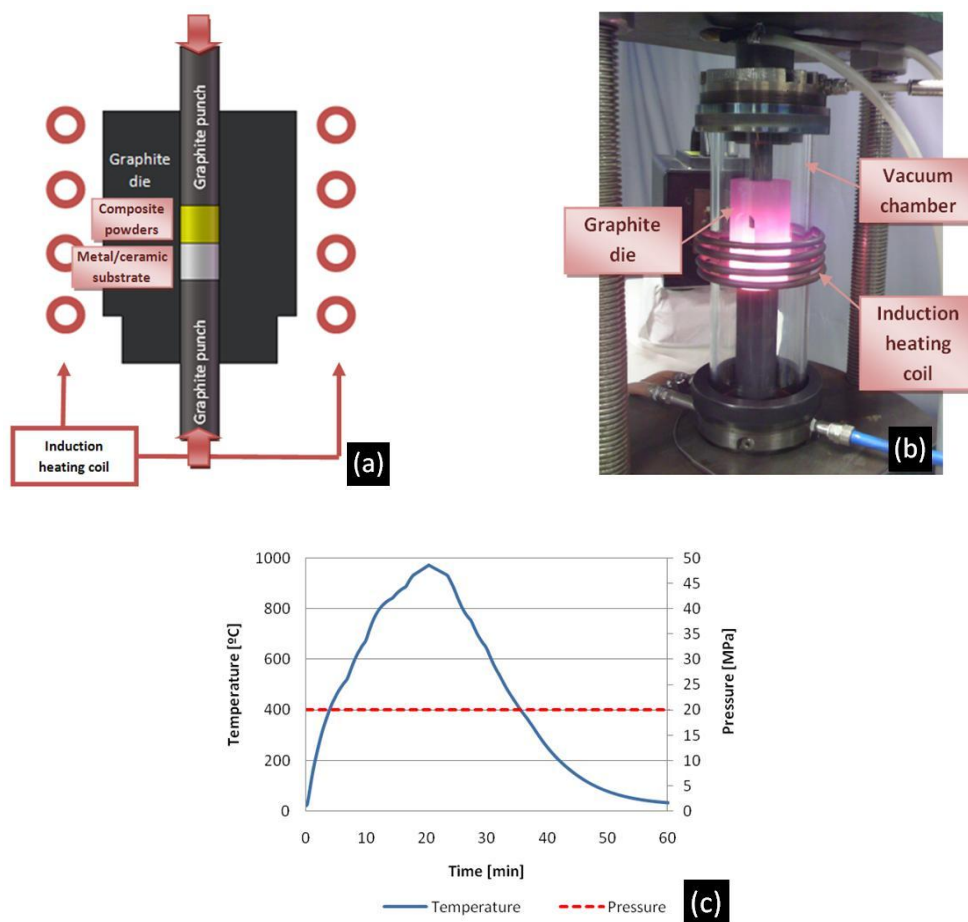


Figure 3.1. Hot pressing apparatus. (a) Hot pressing schematic (b) Processing a specimen in the vacuum chamber (c) Hot pressing cycle.

2.3. Shear tests

The test selected to assess metal-composite and ceramic-composite (Figure 3.2a) bond strength was the shear test due to its recognized reliability based on minimal experimental variables and lower residual stresses induced at metal-ceramic interface (Vásquez et al., 2009). Minimum acceptable values for metal-ceramic bond strength are present in standards ANSI/ADA Specifications N°38 (2000) and ISO Standard 9693 (1999), and is indicated as 25MPa. This value refers to a three-point bending test that measures bond strength. Due to geometrical differences of the specimens used in both tests (shear and three-point bending), no direct comparison should be made of the results of different tests.

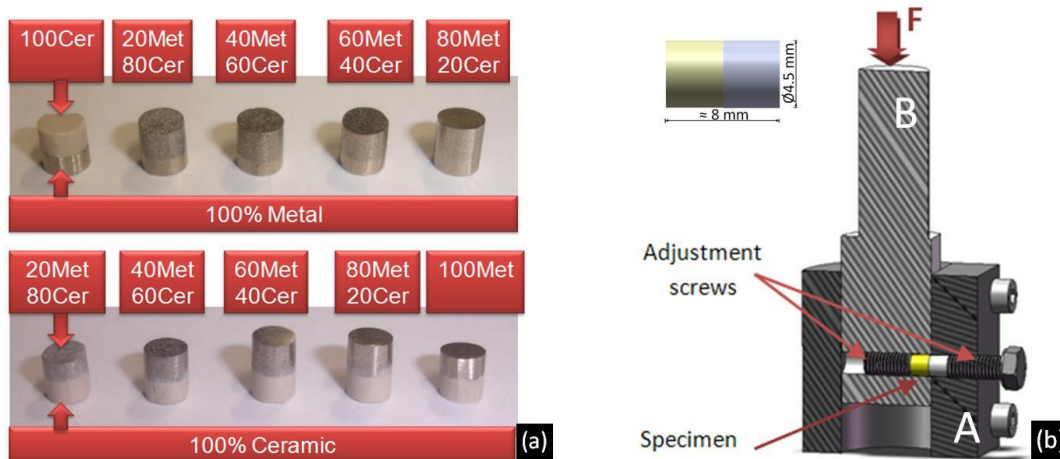


Figure 3.2. Shear test apparatus. (a) Metal-composite and ceramic-composite specimens (b) Cross-section schematic of the shear test device.

Shear bond strength tests were carried out at room temperature and performed in an universal testing machine (Instron 8874, MA, USA), with a load cell having 25 kN capacity and under a crosshead speed of 0.5mm/s. Tests were performed in a custom-made stainless steel apparatus consisting in two sliding parts A and B (Figure 3.2b), each one with a hole perfectly aligned to the other. After alignment of the holes, the

specimen is inserted into it and the specimen's interface is moved to the sliding plane with the help of the adjusting screws. A compressive force is then applied in the upper side of part B until a fracture occurs due to shear loading. Shear bond strength (MPa) was calculated by dividing the highest recorded fracture force (N) by the area of adherent composite (mm^2).

3. Results

Shear bond strength for PMCC (Pressed Metal-Ceramic Composites), specimens are presented in Figure 3.3 and exhibited a range of values between 162.1 ± 45.4 MPa and 235.1 ± 13.0 MPa.

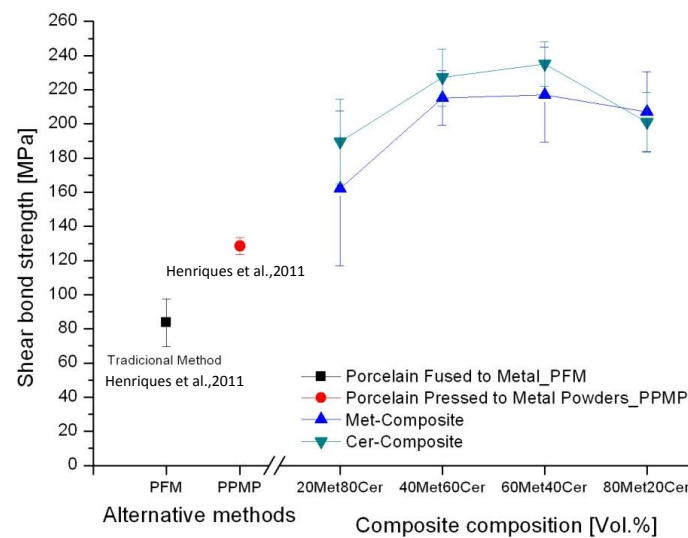


Figure 3.3. Shear bond strength results for the metal and ceramic bonding to different pressed metal-ceramic composites (PMCC) and comparison to alternative processing methods (Henriques et al., 2011).

The 20Met80Cer composite bonded to the metal base showing a shear bond strength of 162.1 ± 45.4 MPa whereas when bonded to the ceramic substrate showed a strength of 189.7 ± 24.8 MPa. In the case of 40Met60Cer and 60Met40Cer results obtained were quite similar being slightly higher in the latter case. 40Met60Cer composite exhibited a shear bond strength of 215.1 ± 15.9 MPa when bonded to a metal substrate and

227.1±16.7 MPa when bonded to a ceramic one. Regarding 60Met40Cer composite the values recorded in the shear test were 217.0±27.9 MPa in the connection to the metal and 235.1±13.0 MPa in the connection to the ceramic substrate. Finally, the shear bond strengths registered for 80Met20Cer composite were 207.2±23.3 MPa and 201.1±17.6 MPa to metal and ceramic substrates, respectively.

The analysis of the fracture surfaces of PMCC (Pressed Metal-Ceramic Composites) specimens showed remnants of the interlayer composites in all tested specimens.

After these tests, and attending to the results obtained (Figure 3.4), some metal-composite-ceramic specimens (Figure 3.4a) were produced using a 50Met50Cer composite interlayer and tested like all the other specimens before. To produce these specimens, a small amount (enough to produce an aprox. 0.5 mm interlayer) of pre-mixed metal-ceramic powders were placed on the metal green compact, previously inserted in the graphite die, and stacked to turn the layer uniform. Ceramic powders were then inserted in the graphite die, and the set was hot pressed in the conditions described in 2.2.

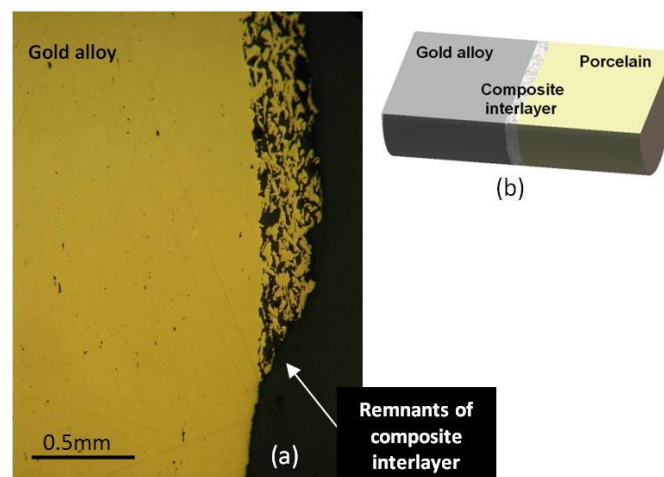


Figure 3.4. Cross section view of metal-ceramic specimen's with 50Met50Cer composite interlayer. a) Fracture zone showing remnants of the composite interlayer in the metal surface. b) Schematic of the specimen's cross-section.

Shear bond strength obtained for 50Met50Cer composite interlayer specimens was 201.8 ± 11.4 MPa. The fracture typology observed for these specimens exhibited the same behavior registered before for the other tested specimens, with remnants of the composite interlayer in both metal and ceramic substrates (Figure 3.4b).

Figure 3.5 presents a SEM/ EDS analysis of the metal-ceramic interface (Watari et al., 1997). Inter-diffusion of some elements was verified between the two materials. Elements constituting of the gold alloy (e.g. Au, Pt, Pd, Ag and In) were found in the vicinity of the interface, but in a very small range (Figure 3.5a). On the other hand, elements of porcelain (e.g. O, Sn, Al, Si, Ca, Na and K) were the ones that diffused the most and with the biggest range. A remark should be made relatively to Oxygen, which was the ceramic's element with the highest concentration found in metal's side (Figure 3.5b).

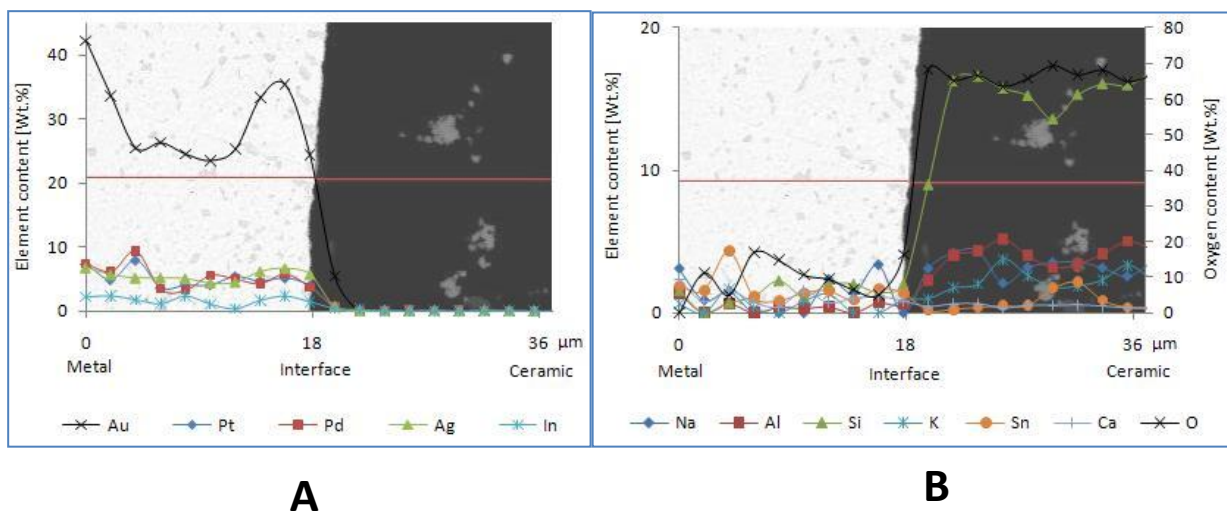


Figure 3.5. EDS line analysis of metal/ceramic interface. a) Inter-diffusion of metal alloy elements in ceramic. b) Inter-diffusion of ceramic elements in metal.

4. Discussion

4.1. Materials

This study aims to evaluate the influence, in bond strength, of a composite in the interface of a gold alloy-porcelain restoration.

Keramit 750 is a gold based alloy with several elements (Pd, Pt, In, Fe and Ir), each of them playing different roles. The significant presence of Pd and Pt, contributes for a considerable solution hardening and leads to a widening of the separation between the solidus and the liquidus line of the solid solution phase diagram. These elements are also used to decrease the melting point and recrystallization temperature of gold alloys, an important fact in metaloceramic prosthetics. This alloy also contains In in its composition which is used to improve the bonding strength between porcelain and metal, and the mechanic properties of the metallic framework (Hautaniemi, 1995; Liu and Wang, 2007; Fischer, 2002). Elements like Fe and Ir help in grain refinement and consequently, mechanical properties enhancement. As reported in the literature (Vásquez et al., 2009; Donovan and Swift, 2009; Shell and Nielsen, 1962; Drummond et al., 1984; Haselton et al., 2001; Chang et al., 2002) dental restorations involving gold alloys present more longevity than others performed with base materials (CoCr and NiCr alloys).

Due to its mechanical properties as well as its good adhesion to dental gold alloys (Rizakalla and Jones, 2004), Ceramco3 Opaque was the selected porcelain to carry out this study (Vásquez et al., 2009; Shell and Nielsen, 1962; Drummond et al., 1984).

4.2. Metal-ceramic sharp transition vs. smooth transition

Reporting to a previous study (Henriques et al., 2011), hot pressing (pressure + temperature) proved to enhance, in over 50% (up to 120 ± 25.4 MPa), the bond strength between this gold alloy and porcelain relative to a conventional PFM (Porcelain Fused

to Metal) ($83.7 \pm 14.0 \text{ MPa}$) (PFM is a firing process without pressure). This was explained by a more intimate contact between the materials to bond, due to pressure, leading to an enhancement of diffusion mechanisms and avoidance of undesired interface defects like porosity and cracks.

The increase on the surface roughness also proved to positively influence the metal-porcelain bonding strength ($128.5 \pm 4.9 \text{ MPa}$). In this case, an approximately 7% higher bond strength was registered for a 10 times higher surface roughness. Surface roughness contributes to a better mechanical interlocking and to a higher adhesion surface area. This means that when one combines temperature with pressure and surface roughness the bond strength of metal-ceramic composite is highly improved.

Based on these outputs, the presence of a smooth interface between metal and ceramic was considered and studied, through the use of a metal-ceramic composite interlayer. Figure 3.6 is an example of a metal-ceramic smooth transition using a 50Met-50Cer composite interlayer. The interlayer was obtained by powder metallurgy technique, which is a very simple way to tailor a metal-ceramic composite through the blending of different volume fractions of the desired materials for the interface (Liu et al., 2006; Chenglin et al., 1999; Kawasaki and Watanabe, 1997; Watari et al., 1997; Kieback et al., 2003).

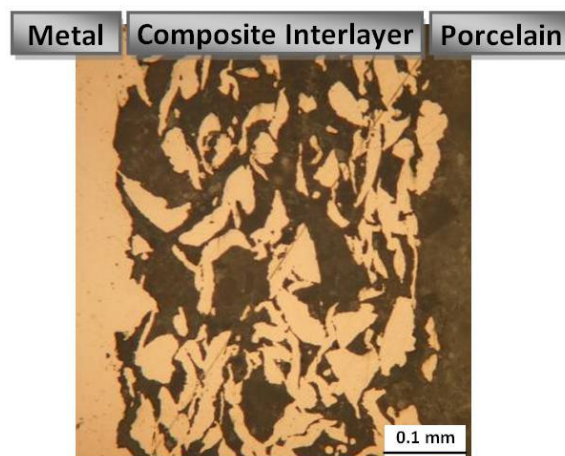


Figure 3.6. Optical microscope view of a 50Met-50Cer composite interlayer 200x.

In a conventional PFM (Porcelain Fused to Metal) restoration, there is a sharp transition between metal and ceramic which induces a properties mismatch (Young Modulus, hardness, chemical composition, etc) between materials involved. A Young Modulus mismatch causes different elastic behaviors of the two materials in the interface, upon loading, that can cause failure of the system. Using a composite interlayer, composed by the two materials to bond (metal+ceramic), we are introducing in the interface a material that has mixed properties between metal and ceramic ones, thus avoiding a sharp transition of material properties. This feature is something that nature already provides for natural teeth in dentin-enamel-junction (DEJ), for instance. Dentin and enamel are the two materials that constitute natural teeth. Enamel with ~65 GPa Young's Modulus and dentin with ~20 GPa Young's modulus are bonded by DEJ. In DEJ, the Young's Modulus changes linearly from that of enamel to that of dentin reducing dramatically the stress in the enamel or crown layer (Huang et al., 2007). The use of a functionally graded material (FGM) layer between ceramic crowns and cements proved to significantly reduce interface stresses between crown and cement (Huang et al., 2007). Stresses are regarded to be responsible for many dental restorations failures (dental ceramic + cement) mainly due to sub-surficial radial cracks (Lawn et al., 2002; Soboyejo, 2001).

Shear strength results registered for PMCC (Pressed Metal-Ceramic Composites) specimens were substantially higher than those referred in literature for sharp transition interfaces (Henriques et al., 2011) even when hot pressed techniques are employed (Vásquez et al., 2009; Shell and Nielsen, 1962; Drummond et al., 1984; Liu et al., 2008; dos Santos et al., 2006; Fischer, 2002; Chang et al., 2002; Henriques et al., 2011). From Figure 3.3 it is possible to see that the range of results go from ~160 MPa to 230 MPa, to Cer-Composite(20Met80Cer) and Met-Composite(60Met40Cer), respectively. Composites, regardless of their composition, showed a generally better adhesion to ceramic substrate than to a metal one. The highest values were registered for the 60Met40Cer and 40Met60Cer composites composition with preponderance to the second one. This means that the best results are obtained for composites with a composition of similar metal/ceramic quantities.

The higher bond strength results obtained in PMCC (Pressed Metal-Ceramic Composites), relatively to PPMP (Porcelain Pressed to Metal Powders), are explained by the introduction of the smooth transition zone between the base materials. This allows a smooth transition of the materials' properties along the interface (Figure 3.6). Stresses in the interface are also very different from a conventional PFM (Porcelain Fused to Metal) and PPMP (Porcelain Pressed to Metal Powders) restoration, as indicated in Figure 3.7. A smooth transition, instead of a sharp one, provided by the presence of a composite interlayer allows a reduction of stress mismatch in the vicinity of the interface (obtained by the combined effect of the reduction of the stress maximum level obtained at sharp interface ($\tau_2 < \tau_1$ in Figure 3.7) and by the distribution of the developed stresses by a higher volume of material).

Also, the presence of a composite interlayer increases the bonding area between the two materials.

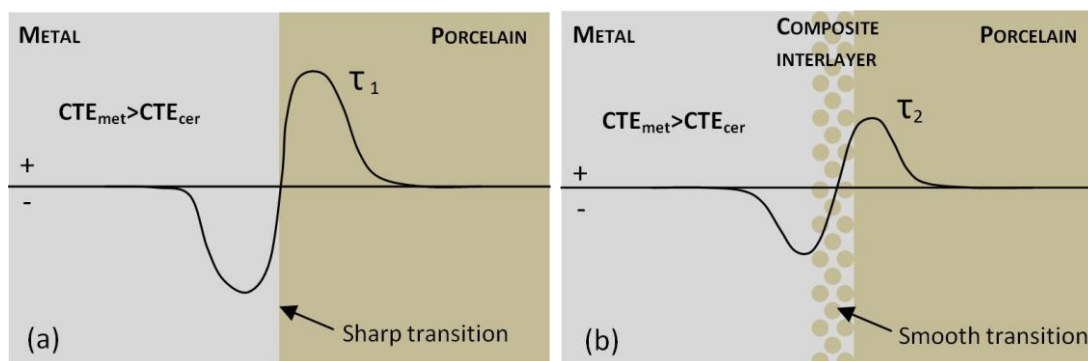


Figure 3.7. Schematic of shear stresses in metal-ceramic interface. (a) conventional PFM restoration – sharp interface; (b) Hot pressed metal-ceramic restoration with a composite interlayer – smooth transition.

4.3. Toughening mechanisms of the metal-ceramic composite interlayer

In fact the metal-ceramic composite interlayer is nothing more than a metal matrix composite (MMCp). It is generally recognized that two types of strengthening may

occur in MMCp: direct and indirect (Dai et al., 2001). Direct strengthening results from load transfer from metal matrix to the reinforcing particles (phase) whereas indirect strengthening results from the influence of the reinforcement on matrix microstructure or deformation mode. Therefore, strain hardening phenomena might be occurring in the metal and the restriction to its plastic deformation due to the presence of ceramic particles (enhancing mechanical resistance). Simultaneously, the presence of a metal phase surrounding the ceramic phase avoids a premature fracture of ceramic particles due to the capacity of the metal to accommodate their strain. Considering the Figure 3.4, the increase of the shear strength from composition 20Met80Cer to 50Met50Cer is explained by the increase of the metal phase with the hardening effect being predominant. From the 80Met20Cer to 50Met50Cer, the increase in ceramic particles is responsible for the deformation constraint of the metal phase, leading to increased shear strength.

In MMCp toughness depends on a complex interaction between the constituent phases. Fracture toughness is a measure of resistance to crack propagation. When a crack propagates through a particulate reinforced composite there are many mechanisms which may, to a larger or smaller extent, hinder the crack growth (Figure 3.8). Each of these mechanisms absorb energy, whereby requiring more work to be done by the external load (Davidson, 1991). They are: (1) deformation within plastic zone, (2) formation of voids along fracture surface, (3) fracture of reinforcement particles along crack path, (4) interfacial separation between matrix and reinforcement, (5) fracture of reinforcement with plastic zone, (6) tortuous fracture path, increasing fracture surface area and (7) matrix crack near, but not continuous with the main crack.

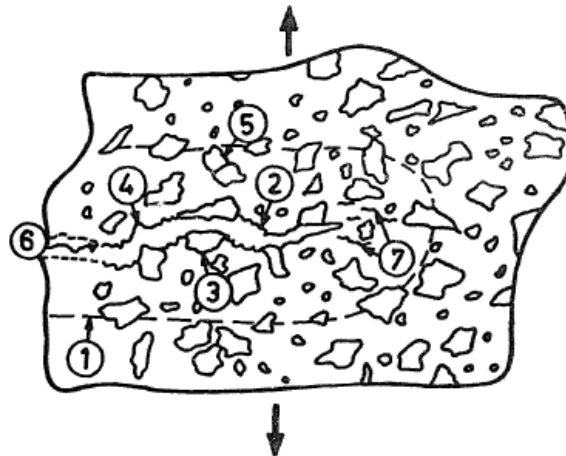


Figure 3.8. Different energy absorption mechanisms in metal matrix composites with discontinuous reinforcements (Davidson, 1991).

Detrimental effects of an increased amount of metal-ceramic interface, like fragile intermetallic phases, porosity, stress concentration, etc., must also be considered. However, obtained results show that these effects are not predominant for the studied metal-ceramic system.

The analysis of the fracture surfaces of PMCC (Pressed Metal-Ceramic Composites) specimens showed remnants of composites in all tested specimens which indicates a good adhesion of the composites to the substrates, whether they are metal or ceramic.

With the introduction of the transition zone, in the case of 40Met60Cer composite, there was an improvement of 70% in bond strength, relatively to results obtained for hot pressed specimens with metal-ceramic sharp transition, and 160% relatively to the conventional PFM (Porcelain Fused to Metal) (Henriques et al., 2011).

Attaining to experimental results presented in Figure 3.4, one can conclude that shear bond strength is maximized for composites with similar metal:ceramic [%Vol.] content. Hence, several metal ceramic specimens were produced with a 50Met50Cer composite interlayer. Shear strength results obtained were very promising (201.8 ± 11.4 MPa) proving that the interlayer had the expected effect of improving metal/ceramic bond

strength. The fracture zone of the specimens showed remnants of the interlayer's composite (Figure 3.4) as observed previously for metal-composites and ceramic-composites specimens. Composites showed, once more, a very good adhesion to metal and to ceramic substrates.

4.4. Practical application

In what concerns to practical application of the outputs of this study, a method that can be used to create a composite interlayer in a metal ceramic interlayer is painting the metal framework with a slurry of blended metal and ceramic powders prior to the ceramic veneering. This can be done using the traditional PFM (Porcelain Fused to Metal) technique. However, in order to reduce the interface defects (porosity, microcracks, etc), it can be used a uniform pressure during sintering. Therefore, it might be used a laboratorial Hot Isostatic Pressing (HIP) furnace using inert gas, such as argon.

Another approach is using rapid manufacturing (RM) techniques. Recently, great advances in (RM) of dental prostheses using powder metallurgy have been made, and the commercial manufacturing of multi-material parts is not very far in time. It has already been developed multi-material laser-assisted densification processes for dental restorations, in which dental restorations are built with powders (dental alloy and porcelain) delivered by slurry extrusion, followed by laser densification of these extruded slurries (Wang et al., 2002; Li et al., 2000; Li et al., 2001a; Li et al., 2001b). Because this is a layer-by-layer process, it can be easily used to create the complete coping with a metal base, followed by a composite interlayer and finally the ceramic veneer. All this can be done with no human intervention, once it is produced directly from a computer model.

5. Conclusions

From this study, the following conclusions can be drawn:

1. The metal-ceramic composites showed better bond strength to metal and to ceramic frameworks than those observed in a sharp transition between metal and porcelain. Improvements in bond strength can reach 160% when compared with a conventional PFM;
2. Powder metallurgy based dental restoration appears to be a feasible method and can, inclusively, produce better results than those obtained by other methods.

6. References

Anusavice KJ. Phillips' science of dental materials. 11th ed. Philadelphia:W.B. Saunders; 2003. pp. 621-54.

Chang JC, Koh SH, Powers JM, Duong JH. Tensile bond strengths of composites to a gold-palladium alloy after cycling. *J Prosthet Dent* 2002; 87(3): 271-276.

Chenglin C, Jingchuan Z, Zhongda Y, Shidong, W. Hydroxyapatite-Ti functionally graded biomaterial fabricated by powder metallurgy. *Mater Sci and Eng A*, 1999; 271: 95-100.

Dai, LH, Ling Z, Bai YL. "Size-dependent inelastic behaviour of particle-reinforced metal-matrix composites." *Compos Sci Tech*, 2001; 61: 1057-1063.

Davidson DL. Fracture toughness of particulate of particulate metal matrix composites, in R.K. Everett and R.J. Arsenault (eds.), *Metal matrix composites: Mechanisms and properties*, Academic Press, London, 1991, pp. 217-234

de Souza JCM, Avaliação de sistemas metalocerâmicos dentários metalizados mecanicamente com titânio. MSc Thesis. 2006

Donovan TE, Swift EJJr. Porcelain-Fused-to-Metal (PFM) Alternatives. *Journal Compilation*, 2009; 1: 4-6.

dos Santos JG, Fonseca RG, Adabo LG, Cruz CAS. Shear bond strength of metal-ceramic repair systems. *J Prosthet Dent*, 2006; 96(3); 165-173.

Drummond JL, Randolph RG, Jekkals VJ, Lenke JW. Shear Testing of the Porcelain-Metal Bond. *J Dent Res*, 1984; 63: 1400.

Eames WB, Rogers LB, Feller PR, Price WR. Bonding agents for repairing porcelain and gold: an evaluation. *Oper Dent*, 1977; 2: 118-122.

Fischer J. Ceramic bonding to a dental gold-titanium alloy. *Biomaterials*, 2002; 23: 1303-1311

Haselton DR, Diaz-Arnold AM, Dunne JT Jr. Shear bond strengths of 2 intraoral porcelain repair systems to porcelain or metal substrates. *J Prosthet Dent*, 2001; 86: 526-531.

Hautaniemi JA. The effect of indium on porcelain bonding between porcelain and Au-Pd-In alloy. *J Mater Science: Materials in Medicine*, 1995; 6: 46-50.

Henriques B, Soares D, Silva F. Shear bond strength of a Hot Pressed Au-Pd-Pt alloy-porcelain dental composite. *J Mech Behav Biomed Mater*, 2011; 4(8):1718-26

Huang M, Wang R, Thompson V, Rekow D, Soboyejo WO. Bioinspired design of dental multimaterials. *J Mater Sci*, 2007; 18: 57-64.

Kawasaki A, Watanabe R. Concept and P/M Fabrication of Functionally graded materials. *Ceramics International*, 1997; 23: 73-83.

Kelly JR. Ceramics in restorative and prosthetic dentistry. *Annu Rev Mater Sci*, 1997; 27: 443-36.

Keramit 750 Alloy data. Online. 2010. Available from URL: http://www.nobilmetal.it/english/pages/non_precious_alloys.html

Kieback B, Neubrand A, Riedel H. Processing techniques for functionally graded materials. *Materials Science and Engineering*, 2003; A362: 81–105.

Knosp H, Holliday RJ, Corti CW. Gold in dentistry: Alloys, Uses and Performance. *Gold Bulletin*, 2003; 36(3): 93-102.

Lawn BR, Deng Y, Lloyd IK, Janal MN, Rekow ED, Thompson VP. Material design ceramic based layer structures for crown. *J Dent Res*, 2002; 81: 433-438.

Lavine MH, Custer F. Variables affecting the strength of bond between porcelain and gold. *J Dent Res*, 1966; 45(1):32-6.

Li X, Crocker J, Geiss E, Shaw L, Marcus H, Cameron T. Evaluation of microstructure and properties for multi-materials laser densification of dental restorations. In: Proceedings of 11th Solid Freeform Fabrication Symposium, Austin, TX, 7–9 August 2000, pp 159–167 335

Li X, Crocker J, Shaw L, Marcus H, Cameron T (2001) Laser densification of nickel powder for dental restorations. In: Proceedings of the 2001 NSF Design, Manufacturing & Industrial Innovation Research Conference, Tampa, FL, 7–10 January 2001, pp 1–8

Li X, Wang J, Augustine A, Shaw L, Marcus H, Cameron T. Microstructure evaluation for laser densification of dental porcelains. In: Proceedings of 12th Solid Freeform Fabrication Symposium, Austin, TX, 6–8 August 2001, pp 195–202.

Liu J, Qiu XM, Zhu S, Sun DQ. Microstructures and mechanical properties of interface between porcelain and Ni-Cr alloy. *Mat Sci and Eng A*, 2008; 497: 421-425.

Liu Q, Leu MC, Schmitt SM. Rapid prototyping in dentistry: technology and application. *Int J Adv Manuf Technol*, 2006; 29: 317-335.

Liu WB, Wang JN. Strengthening of Pd-free high gold dental alloy for porcelain bonding by a pre-firing heat treatment. *Dent Mater* 2007; 23:1136-1141.

Özcan M. Fracture reasons in ceramic-fused-to metal restorations. *Journal of Oral Rehabilitation*, 2003; 30: 265-269.

Rizkalla AS, Jones DW. Indentation fracture toughness and dynamic elastic moduli for commercial feldspathic dental porcelain materials. *Dent Mater*, 2004; 20: 198-206.

Shell JS, Nielsen JP. Study of the Bond between Gold Alloys and Porcelain. *J Dent Res*, 1962; 41: 1424-1437.

Soboyejo WO, Wang R, Katsube N, Seghi R, Pagedas C, Skraba P, Mumm DR, Evans AG. Contact damage of model dental multilayers: Experiments and finite element simulations. *Key Eng Mater.* 2001; 198-199: 135-178.

Strauss JT. Rapid Manufacturing and Precious Metals. *Proceedings of the 23rd Santa Fe Symposium*, 2009; 395-416.

Vásquez VZC, Oscar M, Kimpara ET. Evaluation of interface characterization and adhesion of glass ceramics to commercially pure titanium and gold alloys after thermal- and mechanical-loading. *Dent Mater*, 2009; 25: 221–31.

Wang J, Li X, Shaw L, Marcus HL. Studies on slurry extrusion for dental restoration. In: *Proceedings of the 13th Annual Solid Freeform Fabrication Symposium*, Austin, TX, 5–7 August 2002.

Watari F, Yokoyama A, Saso F , Uo M, Kawasaki T. Fabrication and properties of functionally graded dental implant. *Composites Part B*, 1997; 28B:5-11.

Chapter 4

Influence of preoxidation cycle on the bond strength of CoCrMoSi-porcelain dental composites

Published in the journal Materials Science and Engineering C, 2012, doi: 10.1016/j.msec.2012.07.010

B. Henriques, D. Soares, F.S. Silva

*Centre for Mechanical and Materials Technologies (CT2M) and Department of Mechanical Engineering,
University of Minho, Azurém, 4800-058 Guimarães, Portugal*

Abstract

Objective: The purpose of this study was to evaluate the effect of preoxidation cycle on the shear bond strength (SBS) of CoCrMoSi alloy-porcelain dental composites.

Methods: The porcelain was fired onto three types of metal surfaces: non-preoxidized, preoxidized and, preoxidized followed by grinding. The bond strength of metal-porcelain composites was investigated by the means of a shear test. The metal-ceramic interfaces and the fractured surfaces were analyzed using Optical Microscopy,

Stereomicroscopy and SEM/EDS. Data was analyzed with Shapiro-Wilk test to test the assumption of normality. The t-test was used to compare shear bond strength results ($p < 0.05$). The analysis of the three types of surfaces was performed prior to porcelain firing. It was also performed a complementary analysis of an alumina-blasted preoxidized CoCrMoSi surface. The greater metal-porcelain adhesion was obtained for non-preoxidized specimens.

Results: Non-preoxidized specimens showed significantly ($p < 0.05$) higher shear bond strength than preoxidized/ground specimens, 115.5 ± 7.5 MPa and 74.8 ± 8.5 MPa, respectively. Porcelain showed no adhesion to preoxidized specimens. All preoxidized specimens exhibited adhesive failure type while non-preoxidized presented both adhesive and mixed failure types. Preoxidation heat treatment revealed a detrimental effect on the adhesion of CoCrMoSi-porcelain composites for dental restorations.

Significance: Hence, in order to enhance CoCrMoSi-porcelain adhesion, the preoxidation heat treatment conditions, as performed in this study, should not be performed.

1. Introduction

Despite the use of all-ceramic restorations rapidly growing, porcelain fused to metal (PFM) restorations is still the most used technique within prosthetic dentistry. With its history of nearly 50 years serving dentistry, PFM technique is known to produce aesthetic and reliable restorations proved by their great survival rates (Coonaert et al., 1984). Some studies reported that up to 88.7% of metal-ceramic crowns and 80.2% of metal-ceramic fixed partial dentures (FPDs) were still in function after 10 years (Özcan, 2003). All-ceramic crowns are regarded to provide generally better aesthetics for anterior teeth than metal-ceramic ones but they do not warrant the necessary strength to be used for posterior teeth. Although failure reports are decreasing over

the last years, especially for pressed ceramics, its recent history does not allow drawing conclusions in respect to their long term clinical performance.

For many years gold based alloys were the primary choice for dental restorations because of their high biocompatibility. In 1971, the United States abandoned the gold standard and, as result, its price together with other noble metals increased sharply over the next nine years. Because of the unstable price of the noble metals during this period, most dental laboratories started using alternative materials such as Ni-Cr and Co-Cr alloys. Besides their low price, the obvious advantages of base metal alloys are their lower weight, greater stiffness (elastic modulus) and other beneficial mechanical properties (Anusavice, 2006; Roberts et al., 2009). Co-Cr alloys have an advantage over Ni-Cr alloys based on its great biocompatibility relative to the allergenic potential of the nickel (Roberts et al., 2009; Kelly and Rose, 1983; Baran, 1985). Studies are divergent about the bond strength of non-precious alloy systems. Anusavice (2006), based on in vivo studies, states that there is no evidence of inferior or superior bond strength values of Ni-Cr or Co-Cr alloys, relative to those observed in noble metal alloys. He also reports no difference in failure incidence between metal-ceramic restorations made by base metal alloys and those obtained by noble metal alloys. On the contrary, Drummond et al. (1984) found a significant decrease, in a range of 40%, in shear bond strength of non precious alloys-porcelain systems vs. gold-porcelain systems.

Base metal alloys are formed by elements that are able to be oxidized, especially chromium. Therefore, one of the challenges in this type of alloys is controlling the excessive formation of chromium oxide that results in lower bond strength between metal and porcelain (Rokni and Baradaran, 2007; Mackert et al., 1984; Mclean and Sced, 1973; Sced and Mclean, 1972).

The way this oxide interacts with porcelain during firing cycle has originated several theories. Kautz (1936) suggested that the adherent-to-metal oxide scale is wetted by the porcelain and becomes the transition zone between the two materials. Later, King et al. (1959) believed that the layer of glass nearest the metal dissolves the oxide on

the surface of the metal and that a layer of oxide-saturated glass bonds directly with the metal surface. This thinking was based on the premise that “few oxides are sufficiently adhesive to their metals to produce excellent [porcelain] adherence”. This theory was later adopted by Pask and Fulrath (1962) and Pask (1977), although they do consider the possibility of existence of a discrete oxide layer at the interface and state that once it is present, it must be adherent to the metal.

Posterior studies performed by Miyagawa (1978) and Ritchie et al. (1983) have shown that a discrete oxide layer must be present at the interface. Therefore, Mackert et al. (1984) tried to ascertain whether the oxides formed on dental PFM alloys were sufficiently adherent to their alloys to allow for excellent porcelain adherence and concluded that adherence between oxide formed on the metal surface and porcelain plays a dominant role in porcelain.

There are several oxidation heat treatments of the metal for different purposes: degassing removes the entrapped gas; outgassing eliminates surface contaminants and preoxidation creates an oxide scale (Anusavice, 2006). Besides their main purpose, these treatments may cause collateral effects such as stress releases and framework distortions (Yashihiro, 1984; Bryant and Nicholls, 1979). Wu et al. (1991) determined the effect of oxidation heat treatment on porcelain bond strength in selected base metal alloys and concluded that it didn't have a significant effect on them.

On the contrary, Dekon et al. (1999) and Rokni and Baradaran (2007) found a significant difference in NiCr-porcelain bond strength between oxidized and non-oxidized samples but with divergent results. The former author registered the best results for non-oxidized samples and the latter for oxidized ones. Wagner et al. (1993) found an improvement of 152% on bond strength for preoxidized palladium alloys. Daftary et al. (1986) used different pretreatments on noble and base metal alloys to evaluate their effect on metal-porcelain bond strength. They found significant differences between the different metals and pointed out that each alloy should be treated differently.

This study evaluated the effect of preoxidation heat treatment on the bond strength of a commercial CoCrMoSi alloy to porcelain. It was developed an integrated investigation in terms of the element diffusion profiles at the interaction zone, the ceramic fracture types and the alumina-blasting surface treatment for oxide removal.

2. Materials and methods

2.1. Specimens composition and preparation

For this work a CoCrMoSi dental alloy (Nobil 4000, Nobilmetal, Villafranca d’Asti, Italy) and a dental opaque ceramic (Ceramco3, Dentsply, York, USA) (batch number: 08004925) was used (Nobil4000, 2010; Ceramco3, 2010). The chemical composition of the commercial base alloy Nobil 4000 is presented in Table 4.1. Every alloying element plays a specific role in this alloy. Hence, cobalt is the main constituent in this alloy and chromium is added to provide strength and corrosion resistance via passivation (Metikoš-Huković and Babić, 2007; Hiramoto et al., 2005). Molybdenum, iron and tungsten are added for solid solution hardening (Roberts et al., 2009; Mankins and Lamb, 1990). Molybdenum has the added benefit of influencing the coefficient of thermal expansion (Kelly, 1983; Crook, 1990). Silicon imparts good casting properties and increases alloy ductility (McCabe and Walls, 2008).

In Table 4.2 is presented the chemical composition of Ceramco3 Opaque porcelain. This porcelain was selected for this study because of its recognized mechanical properties (Rizkalla and Jones, 2004) and due to its suitability to bond to CoCr dental alloys (Nobil4000, 2010).

Table 4.1. Base alloy composition (wt.%) (according to manufacturer).

Co	Cr	Mo	Si	Others
62	31	4	2.2	Mn – Fe – W

Table 4.2. Ceramic chemical composition (wt.%).

SiO ₂	Al ₂ O ₃	K ₂ O	SnO ₂	ZrO ₂	CaO	P ₂ O ₅	Na ₂ O	Others
41.3	14.5	14.0	11.9	5.8	4.1	4.1	3.0	MgO, SO ₃ , ZnO, Cr ₂ O ₃ , Fe ₂ O ₃ , CuO, Rb ₂ O

Metal substrates were directly produced from metal rods supplied by the manufacturer. Rods were machined to a diameter of 4.5mm and then cut into several 4mm high substrates using a precision cut-off machine (Minitom, Struers). Afterwards, all substrates were finely ground with 2400-grit SiC paper, ultrasonically cleaned in an alcohol bath for 10 min and rinsed in distilled water for 10 min to remove contaminants. Then they were dried with adsorbent paper towels.

Metal substrates were split in two groups: non-preoxidized and preoxidized substrates. Preoxidation heat treatment comprised a 10 min stage in air at 1000°C. After preoxidation, substrates were again split in two groups. Part of them were stored with the oxide scale formed during preoxidation cycle and the rest was light ground with 2400-grit SiC paper to remove the non-adherent oxide layer formed on metal surface. Indeed, manufacturer instructions recommended a light alumina blasting of metal's surface to remove the oxide scale. The grit-blasting, however, would introduce a substantial amount of surface roughness, which is very important in metal-ceramic adherence but was not desired for this study. In order to avoid the introduction of this new variable (roughness), it was decided to perform this study without the influence of complicating surface-roughness effects, thus this step (grit-blasting) was omitted and replaced by a fine grinding of the surface (2400-grit SiC paper) that would not introduce any surface roughness. This allows the study of the influence of the preoxidation heat treatment on the chemical bonding between the metal and the porcelain without the effect of mechanical interlocking provided by metal surface roughness.

In order to guarantee a flawless interface, porcelain powders were hot pressed onto the metal substrate. First, graphite die was painted with ZrO₂ in order to impede

carbon diffusion to specimen. Then, the metal substrate was placed in die's cavity followed by the porcelain powder. Finally, the set was heated up to 970°C at a heating rate of approximately 60°C/min and remained at that temperature for 2 minutes. Hot pressing was performed under vacuum ($\sim 10^{-2}$ mBar) and at a pressure of ~ 20 MPa.

A SEM-EDS analysis was performed on the surface of the following specimens: (1) non-preoxidized; (2) preoxidized and (3) preoxidized specimens followed by oxide removal with P2400-grit SiC paper. Although sandblasting effect had been omitted for bond strength purposes, it was decided to conduct a broad surface analysis also on an (4) alumina blasted preoxidized specimen comprising a mechanical (surface hardness and roughness) and a chemical (SEM-EDS) component. Alumina blasting of the preoxidized metal surface was performed according to manufacturer's instructions with $\varnothing 110 \mu\text{m}$ grains at a pressure of 0.5 bar (Protempomatic, Bego, Germany). After sandblasting, samples were ultrasonically cleaned in an alcohol bath for 10 minutes and rinsed in distilled water for another 10 minutes. Amongst other things, this step allowed to quantify the oxidation level of the CoCrMoSi surface after sandblasting treatment.

2.2. Shear bond strength tests

Metal-porcelain bond strength was assessed by the means of shear bond strength test. Several tests have been used to assess metal-ceramic bond strength, namely the Schwickerath crack initiation test used in ISO 9693:1999, the three-point-flexure test, the four-point-flexure test, the biaxial flexure test, etc. However, based on literature data, all of them show great variability in the mean bond strength values with large standard deviations (Anusavice, 2006; Anusavice et al., 1980; Chong et al., 1980). The planar interface shear bond strength test used in this study is not influenced by the Young's Modulus of the alloy as happens in bending tests and is considered to be suitable for evaluation of metal-ceramic bonds (Anusavice et al., 1980; Ihab and Yourself, 1996).

The current standards that indicate the minimum acceptable bond strength for metal-ceramic composites are ANSI/ADA Specifications N°38 (2000) and ISO Standard 9693 (1999). Both employ the three-point-bending test and suggest a minimum value of 25 MPa for bond strength. Anusavice (2006) in his textbook suggests the minimum of 51 MPa as lower limit for bond strength, and points out that different values of bond strength are expected with different testing modes. Hence, due to geometrical differences of the specimens employed in the different bond strength tests, no direct comparison should be made with their results.

Tests were carried out at room temperature and performed in a universal testing machine (Instron 8874, MA, USA), with a load cell of 25 kN capacity and under a crosshead speed of 0.5mm/s. To perform the tests a custom-made stainless steel apparatus was built consisting of two sliding parts A and B, each one with a hole perfectly aligned. After the alignment of the holes, the specimens were placed in the apparatus letting the metal-porcelain interface aligned with the sliding plane of parts A and B. Then, a compressive load was applied in the push rod (part B) until fracture occurred. The shear bond strength (MPa) was calculated by dividing the highest recorded fracture force (N) for the area of adherent porcelain (mm^2) (area of cross section of the specimen).

2.3. Analysis of the metal-porcelain interface

The metal-ceramic interface as well as representative fracture surfaces were evaluated by stereomicroscope (SMZ-2T, Nikon, Japan), optical microscope (Axiotech, Carl Zeiss, USA) and SEM/EDS (Nova 200, FEI, Oregon, USA). For interface analysis, the specimens were embedded in auto-polymerizing resin, ground finished to 1200 grit SiC paper and polished with diamond paste first in $6\mu\text{m}$ and finally in $1\mu\text{m}$ felt disc. Morphologic and chemical analyses were performed. The elemental distribution across the metal-ceramic interface was determined by using line scan EDS analysis, allowing to obtain

the chemical composition profile along the metal-ceramic transition that comprised the metal side, the interfacial zone and porcelain side (20 points in the metal side and 20 points in the porcelain side).

The thickness measurement of the oxide layer formed at the metal-ceramic interface after porcelain sintering was obtained by analyzing 10 interface micrographs (SEM), 5 per condition (non-preoxidized and preoxidized/ground).

2.4. Metal surface characterization

Microhardness tests (Microhardness tester, type M, Shimadzu, Japan) were performed on the surface of a non-preoxidized CoCrMoSi substrate, prior and after alumina sandblasting ($\varnothing 110\mu\text{m}$; 3bar). This test intended to quantify the amount of work hardening produced on an alumina-blasted CoCrMoSi specimen's surface. The average surface roughness (Ra) of both types of specimens (finely ground and alumina-blasted) was measured using a profilometer (Mahr S5P, Germany) to make two orthogonal line measurements of 4mm length in each sample.

2.5. Statistical analysis

Data were analyzed using SPSS statistic software (Release 18.0.0 for windows). The Shapiro-Wilk test was first applied to test the assumption of normality. In order to find significant differences, in terms of bond strength results, between non-preoxidized and preoxidized specimens, a t-test was performed. A p-value of 0.05 was considered to be statistically significant.

3. Results

Shear bond strength results are presented in Figure 4.1 for non-preoxidized and preoxidized (ground and not ground) specimens. In preoxidized specimens, porcelain was directly fired over the greenish oxide layer present on the metal's surface, and showed no adhesion to it (Figure 4.1). Porcelain detached from metal substrate without the need of any external load, just by normal handling of the specimen.

Non-preoxidized specimens exhibited significantly ($p < 0.0001$) greater bond strength values than preoxidized/ground ones, 115.5 ± 7.5 MPa and 74.8 ± 8.5 MPa, respectively.

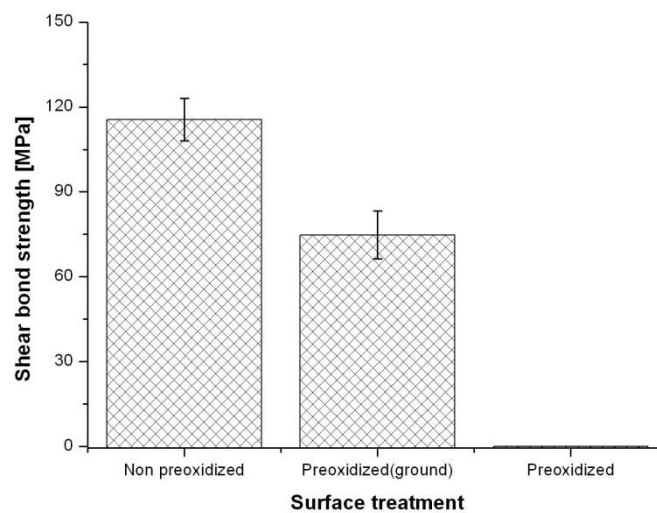


Figure 4.1. Plot of the shear bond strength results of CoCrMoSi-porcelain composites with different metal surface treatments: non-preoxidized, preoxidized/ground and preoxidized, respectively.

Specimens were classified under their failure type as adhesive, cohesive or mixed. The analysis of specimens' fracture surfaces revealed two types of failures: adhesive, when no remnants of ceramic were found on metal's surface; and mixed, when remnants of ceramic were detected on metal's surface. All non-preoxidized specimens exhibited adhesive failure. Half of preoxidized/ground specimens presented adhesive failures while the rest showed mixed failure type (Figure 4.2).

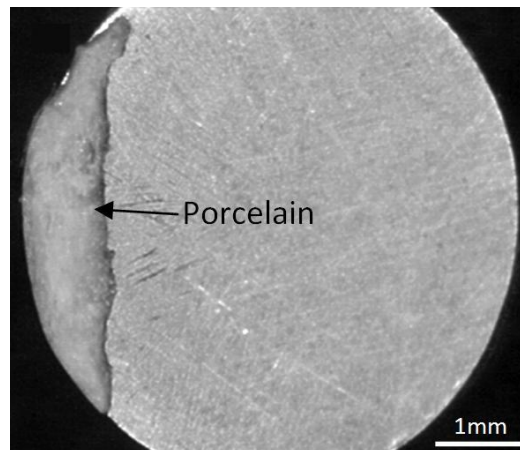


Figure 4.2. Fracture surface of preoxidized/ground specimen – mixed failure type.

Figure 4.3 shows an EDS line scan analysis (in white) for both non-preoxidized and preoxidized specimens. This analysis allows the comparison of element concentration profiles at the interaction zone for both situations. Element concentration profiles for all elements showed to be very similar in both cases and no significant change could be observed. Results show no diffusion of Co, Cr and Mo into porcelain. However, it is possible to see that Cr is present in the oxide layer formed on metal surface. Regarding porcelain elements, it was observed an extensive diffusion of all its elements (O, Si, Al, K, Sn, Na, Ca, Mg) into metal. Special relevance must be given to the O₂ in the metal zone, that was detected in a higher concentration.

The oxide layer, created during porcelain firing, at the metal-ceramic interface was subjected to a thickness measurement and to a chemical analysis. The preoxidized/ground specimens exhibited greater oxide layer thickness values than in the case of non-preoxidized ones, $0.47 \pm 0.09 \mu\text{m}$ and $0.27 \pm 0.20 \mu\text{m}$ respectively.

Elemental content analysis of oxide layer are presented in Table 4.3 and it is in line with results of Figure 4.3, which shows that oxide layer is formed by elements coming from the two base materials, metal and porcelain.

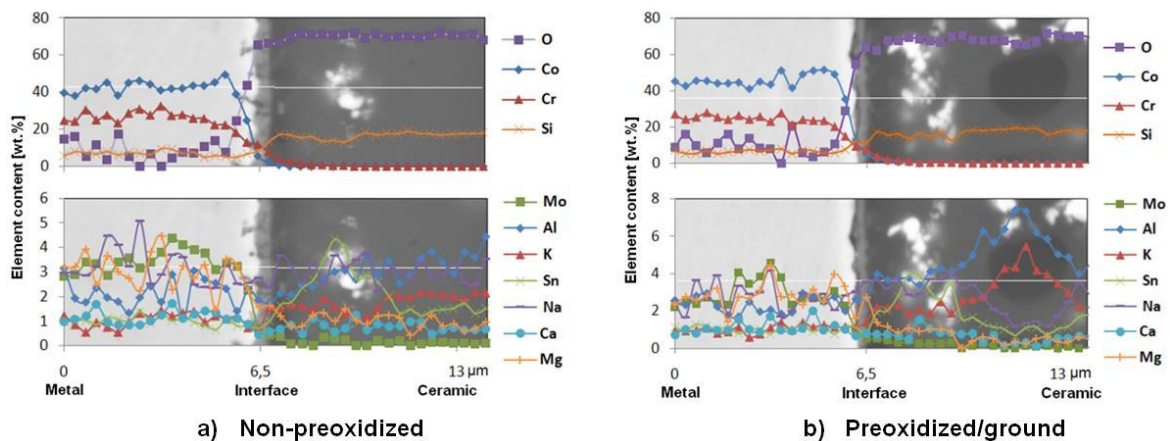


Figure 4.3. EDS line analysis of metal/ceramic interface. (a) Inter-diffusion elements in non-preoxidized specimens. (b) Inter-diffusion elements in preoxidized/ground specimens.

Table 4.3. Typical oxide layer element content (wt.%), after porcelain firing, obtained by EDS.

O	Co	Cr	Mo	Si	Al	K	Sn	Na	Mg
39.02	17.69	22.9	2.2	7.6	1.5	1.01	1.83	1.34	0.34

Table 4.4 shows a comparison of the elemental composition for four different types of surface conditions: 1- non-preoxidized finely ground surface; 2- preoxidized finely ground surface (Figure 4.4); 3 – alumina-blasted surface after preoxidation (Figure 4.4); 4 – finely ground preoxidized surface (Figure 4.5).

Results from Table 4.4 shows that grit-blasting does not remove the oxides from the metal surface in a great extent. It is possible to see that the amount of oxygen in the surface remains at a high level (Type 3). Aluminum traces were found on the alumina-blasted surface which has its origin in alumina particles that were retained at the surface. This finding should be considered when analyzing the amount of oxygen present in the surface, because part of it should belong to alumina particles (Al_2O_3). Therefore, the corrected value for the amount of oxygen found in the surface is 14.6%. Nevertheless, it is still twice the amount of oxygen's content found in the non-preoxidized surface (Type1).

The same table shows that the amount of oxide found in the surface of the finely ground preoxidized specimens (Type 4) is substantially lower when compared to Type 2 and Type 3 surface conditions. Within Type 4 surface condition, were identified three different zones (Figure 5): Z1 – remnants of the oxide layer, Z2 – Co rich and Mo poor content phase and Z3 – Co poor and Mo rich content phase.

Table 4.4. Elemental analysis of four types of surface conditions (wt.%).

Elements	Surface condition						
	Type 1	Type 2	Type 3	Type 4			
	Non-preoxidized	Preoxidized	Alumina-blasted after preoxidation	Finely ground (2400-mesh) after preoxidation			
	General	General	General	General	Z1	Z2	Z3
C	6.02	1.95	2.22	3.32	2.34	2.64	3.14
O	7.86	28.12	23.01	14.44	29.18	10.3	10.77
Al	--	--	7.75	--	--	--	--
Si	0.73	2.03	1.64	2.17	2.05	2.43	3.88
Mo	6.33	3.66	3.29	4.34	2.18	4.23	13.16
Cr	22.35	21.89	19.50	22.58	20.41	23.68	23.43
Co	56.71	42.35	42.59	53.15	43.83	56.72	45.62

Alumina-blasting treatment produced an approximately ten times rougher surface relative to finely ground one, $R_a=0.58\pm 0.01\mu\text{m}$ and $R_a=0.05\pm 0.01\mu\text{m}$, respectively.

The microhardness tests revealed an increase of 84% in the surface hardness of the alumina-blasted surface relative to the finely ground surface, corresponding to $614\text{HV}/1\pm 62$ and $334\pm 31\text{ HV}/1$, respectively.

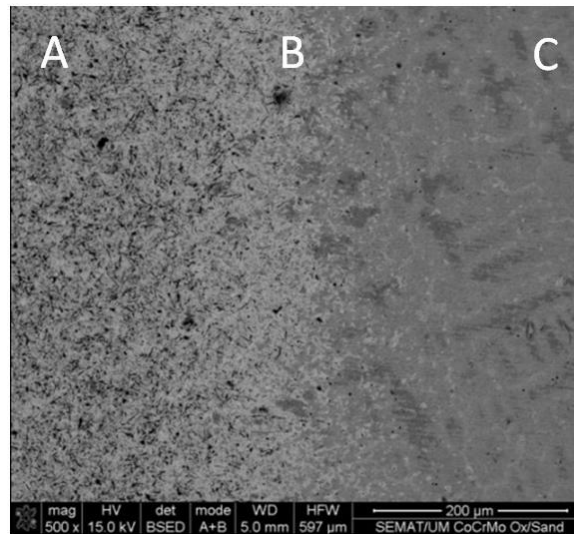


Figure 4.4. SEM micrographs (x500) of two CoCrMoSi surface conditions: (A) alumina-blasted surface; (B) transition zone between alumina-blasted and non-blasted oxidized surface; (C) finely ground surface after preoxidation.

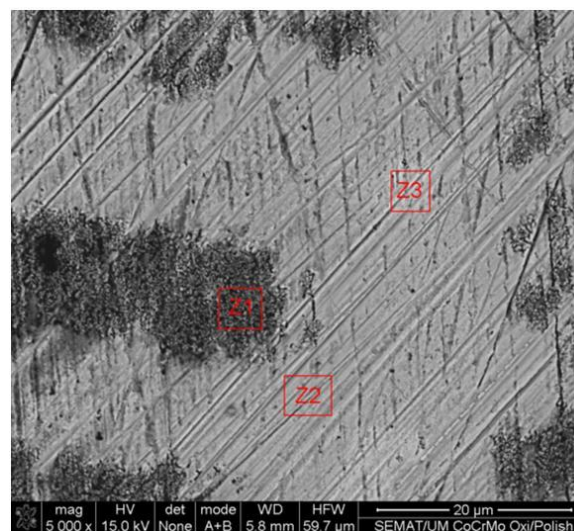


Figure 4.5. SEM micrograph: detailed view (5000x) of oxide layer remnants present on metal's surface, after fine grinding (2400-grit SiC).

4. Discussion

4.1. Preoxidation heat treatment

Preoxidation heat treatment of base metal alloys is a controversial subject (Wu et al. 1991). Despite the recommendation of the manufacturer for performing a preoxidation heat treatment prior to porcelain veneering, the current study showed a significant ($p < 0.001$) decrease on metal-ceramic bond strength for preoxidized specimens. The manufacturer's preoxidation cycle comprised the metal oxidation in a furnace at high temperature followed by grit-blasting for oxide removal. As mentioned before, grit-blasting of the preoxidized specimens was not performed, prior to ceramic bonding. The reason was that grit-blasting stage besides the oxide removal would introduce a substantial amount of surface roughness. Instead, the oxide scale was removed by fine grinding the oxidized surface (Type4) with fine sandpaper (P2400) in order to remove the oxide scale in excess and maintain the same surface roughness of the non-preoxidized specimens. This procedure removed approximately 85% of the oxide scale existing on the oxidized surface (Figure 4.5). This way, it was possible to test the bond strength between metal and ceramic without the action of mechanical interlocking effects provided by surface roughness introduced at the grit-blasting stage. For this research, the relative bond strength resulting from the two types of surface conditions (non-preoxidized and preoxidized) was considered to be more important than the absolute bond strength. Only one variable (oxidation) is evaluated instead of two simultaneous variables (oxidation and roughness).

The oxide formed on CoCrMoSi surface during preoxidation heat treatment (Type 2) proved to have very poor adherence to its metal. Actually, this is pointed as being the main cause for the premature failure of specimens where porcelain had been directly fired onto the preoxidized metal substrate, and where the metal-ceramic debonding occurred during specimens' handling. Mackert et al. (1984) found poor oxide adherence values for CoCrMoSi alloys, especially in the absence of their proprietary bonding agents.

The presence of oxide remnants at the preoxidized/ground specimens' surface (Figure 4.5) could, therefore, have accounted for their lower metal-ceramic bond strength relative to non-preoxidized specimens. The greater oxide thickness registered on the preoxidized/ground specimens (~75% greater than the one registered in non-preoxidized specimens) may also explain such behavior.

Studies on grit-blasted preoxidized specimens revealed divergent findings: Rokni and Baradaran (2007) found a statistically significant relation between the oxide layer and bond strength. They concluded that oxidation in air resulted in thicker oxide layers and lower bond strength in comparison with oxidation under vacuum. They pointed the excessive oxidation of the alloy as the reason for fracture through the metal oxide. On the other hand, Wu et al. (1991) found that the oxide film thickness did not have a relationship to porcelain bonding because the oxide adherence is related to vacancy accumulation Mackert et al. (1984). In the present study, some lenticular pocket accumulation was identified at the metal-oxide interface for both types of specimens (Figure 4.6 a-b). Such pockets might have their origin in the chromium-ion diffusion through the oxide layer, according to the chromium oxide growing mechanism (Lees and Calvert, 1976; Kofstad and Lillerud, 1980). This mechanism is regarded to produce metal-atom lattice vacancies at the metal-oxide interface (Giggs and Halles, 1977; Giggins and Petit, 1977) thus resulting in loss of oxide adherence. Nevertheless, no relevant difference was detected, in pockets' type and number, between preoxidized/ground and non-preoxidized specimens in this study. Therefore, this fact cannot be pointed as the cause for the different bond strength behavior of specimens.

4.2. Analysis of CoCrMoSi alumina-blasted surface

The microhardness and chemical tests performed on CoCrMoSi alumina-blasted surfaces allowed to characterize the hardening mechanisms and chemical modifications produced in non-preoxidized and preoxidized surfaces. Sandblasting not

only roughened the surface but also introduced considerable cold work into the surface layer of the metal, yielding an 84% increase on surface hardness, relative to finely ground surface. Cold work is regarded for changing the oxidation behavior, which can improve the oxide adherence (Petit, 1969; Caplan et al., 1970).

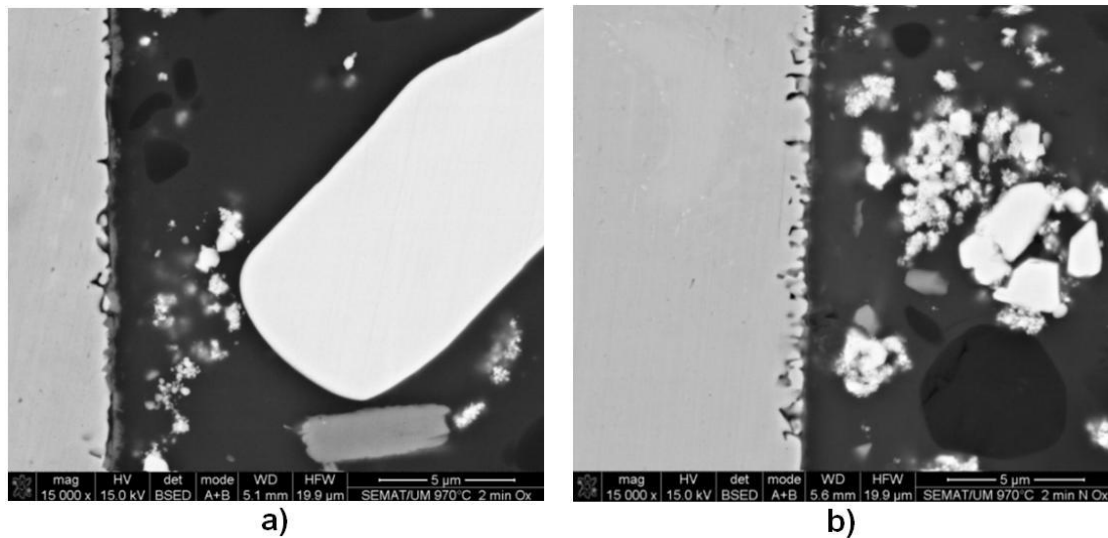


Figure 4.6. SEM micrograph (x15000) of (a) non-preoxidized and (b) preoxidized metal-porcelain interaction zone showing some lenticular pockets accumulation at the metal-oxide interface.

Sandblasting treatment is often performed to remove from the metal surface the oxide formed during preoxidation heat treatment. However, the oxygen concentration found in alumina-blasted surface (Type 3) was more than twice of the oxygen level found in a non-preoxidized surface (Type 1), see Table 4.4. Therefore, it suggests that a considerable amount of oxygen remains in the surface after alumina-blasting due to the disruption of the oxide layer and its inclusion on the deformed surface thus produced (Figure 4.7).

The elemental analysis of the alumina-blasted surface traced the presence of aluminum in a significant level as it is showed in Figure 4.8. Grit-blasting was performed with alumina particles and they are the natural origin of the aluminum

found on the surface. Johnson et al. (2006) in their analysis of the surface conditions of porcelain fused to metal systems also found the presence of Al_2O_3 on the surface of the investigated alloys after the alumina blasting stage. Studies have showed that the presence of alumina or aluminum on the metal surface alloys can have a positive effect on metal-ceramic bond strength (Wagner et al., 1993, Mackert et al., 1984, Whu et al., 1991). Aluminum is an easily oxidized element that can modify the oxide growth mechanism and suppress chromic oxide formation. This is regarded for the metal-ceramic bond strength improvement in NiCr and CoCr alloys, promoted by the enhancement in oxide adherence (Whu et al., 1991). Therefore, alumina-blasting can be regarded for a dual-effect surface treatment which results in mechanical and chemical surface modifications: 1) surface roughening and hardening through cold work; and 2) alumina embed on the metal's surface, respectively. Additionally, the increase of surface area created by sandblasting treatment also accounts for the increase of metal-ceramic adherence levels (Wagner et al., 1993).

It must be pointed out that these effects produced in metal surface by the alumina blasting treatment was not considered in the metal-ceramic bond strength assessment after preoxidation heat treatment performed in this study (section 4.1). In fact, the removal of the oxide layer in excess from metal surface after preoxidation can be done by several ways, namely: grit-blasting (with particles of alumina, silica, zirconia, etc.) or using burs (diamond, SiC, etc). Because alumina particles are often used by prosthetic technicians in this proceeding, it was decided to include an analysis to the surface modifications undergone by the preoxidized metal structure after alumina blasting treatment. Nevertheless, the contribution of this study, which do not recommend the preoxidation heat treatment for CoCrMo alloys, still valid regardless of the method used to remove the oxide layer formed during preoxidation heat treatment.

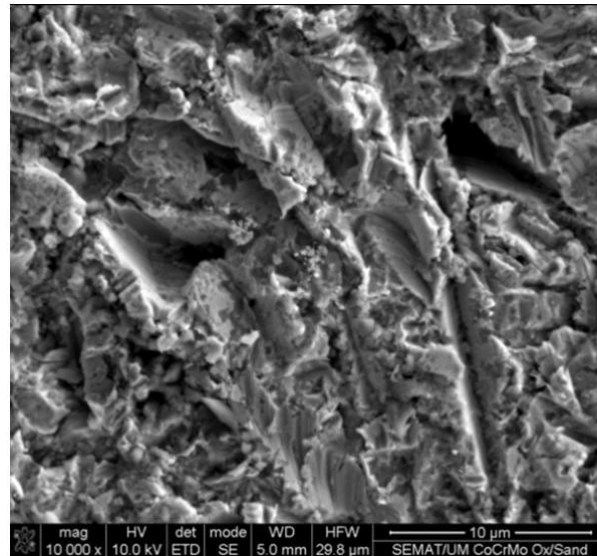


Figure 4.7. SEM micrograph showing the topography of an alumina-blasted CoCrMoSi surface after preoxidation heat treatment.

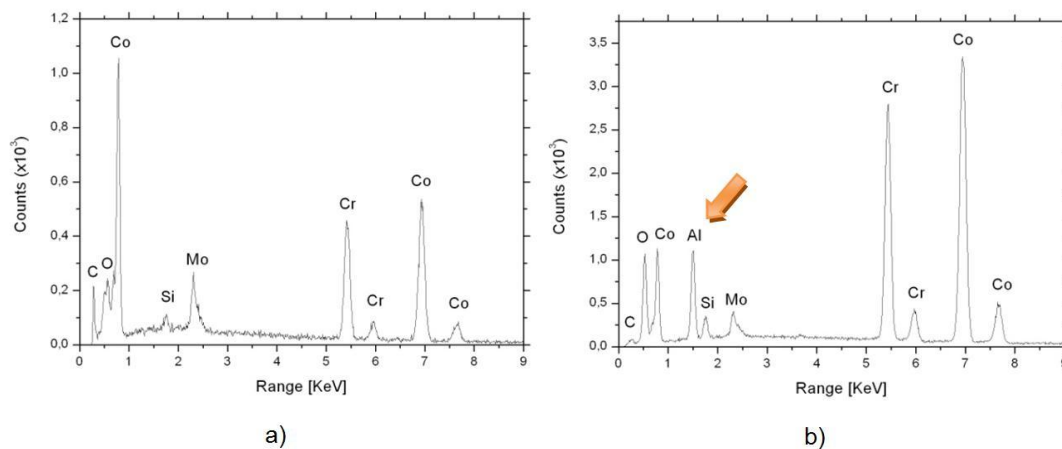


Figure 4.8. (a) EDS analysis of the CoCrMoSi alloy surface before Al_2O_3 -blasting --- no Al peak detected. (b) EDS analysis of the CoCrMoSi alloy surface after Al_2O_3 -blasting --- an Al peak detected (see arrow).

4.3. Reaction zone EDS analysis

Adhesion between metal and oxide is probably one of the least well-understood aspects of oxidation reactions (Mackert et al., 1984). Besides the static phenomena -

van der Waals forces for instance - metal-oxide adhesion also involves dynamic processes of atom transfer across the interfaces as well as diffusion within the metal and the oxide. The EDS line scan analysis performed at metal-ceramic interfaces, for preoxidized and non-preoxidized specimens, did not reveal any Co or Cr accumulation at the interface as reported by Anusavice et al., 1977). They noticed the accumulation of Ni and Cr at the interface which appeared to originate from specific depletion zones in the alloy.

The presence of porcelain elements such as Si, Al, Ca, Na, Sn and Oxygen, on the metal side in a great extent, suggests a considerable width of reaction zone. The presence of Si and Zr at the interface contribute to significantly improve the adherence of oxide to metal (Wu et al., 1991). Because of Al and Zr are easily oxidized elements, they can modify the oxide growth mechanism and suppress excessive chromium oxide formation (Wu et al., 1991). However, in this study these elements were not found, at a high concentration, on the oxide layer. From the analysis of the oxide layer content (Table 4.3) is possible to see that it is formed by a mix of oxides containing especially Cr, Co and Si.

4.4. Fracture type analysis

Stereomicroscope observations of the fracture surfaces revealed two types of failure types: mixed failure and adhesive failure. The same kind of fracture types were reported by Akova et al. (2008), Lombardo et al. (2010) and de Melo et al. (2005) for CoCr alloys-porcelain systems. Half of the preoxidized specimens presented mixed failure type (adhesive between the metal and porcelain, and cohesive within the porcelain). The other half as well as all non-preoxidized specimens exhibited total adhesive fracture. However, the bond strength registered for non-preoxidized specimens was significantly greater ($p < 0.001$) than that of preoxidized ones. Indeed, in this study no correlation was found between the failure types and the shear bond strength values. This is in accordance with de Melo et al. (2005) and Akova et al. (2008)

findings. Base metal alloys display a typical fracture at the interface, which is different from that often exhibited by gold based alloys systems (Sced and Mclean, 1972; Uusalo et al., 2005).

In this study, irrespective of oxidation heat treatment, bond strength results exhibited higher values than those registered in similar studies involving CoCrMoSi alloys-porcelain systems (de Melo et al., 2005, Akova et al., 2008, Salazar et al. 2007). This fact might be explained by the use of hot pressing in the processing of the specimens. The hot pressing technique is regarded for higher metal-ceramic bond strengths relative to conventional porcelain fused to metal technique (Salazar et al., 2007; Henriques et al., 2011).

5. Conclusions

From this study, the following conclusions can be drawn:

1. Preoxidation heat treatment in CoCrMoSi alloys might be a dispensable treatment because it can account for the decreasing of metal-ceramic bond strength.
2. Alumina-blasting treatment does not entirely remove the oxide layer formed during preoxidation heat treatment. It rather disrupts and embeds part of it in the deformed metal surface.
3. Alumina-blasting produces surface contamination with alumina particles, thus creating surface chemical modifications.
4. Alumina-blasting produce both a mechanical and a chemical effect on metal's surface, converging in two complementary effects of metal-ceramic bond strength enhancement.

6. Acknowledgements

This work has been supported by PhD Grant of FCT (Portuguese Foundation for Science and Technology) with the reference SFRH / BD / 41584 / 2007.

Special thanks to DentalCastro – Prosthetic Laboratory for their contribution in this work.

7. References

Akova T, Ucar Y, Tukay A, Balkaya MC, Brantley WA. Comparison of the bond strength of laser-sintered and cast base metal dental alloys to porcelain. *Dent Mater*, 2008; 24:1400-1404

Anusavice KJ. *Phillips' science of dental materials*. 11th ed. Philadelphia:W.B. Saunders. 2006 pp. 621-54.

Anusavice KJ, Dehoff PH, Fairhurs CW. Comparative evaluation of ceramic-metal bond tests using finite element stress analysis. *J Dent Res*, 1980; 59:608-13

Anusavice, KJ, Horner, JA, Fairhurst, CW. Adherence controlling elements in ceramic-metal systems. II. NonPrecious alloys. *J Dent Res*, 1977; 56, 1053.

Baran GR. Selection criteria for base metal alloys for use with porcelains. *Dent Clin North Am*, 1985; 29:779-787

Bryant RA, Nicholls JI. Measurement of Distortions in fixed partial dentures; resulting from degassing. *J Prosthet Dent*, 1979; 42: 515-520.

Caplan D, Sproule GI, Hussey RJ. Comparison of kinetics of high-temperature oxidation of Fe as influenced by metal purity and cold work. *Corros Sci*, 1970; 10:9-17.

Ceramco3 firing data. Online 2010.
<http://www.ceramco.com/documents/090017CeramcoFiringChart.pdf>

Chong MP, Beech DR, Chem MRIC. A simple shear test to evaluate the bond strength of ceramic fused to metal. *Aust Dent J*, 1980; 25: 357-61

Coornaert J, Adriaens P, and De Boever: Long-term clinical study of porcelain fused to gold restorations. *J Prosthet Dent*, 51(3):338-342, 1984

Crook P. *Metals Handbook: Properties and Selection: Non ferrous alloys and special-purpose alloys (ed10), Volume 2*. Metals Park, OH, ASM International, 1990, pp. 446-454.

Daftary FD, Donovan T. The effect of four pretreatment technique on porcelain to metal bond strength. *J Prosthet Dent*, 1986; 56: 535-539.

de Melo RM, Travassos AC, Neisser MP. Shear bond strengths of a ceramic system to alternative alloys. *J Prosthet Dent*, 2005; 93:64-69

Dekon SFC, Vieira LF, Bonfante G. Evaluation of the bond resistance between metal and ceramics, resulting from different previous oxidation times. *Rev Odontol Univ São Paulo*, 1999; 13(1):57-60

Drummond JL, Randolph RG, Jekkals VJ, Lenke JW. Shear Testing of the Porcelain-Metal Bond. *J Dent Res*, 1984;63:1400

Giggs GB, Halles R. Influence of metal lattice vacancies on the oxidation of high temperature materials. In: *Vacancies'76, Proc conf. on point defect behavior and diffusion processes*, Smallman, RE and Harries, JE, Eds., London: The Metals Society 1977; pp 201-207.

Giggins CS, Petit FS. The effect of alloy grain size and surface deformation on the selective oxidation of chromium in Ni-Cr alloys at temperature of 900° and 1100°C. *Trans TMS-AIME* 1969, 245:2509-2514

Henriques B, Soares D, Silva F. Optimization of bond strength between gold alloy and porcelain through a composite interlayer obtained by powder metallurgy. *Mater Sci Eng A*, 2011; 528: 1415-1420.

Hiromoto S, Onodera E, Chiba A, Asami K, Hanawa T. Microstructure and corrosion behaviour in biomedical environments of the new forged low-Ni Co-Cr-Mo alloys. *Biomaterials*, 2005; 26:4912-4923

Ihab, AH, Yourself, FT. Designs of bond strength tests for metal-ceramic complexes: Review of literature. *J Prosthet Dent*, 75; 1996: 602-608.

Johnson T, van Noort R, Stokes CW. Surface analysis of porcelain fused to metal systems. *Dent Mater*, 2006; 22: 330–337.

Kautz K. Further data on enamel adherence. *J Am Ceram Soc*, 1936; 19:93-108

Kelly JR, Rose TC. Nonprecious alloys for use in fixed prosthodontics: a review of literature. *J Prosthet Dent*, 1983; 49: 363-370

King BW, Tripp HP, Duckworth WH. Nature of adherence of porcelain enamels to metals. *J Amer Ceram Soc*, 1959; 42:504-525.

Kofstad P, Lillerud KP. On high temperature oxidation of chromium. II. Properties of CrO and the oxidation mechanism of chromium. *J Electrochem Soc*, 1980; 127:2410-2419.

Lees DG, Calvert JM. The use of ^{18}O as a tracer to study the growth mechanism of oxide scales. *Corros Sci*, 1976; 16:767-774.

Lombardo G, Nishioka RS, Souza ROA, Michida SMA, Kojima NA, Mesquita AMM, Buso L. Influence of Surface Treatment on the shear bond strength of ceramics fused to Cobalt-chromium. *J Prosthodont*, 2010; 19:103-111.

M. Salazar SM, Pereira SMB, V. Ccahuana VZ, Passos SP, Vanderlei AD, Pavanelli CA, Bottino MA. Shear bond strength between metal alloy and a ceramic system, submitted to different thermocycling immersion times. *Acta Ontolog Latinoam*, 2007; 20(2):97-102

Mackert JR, Parry EE, Hashinger DT, Fairhurst CW. Measurement of oxide adherence to PFM alloys. *J Dent Res*, 1984; 63(11):1335-1340.

Mankins WL, Lamb S: Nickel and nickel alloys. Metals Handbook: Properties and selection: Non ferrous alloys and special-purpose materials (ed10), Volume 2. Metals Park, OH, ASM International, 1990, pp. 428-445.

McCabe JF, Walls AWG. Applied dental materials. 9th ed. Blackweell Publishing. 2008. P 71.

Mc lean JW, Sced IR. Bonding of dental porcelain to metal. II. The base metal alloy/porcelain bond. Trans J Br Ceram Soc, 1973;72:235-238.

Metikoš-Huković M, Babić R. Passivation and corrosion behaviours of cobalt and cobalt-chromium-molibdenium alloy. Cor Sci, 2007; 49: 3570-3579

Miyagawa Y. X-ray diffraction at the metal-ceramic interface. Part1. Commercial gold alloy-porcelain interface. Nippon Dent U Annual Pub, 1978; 12:57-61

Nobil4000 Alloy data. Online. 2010. Available from URL: http://www.nobilmetal.it/english/pages/non_precious_alloys.html

Özcan M. Fracture reasons in ceramic-fused-to metal restorations. Journal of Oral Rehabilitation, 2003; 30: 265-269

Pask JA, Fulrath RM. Fundamentals of glass to metal bonding VIII, nature of wetting and adherence. JAM Ceram Soc, 1962; 45:592-595.

Pask JA. Fundamentals of Wetting and Bonding Between Ceramics and Metals. In: Alternatives to Gold Alloys in Dentistry, T.E. Valega, Ed., Bethesda. 1977: 235-254.

Ritchie D, Schaeffer HA, White D. The Presence of an Iron Oxide Layer at the Enamel/Steel Interface in One-coat Porcelain Enamelling. J Mater Sci, 1983; 18: 599-604.

Rizkalla AS, Jones DW. Indentation fracture toughness and dynamic elastic moduli for commercial feldspathic dental porcelain materials. Dent Mater, 2004; 20:198-206

Roberts HW, Berzins DW, Moore BK, Charlton DG. Metal-Ceramic Alloys in Dentistry: A Review. Int J Prosthodont, 2009; 18:188-194

Rokni SR, Baradaran H. The effect of oxide layer thickness on the bond strength of porcelain to Ni-Cr alloy. *J Mashhad Dental School*, 2007; 31:17-21.

Sced IR, Mclean JW. The strength of metal ceramic bonds with base metals containing chromium (a preliminary report). *Br Dent J*, 1972; 2: 232-4.

Uusalo EK, Lassila VP, Yil-Urpo AU. Bonding of dental porcelain to ceramic-metal alloys. *J Prosthet Dent*, 1987;57:26-28

Wagner WC, Asgar K, Bigelow W, Flinn RA. Effect of interface variables on metal-porcelain bonding. *J Biomed Mater Res*, 1993;27: 531-537.

Wu Y, Moser JB, Jameson LM, MaloneWFP. The effect of oxidation heat treatment on porcelain bond strength in selected base metal alloys. *J Prosthet Dent*, 1991; 66:439-444.

Yashihiro T. Radiograph Stress measurement of porcelain fused to metal. *J Prosthet Dent*, 1984; 52: 349-252.

Chapter 5

Microstructure, hardness, corrosion resistance and porcelain shear bond strength comparison between cast and hot pressed CoCrMo alloy for metal-ceramic dental restorations

Published in Journal of the Mechanical Behavior of Biomedical Materials, 12 (2012) 83-92

B. Henriques, D. Soares, F.S. Silva

*Centre for Mechanical and Materials Technologies (CT2M) and Department of Mechanical Engineering,
University of Minho, Azurém, 4800-058 Guimarães, Portugal*

Abstract

Objectives: The purpose of this study was to compare the microstructure, hardness, corrosion resistance and metal-porcelain bond strength of a CoCrMo dental alloy obtained by two routes, cast and hot pressing.

Methods: CoCrMo alloy substrates were obtained by casting and hot pressing. Substrates' microstructure was examined by the means of Optical Microscopy (OM) and by Scanning Electron Microscope (SEM) and Energy Dispersive X-Ray Spectroscopy

(EDS). Hardness tests were performed in a microhardness indenter. The electrochemical behavior of substrates was investigated through potentiodynamic tests in a saline solution (8g NaCl/L). Substrates were bonded to dental porcelain and metal-porcelain bond strength was assessed by the means of a shear test performed in a universal test machine (crosshead speed: 0.5mm/min) until fracture. Fractured surfaces as well as undestroyed interface specimens were examined with Stereomicroscopy and SEM-EDS. Data was analyzed with Shapiro-Wilk test to test the assumption of normality. The t-test ($p < 0.05$) was used to compare shear bond strength results.

Results: Cast specimens exhibited dendritic microstructures whereas hot pressed specimens exhibited a typical globular microstructure with a second phase spread through the matrix. The hardness registered for hot pressed substrates was greater than that of cast specimens, $438 \pm 24 \text{HV}/1$ and $324 \pm 8 \text{HV}/1$, respectively. Hot pressed substrates showed better corrosion properties than casted ones, i.e. higher OCP; higher corrosion potential (E_{corr}) and lower current densities (i_{corr}). It was found no significant difference ($p < 0.05$) in metal-ceramic bond strength between cast ($116.5 \pm 6.9 \text{MPa}$) and hot pressed ($114.2 \pm 11.9 \text{MPa}$) substrates. The failure type analysis revealed an adhesive failure for all specimens.

Significance: Hot pressed products arise as an alternative to cast products in dental prosthetics, as they impart enhanced mechanical and electrochemical properties to prostheses without compromising the metal-ceramic bond strength.

1. Introduction

Metal-ceramic prostheses have been used in dentistry for many decades and have a record of good clinical performance, esthetic and durability (Anusavice, 2006; McCabe and Walls, 2008). They are composed by a metallic framework and by a ceramic veneer. The former is regarded for the mechanical resistance and the latter for the

aesthetic part of the prostheses. For many years gold alloys were employed in dental prosthetics because of their biocompatibility and ease of use (Knosp et al., 2003). Due to the sharp increase in gold's price in the seventies, other alloys arose as alternative such as gold-silver-palladium and palladium-silver alloys. Nevertheless, they still were very expensive comparatively to base metal alloys such as Ni-Cr and Co-Cr alloys that started to be alternatively used in dental prosthetics. Co-Cr alloys have advantages over Ni-Cr alloys like their biocompatibility and the absence of allergic problems as happens with the latter alloys (Roberts et al., 2007). CoCr alloys are also very resistant to corrosion because of chromium (Cr), which forms a protective oxide layer upon the metal's surface (Roberts et al., 2007; Metikoš-Huković and Babić, 2007; Giacomelli et al., 2004; Hsu et al., 2005).

Base metal alloys, though, have some drawbacks, namely: higher melting temperatures; require special care in casting procedure because of their high reactivity; and imparts more difficulty to the finishing process because of their higher hardness.

Powder metallurgy (PM) is an alternative method of fabricating base metal parts and has been shown to produce finer grain structures with enhanced properties, especially strength, toughness and ductility (Patel et al., 2010; Dewidar et al., 2006). PM is a technology that is gaining rising attention in medical field, in general, and in prosthetic dentistry in particular (Dewidar et al., 2006). PM based CAD/CAM systems are bringing to the prosthetic profession new opportunities in terms of manufacturing time, with the ability of producing more in less time, and processing materials with special properties, such as gradient pore materials (Dourandish et al., 2008) or composite materials (Henriques et al., 2011; Oksiuta et al., 2009). PM 100 (Phenix Systems) and 3T RPD Ltd are two examples of companies that provide equipments (former) or services (latter) that allow the production of metal prostheses using laser-sintering, directly from a 3D CAD file. These manufacturers claim parts with high density (99.99%), free of pores and with improved mechanical and electrochemical properties. Studies have shown that laser-sintered crowns do not significantly differ from cast

ones in parameters like the internal fit (Akova et al., 2009) and metal-ceramic bond strength (Akova et al., 2008).

There are other CAD/CAM systems based on CNC milling (e.g. Datron D5, Datron Dynamics Inc, Milford, USA) that produces crowns or Fixed-Partial-Dentures (FPDs) from cast CoCrMo blanks. Since PM parts have better properties than cast parts, it would be of great relevance to produce CoCrMo milled crowns from powder processed blanks. The PM process can have great influence on compacts' properties (Dewidar et al. 2006). Press and sinter technique is usually characterized by some porosity within the parts which negatively affects its mechanical and electrochemical behavior (Rodrigues et al., 2010; Krasicka-Cydzik, 2005). Full-dense hot pressed parts are regarded to have better mechanical and electrochemical properties, and can be obtained by the means of hot consolidation powder processes (e.g. Hot Pressing and HIP). Few studies exist on CoCrMo hot pressed compacts in terms of mechanical and electrochemical properties (Sato et al., 2007; Sato et al. 2008; Naoyuki et al. 2006) and none using a CoCrMo dental alloy. Therefore, this is a study on hot pressed dental CoCrMo alloys for metal-ceramic restorations. It compared the CoCrMo alloy substrates obtained by hot pressing and casting techniques, in terms of microstructure, hardness, corrosion resistance and porcelain bond strength.

2. Materials and Methods

A CoCrMo dental alloy (Nobil4000, Nobilmetal, Villafranca d'Asti, Italy) was used in this study in two forms: ingot and powder. The composition of alloy is presented in Table 5.1. The powder was produced by air atomization and supplied by Nobilmetal, the alloy's manufacturer. The alloy powder particles have spherical shape (Figure 5.1) and the particle size distribution is the following: $D_{10}=4.44\mu\text{m}$; $D_{50}=8.27\mu\text{m}$ and $D_{90}=12.76\mu\text{m}$.

It was used an opaque porcelain powder (Ceramco3, Dentsply, New York, USA) (batch number: 08004925) which composition is presented in Table 5.2 and a micrograph shown in Figure 5.1b.

Table 5.1. Chemical composition of CoCrMo alloy according to manufacturer (wt.%).

Element	Composition
Co	62
Cr	31
Mo	4
Si	2.2
Fe	Trace
Mn	Trace
W	Trace

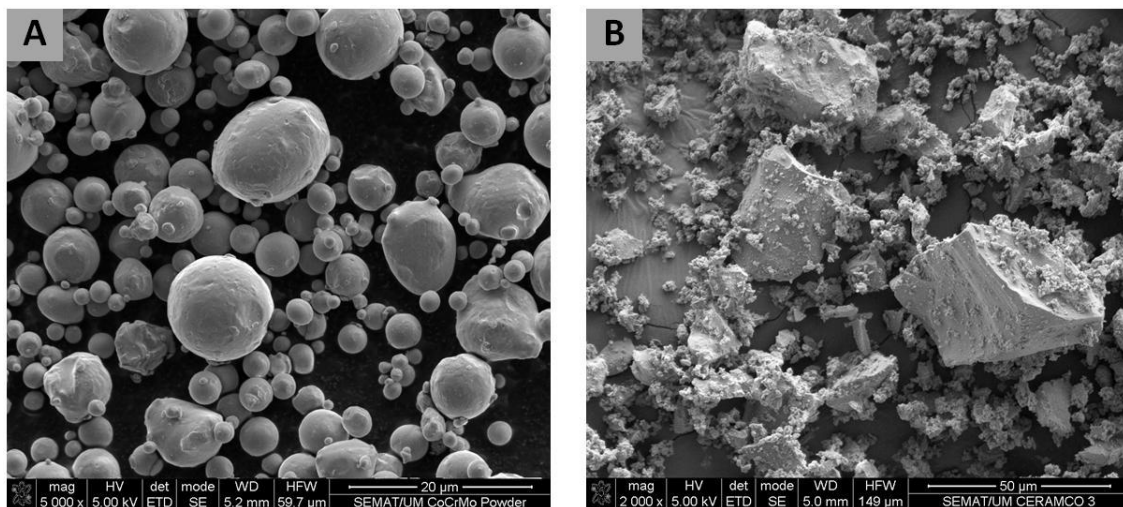


Figure 5.1. SEM micrographs of (A) CoCrMo alloy powders and (B) opaque porcelain powders (Ceramco3).

Cast metal substrates (n=5) were obtained by lost wax casting, using an arc melting furnace (Degumat 2033, Degussa, Germany). Metal rods of approximately 4.5 mm of diameter and 40 mm length were produced. After rods' divesting, several 4 mm height specimens were cut in a precision cut-off machine (Minitom, Struers).

Hot pressed CoCrMo substrates (n=5) were obtained by pressing the metal powders in a graphite die, at high temperatures. The graphite die was painted with zirconium oxide paint in order to impede carbon to diffuse to metal substrates. Hot pressing was performed under vacuum (10^{-2} mbar) at 1000°C for 10 minutes and at a pressure of 60 MPa.

Table 5.2. Chemical composition of porcelain according to manufacturer (wt.%).

ELEMENT	COMPOSITION
SiO ₂	41.3
Al ₂ O ₃	14.5
K ₂ O	14
SnO ₂	11.9
ZrO ₂	5.8
CaO	4.1
P ₂ O ₅	4.1
Na ₂ O	3.0
Others	MgO, SO ₃ , ZnO, Cr ₂ O ₃ , Fe ₂ O ₃ , CuO, Rb ₂ O

All substrates were ground until 2400-grit SiC paper. They were after ultrasonically cleaned in an alcohol bath for 10 min and rinsed in distilled water for another 10 min to remove contaminants. Then they were dried with adsorbent paper towels. No grit-blasting was performed in metal substrates or any preoxidation heat treatment.

In order to guarantee an interface free of defects such as gas bubbles, voids or cracks porcelain powders were hot pressed onto the metal substrates. Metal-ceramic hot pressing procedure comprised the following steps: first, graphite die was painted with a zirconium oxide paint in order to create a shield to avoid carbon diffusion to metal-ceramic compact; then, the metal substrate was placed in die's cavity followed by the porcelain powder; finally, the set was heated up to 970°C, at a heating rate of approximately 70°C/min, and remained at that temperature for 2 minutes. Hot pressing was performed under vacuum ($\sim 10^{-2}$ mBar) at a pressure of ~ 20 MPa.

Microhardness evaluation (Microhardness tester, type M, Shimadzu, Japan) was performed for the two types of substrates, cast and hot pressed. Five indentations were made in each type of substrate and the mean value and standard deviation was calculated.

Microstructures of cast and hot pressed specimens were examined by scanning electron microscopy and energy dispersive spectroscopy - SEM/EDS (Nova 200, FEI, Oregon, USA).

2.1. Electrochemical tests

Electrochemical tests were performed in a standard three-electrode glass cell using a potentiostat/galvanostat (Reference 600, Gamry Instruments, Warminster, USA) with an interface for computer controlled data acquisition. The cylindrical samples were mounted in epoxy resin and ground with 2400-grit SiC paper. The metal-resin interface was sealed with honey wax in order to avoid interstitial corrosion at the specimens' borders. The sample was placed in the glass-cell, letting its front side (9 mm²) exposed to the electrolyte. At the back of the sample, a copper screw promoted the electric contact between the sample and the potentiostat. Open circuit potential and potentiodynamic tests were performed in 8g NaCl/L solution at room temperature. The reference electrode was the SCE (saturated calomel electrode) and the counter electrode was a platinum electrode. The scan rate in the potentiodynamic tests was 1mV/s starting at 0.5V below the E_{OCP} moving in the anodic direction up to 1V. The electrochemical data was obtained out of three tests performed in each of the three cast and hot pressed specimens selected for this purpose. Polarized surfaces were examined by the means of optical microscopy (Axiotech, Carl Zeiss, USA).

2.2. Shear tests

The shear bond strength tests were carried out at room temperature and performed in a universal testing machine (Instron 8874, MA, USA), with a load cell having 25 kN capacity and under a crosshead speed of 0.5mm/s. Tests were performed in a custom-made stainless steel apparatus similar to that described by Henriques et al. (2011a).

The shear bond strength (MPa) was calculated dividing the highest recorded fracture force (N) by the cross sectional area of the bonded porcelain (mm^2).

2.3. Statistical analysis

Data were analyzed using SPSS statistic software (Release 20.0.0 for Windows). The Shapiro-Wilk test was first applied to test the assumption of normality. Differences between cast and hot pressed specimens in terms of shear bond strength were tested using t-test. P values lower than 0.05 were considered statistically significant in the analysis of the results.

2.4. Analysis of the metal-porcelain interface

The metal-ceramic interface as well as representative fracture surfaces were evaluated by stereomicroscopy (SMZ-2T, Nikon, Japan), optical microscopy (Axiotech, Carl Zeiss, USA) and SEM/EDS (Nova 200, FEI, Oregon, USA). For interface analysis, the specimens were embedded in auto-polymerizing resin, ground finished until 1200-grit SiC paper and polished with diamond paste first in $6\mu\text{m}$ and finally in $1\mu\text{m}$ felt disc. Morphologic and chemical analyses were performed. The elemental distribution across the metal-ceramic interface was determined by using line scan EDS analysis (20 points in the metal side and 20 points in the porcelain side).

3. Results

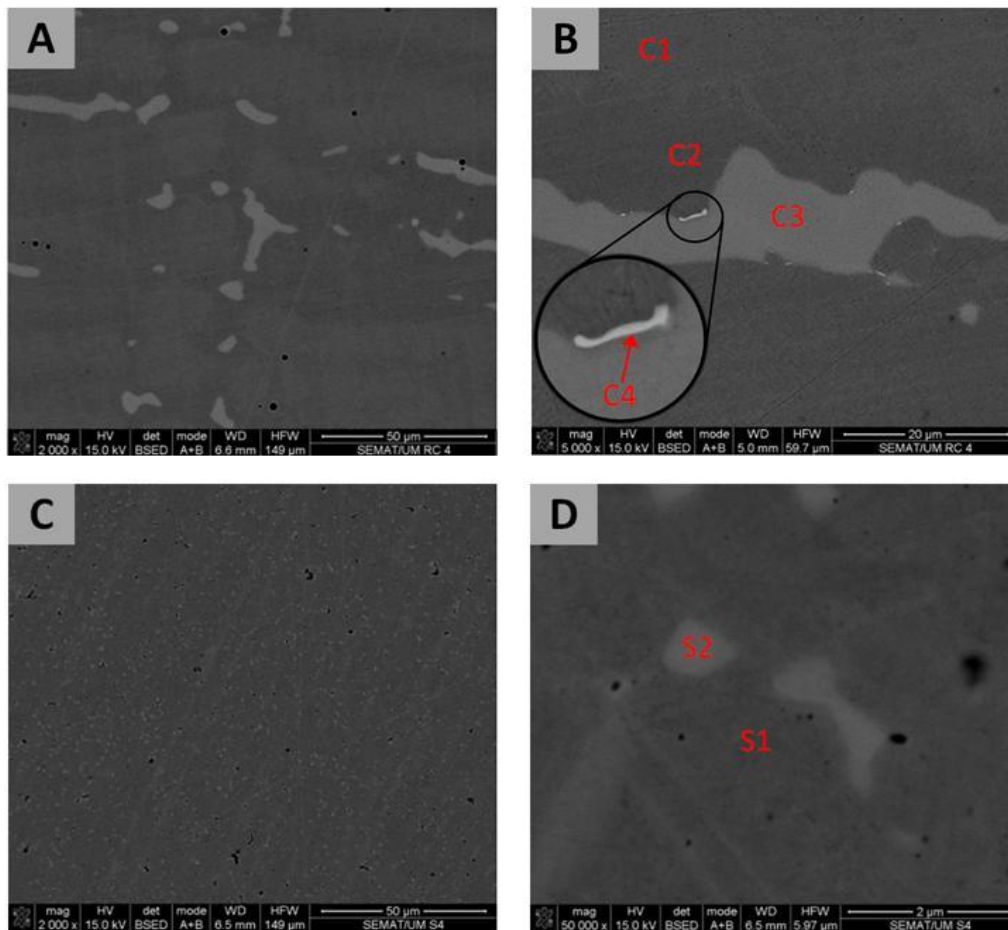
Figure 5.2 shows the microstructure of the cast and hot pressed CoCrMo alloy. It reveals a three-phase dendritic structure in cast specimens and a typical two-phase globular structure in the hot pressed specimens. In Table 5.3 is presented the element composition of the phases present in cast and hot pressed specimens. In cast specimens four different phases were detected and identified as C1 to C4 in Figure 5.2. The dendritic phase, signed here as C1, is a Co rich and Cr and Mo poor phase. The interdendritic region is composed by three phases, mainly C2 and C3 phases, and residual C4 phase. The C3 phase is rich in Mo and Cr, and poor in Co. Regarding C2 phase, it has a halfway composition relatively to C1 and C3 phases, i.e. it has a lower content of Co than C1 phase but higher than in C3 phase, and has higher Cr and Co content than C1 phase but lower than C3 phase. C4 phase was sparsely detected at C3 phase adjacent zones (Figure 5.2) and is characterized to be a Mo and Si rich phase.

The hot pressed specimens are composed by two phases, identified as S1 and S2 (Figure 5.2). S1 phase is rich in Co and poor in Cr and Mo, and has a composition similar to that of the dendritic phase (C1) of cast specimens. Regarding S2 phase, it is poor in Co and rich in Cr and Mo, as verified for interdendritic phase of cast specimens (phase C2).

The volume fraction of dendritic phase in the microstructure of both types of specimens was estimated by the method of point counting (ratio of points on a grid falling on dendritic phase) and revealed 37% of dendritic phase (C1) in cast specimens and 83% of dendritic phase (S1) in hot pressed specimens.

Table 5.3. EDS analysis of the different phases found in cast and hot pressed substrates.

ELEMENTS	TYPE OF SUBSTRATE					
	CAST				HOT PRESSED	
	PHASE					
	C1	C2	C3	C4	S1	S2
Co	64.06	60.17	54.09	52.76	63.94	51.10
Cr	30.42	31.67	34.28	22.00	29.00	34.99
Mo	2.95	4.86	8.75	18.79	5.87	12.38
Si	2.24	2.95	2.77	5.65	1.05	1.38

**Figure 5.2.** Microstructure of cast (A, B) and hot pressed (C, D) CoCrMo alloy metal substrates.

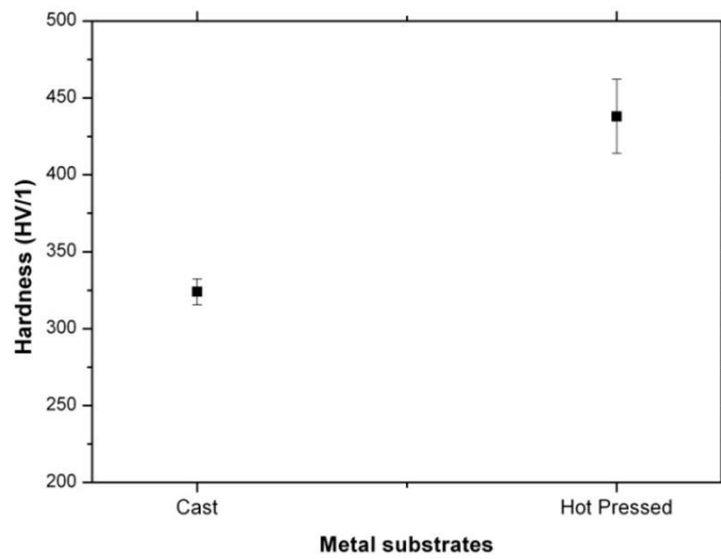


Figure 5.3. Hardness (HV/1) of cast and hot pressed metal substrates.

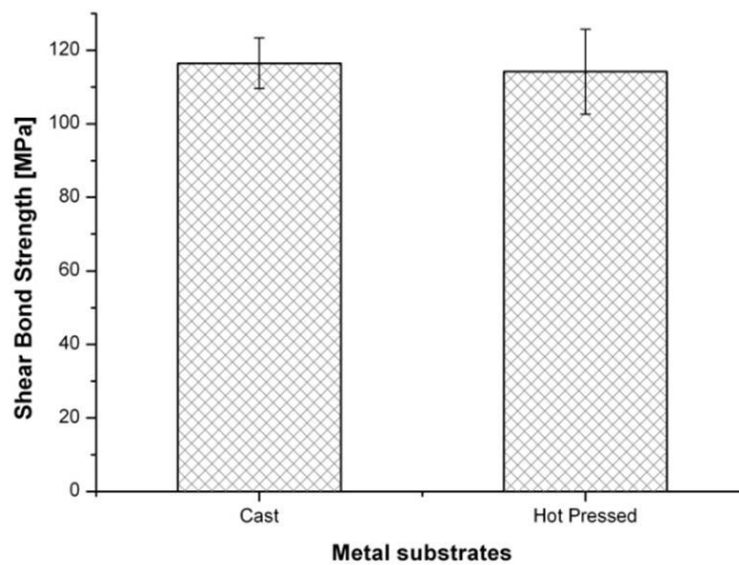


Figure 5.4. Metal-ceramic shear bond strength results for cast and hot pressed metal substrates.

The hardness values recorded for hot pressed specimens were higher than those of cast specimens, $438 \pm 24 \text{HV/1}$ and $324 \pm 8 \text{HV/1}$, respectively.

Metal-ceramic shear bond strength results of cast and hot pressed metal substrates are presented in Figure 5.4. It was found no significant differences ($p > 0.05$) between

these two types of metal substrates. The shear bond strength registered for cast and hot pressed substrates was 116.5 ± 6.9 MPa and 114.2 ± 11.9 MPa, respectively.

Specimens were classified under their failure type as adhesive, cohesive or mixed. All tested specimens exhibited adhesive failures. No remnants of porcelain were found on the specimen's surface, either in cast or in hot pressed specimens (Figure 5.5).

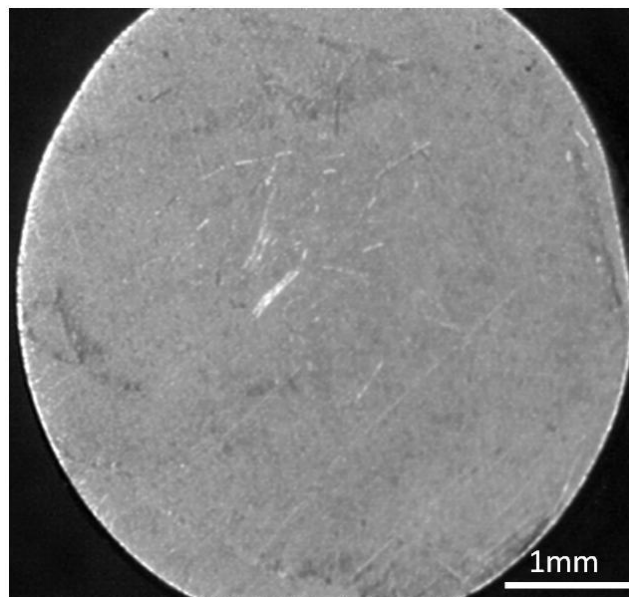


Figure 5.5. Fracture surface of cast CoCrMo alloy-ceramic specimen.

Figure 5.6 shows an EDS line scan analysis (in white) in the metal-ceramic interface region of the cast and hot pressed metal substrates. This analysis allows the comparison between the elements diffusion profiles occurring in both types of specimens. Besides a slightly increase in oxygen content on the metal's side of hot pressed substrates relatively to cast substrates, no significant differences were found in the elements diffusion profiles between the two type of specimens. It must be highlighted the lack of metal elements' diffusion into porcelain (e.g. Co, Cr and Mo), and the broad diffusion of porcelain's elements into metal (e.g. O, Si, Al, K, Sn, Na, Ca, Mg) registered in both situations.

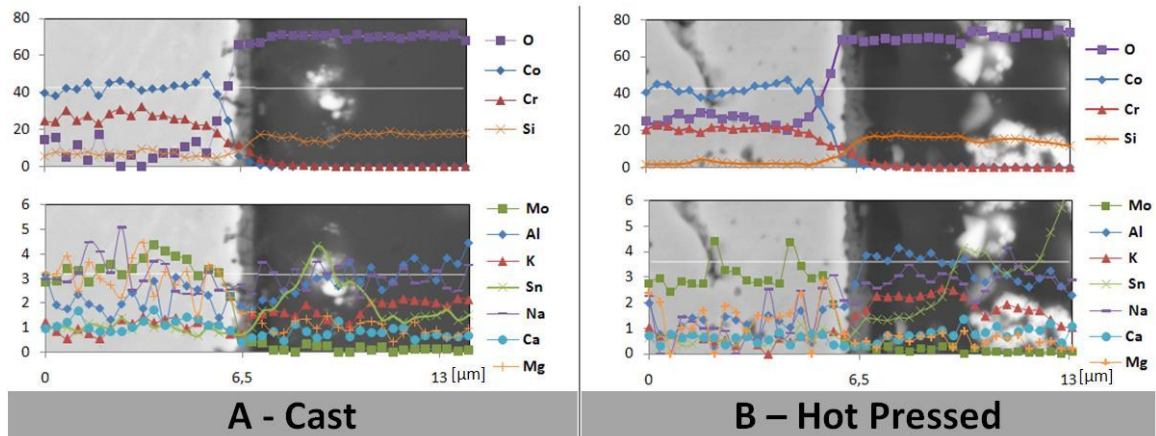


Figure 5.6. EDS line analysis of metal/ceramic interface showing the inter-diffusion of elements in (a) cast and (b) hot pressed specimens.

Figure 5.6a shows the open circuit potential (OCP) for the cast and hot pressed CoCrMo stationary electrodes immersed in a 8g NaCl /L solution at 20°C during 1 h. Following the immersion both curves started to slowly move towards positive potentials, suggesting the growth of an oxide film on the metallic surface. The OCP registered for hot pressed substrate was approximately -280 mV(SCE), which is 70mV nobler than that of cast substrate (-350 mV(SCE)).

The potentiodynamic polarization plots for the cast and hot pressed specimens are presented in Figure 5.7. The corrosion parameters corrosion potential E_{corr} and corrosion current densities i_{corr} were obtained by the Tafel extrapolation method and are presented in Table 5.4. Hot pressed specimens exhibited nobler properties than cast ones, traduced by higher E_{corr} (hot pressed: -328.6 ± 2.1 mV; cast: -515.3 ± 18.5 mV) and lower i_{corr} (hot pressed: $0.4 \pm 0.02 \mu\text{A}\cdot\text{cm}^{-2}$; cast: $1.1 \pm 0.3 \mu\text{A}\cdot\text{cm}^{-2}$). Both specimens' types exhibited a similar region of passivity at a potential of approximately 0.0V to +0.6V (versus SCE).

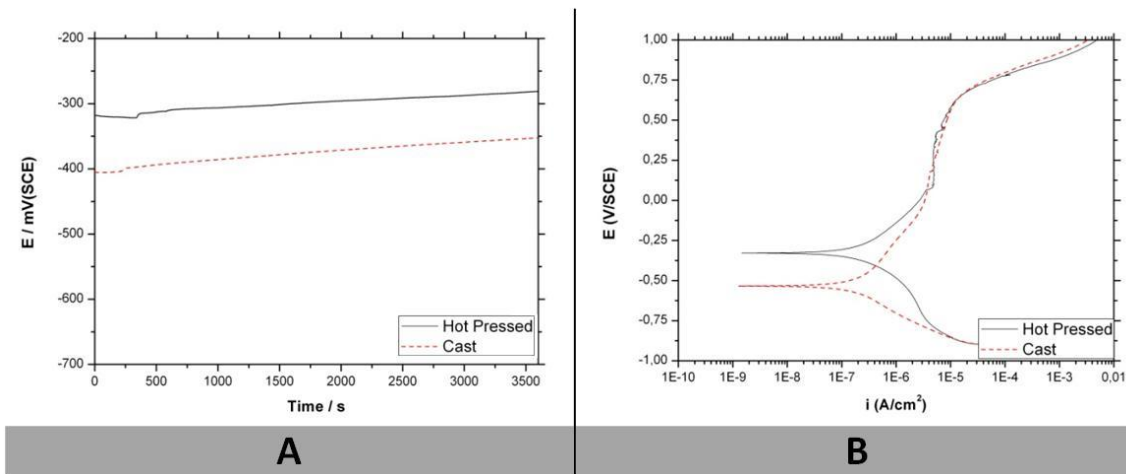


Figure 5.7. Electrochemical curves for CoCrMo substrates: a) Open Circuit Potential (OCP) curves; b) Potentiodynamic polarization curves.

Table 5.4. Corrosion parameters of cast and hot pressed CoCrMo substrates measured in saline solution (8g NaCl/L).

	E_{corr} [mV]	i_{corr} [$\mu\text{A}\cdot\text{cm}^{-2}$]
Cast	-524.4±33.6	1.1±0.3
Hot Pressed	-328.6±2.1	0.4±0.02

4. Discussion

4.1. Metals substrates

This study is concerned with the viability of using hot pressed metal substrates for metal-ceramic dental restorations in comparison with conventional cast ones. Therefore it was made an assessment in terms of microstructure, hardness, electrochemical behavior and metal-ceramic adhesion.

The Co based alloy used in this study is a common cast Co-Cr alloy used in porcelain-fused-to metal restorations that fulfills the ANSI/ADA Specifications No. 14 (ISO 6871)

in terms of chromium and cobalt weight, which should be no less than 20% and 85%, respectively (Table 5.1). The alloy also attends to minimum values required for elongation (1.5%), yield strength (500MPa) and elastic modulus (170 GPa) (Nobil4000 alloy data).

Cobalt is the major element in the alloy and its content in the alloy is regarded for the elastic modulus, strength and hardness (Craig and Powers, 2002). Chromium is the second major element in the alloy (Table 5.1) and is responsible for its tarnish and corrosion resistance. The chromium content on a Co-Cr alloy should not exceed 30% because it gets more difficult to cast. Another point related with this percentage of chromium is that the alloy starts forming a brittle phase known as sigma (σ) phase (Craig and Powers, 2002; Sato et al., 2007; Sato et al. 2008; Naoyuki et al. 2006; Lee et al. 2008). The chemical composition and the microstructure of the cast and hot pressed specimens were analyzed, by optical and SEM microscopy, and revealed the presence of σ phase in both specimens (C3 and S2 phases), where Cr and Mo were found to preferentially segregate. The presence of these phases is in accordance with the ternary Co-Cr-Mo phase diagram (Gupta, 2005) for the tested alloy chemical composition. The amount of σ phase in hot pressed specimens is significantly lower than in the case of cast specimens. Moreover, the σ phase in cast specimens is localized along the interdendritic regions whereas in the hot pressed specimens it is spread throughout the matrix. In the latter case, σ phase was formed during alloy solidification, at powder atomization process. The σ phase is known to cause brittle fracture in the as-cast Co-Cr alloys (Lee et al. 2006). Therefore, its reduction or suppression leads to an improvement in the alloy's ductility (Sato et al., (2007). Lee et al. (2008) were able to inhibit the σ phase formation and the gamma (γ) phase stabilization in Co-Cr-Mo alloys by the addition of N, resulting in improved mechanical properties.

The presence of molybdenum in the alloy contributes to the strength of the alloy. Silicon and manganese imparts increased casting properties to the alloy. A Si rich phase (C4) was randomly detected at the interdendritic region (Figure 5.2).

No carbides were detected in none of the specimens. Carbides are generally found in Co-Cr-Mo alloys along the grain boundaries or spread through the matrix (Placko et al. 1997; Shi et al. 1993; Krasicka-Cydzik et al. 2005; Rodrigues et al. 2011; Asgar and Allan, 1968). Carbon is often added to Co-Cr-Mo alloys to improve mechanical properties due to its ability to stabilize the γ phase, which is an effective way to keep the alloy ductile. However, the presence of carbon contributes to the precipitation of $M_{23}C_6$ carbides (Mineta et al., 2010) which act as preferential sites for fatigue crack propagation (Zhuang and Langer, 1989; Kilner et al., 1986).

Cobalt-chromium alloys are known to have excellent corrosion resistance (Ameer et al., 2004) and results obtained in this study corroborate this fact. Nevertheless, hot pressed specimens exhibited greater corrosion resistance than cast specimens in terms of open circuit potential (OCP), corrosion potential E_{corr} and current densities i_{corr} as shown in Table 5.4 after the polarization tests. The OCP curves show a higher tendency of cast specimens for corrosion in comparison with that exhibited by hot pressed specimens. The corrosion potential E_{corr} as well as the anodic polarization curves show that both cast and hot pressed specimens are in the passive state, which is a characteristic of materials with high resistant to corrosion. Passivation in CoCrMo alloys is related to the formation of a thin layer formed by chromium-oxide (Cr_2O_3) and some hydroxides (Huang, 2002). This layer impedes the transportation of oxygen and metallic ions.

The corrosion current densities i_{corr} observed in cast specimens are greater than those registered in hot pressed specimens ($1.1 \pm 0.3 \mu A \cdot cm^{-2}$ vs. $0.4 \pm 0.02 \mu A \cdot cm^{-2}$), which results in higher corrosion rates occurring in the former ones. The porosity level and the type of microstructure of the specimens might help explain this behavior. Figure 5.2 do not show evidence of significant porosity differences between the two specimens, as the hot pressing produced approximately full-dense powder compacts (>99% density). Therefore the differences in corrosion behavior must come from the microstructure (Matković et al., 2004). Cast specimens exhibit a dendritic phase (C1) fraction of 37%, being the rest interdendritic region (C2-C4). The dendritic phase has

fcc structure and is a noble phase, whereas interdendritic regions has hcp structure and is regarded to be a less noble phase (Matković et al., 2004). Interdendritic regions can be a quaternary mixture of a cobalt-rich γ -phase, a chromium-rich $M_{23}C_6$ phase ($M=Co, Cr$ or Mo); an M_7C_3 carbide; and a chromium and molybdenum-rich σ phase (Craig and Powers, 2002). These are microstructural heterogeneities where the dissolution of the alloy is initiated (Montero-Ocampo and Rodriguez, 1995). Figure 5.8a shows a micrograph of the cast specimen after polarization test and shows the preferential dissolution of interdendritic regions.

The microstructure of hot pressed specimens is mainly composed by S1 phase (83%), which is similar in composition to dendritic phase of cast specimens (C1). The σ phase (S2) was found in hot pressed substrates with globular shape and in less extension than it was observed in cast specimens, where σ phase was found within the interdendritic regions with elongated shapes. The presence of significantly greater amount of a noble phase (S1), in the hot pressed specimens, might explain their better corrosion resistance. Figure 5.8b shows the polarized surface of hot pressed specimens where the dissolution of the regions adjacent to the grain boundaries is visible. This finding is in accordance with Okisuta et al. (2009) study where they observed, in the pure CoCrMo hot pressed specimens, the dissolution of the phase present at the grain boundaries as well as numerous deep pits.

Krasicka-Cydzik et al. (2005), in their study on the corrosion behavior of hot pressed CoCrMo samples for surgical applications, also reported higher corrosion potentials in hot pressed specimens than in cast specimens. However, the corrosion current densities i_{corr} were higher in hot pressed specimens than in cast specimens. This fact might be related to the sintering process they used, which produced substantially porous samples (19% of porosity) which corresponded to a bigger surface area when compared to full dense specimens. Greater surface areas exposed to the electrolyte are regarded for higher current densities (Krasicka-Cydzik et al., 2005; Rodrigues et al., 2010). In the present study, the hot pressed specimens are full dense specimens (>99% density).

Rodrigues et al. (2010) also reported open circuit potentials and corrosion potentials of hot pressed CoCrMo specimens that were considerably nobler for than those found in the literature for cast and wrought CoCrMo alloys under similar testing conditions.

Hardness is an important characteristic in a way that harder alloys, combined with greater elastic modulus allows the manufacture of longer prostheses (Craig and Powers, 2002). The higher hardness, though, may impact the ability to finish/polish the alloy clinically. The greater hardness of hot pressed specimens relatively to cast ones is related with the former's finer microstructure. Fine grain structure coupled with low porosity is regarded to produce hard hot pressed compacts (Rodrigues et al., 2010; Dourandish et al. 2008; Patel et al., 2010). The hardness value registered in cast specimens ($324 \pm 8 \text{HV}/1$) is of the same magnitude of commercial CoCrMo dental alloys with low carbon content (e.g. Wironit) (Matchović et al., 2004). Matchović et al. (2004) demonstrated that interdendritic regions (hcp) had significantly lower hardness than dendritic phase (fcc). This fact might also explain the lower hardness of cast specimens, where the dendritic phase represents 37% of the whole microstructure.

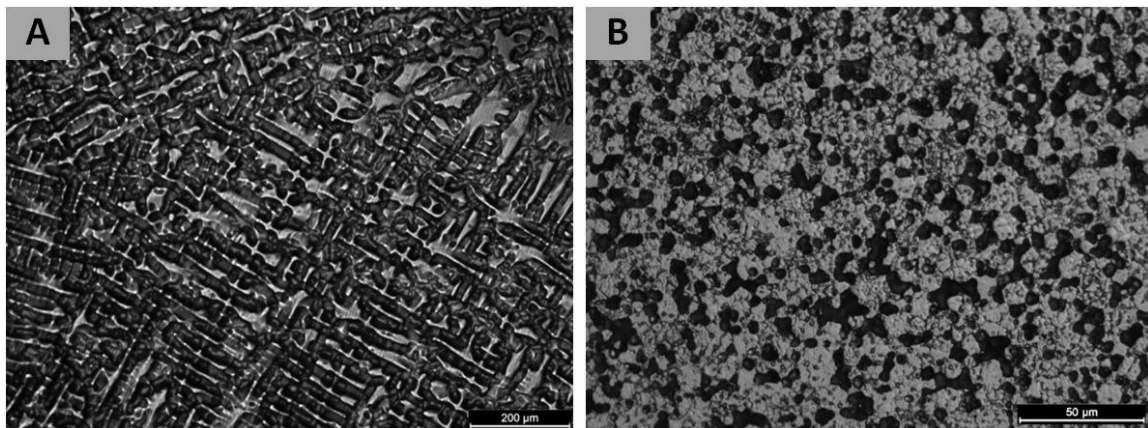


Figure 5.8. Micrographs of metal surfaces after potentiodynamic polarization tests: a) cast (100x); b) hot pressed (500x).

4.2. Metal-ceramic composites

This study has also compared the metal-ceramic shear bond strength of hot pressed and cast CoCrMo alloy. No significant differences ($p < 0.05$) between the two techniques were found. This result is in accordance with Akova et al. (2008) findings in their study of the bond strength between laser-sintered and casted base metal dental alloys to porcelain. They showed that there were no significant differences, on the shear bond strength, between the laser-sintered Co-Cr alloys and conventionally casted Ni-Cr and Co-Cr alloys. In Akova et al. (2008) study, metal substrates were subjected to preoxidation heat treatment, according to manufacturer's specifications, whereas this step was omitted in the present study. Nevertheless, the same findings were observed.

All specimens exhibited adhesive failure type, despite the good metal-ceramic bonding verified for both processes, cast and hot pressed. The lack of surface roughness might help explain the adhesive failure of all specimens. Despite adhesive failures are usually correlated with poor bonding between metal and ceramic, this was not the case in this study. This finding is in accordance with other studies' findings where no correlation could be established between failure type and bond strength (Henriques et al., 2011a; de Melo et al., 2005; Akova et al., 2008).

The bond strength and failure type results of this study must be analyzed taking into account the process that was employed to bond porcelain to metal. In this study, porcelain was hot pressed to the metal substrates and this process is regarded to provide enhanced metal-ceramic interface properties (Henriques et al., 2011a) as well as greater porcelain cohesive strength (Craig and Powers, 2002; Kelly, 1997; Drummond et al., 2000). The external pressure applied on ceramic produces a full contact between the fused porcelain and the metal surface yielding a flawless interface between the two materials, free of defects such as pores and cracks. Even in situations where no surface roughening treatments are performed, as happened in this study, an effective bonding is achieved. It must be though referred that a grit-blasting surface treatment is often performed to metal substructures before porcelain firing. This treatment increases the surface roughness in order to produce micro-mechanical

retention of the porcelain (Craig and Powers, 2002; Wagner et al. 1993; Shell and Nielson, 1962). In this study, it was decided not to consider the effect of surface roughness and, therefore, this treatment was omitted. Regarding porcelain's fracture strength, it was demonstrated elsewhere (Henriques et al., 2011a) that hot pressed porcelains are significantly stronger than conventionally vacuum-sintered porcelains. The high cohesion of porcelain together with the flat metal's surface, can explain the adhesive failures registered in all specimens.

The shear bond strength test was selected among the available tests for metal-ceramic bond strength assessment (e.g. the Schwickerath crack initiation test used in ISO 9693:1999, the three-point-flexure test; four-point-flexure test; biaxial flexure test, etc). It has been pointed as having advantages over other tests, namely: the bond strength results are not influenced by the Young's Modulus of the alloy as happens in bending tests (Hammad and Talic, 1996) and its suitability for evaluation of metal-ceramic bonds (Anusavice et al.,1980; Ihab and Yourself,1996). This test geometry is therefore used by many authors to perform metal-ceramic bond strength assessments (Akova et al, 2008; dos Santos et al, 2006; Vasquez et al, 2009; de Melo et al, 2005; M. Salazar et al., 2007).

The EDS diffusion profiles analysis of cast and hot pressed specimens revealed no relevant differences in the elements' diffusion extent and content. This fact might also support the similar bond strength results registered for both types of specimens. In the absence of significant surface roughness, which accounts for mechanical retention, the chemical bonding is regarded to be the main adhesion mechanism that promotes the bonding between metal and porcelain (Wagner et al., 1993; Shell and Nielson, 1962). A chemical bonding is established by the elements' diffusion through the ceramic and metal, thus the importance of the elements' diffusion profile analysis.

Figure 5.6 shows an oxide layer formed at the metal-ceramic interface of both cast and hot pressed specimens. This oxide layer was formed during porcelain firing, once metal substrates were not submitted to a preoxidation heat treatment, and it is mainly composed by Cr_2O_3 (Mackert et al., 1981). It is interesting to note that elements from

porcelain such as Si, Al, Ca, Na, Sn and Oxygen, were found in the metal's side in a great extent, suggesting a considerable width of diffusion.

This study has demonstrated the applicability of powder processing in the dental prosthetics. The hot pressed CoCrMo alloy substructures have shown superior mechanical and electromechanical properties in comparison with those obtained by casting technique. Moreover, the hot pressed substructures proved to produce metal-ceramic bonds with the same characteristics of those found in cast specimens. Therefore, hot pressed CoCrMo blanks should be considered as an alternative in the production of milled substructures for metal-ceramic dental restorations.

5. Conclusions

From this study, the following conclusions can be drawn:

1. The hot pressed and cast substrates of CoCrMo alloy presented different microstructures, being globular in the former case and dendritic in the latter case, with different constituent's volume fractions;
2. The hot pressed substrates of CoCrMo alloy were substantially harder than those obtained by casting technique;
3. The hot pressed substrates of CoCrMo alloy exhibited greater corrosion resistance than cast substrates.
4. No significant differences ($p < 0.05$) were found, in the metal-ceramic bond strength, between hot pressed and cast CoCrMo alloy substrates.

6. References

Anusavice KJ. Phillips' science of dental materials. 11th ed. Philadelphia:W.B. Saunders, 2006; pp. 621-54.

Anusavice KJ, Dehoff PH, Fairhurs CW. Comparative evaluation of ceramic-metal bond tests using finite element stress analysis. *J Dent Res*, 1980; 59: 608-613.

Akova T, Ucar Y, Tukay A, Balkaya MC, Brantley WA. Comparison of the bond strength of laser-Hot Pressed and Cast base metal dental alloys to porcelain. *Dent Mater*, 2008; 24: 1400-1404.

Ameer MA, Khamis E, Al-Motlaq M. Electrochemical behavior of recasting Ni–Cr and Co–Cr non-precious dental alloys. *Corr Sci*, 2004; 46: 2825–2836.

Asgar K, Allan FC. Microstructure and Physical Properties of Alloys for Partial Denture Castings. *J Dent Res*, 1968; 47(2): 189-197.

Craig RG, Powers JM. Restorative dental materials. 11th ed. Mosby, 2002; pp.480-492.

de Melo RM, Travassos AC, Neisser MP. Shear bond strengths of a ceramic system to alternative alloys. *J Prosthet Dent*, 2005; 93: 64-69

Dewidar MM, Yoon H, Lim JK. Mechanical Properties of Metals for Biomedical Applications Using Powder Metallurgy Process: A Review. *Met & Mater Inter*, 2006; 12(3): 193-206.

dos Santos JG, Fonseca RG, Adabo LG, Cruz CAS. Shear bond strength of metal-ceramic repair systems. *J Prosthet Dent*, 2006; 96(3): 165-173.

Dourandish M, Godlinski D, Simchi A, Firouzdor V. Sintering of biocompatible P/M Co–Cr–Mo alloy (F-75) for fabrication of porosity-graded composite structures. *Mater Sci Eng A*, 2008; 472: 338-346.

Drummond JL, King TJ, Bapna MS, Koperski RD. Mechanical property evaluation of pressable restorative ceramics. *Dent Mater*, 2000; 16; 226-233.

- Giacomelli FC, Giacomelli C, Spinelli A. Behavior of Co-Cr-Mo biomaterial in simulated body fluid solutions studied by electrochemical and surface analysis techniques. *J Braz Chem Soc*, 2004; 15(4): 541-547.
- Gupta KP. The Co-Cr-Mo (Cobalt-Chromium-Molybdenum) System. *J Phase Equilib Diffus*, 2005; 26: 87–95.
- Hammad IA, Talic YF. Designs of bond strength tests for metal-ceramic complexes: Review of the literature. *J Prosthet Dent*, 1996; 75: 602-608.
- Henriques B, Soares D, Silva F. Shear bond strength of a Hot Pressed Au-Pd-Pt alloy-porcelain dental composite. *J Mech Behav Biomed Mater*, 2011a; 4(8): 1718-1726.
- Henriques B, Soares D, Silva F. Optimization of bond strength between gold alloy and porcelain through a composite interlayer obtained by powder metallurgy. *Mater Sci Eng A*, 2011b; 528: 1415-1420.
- Huang HH. Effect of chemical composition on the corrosion behavior of Ni-Cr-Mo dental Casting alloys. *J Biomed Mater Res*, 2002; 60: 458-465.
- Hsu RW, Yang C, Huang C, Chen Y. Electrochemical corrosion studies on Co-Cr-Mo implant alloys. *Mat Chem Phys*, 2005; 93: 531-538.
- Ihab AH, Yourself FT. Designs of bond strength tests for metal-ceramic complexes: Review of literature. *J Prosthet Dent*, 1996; 75: 602-608.
- Kelly JR. Ceramics in restorative and prosthetic dentistry. *Annu Rev Mater Sci*, 1997; 27: 443-468.
- Kilner T, Laanemäe WM, Pilliar R, Weatherly GC, MacEwen SR. Static mechanical properties of cast and sinter-annealed cobalt-chromium surgical implants. *J Mater Sci*, 1986; 21: 1349-1356.
- Knosp H, Holliday RJ, Corti CW. Gold in dentistry: Alloys, Uses and Performance. *Gold Bulletin*, 2003; 36(3): 93-102

Lee S, Nomura S, Chiba A. Significant Improvement in Mechanical Properties of Biomedical Co-Cr-Mo Alloys with Combination of N Addition and Cr-Enrichment. *Mater Trans*, 2008; 49(2): 260-264.

M Salazar SM, Pereira SMB, V Ccahuana VZ, Passos SP, Vanderlei AD Pavanelli CA, Bottino MA. Shear bond strength between metal alloy and a ceramic system, submitted to different thermocycling immersion times. *Acta Ontolog Latinoam*, 2007; 20(2): 97-102.

Mackert JR, Rindle RD, Fairhurst CW. Oxide wrinkling and porcelain adherence on non-precious alloys. *J Am Dent Assoc*, 1982; 60: 377-381.

Matković T, Matković P, Malina J. Effects of Ni and Mo on the microstructure and some other properties of Co–Cr dental alloys. *J Alloys Comp*, 2004; 366: 293–297.

Metikoš-Huković M, Babić R. Passivation and corrosion behaviors of cobalt and cobalt chromium-molibdenium. *Cor Sci*, 2007; 49: 3570-3579.

McCabe JF, Walls AWG. *Applied dental materials*. 9th ed. Blackweell Publishing, 2008; pp. 71

Mineta S, Namba S, Yoneda T, Ueda K, Narushima T. Carbide Formation and Dissolution in Biomedical Co-Cr-Mo Alloys with Different Carbon Contents during Solution Treatment. *Met Trans*, 2010; 41A: 2129-2138.

Montero-Ocampo C, Rodriguez AS. Effect of carbon content on the resistance to localized corrosion of as-Cast cobalt-based alloys in an aqueous chloride solution. *J Biomed Mater Res*, 1995; 29: 441-453.

Naoyuki N, Mariko A, Atsushi K, Shigeo F, Akihiko C, Naoya M, Shuji H. Fabrication and Mechanical Properties of Porous Co-Cr-Mo Alloy Compacts without Ni Addition. *Mater Trans*, 2006; 47(2): 283-286.

Nobil4000 alloy data, online 2011. Available from URL: <http://www.nobilmetal.it/en/products.aspx?id=07EF07EF>

Oksiuta Z, Dabrowskia JR, Olszynab A. Co–Cr–Mo-based composite reinforced with bioactive glass *J Mater Proc Tech*, 2009; 209: 978–985.

Placko HE, Brown SA, Payer JH. Effects of microstructure on the corrosion behavior of CoCr porous coatings on the orthopedic implants. *J Biomed Mater Res*, 1998; 39: 292-299.

Roberts HW, Berzins DW, Moore BK, Charlton DG. Metal-ceramic alloys in dentistry: a review. *J Prosthodont*, 2009; 18: 188-194.

Rodrigues WC, Broilo LR, Lírio S, Knörnschild G, Espinoza FRM. Powder metallurgical processing of Co-28%Cr-6%Mo for dental implants: Physical, mechanical and electrochemical properties. *Pow Tech*, 2011; 206(3), 233-238.

Sato Y, Nomura N, Fujinuma S, Chiba A. Microstructure and Mechanical properties of Hot-Pressed Co-Cr-Mo alloy compacts. *Adv Mat Res*, 2007; (26-28), 769-772.

Sato Y, Nomura N, Fujinuma S, Chiba A. Microstructure and Tensile Properties of Hot-Pressed Co-Cr-Mo Alloy Compacts for Biomedical Applications. *J Japan Inst Metals* 2008, 532-537.

Shell JS, Nielsen JP. Study of the Bond between Gold Alloys and Porcelain. *J Dent Res*, 1962; 41: 1424-1437.

Shi L, Northwood DO, Cao Z. Alloy design and microstructure of a biomedical Co-Cr alloy. *J Mater Sci*, 1993; 28: 1312-1316.

Vásquez, VZC, Öscan M, Kimpara ET. Evaluation of interface characterization and adhesion of glass ceramics to commercially pure titanium and gold alloys after thermal- and mechanical-loading. *Dent Mater*, 2009; 25: 221-231.

Wagner WC, Asgar K, Bigelow WC, Flinn RA. Effect of interfacial variables on metal-porcelain bonding. *J Biom Mater Res*, 1993; 27: 531-537.

Zhuang LZ, Langer EW. Effects of alloy additions on the microstructures and tensile properties of cast Co-Cr-Mo alloy used for surgical implants. *J Mater Sci*, 1989; 24: 4324-4330.

Chapter 6

Hot pressing effect on the shear bond strength of dental porcelain to CoCrMoSi alloy substrates with different surface treatments

Submitted for publication to the journal Materials Science and Engineering C

B. Henriques¹, Faria, S², D. Soares¹, F.S. Silva¹

¹*Centre for Mechanical and Materials Technologies (CT2M) and Department of Mechanical Engineering, University of Minho, Azurém, 4800-058 Guimarães, Portugal*

²*Department of Mathematics and Applications, Research CMAT, University of Minho*

Abstract

Objectives: The purpose of this study was to evaluate the effect of hot pressing on the shear bond strength of a CoCrMoSi alloy to a low-fusing feldspathic porcelain, for two types of surface treatments.

Methods: Metal-porcelain composites specimens were produced by two different routes: conventional porcelain-fused-to-metal (PFM) and hot pressing (HP).

Additionally, two types of surface conditions were tested for each route: polished and grit-blasted. Bond strength of metal-porcelain composites were assessed by the means of a shear test performed in a universal test machine (crosshead speed: 0.5mm/min) until fracture. The shear strength of porcelain compacts obtained by the two routes, namely conventional vacuum sintering and hot pressing, was also assessed. Interfaces of fractured metal-ceramic specimens as well as undestroyed interface specimens were examined with optical microscope, stereomicroscope and SEM/EDS. Data was analyzed with Shapiro-Wilk test to test the assumption of normality. The 2-way ANOVA followed by Tukey HSD multiple comparison test was used to compare shear bond strength results and the t-test was used to compare the porcelain shear strength ($p < 0.05$).

Results: Hot pressed specimens exhibited significantly ($p < 0.001$) higher bond strength values than those obtained by conventional PFM technique. Significant differences ($p < 0.001$) were found in the shear bond strength between grit-blasted and polished specimens. The higher bond strength values were registered for HP specimens with grit-blasted surface, 141.17 ± 2.85 MPa. Significant differences ($p < 0.05$) were also found between the shear strength of vacuum sintered and hot pressed porcelain.

Significance: This study shows that hot pressing yields significantly ($p < 0.05$) higher metal-ceramic bond strengths than conventional PFM technique. Metal-ceramic bond strength gets maximized when porcelain is hot pressed onto rough metal surfaces, thus producing lower variability in results. Hot pressing technique showed also to enhance porcelain's cohesion.

1. Introduction

Metal-ceramic restorations comprise the union of a ceramic (feldspathic porcelain) to a metal substructure, through the fusion of ceramic onto the metallic substructure, hence the common name, porcelain-fused-to-metal (PFM) restorations. The success of this system relies on the strength provided by the metal substructure and by esthetics

coming from ceramic, which mimics the toothlike appearance (Anusavice, 2006). This system is currently used in metal-ceramic dental prostheses for dental restorations (anterior and posterior crowns and fixed partial dentures).

All-ceramic restorations have gained prominence in the last years due to their enhanced esthetic properties (Anusavice, 2006). Within the materials available for ceramic-cored restorations, zirconia is pointed as a very promising material due to its enhanced mechanical and esthetic properties (Zarone et al., 2011; Vichi et al., 2010). They are though more used in single crowns and short-span partial dentures (pre molars and anterior teeth) because of their higher susceptibility for fracture on molars. The veneering porcelain chipping from zirconia-cored restorations is faced as the major problem with this type of restoration (Donovan and Swift, 2009 and Zarone et al., 2011). For comparison, the incidence of ceramic veneer chipping from the zirconia core is 8%-10% in 1-2 years while the rate of chipping with PFM is in the range of 4-10% at 10 years (Donovan and Swift, 2009).

Cobalt-chromium alloys are very popular alloys that are used to produce partial denture frameworks. They have the advantage over nickel containing alloys of not creating any allergic reactions (Roberts et al., 2007). Relatively to gold alloys, it is a much cheaper alloy, hence more democratic, and has enhanced mechanical properties such as higher hardness and Young's modulus (Roberts et al., 2007). Base metal alloys have higher melting ranges (1400-1500°C) than gold alloys (800-1050°C), which requires more expensive melting equipments. Base metal alloys are also generally considered technique-sensitive because processing variables such as mold temperature, temperature of the molten alloy, and the sprue size and arrangement can affect the properties of the finished casting as much as composition does (Craig and Powers, 2002).

Hot Pressing, also called high temperature injection molding, consists on the application of external pressure to sinter and shape the ceramic at high temperature, and was first used in the fabrication of all-ceramic restorations such as crowns, inlays, on-lays, veneers and fixed partial dentures. Recently, this technique became available

also for metal-ceramic restorations (Ishibe et al, 2011). Hot Pressing is characterized to avoid large pores and to promote a good dispersion of the crystalline phase within the glassy matrix, hence resulting in superior mechanical properties within the ceramics (Venkatachalam et al., 2009; Drummond et al., 2000) and in flawless metal-ceramic interfaces. Despite being just a few, there are some studies on the bond strength of Hot Pressed porcelain to metal dental substructures. Schweitzer et al. (2005) and Venkatachalam et al. (2009), performed comparative studies on the bond strength between ceramic pressed to metal versus feldspathic porcelain fused to metal, although the pressable ceramic they used was indicated to all-ceramic restorations and not for metal-ceramic ones. They found no differences between the two techniques for the tested alloys, níquel-chromium vs. gold-palladium and cobalt-chromium vs. gold-palladium, respectively.

Ishibe et al. (2011) performed a study involving recently developed heat pressable ceramics for metal-ceramic restorations, and found no differences on the bond strength between the conventional layering and the heat pressing process. Henriques et al. (2011a) found significant differences on metal-ceramic bond strength between Hot Pressed and conventionally fused porcelain to metal (gold based alloy). Unlike the other studies, Henriques et al. (2011a) used porcelain in powder form and not in ingot form.

The aim of this study was to assess the influence of Hot Pressing on the metal-ceramic bond strength, between a base metal alloy (CoCrMo) and a conventional low-fusing feldspathic porcelain, and for two types of surface treatments.

2. Material and Methods

For this work a CoCrMoSi dental alloy (Nobil 4000, Nobilmetal, Villafranca d'Asti, Italy) and a dental opaque ceramic (Ceramco3, Dentsply, York, USA) (batch number: 10004163) were used. The chemical composition of both materials is presented in Table 6.1 and Table 6.2.

Table 6.1. Base alloy composition (wt.%) (according to manufacturer).

Co	Cr	Mo	Si	Others
62	31	4	2.2	Mn – Fe – W

Table 6.2. Ceramic chemical composition (wt.%).

SiO ₂	Al ₂ O ₃	K ₂ O	SnO ₂	ZrO ₂	CaO	P ₂ O ₅	Na ₂ O	Others
41.3	14.5	14.0	11.9	5.8	4.1	4.1	3.0	MgO, SO ₃ , ZnO, Cr ₂ O ₃ , Fe ₂ O ₃ , CuO, Rb ₂ O

Metal substrates (n=20) were obtained by lost wax process casting in an arc melting furnace, (Degumat 2033, Degussa, Germany). Metal rods of approximately 4.5 mm of diameter and 40 mm length were produced. After divesting, metal rods were cut into several 4mm height metal substrates using a precision cut-off machine (Minitom, Struers).

Porcelain was bonded to metal substrates by two routes: conventional porcelain fused to metal (**PFM**) and hot pressing (**HP**). Two types of metal surface treatment were tested: polished surface and rough surface.

First, all substrates were ground until 1200-grit sandpaper. Polished substrates were ground with 2400 grit-sandpaper and rough ones were grit-blasted with $\varnothing 110\mu\text{m}$ alumina grains at a pressure of 3 bar (Protempomatic, Bego, Germany). All substrates were ultrasonically cleaned in an alcohol bath for 10 min and rinsed in distilled water for another 10 min to remove contaminants. They were dried with adsorbent paper towels. It was not performed any preoxidation surface treatment to the alloy before porcelain bonding.

To produce porcelain fused to metal (**PFM**) specimens an acrylic template was used to ensure that the porcelain height was the same for all specimens (4mm). Porcelain was applied to metal substrates in the form of a creamy paste resulting from the addition

of distilled water to porcelain powders in the ratio of 1:2 (water:porcelain). The excess of water was removed using an adsorbent paper and after the porcelain condensing, metal-porcelain sets were carefully moved to a furnace (Vita 900, Vita, Bad Säckingen, Germany) and vacuum sintered (1mBar) at 970°C and at a heat rate of approx. 70°C/min, following porcelain's manufacturer specifications.

Hot pressed (**HP**) specimens were obtained by pressing the porcelain powders onto the metal substrate in a graphite die under vacuum ($\sim 10^{-2}$ mBar) at a temperature of 970°C, and at a pressure of ~ 20 MPa (Figure 6.1). The cavity of the graphite die was veneered with zirconium oxide to avoid carbon diffusion to specimens. The heat rate was 70°C/min and after a 2 minute stage at 970°C, the power of the induction heating furnace was shut down. The die cooled naturally.

In order to determine the effect of Hot Pressing in the porcelain strength, it was performed a complementary shear test to cylindrical porcelain specimens (\varnothing 4.5x4mm) obtained by two routes, namely conventional vacuum sintering (VS) and hot pressing (HP).

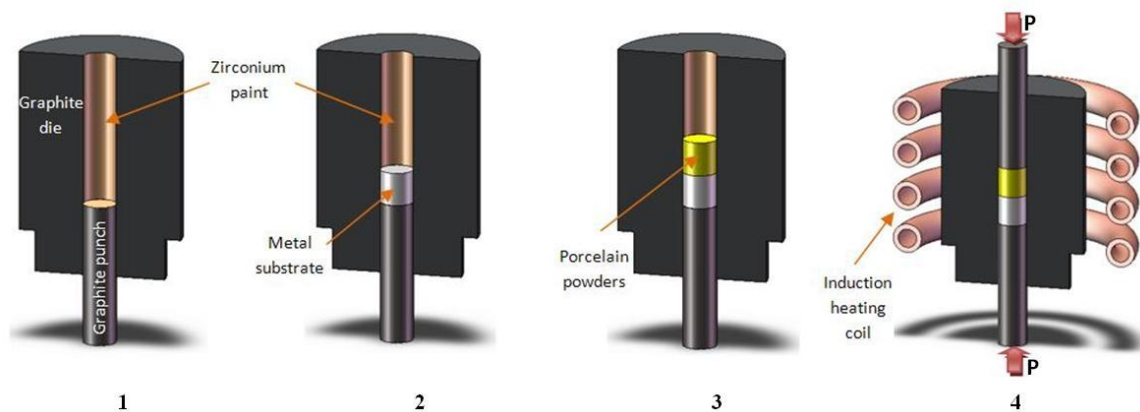


Figure 6.1. Hot pressing procedure: 1 – Painting die's cavity with zirconium oxide; 2 – Place the metal substrate in die's cavity; 3 – Place the porcelain powders in die's cavity; 4 – Hot pressing (pressure+temperature) metal-porcelain set.

2.1. Shear tests

The shear bond strength tests were carried out at room temperature and performed in a universal testing machine (Instron 8874, MA, USA), with a load cell having 25 kN capacity and under a crosshead speed of 0.5mm/s. Tests were performed in a custom-made stainless steel apparatus (Figure 6.2) similar to that described by Henriques et al. (2011a).

The shear bond strength (MPa) was calculated dividing the highest recorded fracture load (N) by the cross sectional area of the bonded porcelain (mm²).

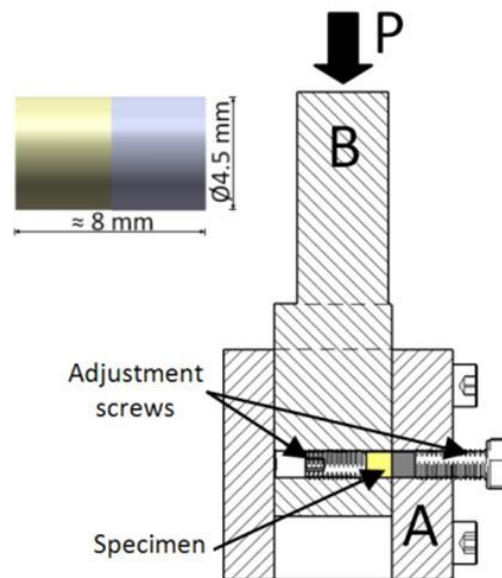


Figure 6.2. Cross-section schematic of the shear test device (A: external part; B internal part). The specimens' dimensions are also shown.

2.2. Analysis of the metal-porcelain interface and failure mode

The metal-ceramic interface as well as representative fracture surfaces were evaluated by optical microscope (Axiotech, Carl Zeiss, USA) and SEM/EDS (Nova 200, FEI, Oregon, USA). For interface analysis, the specimens were embedded in auto-polymerizing resin,

ground finished to 1200 grit SiC sand-paper and polished with diamond paste first in 6 μ m and finally with 1 μ m felt disc. Morphologic and chemical analysis were performed.

The elemental distribution across the metal-ceramic interface was determined by using line scan EDS analysis (20 points in the metal side and 20 points in the porcelain side).

The specimens' failure modes were classified as: (1) adhesive, if no remnants of ceramic were found in the metal surface; (2) cohesive, if fractures occurred within the ceramic side; (3) mixed, if remnants of ceramic were found in the metal surface.

2.3. Statistical analysis

Data were analyzed using SPSS statistic software (Release 18.0.0 for windows). The Shapiro-Wilk test was first applied to test the assumption of normality. Differences between processing type and surface treatment factors in the shear bond strength results were compared using 2-way ANOVA followed by Tukey HSD multiple comparison test. Differences between hot pressed (HP) and conventional vacuum sintered (VS) porcelains in terms of shear strength were tested using t-test. P values lower than 0.05 were considered statistically significant in the analysis of the results

2.4. Metal surface characterization

The average surface roughness (Ra) of both types of specimens (Polished and Grit-Blasted) was measured using a profilometer (Mahr S5P, Germany). Two orthogonal measurements of 4mm length on the surface of each sample were made.

3. Results

Results of the metal-ceramic shear bond strength tests performed for different processing and surface conditions are plotted in Figure 6.3. The conventional porcelain fused to metal (PFM) technique yielded lower mean bond strength values than hot pressing (HP) technique, regardless of the surface treatment used (polished (P) or grit-basted (GB)).

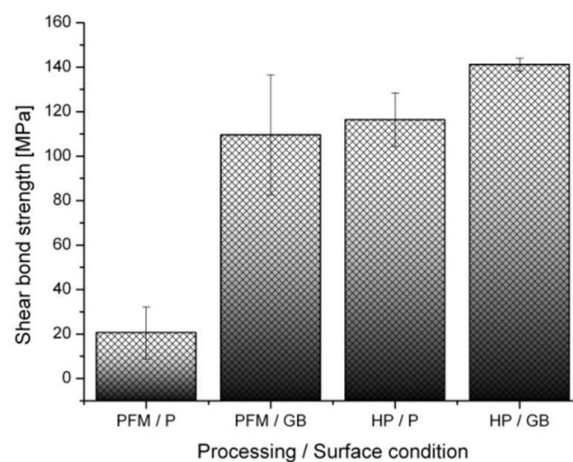


Figure 6.3. Metal-ceramic shear bond strength results for each combination of Processing type (PFM – Porcelain-Fused-to-Metal; HP – Hot Pressing) and Surface treatment (P – Polished; GB - Grit-Blasted).

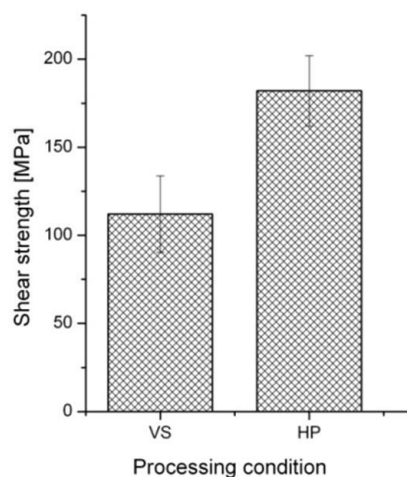


Figure 6.4. Porcelain shear strength results for different processing conditions (VS – conventional Vacuum Sintering technique; HP – Hot Pressing).

The results of 2-way ANOVA for the experimental conditions are presented in Table 6.3. The mean bond strength values were significantly affected by the processing type ($p < 0.001$) and surface treatment ($p < 0.001$). The interaction between the processing type and surface treatment were statistically significant ($p < 0.001$). The results of Tukey's multiple comparison test demonstrated that when the surface treatment was GB the HP processing type showed significantly higher results than the PFM processing type ($p < 0.05$) and when the surface treatment was P the HP processing type also showed significantly higher results than the PFM processing type ($p < 0.05$). When the processing type was PFM the GB surface treatment showed significantly higher results than the P surface treatment ($p < 0.05$). (See Table 6.5 and Figure 6.3).

In terms of processing condition, Hot Pressed porcelain (HP) displayed a significantly higher strength than that of conventionally Vacuum Sintered (VS) porcelain (t-test, $p < 0.001$). (See Figure 6.4 and Table 6.4).

Table 6.3. Two-way ANOVA results according to metal-ceramic shear bond strength data.

	df	SS	MS	F	p
Processing type	1	20280.43	20280.43	79.78	1.29E-7
Surface treatment	1	16172.52	16172.53	63.62	5.76E-7
Interaction	1	5141.40	5141.40	20.23	3.66E-4
Total	19	45661.62			

Statistically significant at a level of $p < 0.05$. **df**: Degrees of freedom; **SS**: Sum of squares; **MS**: Mean square; **F**: F-ratio; **p**: p-value

Table 6.4. Mean \pm standard deviation (SD) of the shear strength of porcelain processed by two routes, hot pressing and vacuum sintering (MPa).

	Processing route	
	Hot Pressing (HP)	Vacuum Sintering (VS)
Porcelain shear strength	182.06 \pm 19.98	112.16 \pm 21.73

Table 6.5. Mean \pm standard deviation (SD) of the shear bond strength results (MPa).

Experimental conditions		Surface treatment		
		Polished	Grit Blasted	Mean \pm SD
Processing type	PFM	20.60 \pm 11.63 ^{a,b,c}	109.55 \pm 26.98 ^{a,d}	65.07 \pm 50.80 ^f
	HP	116.36 \pm 12.08 ^b	141.17 \pm 2.85 ^{c,d}	128.76 \pm 15.47 ^f
	Mean \pm SD	68.48 \pm 51.69 ^e	125.36 \pm 24.59 ^e	

Same superscript letters indicate significant differences (Tuckey's test, $\alpha=0.05$)

Specimens were classified under their failure types as adhesive and mixed. All polished specimens (PFM/P and HP/P) as well 80% of PFM/GB specimens, exhibited adhesive failure. A mixed failure type was observed for 20% of PFM/GB specimens, which showed remnants of ceramic on the metal's surface after fracture.

Figure 6.5 shows an EDS line scan analysis (in white) for PFM and HP specimens. This analysis allows the visualization of element concentration profiles at the metal-porcelain interaction zone. Results show no diffusion of Co, Cr and Mo into porcelain. However, it is possible to see that Cr is present in the oxide layer formed on metal surface. Regarding porcelain elements, it was observed an extensive diffusion of all its elements (O, Si, Al, K, Sn, Na, Ca, Mg) into metal. Special attention must be given to O₂, in the metal zone, which was detected in a higher concentration.

Grit-Blasted (GB) specimens presented approximately ten times rougher surface than Polished (P) ones, Ra=0.58 \pm 0.01 μ m and Ra=0.05 \pm 0.01 μ m, respectively.

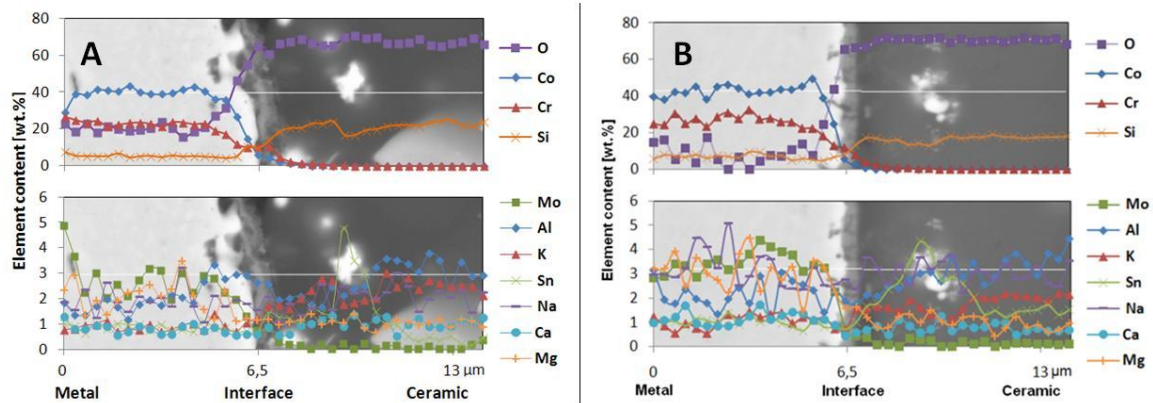


Figure 6.6. EDS line analysis of metal/ceramic interface showing the inter-diffusion of elements in (a) Porcelain-Fused-to-Metal and (b) Hot Pressed specimens.

4. Discussion

4.1. Materials

This study evaluated the effect of hot pressing on the shear bond strength of CoCrMoSi alloy-porcelain composites and made a comparison with conventionally obtained porcelain fused to metal specimens for different surface treatments, polished and grit-blasted.

In this study it was used the cobalt based alloy Nobil 4000 (Co-Cr-Mo-Si). This alloy is mainly composed by cobalt and chromium, containing in its composition several other minor alloying elements (Mo, Si, Mn, Fe, W). The constituents of this alloy develop specific features, such as: chromium - provide strength and corrosion resistance via passivation (Metikoš-Huković and Babić, 2007); molibdenum - provide a solid solution hardening and influences the alloy's coefficient of thermal expansion (CTE) (Roberts et al., 2009; Mankins and Lamb, 1990; Crook, 1990); iron and tungsten - provide a solid solution hardening to the alloy (Roberts et al., 2009; Mankins and Lamb, 1990); silicon - imparts good casting properties and increases alloy ductility (McCabe and Walls, 2008).

The Ceramco 3 porcelain is a high-fusing, leucite based porcelain, used for metal-ceramic and all ceramic restorations. It is characterized by good mechanical properties (Rizkalla and Jones, 2004) and is compatible with high noble, noble and predominantly base alloys.

4.2. Shear bond strength test

There are several available ways to measure metal-ceramic bond strength. Within the most common mechanical tests are the shear test, the Schwickerath crack initiation test used in ISO 9693:1999, the three-point-flexure test, the four-point-flexure test and the biaxial flexure test. The shear bond strength test results are characterized for not being influenced by the Young's Modulus of the alloy as happens for bending tests (Hammad and Talic, 1996; Hammad and Stein, 1990) and by its suitability for evaluation of metal-ceramic bonds (Anusavice et al.,1980; Ihab and Yourself,1996). Special attention must be paid to the device configuration because it can largely influence results. For instance, the shear device composed by a knife without a groove, generates great local stresses in the porcelain caused by small area of contact that can lead to the porcelain failure. Failure at the interface can be triggered by a cohesive failure in the porcelain and consequent propagation through the interface. The test device used in this study consisted in a piston-type shear device with half loop loading which reduces the stress concentration magnitude adjacent to the interface. This is considered an improved loading condition compared with concentrated force application at a single point (knife without a groove) or distributed only over a single layer (deHoff et al., 1995). Based on these facts, many authors used this test configuration in metal-ceramic bond strength characterization (Akova et al, 2008; dos Santos et al., 2006; Vasquez et al., 2009; de Melo et al., 2005; M.Salazar et al., 2007).

4.3. Hot Pressing

This study involves a base metal alloy and a hot pressed veneering porcelain in powder form. Few studies can be found in literature about low-fusing, leucite-based pressable ceramics to metals (Drummond et al., 2000; Schweitzer et al., 2005; Venkatachalam et al., 2009; Ishibe et al., 2011). Within these studies, only Ishibe et al. (2011) tested the recently developed glass-ceramics pressed to metal cores, using a lost wax technique. Other authors (Schweitzer et al. 2005; Venkatachalam et al., 2009) have tested veneering pressable ceramics, designed for all-ceramic restorations, in hot pressed metal-ceramic restorations.

This study showed significantly ($p < 0.05$) higher metal-ceramic shear bond strength of hot pressed specimens when compared to conventional PFM specimens. Conversely, Venkatachalam et al. (2009) and Schweitzer et al. (2005) found no significant differences ($p > 0.05$) on metal-ceramic bond strength between ceramic pressed to metal and feldspathic porcelain fused to metal, either for noble or other base alloys. They pointed out some factors that could have influenced results, such as: the additional steps of divestment and sprue removal of pressed ceramic samples, and the excessive CTE mismatch between pressed ceramic and metal ($> 1 \times 10^{-6} 1/^\circ\text{C}$).

The statistical analysis of bond strength results revealed significant differences ($p < 0.05$) between hot pressed (HP) and porcelain fused to metal (PFM) specimens and between polished (P) and grit-blasted (GB) specimens (Table 6.3). The enhanced bond strength of GB specimens relatively to P is explained by the surface roughness produced by the grit-blasting treatment, causing an increased surface area for chemical bonding (Wagner and et al. 1993) and a metal-ceramic interlocking, which enables mechanical retention of the porcelain (Henriques et al., 2011a; Wagner and et al., 1993).

HP specimens exhibited greater bond strength values than PFM ones. This might be explained by a more effective contact between metal and porcelain resulting from a

superimposed overpressure, producing this way an interface free of defects such as pores or cracks (Figure 6.6a-d) where better chemical bonds can be established.

Regarding PFM/P specimens, the porcelain did not wet the polished metal's surface properly, and the establishment of an effective bond could not occur. This effect is confirmed by the identification of some gaps at the metal-porcelain interface (Figure 6.6a). PFM/GB specimens presented greater bond strength values than PFM/P due to the presence of a greater surface roughness, $R_a=0.58\pm 0.01\mu\text{m}$ vs. $R_a=0.05\pm 0.01\mu\text{m}$. Figure 6.6c shows the PFM/GB specimens' interface where some porosity was detected as processing defects (see arrows in Figure 6.6c). HP/P specimens showed significantly greater bond strength values relatively to PFM/P despite both having the same surface treatment. This fact is owed to hot pressing that enforced the contact between the two materials, thus promoting micromechanical retention and chemical bonding (Figures 6.6a-b). The greater bond strength results were registered for HP/GB specimens. Here, the advantages of hot pressing process are added to the benefits of a rough surface, resulting in a strong and flawless interface. It should be highlighted that HP/GB specimens exhibited the least standard deviation within all tested specimens, similar to what was reported by Henriques et al. (2011a) in a study involving a gold based alloy. The lower variability of results verified for HP/GB specimens represent the manufacture of more reliable restorations with greater reproducibility.

In order to guarantee that thermal based pre-stresses state at interface would not differ from PFM to HP specimens, it was applied an equivalent heating and cooling rates in both processes. The specimens' geometry was selected based on its simplicity and its broad use in similar studies for metal-ceramic bond strength assessment (Akova et al., 2008; dos Santos et al., 2006; Vasquez et al., 2009; de Melo et al., 2005; M. Salazar et al., 2007. Henriques et al., 2011a; Henriques et al., 2011b).

As stated before, a complementary study was conducted to assess the influence of hot pressing in the porcelain strength and a significant ($p<0.05$) increase in the porcelain shear strength was verified for hot pressed (HP) porcelain in comparison with vacuum sintered (VS) porcelain. This finding is in accordance with literature that reports some

advantages of pressable ceramics over traditional porcelains, namely higher compressive strengths and higher flexural strength, which are explained by an increased presence of uniformly distributed leucite phase (Kelly, 1997; Drummond et al., 2000).

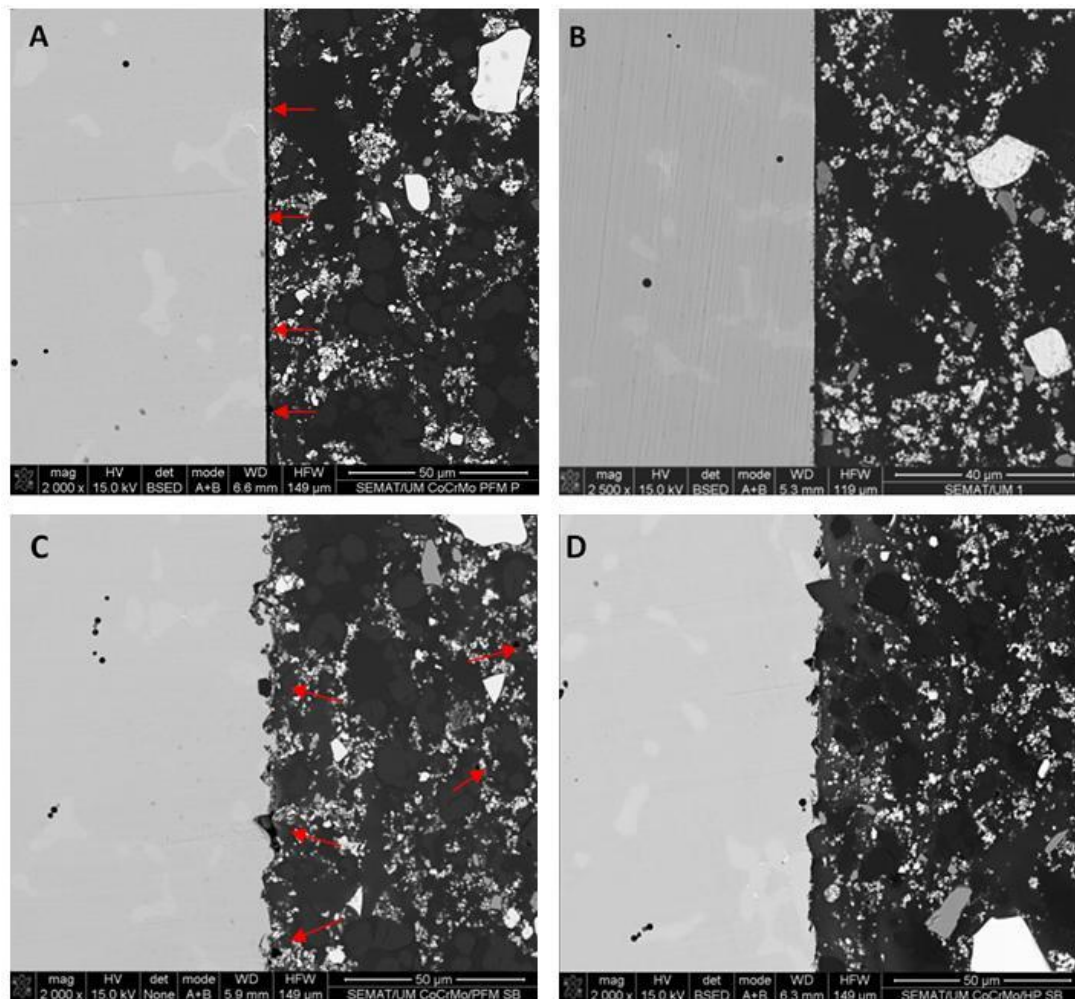


Figure 6.6. Metal-ceramic interface micrographs of Porcelain-Fused-to-Metal (A- Polished; B- Grit-Blasted) and Hot Pressed (C- Polished; D-Grit-blasted). The arrows indicate processing defects at the interface.

4.4. Fracture type analysis

Two fracture types were registered after specimens' testing: mixed and adhesive failure. Except for the case of PFM/GB specimens, which exhibited 20% of mixed failure, all the other specimens exhibited 100% adhesive failures. Considering this fracture type pattern, it cannot be established any correlation between the fracture type and the bond strength results. The same findings were reported by several other authors for manifold processing and base materials types. Henriques et al. (2011a) found no correlation between the type of failure and the bond strength in a study involving conventional fused porcelain (PFM) and hot pressing (HP) for a gold based alloy. de Melo et al. (2005) determined metal-porcelain bond strength for Ni-Cr and Co-Cr base alloys, and have also not found a correlation between the two factors. Akova et al. (2008) evaluated the bond strength of laser sintered (Co-Cr) and cast base metal alloys (Ni-Cr and Co-Cr) and were not able to establish any relation between failure type and bond strength results.

The greater cohesion of hot pressed porcelain could have accounted for the 100% adhesive failure type verified for hot pressed specimens, despite the good metal-ceramic bond strength that was exhibited. Therefore, this can suggest that the bonding between metal and porcelain was not as effective as the enhanced cohesive strength of porcelain.

4.5. EDS analysis

In order to characterize the atoms diffusion phenomena at the metal-ceramic interface, an EDS line scan analysis was performed at that site. Figure 6.5 shows an oxide layer formed at metal-ceramic interface that was formed during the porcelain firing cycle since the alloy was not subjected to a preoxidation heat treatment in any of the hot pressed or porcelain fused to metal specimens. Attending to the elements diffusion profiles, one can see that the oxide layer is composed by several elements

coming from metal and ceramic. Other studies indicate that this layer is commonly composed by a large quantity of Cr_2O_3 (Mackert et al., 1981). Unlike Anusavice et al.(1977) findings, it was not here registered any Co or Cr accumulation at the interface. The lack of a significant presence of Cr at the interface can be related to the absence of a preoxidation heat treatment to the alloy together with the porcelain's firing cycle performed under vacuum, which could have caused some surface chromium volatilization (Cydzik et al., 2005). The presence of porcelain elements such as Si, Al, Ca, Na, Sn and Oxygen, on the metal side in a great extent, suggests a considerable width of diffusion zone.

The present study demonstrates the benefits that hot pressing can provide to the performance of a metal-ceramic restoration, especially in terms of greater metal-ceramic adhesion and porcelain fracture toughness. These findings were obtained by static mechanical tests, which do not correspond to the clinical conditions at which they are subjected in the oral cavity. Therefore, future tests should include metal-ceramic bond stress assessment after thermal and mechanical cycling in order to better simulate real operating conditions of dental materials.

5. Conclusions

From this study, the following conclusions can be drawn:

1. Hot pressing (HP) technique significantly ($p < 0.05$) improved metal-ceramic bond strength relatively to conventional porcelain fused to metal (PFM) technique;
2. Hot pressing technique (HP) provides to the porcelain significantly ($p < 0.05$) higher shear strength than conventional vacuum sintering technique;
3. Grit-blasting (GB) surface treatment significantly ($p < 0.05$) improved metal-ceramic bond strength whether the hot pressing (HP) or the porcelain fused to metal (PFM) techniques are used.

6. Acknowledgements

This work has been supported by PhD Grant of FCT (Portuguese Foundation for Science and Technology) with the reference SFRH / BD / 41584 / 2007.

Special thanks to DentalCastro – Prosthetic Laboratory for their contribution in this work.

7. References

Akova T, Ucar Y, Tukay A, Balkaya MC, Brantley WA. Comparison of the bond strength of laser-sintered and cast base metal dental alloys to porcelain. *Dent Mater*, 2008; 24: 1400-1404.

Anusavice KJ. *Phillips' science of dental materials*. 11th ed. Philadelphia:W.B. Saunders, 2006; pp. 621-54.

Anusavice KJ, Dehoff PH, Fairhurs CW. Comparative evaluation of ceramic-metal bond tests using finite element stress analysis. *J Dent Res*, 1980; 59: 608-613.

Anusavice KJ, Horner JA, Fairhurst CW. Adherence controlling elements in ceramic-metal systems. I. Precious alloys. *J Dent Res*, 1977; 56: 1045.

Craig RG, Powers JM. *Restorative dental materials*. 11th ed. Mosby, 2002; pp.480-492.

Crook P. *Metals Handbook: Properties and Selection: Non ferrous alloys and special-purpose alloys (ed10), Volume 2*. Metals Park, OH, ASM International, 1990; pp. 446-454.

de Melo RM, Travassos AC, Neisser MP. Shear bond strengths of a ceramic system to alternative alloys. *J Prosthet Dent*, 2005; 93: 64-69

DeHoff PH, Anusavice KJ, Wang Z. Three-dimensional finite element analysis of the shear bond strength test. *Dent Mater*, 1995; 11: 126-131.

dos Santos JG, Fonseca RG, Adabo LG, Cruz CAS. Shear bond strength of metal-ceramic repair systems. *J Prosthet Dent*, 2006; 96(3): 165-173.

Donovan TE, Swift EJJr. Porcelain-Fused-to-Metal (PFM) Alternatives. *J Comp*, 2009; 1: 4-6.

Drummond JL, King TJ, Bapna MS, Koperski RD. Mechanical property evaluation of pressable restorative ceramics. *Dent Mater*, 2000; 16: 226-233.

Hammad IA, Stein RS. A qualitative study for the bond and color of ceramometals – Part I. *J Prosthet Dent*, 1990; 75: 602-608.

Hammad IA, Talic YF. Designs of bond strength tests for metal-ceramic complexes: Review of the literature. *J Prosthet Dent*, 1996; 75: 602-608.

Henriques B, Soares D, Silva F. Shear bond strength of a Hot Pressed Au-Pd-Pt alloy-porcelain dental composite. *J Mech Behav Biomed Mater*, 2011a; 4(8): 1718-1726

Henriques B, Soares D, Silva F. Optimization of bond strength between gold alloy and porcelain through a composite interlayer obtained by powder metallurgy. *Mater Sci Eng A*, 2011b; 528: 1415-1420

Ihab AH, Yourself FT. Designs of bond strength tests for metal-ceramic complexes: Review of literature. *J Prosthet Dent*, 1996; 75: 602-608.

Ishibe M, Raigrodski AJ, Flin BD, Chung KH, Spiekerman C, Winter RR. Shear bond strengths of pressed and layered veneering ceramics to high-noble alloy and zirconia cores. *J Prosthet Dent*, 2010; 105: 29-37.

Kelly JR. Ceramics in restorative and prosthetic dentistry. *Annu Rev Mater Sci*, 1997; 27: 443-36.

Krasicka-Cydzik E, Okisiuta Z, Dabrowski JR. Corrosion testing of sintered samples made of the Co-Cr-Mo alloy for surgical applications. *J Mater Sci: Mater Med*, 2005; 16: 197-202.

M Salazar SM, Pereira SMB, V Ccahuana VZ, Passos SP, Vanderlei AD Pavanelli CA, Bottino MA. Shear bond strength between metal alloy and a ceramic system, submitted to different thermocycling immersion times. *Acta Ontolog. Latinoam*, 2007; 20(2): 97-102

Mackert, JR, Rindle RD, Fairhurst CW. Oxide wrinkling and porcelain adherence on non-precious alloys. *J Am Dent Assoc*, 1981; 60: 377-381.

Mankins, WL, Lamb S, 1990. Nickel and nickel alloys. *Metals Handbook: Properties and selection: Non ferrous alloys and special-purpose materials (ed10), Volume 2*. Metals Park, OH, ASM International, pp. 428-445.

McCabe JF, Walls AWG. *Applied dental materials*. 9th ed. Blackweell Publishing, 2008; pp 71.

Metikoš-Huković M, Babić R. Passivation and corrosion behaviors of cobalt and cobalt chromium-molibdenium. *Cor Sci*, 2007; 49: 3570-3579.

Rizkalla AS, Jones DW. Indentation fracture toughness and dynamic elastic moduli for commercial feldspathic dental porcelain materials. *Dent Mater*, 2004; 20: 198-206.

Roberts HW, Berzins DW, Moore BK, Charlton DG. Metal-ceramic alloys in dentistry: a review. *Int J Prosthodont*, 2009; 18: 188-194.

Schweitzer DM, Goldstein GR, Ricci JL, Silva NR, Hittelman EL. Comparison of bond strength of a pressed ceramic fused to metal versus feldspathic porcelain fused to metal. *J Prosthodont*, 2005; 14: 239-247.

Vásquez VZC, Öscan M, Kimpara ET. Evaluation of interface characterization and adhesion of glass ceramics to commercially pure titanium and gold alloys after thermal- and mechanical-loading. *Dent Mater*, 2009; 25: 221–231.

Venkatachalam B, Goldstein R, Pines MS, Hittelman EL. Ceramic Pressed to Metal versus feldspathic porcelain fused to metal: a comparative study of bond strength. *Int. J Prosthodont*, 2009; 22: 94-100.

Vichi A, Louca C, Corciolani G, Ferrari M. Color related to ceramic and zirconia restorations: A review. *Dent Mater*, 2011; 27:97-108.

Wagner WC, Asgar K, Bigelow WC, Flinn RA. Effect of interfacial variables on metal-porcelain bonding. *J Biom Mater Res*, 1993; 27: 531-537.

Zarone F, Russo S, Sorrentino R. From porcelain-fused-to-metal to zirconia: Clinical and experimental considerations. *Dent Mater*, 2011; 27: 83-96.

Chapter 7

Experimental evaluation of the bond strength between a CoCrMo dental alloy and porcelain through a composite metal-ceramic graded transition interlayer

Published in Journal of the Mechanical Behavior of Biomedical Materials, 2012, doi: 10.1016/j.jmbbm.2012.04.019

B. Henriques¹, M. Gasik², D. Soares¹, F.S. Silva¹

¹*Centre for Mechanical and Materials Technologies (CT2M) and Department of Mechanical Engineering, University of Minho, Azurém, 4800-058 Guimarães, Portugal*

²*Department of Materials Science and Engineering, School of Chemical Technology, Aalto University Foundation, 00076 Aalto, Espoo, Finland*

Abstract

Objectives: The purpose of this study was to evaluate the shear bond strength between CoCrMo dental alloy and porcelain restorations by application of different

metal-ceramic transitional interfaces aiming on improvement of the bond strength and fracture tolerances.

Methods: Several metal-ceramic specimens with different composite interlayers were produced. The interlayers consisted in metal/ceramic composites with different metal volume fractions (20M; 40M; 60M; 80M). The metal-ceramic bond strength as well as the fracture strength of the composites and monolithic base materials were assessed by the means of a shear test performed in a universal test machine. The interfaces of fractured and untested specimens were examined by the means optical microscopy. The microstructures of monolithic base materials were analyzed using SEM/EDS. The elastic and inelastic properties of the homogeneous compositions were additionally evaluated using dynamic mechanical analysis.

Results: The bond strength results obtained for metal-ceramic graded specimens were the highest (261 ± 38 MPa) for 40% vol. metal in the interlayer [40M] vs. 109 ± 27 MPa for a direct metal-ceramic joint. The Young's moduli and the fracture resistance of the composites revealed an increasing trend for increasing metal contents.

Significance: This study shows that a graded transition between metal and ceramic, provided by a metal/ceramic composite interlayer, is regarded for an increase by 2.5 times in the bond strength between the two materials relative to conventional sharp transitions. The elastic modulus of the composites used as interlayers might be very reasonably approximated by a micromechanical model.

1. Introduction

A metal-ceramic dental prosthesis comprises a metal shell on which is fused a porcelain veneer in a high heat oven. This technique is called porcelain-fused-to-metal (PFM). The metal framework provides compression and tensile strength, and the porcelain provides the crown a white tooth-like appearance. An alternative to metal-ceramic restorations are the all-ceramic ones, in which the metal framework is

replaced by a ceramic core (e.g. alumina, zirconia) (Anusavice, 2006; Zarone et al., 2011). Although the use of a ceramic framework can lead to better instant aesthetical results, published clinical results are not comparable at the moment with metal-ceramic restorations. There are not enough long-term data for validating the clinical potential of all-ceramic restorations (Zarone et al., 2010). The major drawbacks of such restorations are their high susceptibility on fracture and shock for higher loads and load rates (as it happens on molars) together with the great incidence of veneering porcelain chipping (8-10% in 1-2 years) when compared with PFM restorations (4-10% in 10 years) (Donovan and Swift, 2009). Hence, they are often used in single crowns and short-span partial dentures (pre molars and anterior teeth) (Zarone et al., 2011, Vichi et al., 2010). Therefore, PFM restorations remain the best option when one wishes to combine good aesthetics with maximum clinical longevity (Kelly, 1996; Donovan and Swift, 2001).

Metal-ceramic dental restorations life time strongly depends on the success of the bond between porcelain and the metal substrate (Drummond et al., 1984). The nature of the bond between the metal coping and the ceramic has been extensively studied and it is generally agreed that it is attributed to four mechanisms (Van Noort, 2007): mechanical retention; compression fit; van der Waal's forces and chemical bonding. Hence, in order to obtain a good bond between the metal coping and the ceramic veneer, the metal surface needs to be carefully prepared. To create mechanical retention, metal frameworks are usually sandblasted with alumina particles to promote desired surface roughness, thus increasing the extent of metal-ceramic mechanical interlocking. To assure for a compression fit, the metal's coefficient of thermal expansion (CTE) should be slightly higher than that of the porcelain ($\alpha_M - \alpha_C > 0.5 \times 10^{-6} \text{ 1/}^\circ\text{C}$) (Craig and Powers, 2002). On cooling, the metal contracts more than ceramic, leaving the latter in a state of compression (Craig and Powers, 2002). Finally, before porcelain firing, metal substrates are often submitted to a heat treatment to create a controlled thin oxide coating on the metal's surface that forms chemical bonds (ionic, covalent or metallic) with the porcelain oxides.

In fact, despite the great survival rates of metal-ceramic restorations, failure in these systems still occur (Kerschbaum et al., 1997; Coornaert et al., 1984, Özcan, 2003; Liu et al., 2008) and therefore, they are still the object of extensive studies. Failures are often reported as having the following causes: excessive porosity in the ceramic due to technical processing deviations (Oram, 1984); microcracks in ceramic caused by thermal stresses due to thermal coefficient differences between metal and porcelain (Yamamoto M, 1989); and mechanical and thermal fatigue (Vásquez et al., 2009).

The solution to overcome problems related to the bonding of these two materials with such different natures can have an answer in natural teeth structure. Natural tooth is composed of two distinct materials: enamel and dentin with elastic moduli of ~65 and ~20 GPa, respectively. They are bound by dentin-enamel-junction (DEJ) where the Young's modulus changes linearly from that of enamel to that of dentin, thus reducing dramatically the stress in the enamel (Huang et al., 2007; Niu et al., 2009) when loads are applied and acting as a natural functionally graded material (FGM). By definition, a FGM is a heterogeneous composite material containing a number of constituents which exhibit a compositional gradient from one surface of the material to the other subsequently resulting in a material with continuously varying properties (Suresh and Mortensen, 1998). Experimental and theoretical analyses have proved that gradients in surface composition can improve the mechanical performance of a material and graded materials have better ability to resist thermal and mechanical stresses (Suresh, 2001). It have been demonstrated that using a graded interface in the metal ceramic joints, stresses might be decreased by 3-8 times relative to sharp interfaces (Gasik et al. 2005).

This study aimed at reducing stresses and stresses derivatives at the metal-ceramic interface, caused by material properties mismatch, by the means of creation of a composite interlayer which would act as a smooth transition zone between metal and ceramic. Henriques et al. (2011) have studied this subject for high noble gold dental alloy. The significant improvements on metal-ceramic bond strength was explained by both the smooth transition between base materials provided by the interlayer and by

the use of hot pressing technique, which enabled flawless interfaces (absence of undesired porosity and small cracks) and promoted the full contact between the materials, thus contributing to a better chemical bonding (Henriques et al., 2011a; Henriques et al., 2011b). It is therefore possible to apply a similar concept to dental restorations in general, and using a base metal alloy (CoCrMo) in particular. Such approach and the properties of CoCrMo/porcelain composites have not been yet reported in literature.

Nevertheless, there is a study (Okisuta et al., 2009) reporting significant increase in the hardness, yield strength and corrosion resistance of CoCrMo based composites reinforced with bioactive glass when compared to the pure CoCrMo alloy. This can give a hint about the properties that are expected for the CoCrMo-porcelain composites that will be used in this study as interlayers. Hence, the main purpose of this study was to assess the impact of the presence of a composite interlayer on the metal-ceramic bond strength. Several interlayers with different metal/ceramic volume fractions were tested in order to find the composition that maximizes the bond strength between the two materials that takes part in the restoration.

2. Materials and Methods

2.1. Materials

In this study a CoCrMo alloy (Nobil 4000, Nobilmetal, Villafranca d’Asti, Italy) and a Dental Opaque Porcelain (Ceramco3, Dentsply, York, USA) (batch number: 08004925) were used. Table 1 and Table 2 present the metal and the porcelain chemical compositions, respectively.

Table 7.1. Base alloy composition (wt.%) (according to manufacturer).

Co	Cr	Mo	Si	Others
62	31	4	2.2	Mn – Fe – W

Table 7.2. Ceramic chemical composition (wt.%).

SiO ₂	Al ₂ O ₃	K ₂ O	SnO ₂	ZrO ₂	CaO	P ₂ O ₅	Na ₂ O	Others
41.3	14.5	14.0	11.9	5.8	4.1	4.1	3.0	MgO, SO ₃ , ZnO, Cr ₂ O ₃ , Fe ₂ O ₃ , CuO, Rb ₂ O

2.2. Processing

The manufacturing of the metal-ceramic specimens comprised the following steps: 1) casting the metal substrates; 2) production of the metal/ceramic composites to be used as interlayers and; 3) hot pressing the metal-interlayer-ceramic specimens. Hence, metal substrates were obtained by lost wax investment casting, held in an arc melting furnace (Degumat 2033, Degussa, Germany) in which were produced metal rods of approximately 4.5 mm of diameter and 40 mm length. Metal rods were divested using water and steam jet. After several 4 mm height specimens were cut in a precision cut-off machine (Minitom, Struers). All metal substrates were ground until 1200-grit sand paper and then grit-blasted with Ø110µm alumina grains at a pressure of 3 bar (Protempomatic, Bego, Germany). Then, they were ultrasonically cleaned in an alcohol bath for 10 min and rinsed in distilled water for another 10 min to remove contaminants. Finally they were dried with adsorbent paper towels. It must be pointed out that no preoxidation heat treatment was applied to the metal substrates before porcelain bonding.

Several powder mixtures with different metal/porcelain volume fractions were produced to be used as interlayers. After powders' weighting, the mixtures were blended in a rotary machine at 40 rpm during 10 min. The following mixtures were produced (vol.%): pure porcelain with 0% metal [0M]; 20% metal [20M]; 40% metal [40M]; 60% metal [60M]; 80% metal [80M] and 100% metal [100M]. Finally the sets composed by the metal substrate + composite interlayer + porcelain were hot pressed in a graphite die. The hot pressing sequence comprised the following steps (Figure 7.1): first, the graphite die's cavity was veneered with ZrO₂ paint to prevent carbon

diffusion to specimens after which the metal substrate was there placed. After the metal substrate was in place, the metal-ceramic powder mixture was inserted into the cavity. For last, the porcelain powders were inserted into the cavity. The porcelain sintering (hot pressing) was performed under vacuum ($\sim 10^{-2}$ mBar) at a temperature of 970°C and a constant pressure of ~ 20 MPa. The selected heat rate was $70^{\circ}\text{C}/\text{min}$ and after a 2 minute stage at 970°C , the cooling rate was natural after the power of the induction heating furnace was shut down. All studied interlayers had the same thickness of ~ 500 μm .

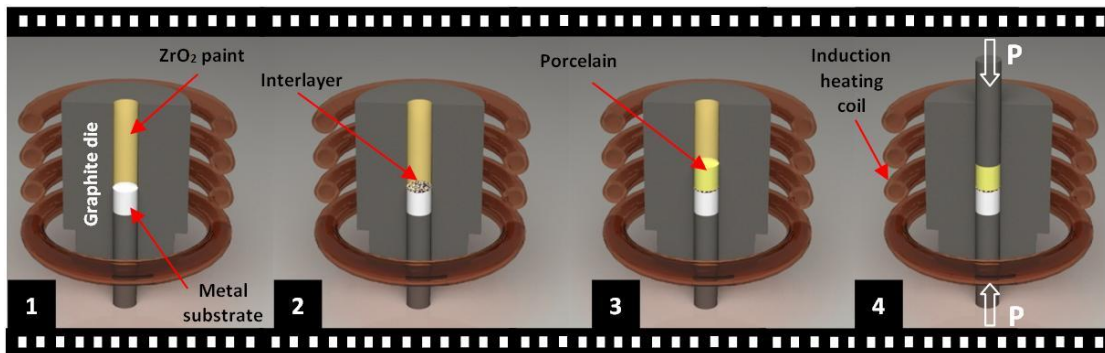


Figure 7.1. HSMP specimens' manufacturing procedure: **1** – Die's cavity painting with zirconium paint followed by metal substrate's placement; **2** – Placement of metal/ceramic composite powders in the die's cavity; **3** – Porcelain powders placement; **4** - Hot pressing (pressure+temperature) the metal-interlayer-porcelain specimen.

To be used as control group, several porcelain-fused-to-metal (PFM) specimens were also produced ($n = 5$). Porcelain was applied onto metal substrates in the form of a creamy paste resulting from the addition of distilled water to porcelain powders (the mass ratio of 1:2). The excess water was removed using an adsorbent paper and the green specimens were carefully moved to a furnace (Vita 900, Vita, Bad Säckingen, Germany) and vacuum sintered (1 mBar) at 970°C and at a heat rate of approximately $70^{\circ}\text{C}/\text{min}$, following the porcelain's manufacturer firing schedule.

In order to assess the fracture shear strength of the metal/ceramic composites used as interlayers and their base materials (i.e. metal and porcelain), shear tests were performed in specimens specially prepared for that purpose.

The homogeneous m/c composites and monolithic base materials were characterized in terms of their Young's Modulus (YM). The YMs were measured using a Dynamic Mechanical Analysis equipment (DMA 242 C, Netzsch, Germany) with a three-point bending sample holder. The preliminary analysis had shown that the composite specimens did not have frequency-dependent features either substantial inelastic contribution, so all the tests were further performed at room temperature and at a frequency of 1 Hz. The samples used for DMA had the following dimensions: 40 mm × 6 mm × 2 mm.

2.3. Shear tests

The shear bond strength tests were carried out at room temperature and performed in a universal testing machine (Instron 8874, MA, USA), with a load cell of 25 kN capacity and under a crosshead speed of 0.5mm/s. Tests were performed in a custom-made stainless steel apparatus (Figure 7.2) similar to that described by Henriques et al. (2011a). The apparatus consisted in two sliding parts A and B, each one with a hole perfectly aligned to the other. After aligning the holes, the specimens were inserted and loaded in the interface in the interface until fracture. The shear bond strength (MPa) was calculated by the dividing the highest recorded load (N) by the cross sectional area of resistant porcelain (mm²).

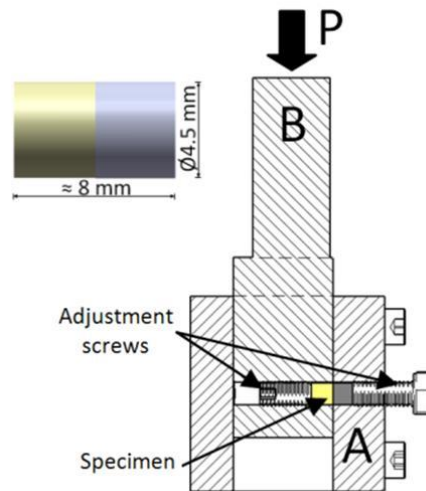


Figure 7.2. Cross-section schematic of the shear test device (A: external part; B internal part). The specimens' dimensions are also shown.

2.4. Analysis of the metal-porcelain interface and failure mode

The metal-ceramic interface as well as representative fracture surfaces were evaluated by optical microscopy (AxioTech, Carl Zeiss, USA) and SEM/EDS (Nova 200, FEI, Oregon, USA). For interface analysis, the specimens were embedded in auto-polymerizing resin, ground finished to 1200 grit SiC sand-paper and polished with diamond paste first in 6 μm and finally in 1 μm felt disc.

3. Results

Figure 7.3 exhibits the shear bond strength results of metal-ceramic specimens with different interlayers and also of conventional porcelain fused to metal specimens (PFM), which were used as control group. The hot pressed specimens with composite interlayers showed generally higher bond strength values than those of PFM specimens ($109.5 \pm 27\text{MPa}$), which were the control group. Hence, the results registered for specimens with the interlayer's compositions of 0M / 100M (interlayer's

compositions corresponding to hot pressed metal-ceramic specimens with a sharp metal-ceramic transition), 20M, 40M, 60M and 80M, were 141.2 ± 2.8 MPa, 168.1 ± 37.7 MPa, 261.1 ± 38.0 MPa, 229.8 ± 28.1 MPa and 171.7 ± 34.7 MPa, respectively.

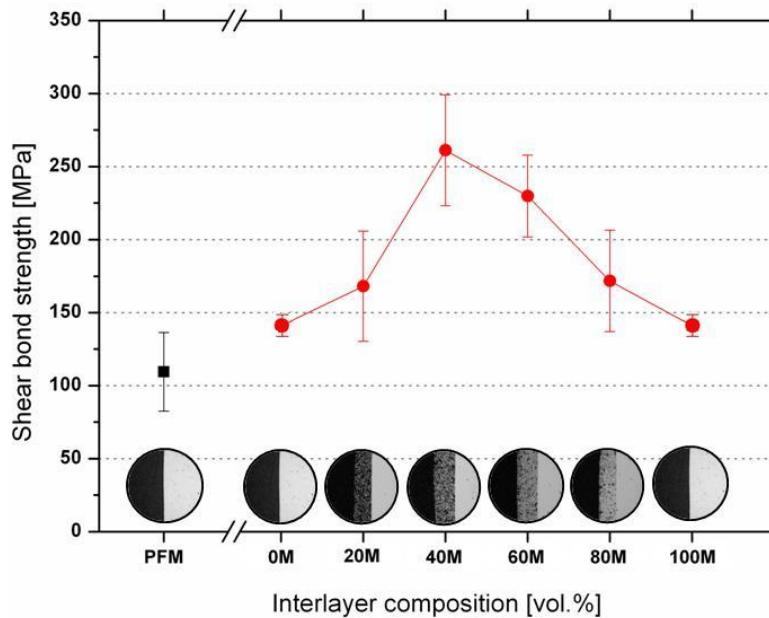


Figure 7.3. Plot of the shear bond strength results for metal-ceramic restorations with interlayers of different compositions, and for PFM specimens, the control group.

Representative micrographs of all metal-ceramic volume fraction specimens' combinations are presented in Figure 7.4. Here, it is shown a general view of the metal-interlayer-ceramic region for the interlayer compositions used in this study, as well as detailed micrographs of three specific regions, as follows: 1) metal-interlayer transition; 2) interlayer and, 3) interlayer-ceramic transition.

Figure 7.5 shows SEM micrographs of ceramic and metal revealing their microstructure. Ceramic (porcelain) is mainly composed by SiO_2 , Al_2O_3 , K_2O , SnO_2 and ZrO_2 . The metal microstructure is the typical dendritic microstructure found in cast CoCrMo alloys (Henriques et al., 2012).

In Figure 7.6 are plotted the volume fractions of the experimentally obtained composites in comparison with the designed values. These results, which resulted from image analyses, show small deviations between the designed and experimental values.

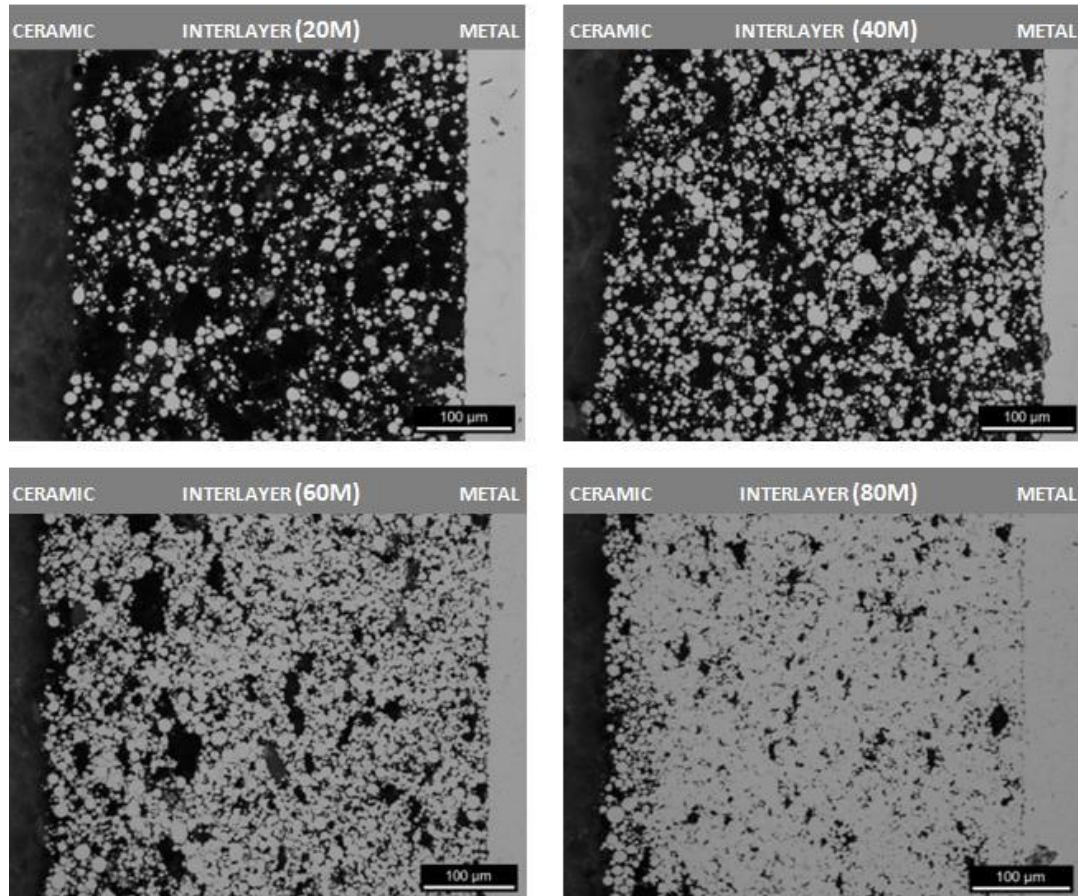


Figure 7.4. Micrographs of the ceramic-interlayer-metal region for specimens having interlayers with different metal/ceramic contents.

The fracture surfaces of the specimens were also analyzed and the fracture micrographs are presented in Figure 7.7. This analysis revealed different fracture patterns for the selected interlayers. Hence, the specimens with 0M and 100M interlayers as well as most of the PFM specimens (80%) exhibited adhesive failure, i.e. no remnants of ceramic were left on the metal surface. The specimens with 20M interlayer showed adhesive fracture on the interlayer-metal interface. In their turn, specimens with 40M interlayer exhibited mixed fracture, i.e. there were some interlayer's remnants visible on the metal's surface. The specimens with the 60M

interlayer also exhibited mixed fracture but in this case the ceramic fracture occurred at the interlayer-ceramic interface rather than at the metal surface, and it was noticed a slight cohesive fracture within the interlayer. Finally, specimens having the 80M interlayer displayed a ceramic's fracture that occurred at the ceramic-interlayer interface, but unlike the 60M specimens, it was not detected any cohesive damage of the interlayer.

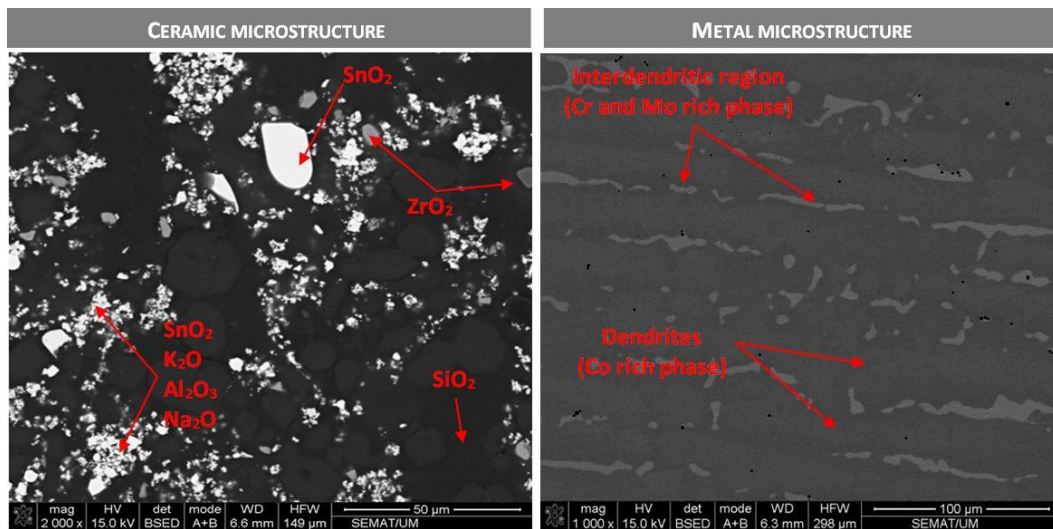


Figure 7.5. SEM micrographs showing the microstructure of monolithic base materials- ceramic (porcelain and metal (CoCrMo alloy)).

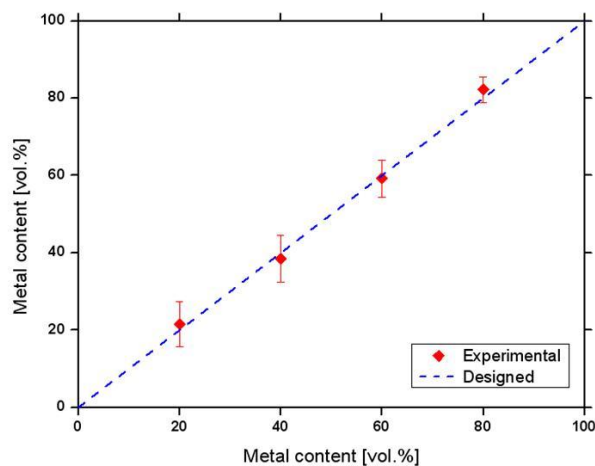


Figure 7.6. Comparison between the designed and the experimental volume fractions in different composites.

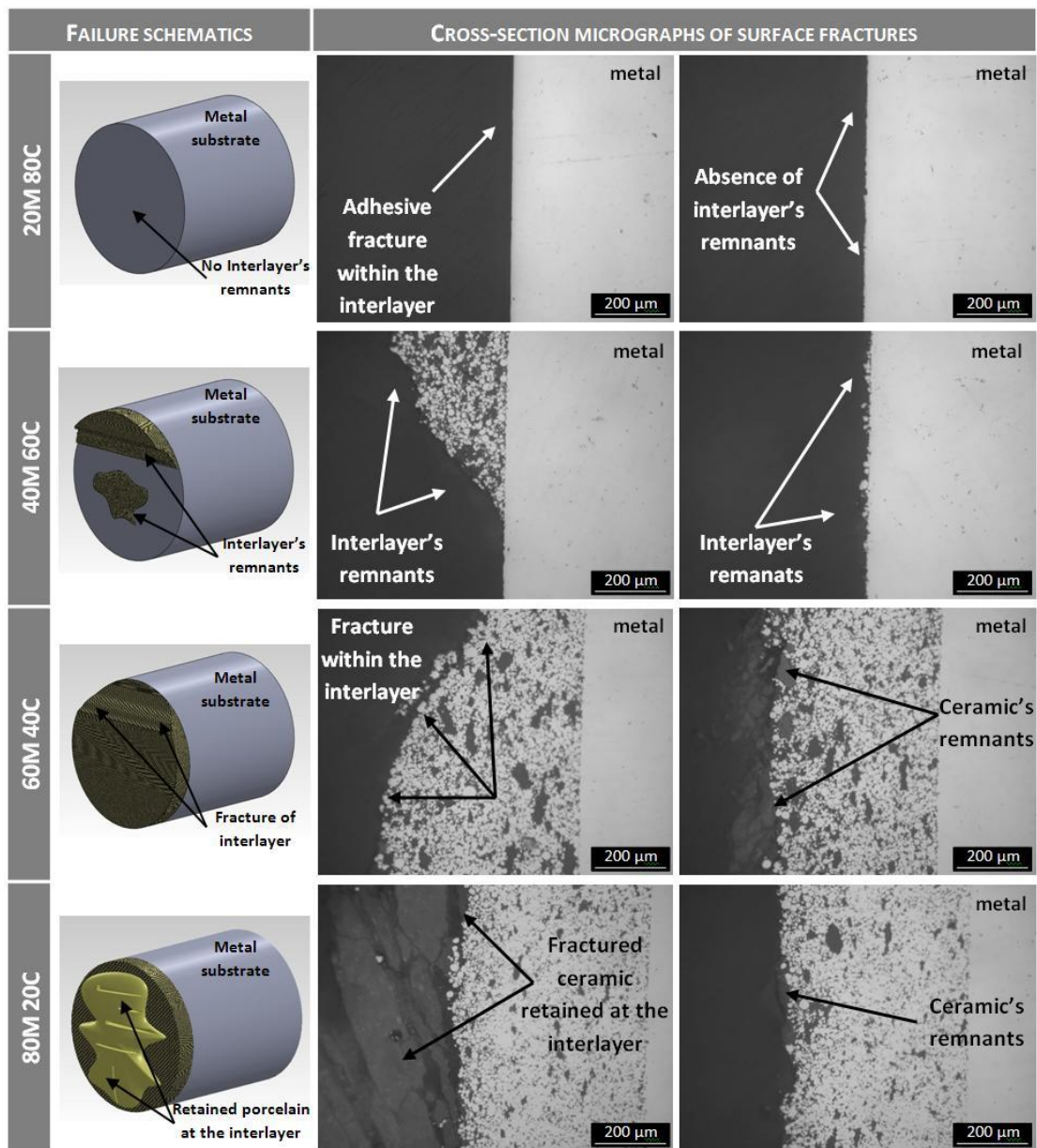


Figure 7.7. Micrographs showing a cross-section view of the fracture zones for specimens with different interlayers (20M; 40M; 60M; 80M). After bond strength tests, fractured specimens were embedded in resin and ground until reaching the longitudinal mid-plane, to allow the analysis of fracture zone in cross-section.

In order to better understand the behavior of the metal-interlayer-ceramic system, it was characterized the inelastic (fracture strength - Figure 7.8) and the elastic (elastic modulus - Figure 7.8) behavior of the monolithic and composite materials.

Figure 7.8 shows the Fracture Strength (FS) of the monolithic base materials (metal and ceramic) and of metal/ceramic composites that were used in this study as interlayers. Here the fracture strength values have been normalized to their minimal value, which is of that for pure ceramic (porcelain), because the shear test geometry used to assess composites' FS was different from that used to perform the metal-ceramic shear bond strength tests. In this way a direct comparison between the composites' fracture strengths and the metal-interlayer-porcelain bond strength results is avoided as it could be misleading. The composites' fracture strength evolution is characterized by an upward trend following the increasing in the metal content, as one might expect, but this trend is not very linear.

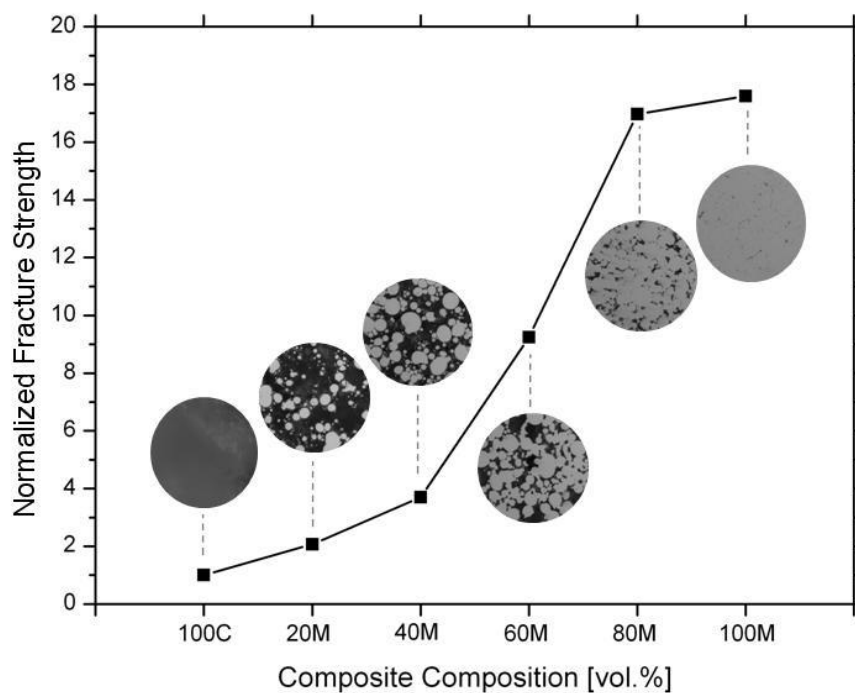


Figure 7.8. Normalized Fracture Strength of the different homogeneous composites used as interlayers (20M; 40M; 60M; 80M) and their respective monolithic base materials (100C; 100M). Normalization method consisted in dividing the Fracture Strength data by the minimum value.

Figure 7.8 shows the experimental Young's Moduli (YM) values obtained for the composites used as interlayers and for the monolithic base materials. In this figure is also plotted the composites' YM estimation by the universally used linear (Voigt rule) and inverse (Reuss rule) models of the rules of mixtures. Additionally an evaluation has been made by a micromechanical model (Gasik, 2009) which shows a very good fit for ceramic rich specimens. The deviations observed at high metal fractions might be explained by the changed microstructure where percolation level and the matrix-inclusion roles are changed.

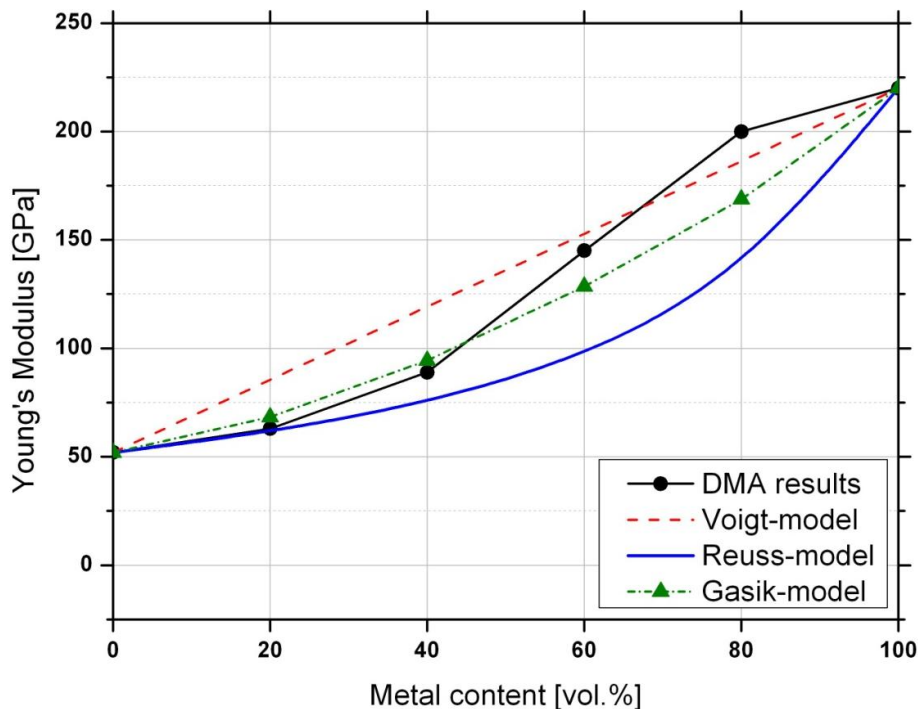


Figure 7.9. Young's Moduli plot of the metal-ceramic composites and monolithic base materials, obtained experimentally by DMA. It is also shown the Voigt- and Reuss-models based on the rule of mixtures, and Gasik's micromechanical model (Gasik, 2009).

4. Discussion

4.1. Sharp vs. graded metal-ceramic transition

Metal-ceramic restorations are composed by two types of materials which, due to their different natures, have distinct physical and mechanical properties (e.g. Young's modulus, CTE, hardness, etc.), thus resulting in significant properties' mismatch at their interface (Figure 7.9A). These properties' mismatch can cause excessive thermal and mechanical stresses in clinical conditions (thermal and mechanical cycling) which might ultimately lead to the bond's failure. The presence of a composite interlayer, which proved to significantly increase the metal-ceramic bond strength under static bond strength testing, can address a good answer to this issue concerned with fatigue resistance. Therefore, using an interlayer with base materials' intermediate properties can result in a lower stress state level at the interface under clinical conditions (mechanical and thermal cycling). The 40M interlayer showed to maximize the metal-ceramic bond strength, when tested under static conditions as happened in this study. This interlayer's composition, 40M, should also exhibit the best performance when tested under clinical conditions (mechanical and thermal cycling). The reason relies in its Young's modulus, which has an intermediate value between that of metal and porcelain (Figure 7.9 and Figure 7.10B).

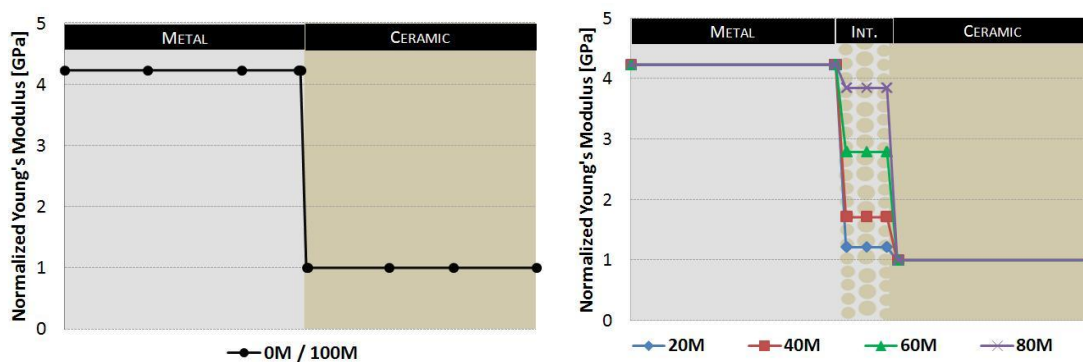


Figure 7.10. Normalized Young's Moduli schematic plot of the metal-ceramic interface for a sharp transition (A) and for a smooth transition provided by different interlayers (B). Normalization method consisted in dividing the Young's modulus data by the minimum value.

4.2. Bond strength and Fracture Analysis

The bond strength results present in Figure 7.3 shows that specimens provided with an interlayer exhibited higher adhesion than those with a sharp transition, namely PFM and 0M / 100M specimens. As previously stated, the PFM specimens worked as the control group and they differed from the 0M / 100M specimens as they were obtained by the conventional porcelain-fused-to-metal technique (PFM) in a vacuum sintering furnace. Despite different processing method both specimens' types exhibited a sharp transition between metal and ceramic, the greater bond strength values observed for 0M /100M specimens relative to those of PFM specimens are explained by the hot pressing effect (Henriques et al, 2011a; Henriques et al., 2011b).

It was also observed an increase in the bond strength values for interlayers containing rising metal content in its composition until a maximum volume fraction of 40% (40M), which exhibited the highest bond strength value recorded in this study ($261.1 \pm 38.0\text{MPa}$). When the metal content in the interlayer exceeded this amount, it was noticed an inflection of the bond strength trend and a decrease was successively observed for interlayers containing metal volume fractions of 60% and 80% (60M and 80M). A careful analysis of the micrographs can be helpful in the understanding of such behavior. Hence, the bond strength increase observed with the 20M interlayer relative to the sharp interface (0M) is explained by an increase in the mechanical interlocking provided by the respective interlayer. Figure 7.4 shows a coarse mechanical interlocking at the ceramic-interlayer interface and also at the interlayer-metal interface where is visible a few metal particles bonded to the metal substrate. However, the observation of the fracture surface (Figure 7.7) shows an adhesive failure between the interlayer and the metal surface, pointing this site as the weakest site of the ceramic-interlayer-metal system.

The increase in the metal particles observed in the 40M interlayer was followed by an increase in the bond strength values. Figure 7.4 shows an increase in the number of metal particles that are bonded to the metal substrate wall and some bridging effects between metal particles as well, thus creating an enhanced roughening. The analysis of

the fracture surface (Figure 7.7) revealed a mixed fracture within the interlayer, with remnants of interlayer present on the metal substrate's surface. This fact shows an increase in adhesion between the interlayer and the metal surface which can be directly related to the bond strength improvement registered over the previous interlayer composition (20M). Experimental results showed that a 50M interlayer yield bond strength values in the range of those found in 40M interlayer. This shows that the inflection point of the bond strength curve (Figure 7.3) is between 40M and 60M.

The 60M interlayer caused a bond strength drop and the yet verified trend of adhesion improvement, parallel to the interlayer's metal content increase, had ceased. The high content of metal particles in the interlayer allowed, on one side, an improved adhesion to the metal surface (Figure 7.4) and, on the other side, a great strengthening in fracture strength of the interlayer itself (Figure 7.8). The failure thus occurred in the weakest site of the porcelain-interlayer-metal system which was at the porcelain-interlayer interface, as the fracture analysis revealed (Figure 7.7). After the bond strength tests, almost all of the 60M interlayers remained bonded to the metal substrates, despite some minor cohesive failures observed within the interlayer, especially at the specimens' borders.

The metal-ceramic bond strength followed its downward trend for the specimens provided with the 80M interlayers. The rationale for such behavior is similar to that above described for specimens with 60M interlayers. In this case the interlayer acted as an extension of the metal substrate and the failure occurred at the porcelain-interlayer interface. No cohesive fracture of the interlayer was observed for this particular case and this fact may be explained by the great fracture strength of this interlayer (Figure 7.8), which is comparable to that of metal substrate.

It is important to point out that residual stresses may affect the results, as they are greatly dependent on processing history. The processing cycle was the same for all specimens with interlayer and slightly different from that of conventional PFM specimens (especially in the cooling rate, which was faster for PFM specimens). Therefore, despite these stresses might affect the absolute values they are present in all the specimens to a compatible extent and thus implicitly included in the normalized

results. Nevertheless thermal stresses evaluation at different stages of the processing and testing would require a separate study.

4.3. Fracture strength of the composites used as interlayers

So far, the results showed that the type of composite used as interlayer strongly influences the behavior of the metal-interlayer-ceramic system. Therefore, understanding the mechanisms that are behind the fracture strength (Figure 7.8) of the homogeneous composites used as interlayers can be of extreme importance to understand the behavior of the metal-interlayer-ceramic systems as a whole. The analysis of the composites used in this study as interlayers can be divided in two types: the ceramic matrix composites (CMCs) and the metal matrix composites (MMCs). The CMCs are the 20M and 40M composites, and corresponds to the composites where ceramic is in higher content relative to metal particles. On the other side, the 60M and 80M composites are MMCs because metal is present in a higher content and therefore it turned the matrix.

The strengthening mechanisms provided by the metallic particles in CMCs are explained by the higher elastic modulus of the reinforcement phase (metallic particles) relative to that of the matrix (porcelain). The incorporation of a ductile, metallic, secondary phase in glass and glass-ceramics matrix, thus forming a composite, improved the latter's mechanical properties, in particular the fracture resistance (Dlouhy and Boccaccini, 1995). The fracture toughness was then increased by exploiting the plastic deformation of the ductile phase provided by the metal particles. In this case MMCs, ceramic particles which had lower yield strength and lower Young's modulus than the metallic matrix, acted as defects rather than as reinforcing elements. This explains the drop in fracture resistance of these composites for increasing ceramic contents.

5. Conclusions

From this study, the following conclusions can be drawn:

1. The metal-ceramic bond strength can be highly enhanced by using a composite interlayer at the interface;
2. The interlayer with the composition of 40M [vol.%] was the one that maximized the metal-ceramic bond strength, yielding a ~140% bond strength improvement relative to the control group (conventional porcelain fused to metal specimens);
3. The approach of a thin graded transition between metal and ceramic rather than a sharp one comes out of this study as a better solution for metal-ceramic dental restorations.

6. Acknowledgements

This work has been supported by PhD Grant of FCT (Portuguese Foundation for Science and Technology) with the reference SFRH / BD / 41584 / 2007. Special thanks to DentalCastro – Prosthetic Laboratory for their contribution in this work. Assistance by M.Sc. M. Friman in making DMA experiments is also acknowledged.

7. References

- Anusavice KJ. Phillips' science of dental materials. 11th ed. Philadelphia:W.B. Saunders, 2006.
- Craig, R.G., Powers, J.M. 2002. Restorative dental materials. 11th ed. Mosby. pp.576-580.
- Coornaert J, Adriaens P, De Boever. Long-term clinical study of porcelain fused to gold restorations. J Prosthet Dent, 1984; 51(3):338-342.

- Dlouhy I, Boccaccini AR. Preparation, microstructure and mechanical properties of metal-particulate/glass-matrix composites. *Comp Sci Tech*, 1996;56:1415-1424
- Donovan TE, Swift EJJr. Porcelain-Fused-to-Metal (PFM) Alternatives. *J Comp*, 2009; 1: 4-6.
- Gasik M. Elastic properties of lamellar Ti–Al alloys. *Comp Mater Sci*, 2009; 47:206–212
- Gasik M, Kawasaki A, Kang Y. Optimization of FGM TBC and their thermal cycling stability. *Mater Sci For*, 2005; 492-493.
- Henriques B, Soares D, Silva FS. Optimization of bond strength between gold alloy and porcelain through a composite interlayer obtained by powder metallurgy. *Mater Sci Eng A*, 2011a; 528: 1415-1420.
- Henriques B, Soares D, Silva F. Shear bond strength of a Hot Pressed Au-Pd-Pt alloy-porcelain dental composite. *J Mech Behav Biomed Mater*, 2011b; 4(8):1718-26
- Henriques B, Soares D, Silva F. Microstructure, hardness, corrosion resistance and porcelain shear bond strength comparison between cast and hot pressed CoCrMo alloy for metal–ceramic dental restorations. *J Mech Behav Biomed Mater*, 2012; doi:10.1016/j.jmbbm.2012.03.015
- Huang M, Wang R, Thompson V, Rekow D. Bioinspired design of dental multilayers. *J Mater Sci: Mater Med*, 2007; 18:57-64
- Kelly JR. Ceramics in restorative and prosthetic dentistry. *Annu. Rev. Mater. Sci.* 1997; 27: 443-36.
- Drummond JL, Randolph RG, Jekkals VJ, and Lenke JW. Shear testing of the Porcelain-Metal Bond. *J Dent Rest*, 1984; 63: 1400.
- Kerschbaum T, Seth M, Teeuwen U. Verweildauer von Kunststoff-und Metal–Keramisch verblendeten Kronen und Brucken. *Deutsche Zahnärztliche Zeitschriften*. 1997; 52: 404.
- Liu J, Qiu XM, Zhu S, Sun DQ. Microstructures and mechanical properties of interface between porcelain and Ni-Cr alloy. *Mat Sci Eng A*, 2008: 497, 421-425.

- Özcan M. Fracture reasons in ceramic-fused-to metal restorations. *J Oral Rehab*, 2003; 30: 265-269.
- Oram DA, Cruickshank-Boyd EH. Fracture of ceramic and metaloceramic cylinders. *J Prosthet Dent*, 1984; 52: 221.
- Niu X, Rahbar N, Farias S, Soboyejo W. Bio-inspired design of dental multilayers: Experiments and model. *J Mech Behav Biom Mater*, 2009; 2: 596-602
- Nobil 4000 - Alloy Data. [Online] [Cited: November, 2011.] http://www.nobilmetal.it/public/products_attach/st_nobil_4000.pdf
- Rizkalla AS, Jones DW. Indentation fracture toughness and dynamic elastic moduli for commercial feldspathic dental porcelain materials. *Dent Mat*, 2004; 20: 198-206.
- Suresh S, Mortensen A. *Fundamentals of functionally graded materials*. London: Maney publishing; 1998
- Suresh S. Graded materials for resistance to contact deformation and damage. *Science*, 2001; 292: 2447-51
- Van Noort R. *Introduction to Dental Materials*. 3rded. Elsevier, 2007.
- Vásquez VZC, Özcan M, Kimpara ET. Evaluation of interface characterization and adhesion of glass ceramics to commercially pure titanium and gold alloys after thermal- and mechanical-loading. *Dent. Mater*, 2009; 25:221–31.
- Vichi A, Louca C, Corciolani G, Ferrari M.. Color related to ceramic and zirconia restorations: A review. *Dent Mater*, 2011; 27: 97-108.
- Yamamoto M. In: *Metal Ceramics, Principles and Methods* of Makoto Yamamoto, 1989, pp. 447. Quintessence Publishing Co., Chicago, IL, USA
- Zarone F, Russo S, Sorrentino R. From porcelain-fused-to-metal to zirconia: Clinical and experimental considerations. *Dent. Mater*, 2011; 27: 83-96.

Chapter 8

Shear bond strength comparison between conventional porcelain fused to metal and new functionally graded dental restorations after thermal-mechanical cycling

Published in Journal of the Mechanical Behavior of Biomedical Materials, 2012, doi: 10.1016/j.jmbbm.2012.06.002

B. Henriques¹, S. Gonçalves¹, D. Soares¹, F.S. Silva¹

¹*Centre for Mechanical and Materials Technologies (CT2M) and Department of Mechanical Engineering, University of Minho, Azurém, 4800-058 Guimarães, Portugal*

Abstract

Objectives: The aim of this study was to evaluate the effect of thermo-mechanical cycling on the metal-ceramic bond strength of conventional porcelain fused to metal restorations (PFM) and new functionally graded metal-ceramic dental restorations (FGMR).

Methods: Two types of specimens were produced: PFM and FGMR specimens. PFM specimens were produced by conventional PFM technique. FGMR specimens were hot pressed and prepared with a metal/ceramic composite interlayer (50M, %vol.) at the metal-ceramic interface. They were manufactured and standardized in cylindrical format and then submitted to thermal (3000, 6000 and 12000 cycles; between 5°C and 60°C; dwell time: 30s) and mechanical (25000, 50000 and 100000 cycles under a load of 50N; 1.6Hz) cycling. The shear bond strength tests were performed in a universal testing machine (crosshead speed: 0.5 mm/min), using a special device to concentrate the tension at the metal-ceramic interface and the load was applied until fracture. The metal-ceramic interfaces were examined with SEM/EDS prior and after shear tests. The Young's modulus and hardness were measured across the interfaces of both types of specimens using nanoindentation tests. Data was analyzed with Shapiro-Wilk test to test the assumption of normality. The 2-way ANOVA was used to compare shear bond strength results ($p < 0.05$).

Results: FGMR specimens showed significantly ($p < 0.001$) higher shear bond strength results than PFM specimens, irrespective of fatigue conditions. Fatigue conditions significantly ($p < 0.05$) affected the shear bond strength results. The analysis of surface fracture revealed adhesive fracture type for PFM specimens and mixed fracture type for FGMR specimens. Nanoindentation tests showed differences in mechanical properties measured across the metal-ceramic interface for the two types of specimens, namely Young's Modulus and hardness.

Significance: This study showed significantly better performance of the new functionally graded restorations relative to conventional PFM restorations, under fatigue testing conditions and for the materials tested.

1. Introduction

A metal-ceramic dental restoration (e.g. crown or fixed partial denture) consists of a metal substructure onto which is fired a ceramic veneer. In these restorations the strength of the metallic substructure is combined with the tooth like appearance of the porcelain to form strong artificial prostheses with natural look (Craig and Powers, 2002; Jörn et al., 2010). All-ceramic restorations, especially zirconia-cored restorations, are nowadays an alternative to metal-ceramic systems mainly due to their enhanced aesthetic properties (Zarone et al., 2011). Zirconia-cored restorations have demonstrated suitable strength and mechanical performance when applied as single crowns and short-span fixed partial dentures. The long-span zirconia structures started more recently to be used with more reliability. The latest generation of these structures is currently under evaluation and further *in vivo*, long-term clinical studies are necessary for drawing solid conclusions about their performance (Zarone et al., 2011, Vichi et al., 2010). The major problem related with zirconia-cored restorations is the greater incidence of veneering porcelain chipping (8-50% at 1-2 years) when compared with porcelain fused to metal restorations (4-10% at 10 years) (Donovan and Swift, 2009), although the chipping rate in metal-ceramic restorations depends on the type of metal: precious-alloy based reconstructions have fewer chipping rates than titanium or non-precious alloy based systems (Pjetursson et al., 2004; Walter et al., 1999; Eliasson et al., 2007; Napankangas et al., 2002). Therefore, the metal-ceramic restorations still represent the majority and the most reliable dental restorations especially when a good adhesion between the two materials is achieved (Salazar et al., 2007; Anusavice, 2006). Indeed, the good adhesion between materials is of great importance since, despite the high longevity and survival rates of metal-ceramic restorations, failures still occur chiefly due to interfacial breakdown of the metal-ceramic bond (Van Noort, 2007). Authors have been seeking methods and techniques that are capable of producing strong metal-ceramic bonds (Elsaka et al., 2010a; Elsaka et al., 2010b, Wu et al., 1991; Wagner et al., 1993; Henriques et al., 2011a; Henriques et al., 2011b). These studies have focused on the three main mechanisms involved in the metal-ceramic bonding: (1) mechanical adhesion, which is

related to the mechanical interlocking occurring on surface irregularities of both materials (Van Noort, 2007); (2) physical adhesion, governed by Van der Waal's forces and; (3) chemical adhesion, in which covalent or ionic forces form chemical bonds between the ceramic and the oxide layer formed on metal's surface (Van Noort, 2007). Henriques et al. (2011a) have tested a functionally graded approach for metal-ceramic restorations. Suresh and Mortensen (1998) defined functionally graded material (FGM) as a heterogeneous composite material containing a number of constituents that exhibit a compositional gradient from one surface of the material to the other subsequently resulting in a material with continuously varying properties. Graded materials are known for their ability to better resist thermal and mechanical stresses (Suresh, 2001). Natural teeth display a graded transition between enamel and dentin, which are materials with a significant difference in Young's modulus (~65GPa and ~20 GPa, respectively). Huang et al., 2007 and Niu et al., 2009 demonstrated that the Young's modulus changes linearly from that of enamel to that of dentin, at the dentin-enamel-junction (DEJ), promoting a stress reduction in the enamel. The solution tested by Henriques et al. (2011a) relied on the introduction of a metal-ceramic composite interlayer at the interface between the metal substructure and the ceramic veneer, to impart a graded transition between the two materials. A significant increase on metal-ceramic shear bond strength has been shown for static tests. These results were explained by the graded transition between base materials provided by the composite interlayer and by the use of hot pressing technique. Hot pressing enabled the fabrication of flawless interfaces (absence of undesired porosity and small cracks) and promoted the full contact between base materials, thus enhancing the diffusion of elements in the interface and contributing to a better chemical bonding (Henriques et al., 2011a; Henriques et al., 2011b).

Dental materials should be tested in conditions similar to those they will find in the oral cavity. Structures in oral environment are constantly exposed to thermal, physical and chemical changes, due to the contact with food, drinks and drugs, or even due to thermal shocks from surrounding environment (Gale and Darvel, 1998). The fact is that conventional methods often used in metal-ceramic adhesion assessment (shear,

tensile, flexural and torsion strength tests) do not include a fatigue component, which might result in optimistic results that do not reflect real clinical behavior. Therefore, thermal and mechanical cycling tests are proposed to simulate the oral conditions prior to mechanical tests (Gale and Darvel, 1998; Vásquez et al., 2008; Vásquez et al., 2009; Oyafuso et al., 2008). Thermal cycling tests are based on temperature changes that induce repeated stresses at the interface of the two materials. Such stresses arise due to differences in the thermal expansion coefficients of both materials and can lead to adhesion losses (Vásquez et al., 2008). Mechanical tests intend to simulate chewing conditions and are based on the incidence of repeated loads on the metal-ceramic system, thus producing alternate stresses (Oyafuso et al., 2008). These stresses forms at the metal-ceramic interface due to the Young's Modulus mismatch between the dissimilar materials.

The aim of this study was to compare the shear bond strength of conventional porcelain fused to metal restorations with the new functionally graded restorations after thermal and mechanical fatigue tests.

2. Materials and Methods

2.1. Materials

In this study a CoCrMo alloy (Nobil 4000, Nobilmetal, Villafranca d'Asti, Italy) and a dental opaque porcelain powder (Ceramco3, Dentsply, York, USA) (batch number: 08004925) were used. In Table 8.1, Table 8.2 and Table 8.3 are presented the chemical compositions as well as some relevant properties of metal and ceramic, respectively.

Table 8.1. Base alloy composition (wt.%) (according to manufacturer).

Co	Cr	Mo	Si	Others
62	31	4	2.2	Mn – Fe – W

Table 8.2. Ceramic chemical composition (wt.%).

SiO ₂	Al ₂ O ₃	K ₂ O	SnO ₂	ZrO ₂	CaO	P ₂ O ₅	Na ₂ O	Others
41.3	14.5	14.0	11.9	5.8	4.1	4.1	3.0	MgO, SO ₃ , ZnO, Cr ₂ O ₃ , Fe ₂ O ₃ , CuO, Rb ₂ O

Table 8.3. Relevant materials' properties.

Materials	Density [g/cm ³]	CTE [10 ⁻⁶ K ⁻¹]		Young's Modulus [GPa]
		[25-500°C]	[25-600°C]	
CoCrMo alloy - Nobil 4000 ^a	8.6	14.4	14.9	220
		14.9 ^c	15.4 ^c	
Porcelain - Ceramco3 Opaque	2.8 ^b			83 ^b

^a Nobil 4000 Manufacturer (2011); ^b Souza et al. (2010); ^c Rizkalla and Jones (2004).

2.2. Specimens Manufacturing

In this study, two types of metal-ceramic specimens were tested: a) conventional porcelain to metal specimens (PFM), characterized by a sharp metal-ceramic interface and; b) hot pressed metal-ceramic specimens with a composite interlayer at the metal-ceramic interface, hereafter designated as functionally graded restorations (FGMR). The manufacturing procedure of the metal substrates was common for both types of specimens, as follows: Metal substrates (N=34) were obtained by hot pressing technique, which consisted in pressing the CoCrMo powders in a graphite die, at high temperatures. The graphite die was painted with zirconium oxide in order to impede carbon diffusion to metal substrates. Hot pressing was performed under vacuum (10⁻² mbar) at 1000°C for 10 minutes and at a pressure of 60 MPa.

All metal substrates were ground until 1200-grit sand paper and then grit-blasted with Ø110µm alumina grains at a pressure of 3 bar (Protempomatic, Bego, Germany). Then, they were ultrasonically cleaned in an alcohol bath for 10 min and rinsed in distilled water for another 10 min to remove contaminants. Finally they were dried with absorbent paper towels. It must be pointed out that no preoxidation heat treatment was applied to the metal substrates before porcelain bonding.

To produce porcelain fused to metal (PFM) specimens (N=18) an acrylic template was used to ensure that the porcelain height was the same for all specimens (4 mm). Porcelain was applied onto metal substrates in the form of a creamy paste resulting from the addition of distilled water to porcelain powders in a ratio of 1:2 (water:porcelain). The excess of water was removed using an adsorbent paper and after the porcelain condensing, metal-porcelain sets were carefully moved to a furnace (Vita 900, Vita, Bad Säckingen, Germany) and vacuum sintered (1mBar) at 970°C and at a heat rate of approximately 70°C/min, following the porcelain manufacturer firing schedule.

The functionally graded specimens (FGMR) (N=16) were obtained by hot pressing the set composed by the metal substrate + composite interlayer + porcelain in a graphite die. The composite interlayer was made up of a mixture of metal powders and porcelain powders (50% metal-50% porcelain; %vol.). The metal powders used had the same composition of the metal substrates and the following size distribution: $D_{10}=4.44\mu\text{m}$; $D_{50}=8.27\mu\text{m}$ and $D_{90}=12.76\mu\text{m}$. The mixture was blended using a rotary machine at 40 rpm during 10 min.

The production sequence of FGMR specimens comprised the following steps (Figure 8.1): first, the cavity of the graphite was painted with zirconium oxide to prevent carbon diffusion to specimens and then the metal substrate was placed inside. After the metal substrate was in place, a metal-porcelain powder mixture (50% metal-50% porcelain - %vol.) was inserted into the cavity. The porcelain powders were at last inserted into the cavity. The porcelain sintering (hot pressing) was performed under vacuum ($\sim 10^{-2}$ mBar) at a temperature of 970°C and a pressure of ~ 20 MPa. The heat rate was 70°C/min and the sintering stage was 2 minute at 970°C. The cooling rate was natural after the power of the induction heating furnace was shut down. After sintering, the thickness of the composite interlayer in FGMR specimens was determined by image analysis of the interfacial region and revealed a mean value of 500 μm .

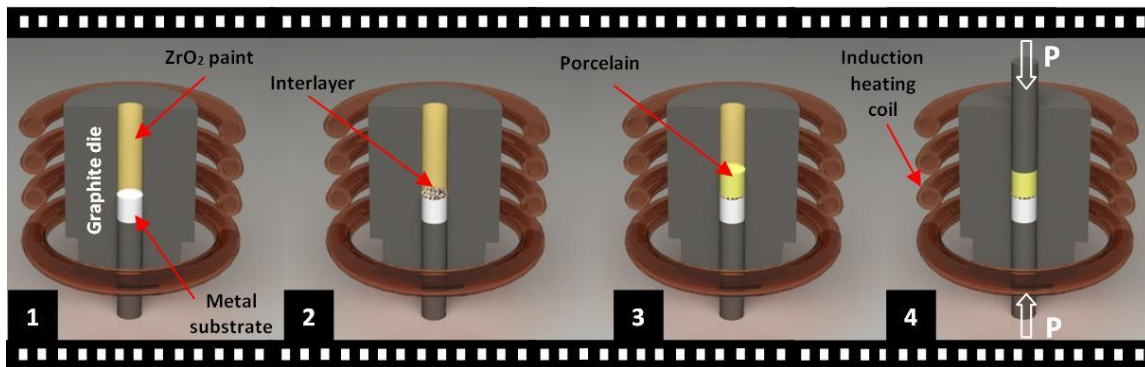


Figure 8.1. FGMR specimens manufacturing procedure: 1 – Painting the cavity of the die with zirconium oxide followed, and metal substrates placement; 2 – Placement of the composite mixture in the die's cavity; 3 – Porcelain powders placement; 4 - Hot pressing (pressure+temperature) the metal-interlayer-porcelain specimen.

2.3. Thermal and mechanical cycling

The fatigue tests applied to the metal-ceramic specimens comprised thermal cycling followed by mechanical cycling tests.

Thermal cycling tests were performed in Fusayama's artificial saliva (AS) (Fusayama et al., 1963), which chemical composition is given in Table 8.4. The pH of this solution was approximately 5.7. These tests consisted in 3000, 6000 and 12000 thermal cycles between 5°C and 60°C. The dwelling time at each temperature was 30s and the transfer time between baths was 10s.

Table 8.4. Chemical composition of Fusayama's artificial saliva.

COMPOSITION	QUANTITY (g/L)
NaCl	0.4
KCl	0.4
CaCl ₂ .2H ₂ O	0.795
Na ₂ S.9H ₂ O	0.005
NaH ₂ PO ₄ .2H ₂ O	0.69
Urea	1

The mechanical cycling tests were performed in a mechanical cycling machine (custom made, CT2M, University of Minho, Portugal), similar to that described by Vázquez et al. (2009), designed with the purpose of simulating the mechanical loads generated in the teeth during chewing cycles. The device was composed by 5 upper rods that were fixed on an upper metal plate (Figure 8.2). The stainless steel loading stylus with 6 mm diameter induced a load of 50N in the centre of the veneering ceramic, at a frequency of 1.6Hz, during 25000, 50000 and 100000 cycles. These tests ran at room temperature in a dry environment and were performed after the specimens have been subjected to thermal cycling tests.

Table 8.5 shows the fatigue test conditions arranged by the combination of thermal and mechanical number of cycles.

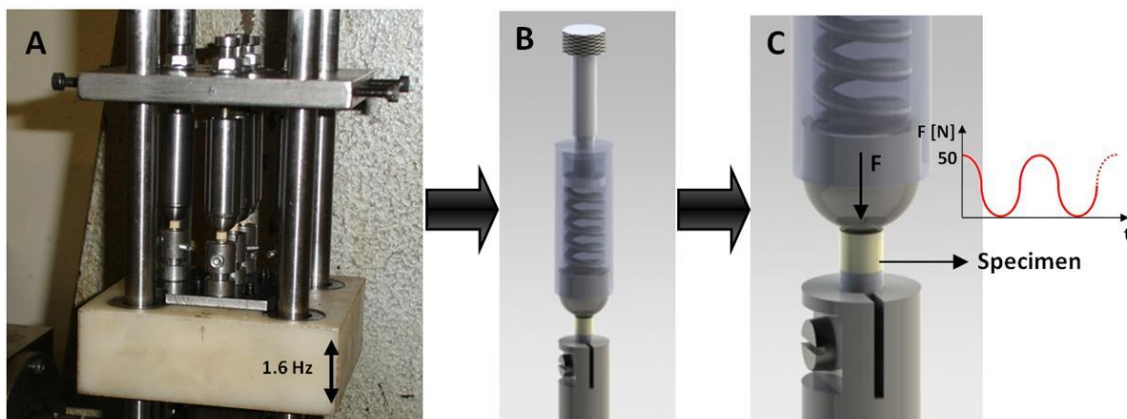


Figure 8.2. Mechanical cycling device used for dynamic loading of metal-ceramic specimens.

Table 8.5. Fatigue tests conditions based on the thermal and mechanical number of cycles.

	Condition 0	Condition 1	Condition 2	Condition 3
Thermal cycles	0	3000	6000	12000
Mechanical cycles	0	25000	50000	100000

2.4. Shear Test

The shear bond strength tests were carried out at room temperature and performed in a universal testing machine (Instron 8874, MA, USA), with a load cell of 25 kN capacity and under a crosshead speed of 0.5mm/s. Tests were performed in a custom-made stainless steel apparatus similar to that described by Henriques et al. (2011a). The apparatus consisted in two sliding parts A and B, each one with a hole perfectly aligned to the other. After aligning the holes, the specimens were there inserted and loaded in the interface until fracture (Figure 8.3).

The shear bond strength (MPa) was calculated dividing the highest recorded fracture force (N) by the cross sectional area of the bonded porcelain (mm^2).

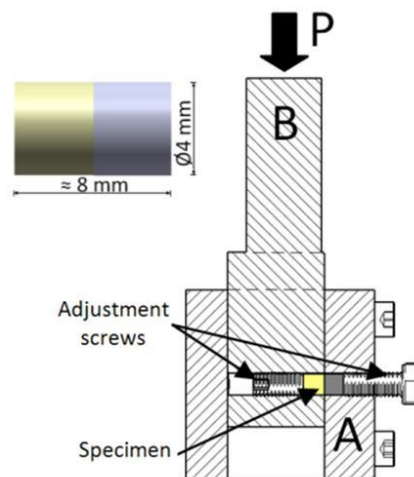


Figure 8.3. Cross-section schematic of the shear test device (A: external part; B internal part). The specimens' dimensions are also shown.

2.5. Analysis of the metal-ceramic interface and failure mode

The interface of metal-ceramic specimens was examined prior and after thermal and mechanical cycling tests by the means of SEM/EDS analysis (Nova 200, FEI, Oregon, USA). The specimens subjected to SEM/EDS analysis were longitudinally cross-

sectioned to allow the interface investigation. The purpose was to detect damages on the interfacial region caused by fatigue tests. It was also performed nanoindentations (Nano test, Micro Materials, UK) across the specimens' interface in both types of specimens (PFM and FGMR) to look for Young's modulus and hardness variations. The samples were indented with the pyramidal Berkovich indenter at a loading force of 300mN during 30s. The distance between two indents on the surface of the sample was 30 μm to avoid the influence of residual stressed from other impressions. The Berkovich indenter has a three-sided pyramid geometry, which is geometrically self similar, and has the same projected area to depth ratio as a Vickers indenter.

The types of fracture observed in the shear tests were also considered in this study and were registered for all specimens. Hence, failure modes were classified as follows: (1) adhesive, if no remnants of ceramic were found on the metal surface; (2) cohesive, if fracture occurred within the ceramic side; (3) mixed, if remnants of ceramic were found in the metal surface.

2.6. Statistic Analysis

Data were analyzed using SPSS statistic software (Release 20.0.0 for Windows). The Shapiro-Wilk test was first applied to test the assumption of normality. Differences between processing type and fatigue conditions factors in the shear bond strength results were compared using 2-way ANOVA. P values lower than 0.05 were considered statistically significant in the analysis of the results.

3. Results

3.1. Shear bond strength

Figure 8.4 shows a plot of the shear bond strength results of metal-ceramic specimens after thermal and mechanical cycling.

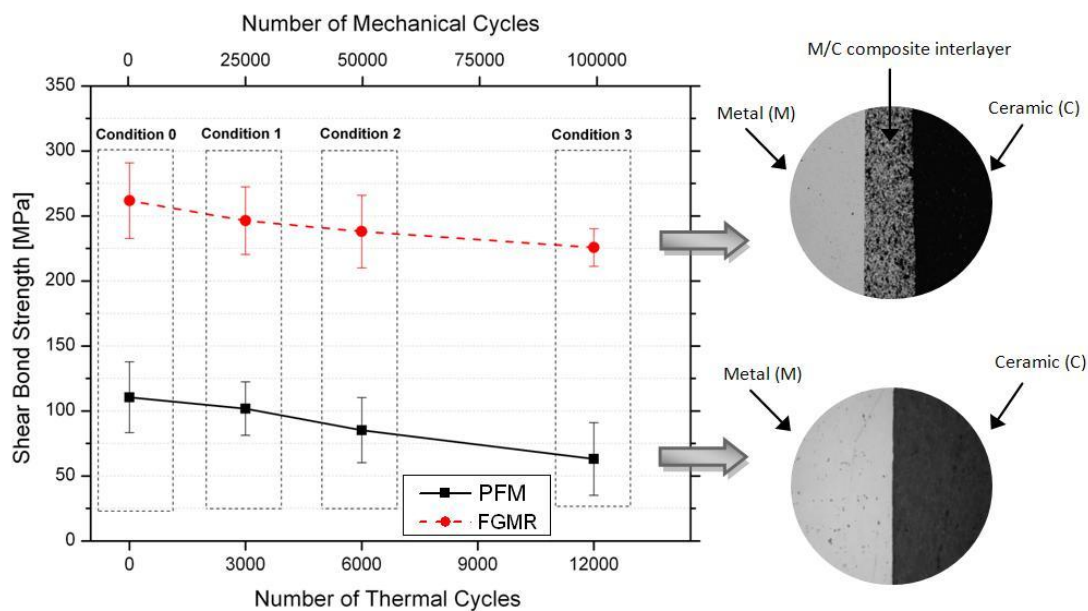


Figure 8.4. Mean \pm standard deviation (SD) of the shear bond strength results for conventional porcelain fused to metal specimens (PFM) and for functionally graded specimens (FGMR), after thermal and mechanical cycling. At the right side is shown a micrograph of each type of interface.

The functionally graded specimens (FGMR) exhibited greater shear bond strength values than those observed for porcelain fused to metal (PFM) specimens, irrespective of the fatigue conditions. The shear bond strength registered for FGMR specimens was 255 ± 29 MPa; 246 ± 26 MPa; 238 ± 28 MPa and 226 ± 15 MPa for *conditions 0 to 3*, respectively. Regarding PFM specimens, the shear bond strength values registered were 109 ± 27 MPa; 102 ± 20 MPa; 85 ± 25 MPa and 63 ± 28 MPa for *conditions 0 to 3*, respectively.

Table 8.6 presents the results of 2-way ANOVA for experimental conditions. The mean shear bond strength values are significantly affected by the processing type ($p < 0.001$) and fatigue conditions ($p < 0.05$).

The mean shear bond strength values of PFM and FGMR specimens for *condition 3* decreased 47MPa and 29MPa, respectively, which represents a bond strength loss of 43% and 11% of their initial bond strength values (*condition 0*). After *condition 3* fatigue tests, which corresponded to the most severe testing conditions, the shear bond strength of FGMR specimens was 210% higher than that of PFM specimens.

Table 8.6. Two-way ANOVA results according to metal-ceramic shear bond strength data.

	df	SS	MS	F	p
Processing type	1	171624.85	171624.85	284.42	1.66E-15
Fatigue conditions	3	7295.95	2431.98	4.03	0.02
Model	4	182119.98	45529.99	75.45	6.37E-14
Total	33	197808.84			

Statistically significant at a level of $p < 0.05$. **df**: Degrees of freedom; **SS**: Sum of squares; **MS**: Mean square; **F**: F-ratio; **p**: p-value

3.2. SEM observation

A SEM/EDS inspection of both specimens' interfaces was performed. The micrographs of the PFM specimens' interface, before (*condition 0*) and after fatigue tests (*condition 3*), are presented in Figure 8.5A-B. The cycled specimens showed some cracks within the porcelain, along with some residual porosity due to the manufacturing process (Figure 8.5B). A similar analysis was performed to FGMR specimens, before (*condition 0*) and after fatigue tests (*condition 3*) (Figure 8.5C-D).

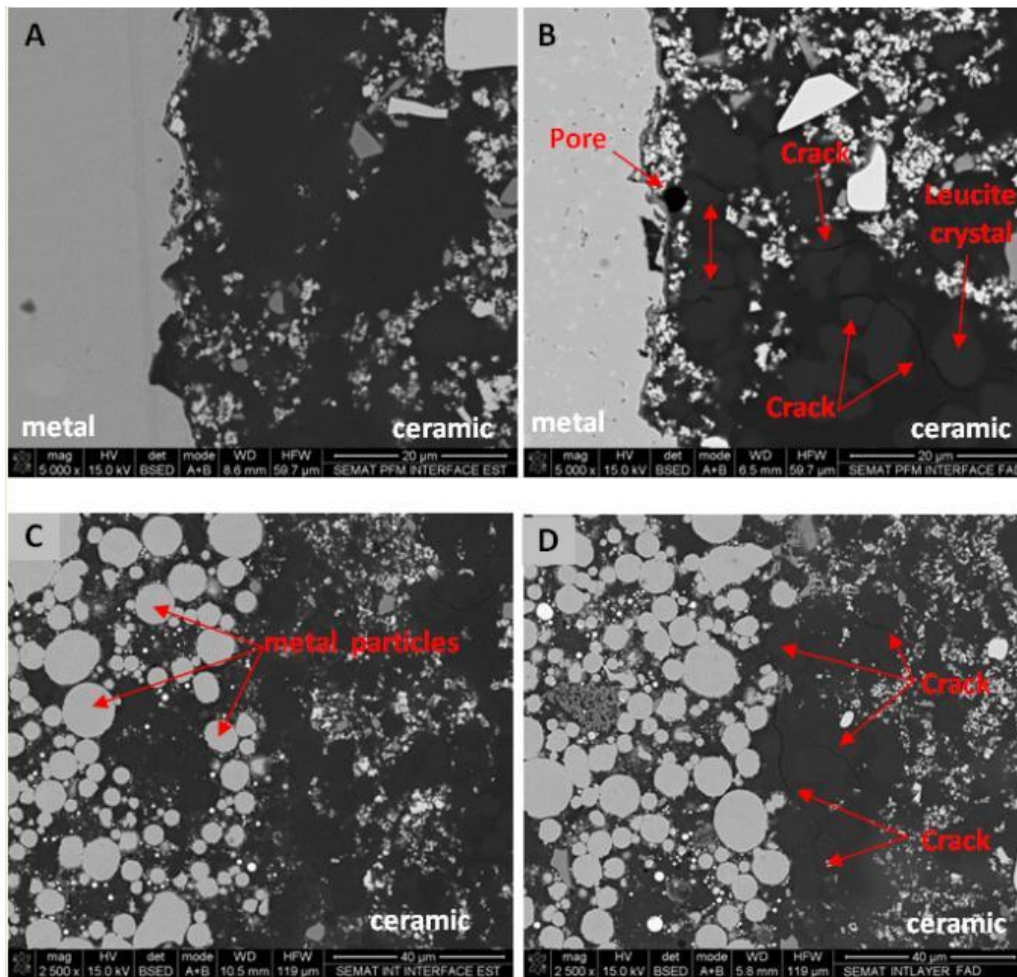


Figure 8.5. Representative SEM micrographs of PFM (A,B) and FGMR (C,D) metal-ceramic interfaces, before fatigue tests (A,C) and after fatigue tests (12000 thermal cycles + 100000 mechanical cycles) (B,D), respectively. Figures 4B and 4D show cracks within porcelain formed during fatigue tests.

The presence of cracks within the porcelain was also detected in these type of specimens (Figure 8.5D). However, no manufacturing flaws, such as pores, were detected, like it happened for PFM specimens. A detailed micrograph of the ceramic-interlayer-metal region, before fatigue tests, is presented in Figure 8.6.

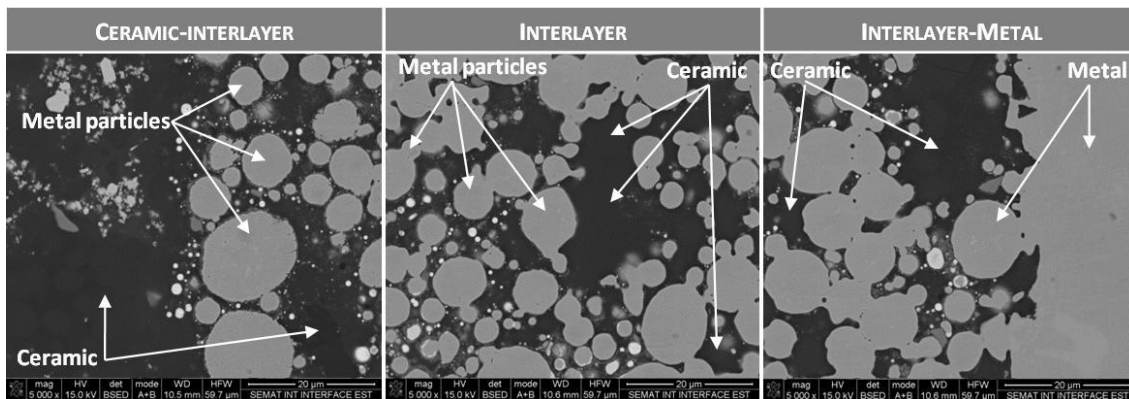


Figure 8.6. SEM micrograph showing a detailed view of the ceramic-interlayer-metal region of the new functionally graded specimens.

The fracture surfaces of PFM and FGMR specimens after fatigue tests (*condition 3*) were also examined by SEM/EDS. PFM specimens displayed an adhesive fracture type, i.e., no remnants of ceramic were visible on the metal's surface. Traces of salts were identified in the metal's surface (Figure 8.7A and 8.7B). The EDS analysis to these salts revealed the presence of P and Ca (Figure 8.8), which are constituents of the artificial saliva. This shows that the artificial saliva was able to penetrate through interface during thermal cycling.

The FGMR specimens exhibited mixed fracture type within the interlayer. Figures 7 C-D show remnants of interlayer on the metal surface. In Figure 8.9 are also visible metallic particles from the interlayer attached to the metal substrate, which contributed to the mechanical retention of the interlayer. Unlike PFM specimens, no traces of liquid ingress were detected on the fracture surface of FGMR specimens (Figure 8.10). For this purpose, all fractured surfaces of condition 3 specimens were analyzed in randomly selected regions.

Figure 8.11 shows the mechanical properties (Young's modulus and hardness) across the metal-ceramic interfaces of PFM and FGMR specimens, obtained by nanoindentations tests. PFM specimens exhibited a great mismatch in mechanical properties at the metal-ceramic interface. Concerning FGMR specimens, they exhibited a graded transition in mechanical properties across the metal-ceramic interface. The

significant mismatch in mechanical properties observed in PFM specimens was mitigated in the FGMR specimens.

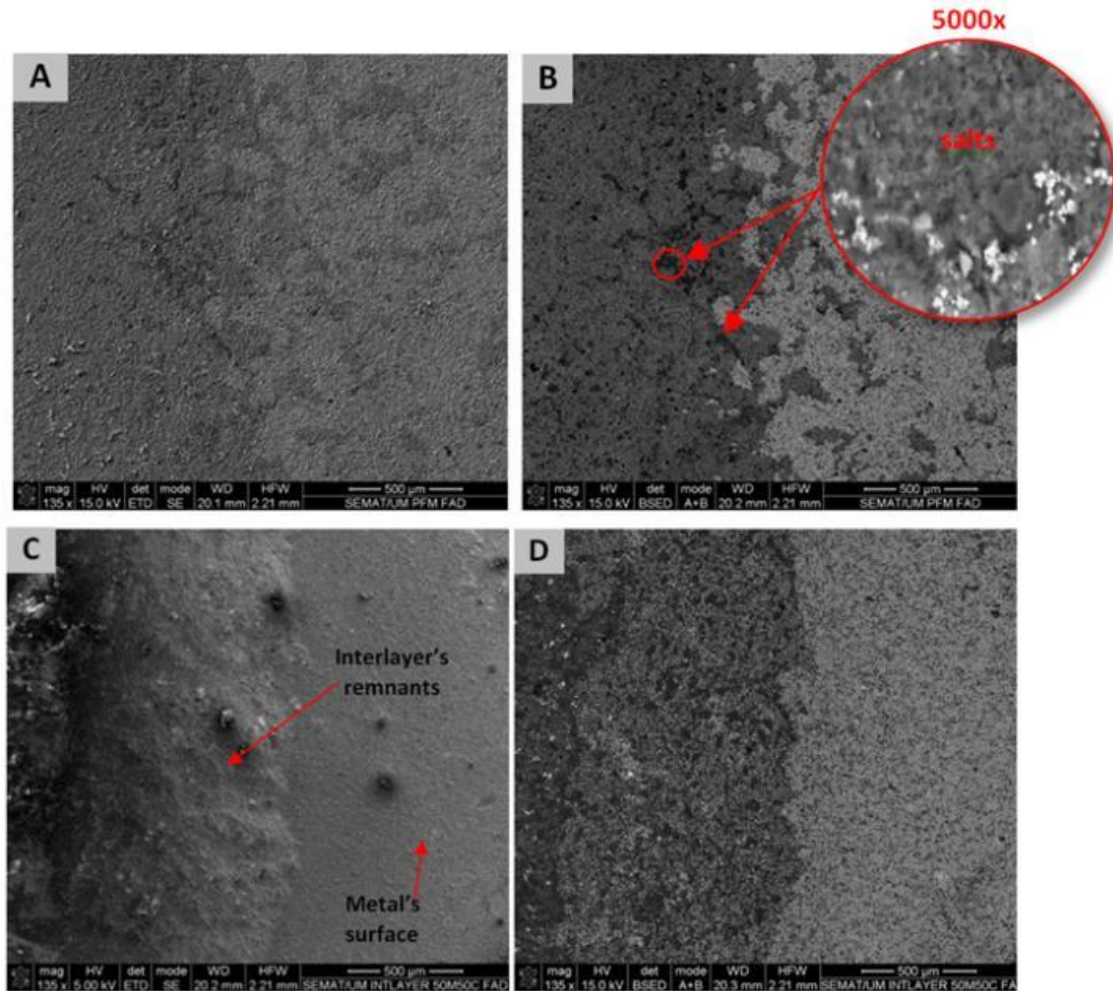


Figure 8.7. SEM micrographs of PFM and FGMR specimens' fracture surfaces, after fatigue tests (*condition 3*- 12000 thermal cycles + 100000 mechanical cycles). **PFM** specimens: **A**- topography; **B**-chemical composition. **FGMR** specimens: **C**- topography; **D**- chemical composition. **FGMR** specimens: **C**- topography; **D**- chemical composition.

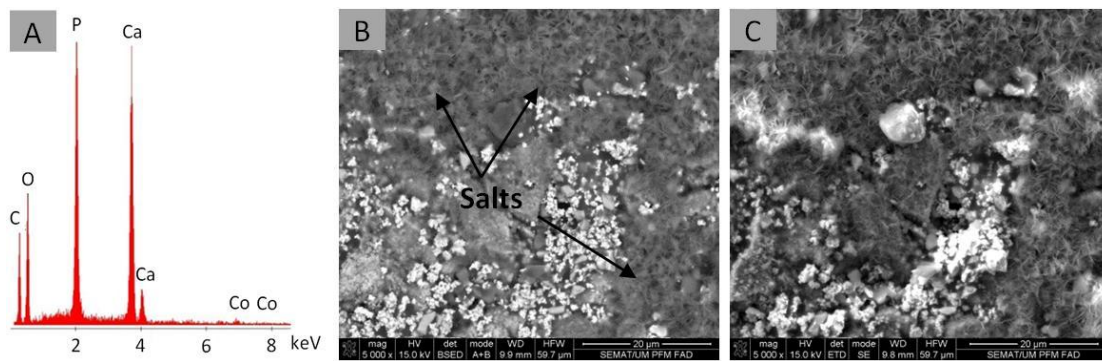


Figure 8.8. SEM/EDS analysis of salts found on fracture surface of PFM cycled specimens after *condition 3* fatigue tests. A- The spectrum reveals traces of P and Ca with probable origin in artificial saliva; B- Chemical composition; C- Topography.

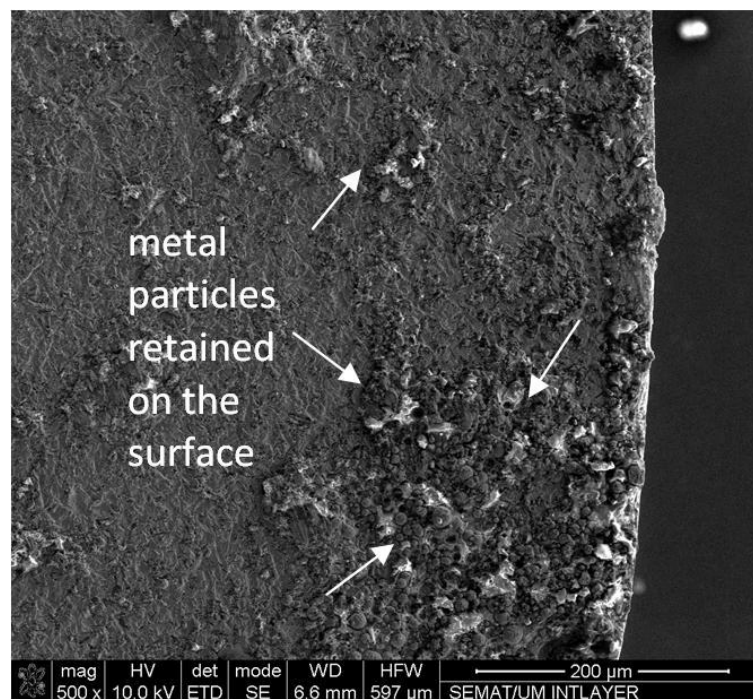


Figure 8.9. Fracture micrograph of the new functionally graded specimens showing remnants of metal particles from the interlayer retained at the metal surface.

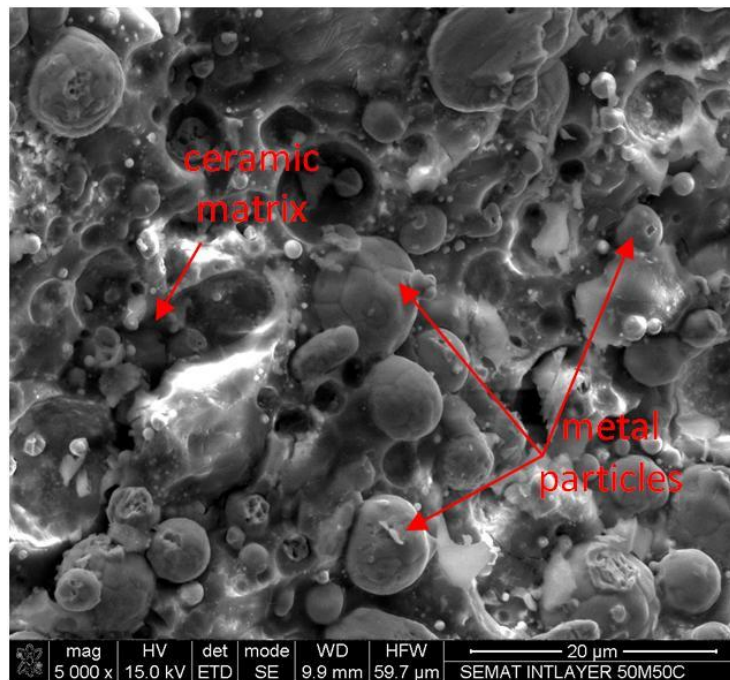


Figure 8.10. Fractography of the composite interlayer, showing no traces of liquid ingress. It is also shown the metal particles embedded in the ceramic matrix after fracture.

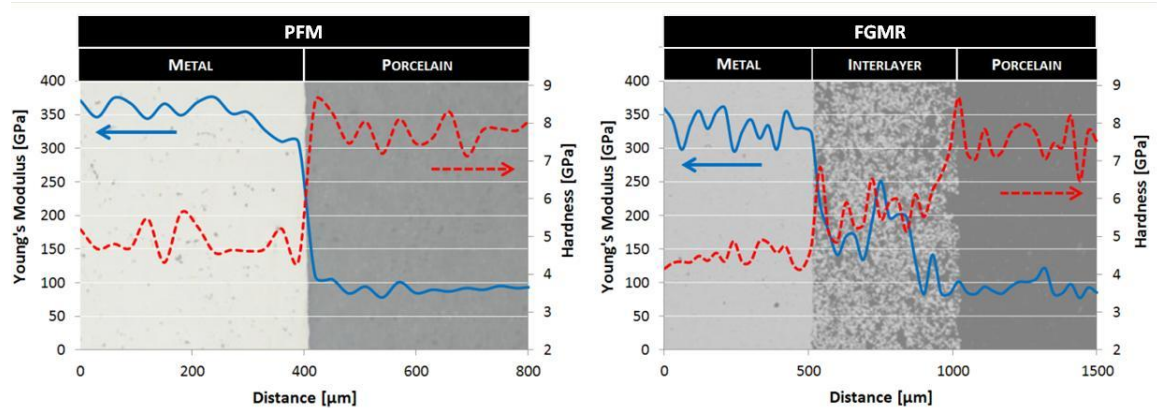


Figure 8.11. Mechanical properties measured at the metal-ceramic interface for a sharp (PFM) and a graded transition (FGMR). Young's Modulus (—) and Hardness (---).

4. Discussion

This study evaluated the effect of thermo-mechanical cycling on the metal-ceramic bond strength of conventional porcelain fused to metal restorations (PFM) and the new functionally graded restorations (FGMR).

4.1. Shear test

The shear bond strength test was selected among the available tests for metal-ceramic bond strength assessment (e.g. the Schwickerath crack initiation test used in ISO 9693:1999, the three-point-flexure test; four-point-flexure test; biaxial flexure test, etc). This test is considered to be suitable for evaluation of metal-ceramic bonds (Anusavice et al.,1980) and one of the advantages over the bending tests is that the results are not influenced by the Young's Modulus of the alloy (Hammad and Talic, 1996; Hammad and Stein, 1990). This test geometry has therefore been used by many authors to perform metal-ceramic bond strength tests (Akova et al., 2008; dos Santos et al., 2006; Vasquez et al., 2009; de Melo et al., 2005; M. Salazar et al., 2007).

The geometry and dimensions of the specimens used in this study were similar to specimens used in other studies on metal-ceramic shear bond strength assessments (Salazar et al., 2007; Vásquez et al., 2008; Vásquez et al., 2009; de Melo et al.,2005).

4.2. Fatigue tests

The metal-ceramic bond strength assessment of dental materials is often performed by the means of static mechanical tests (Akova et al., 2008; dos Santos el al., 2006; Vasquez et al., 2009; de Melo et al., 2005; Salazar et al., 2007), which do not

correspond to the clinical conditions at which they are subjected in the oral cavity. When in service, dental restorations are subjected to cyclic thermal and mechanical stresses, originated by the daily feeding routines, which must be considered when performing in-vitro studies involving restorative dental materials (Scherrer et al., 2003). Several studies on metal-ceramic bond strength after thermal and mechanical fatigue tests have been conducted, although the number of variables involved in such tests (number of cycles, temperature changes, dwell times, test medium, loads, etc.) have turned difficult or almost impossible the comparison between studies. In that way, one can find in literature studies where fatigue tests significantly affected the metal-ceramic bond strength and others where that did not occur (Salazar et al. (2007); Fisher et al., 2009; Tróia et al., 2003; Shimoe et al., 2004; Vásquez et al., 2009).

This study comprised thermal and mechanical fatigue tests applied to metal-ceramic specimens to simulate the clinical operating conditions of regular dental restorations. Thermal cycling conditions were selected based on Pröbster et al. (1996), Leibrock et al. (1999) and Fischer et al. (2009) studies which suggested that 6000 thermal cycles would correspond to 5 years in clinical service. The values of 3000 and 12000 thermal cycles were then extrapolated for 2.5 years and 10 years of clinical service, respectively. In order to simulate more severe clinical conditions, it was not used the baths temperatures of 5°C and 55°C as found elsewhere (Salazar et al 2007; Vásques et al, 2008; Vásquez et al., 2009), but instead, the temperatures of 5°C and 60°C which have also been referenced (Atta et al, 1990; Crim and Mattingly, 1990; Rees et al. 1990). The dwelling time at each temperature was 30s and was similar to that used by Salazar et al. (2007) in their study. This time was selected attending to the specimens' size, which was quite massive when compared to specimens used for flexural tests. A shorter dwell time would not create the desired temperature gradients along the specimens. Same concerns were reported by Vásquez et al. (2009) that referred that a dwell time of 10s could be considered short for this specimens' size. The medium used to perform thermal fatigue tests was artificial saliva as proposed by Gale and Darvel (1999). It is common to find distilled water as fatigue tests medium (Tróia et al. 2003; Vásquez et al. 2008; Vásquez et al. 2009; Oyafuso et al. 2008; Nikaido et al. 2002),

although it is considered entirely inadequate, if benign, to such test (Gale and Darvel, 1999).

Mechanical cycling simulated the loads withstood by the dental restorative systems during chewing actions. In this study, the applied load was 50N and the number of cycles was 25000, 50000 and 100000 at a frequency of 1.6Hz. Sartory et al. (2007) and Morgan et al. (1993) fixed a number of 100000 mechanical cyclic tests in dental implants, thus estimating a 5 year period in the oral cavity. The same extrapolation that was previously done for thermal fatigue tests can also be used for mechanical cyclic tests. Therefore, one can make a correspondence of 25000 and 50000 mechanical cycles as 1.25 and 2.5 years of clinical service, respectively.

Despite the number of thermal and mechanical cycles selected for this study intended to simulate those occurring in clinical service, it is important to point out that in-vitro studies involving geometric metal-ceramic specimens instead of complete dental restorations (Rosentritt et al., 2011; Rosentritt et al., 2009) should be only used for comparisons of relative effects of material properties, material microstructure and treatment/processing conditions that may impact the performance of metal-ceramic system (e.g. resistance to fracture) and no clinical inferences on its performance (e.g. susceptibility to fracture) should be made.

4.3. Shear bond strength after fatigue tests

Results present in Figure 8.4 indicated that the new functionally graded restorations exhibited significantly ($p < 0.001$) higher bond strength values than those observed for conventional PFM restorations, irrespective of fatigue testing conditions. The improvement in bond strength resistance exhibited by the new functionally graded restorations relative to conventional PFM ones was in excess of 130%. The hot pressing

techniques and the presence of the m/c composite interlayer (50M) played a determinant role in the enhancement of the global performance of the metal-ceramic interface. Hot pressing technique is regarded for improved physical and chemical adhesion (Henriques et al, 2011a; Henriques et al., 2011b) and for flawless ceramics with enhanced fracture toughness (Henriques et al., 2011b).

The interlayer is composed by metal particles surrounded by a ceramic matrix, forming a ceramic matrix composite (CMC) (Figure 8.6 and Figure 8.10). The CMCs have higher fracture strength than plain ceramic due to the higher elastic modulus of the metallic particles (reinforcement phase) relative to the matrix (ceramic) (Dlouhy and Boccaccini, 1995). Metallic particles also accounted for a dramatic increase in the mechanical retention of the porcelain. This feature is shown in Figure 8.6 where several metallic particles of the interlayer are bonded to the metal substrate and also bonded to each other, thus creating bridging effects that are regarded for bond strength enhancements. Figure 8.9 shows a micrograph of a fractured functionally graded specimens where metallic particles are retained on the surface of the metal substrate.

Besides their higher bond strength, the new functionally graded restorations also showed to be less affected by fatigue tests than conventional ones. After the most aggressive testing conditions (*condition 3*) these specimens displayed a bond strength loss of 11% whereas the conventional PFM displayed 43% of loss. The improved fatigue results of the new functionally graded restorations over the traditional ones can be explained by the effect of a metal-ceramic graded transition. The graded transition between metal and ceramic yields a significant reduction in properties' mismatch (e.g. CTE – coefficient of thermal expansion, Young's modulus, hardness, etc.) at the interface, relative to conventional PFM restorations. Figure 8.10 shows the Young's moduli and hardness evolution across the two types of interfaces tested in this study, namely sharp and graded ones. Unlike conventional PFM restorations, the new functionally graded restorations exhibited a graded profile of properties at the interface, which led to the suppression of properties' mismatch. Since the stresses

formed at the interface result from the properties' mismatch between the two materials, the reduction or suppression of these mismatches result in lower thermal and mechanical based stresses at the interface (Gasik et al.,2005). This explains the lower incidence of cracks at the interface of the FGMR specimens when compared to PFM specimens (Figure 8.5). Unlike PFM specimens, where cracks propagated freely throughout the ceramic and the interface, the new functionally graded specimens showed crack retention features provided by the metallic particles of the interlayer, which acted as cracks stoppers (Figure 8.5D). They retarded the crack propagation and thus the degradation of the interface.

Although the micrographs of the metal-ceramic interface region of both types of specimens after fatigue tests (Figure 8.5) revealed damages within porcelain in both situations (Figures 5B and 5D), they were found in higher extent in the conventional PFM specimens. Several cracks were detected at the boundaries of leucite crystals and glassy matrix, and they are explained by the large mismatch in the coefficient of thermal expansion of leucite and glassy matrix (Hamouda et al, 2010; Van Noort, 2007; Lorenzoni et al. 2010). During thermal cycling tests, these two phases behaved differently to temperature variations, leading to cracks' generation.

The SEM/EDS analysis of the specimens submitted to longer fatigue testing conditions (*condition 3*), disclosed the presence of salts on the surface fracture of PFM specimens. The EDS analyses of those salts indicated they are essentially constituted by phosphorus and calcium (Figure 8.8), which are constituents of artificial saliva that was used as medium to thermal cycling tests. This suggests that the liquid was able to ingress through the metal-ceramic interface at some points, thus promoting the degradation of the bond between the two materials. Cracks formed along the metal-ceramic interface together with the corrosion of the oxide layer formed at the same site (Fisher et al., 2009), are pointed as the causes of liquid ingress. Moreover, the Co-Cr alloys have shown poor resistance to attack in solutions containing chlorine (Upadhyay et al., 2006), which is one of the constituents of the artificial saliva. The stresses generated by thermal cycling tests were considered to increase the

occurrence of degradation in wet (Upadhyay et al., 2006) and aqueous environments, and also to encourage the effect of mechanical fatigue, which weakens the materials and their interfaces (Fischer et al., 2009; Vásquez et al., 2009; Lorenzoni et al., 2010; Nikaido et al., 2002).

The SEM/EDS analysis of the fracture surfaces of the new functionally graded restorations (Figures 9 and 10) did not reveal traces of liquid ingress as occurred with the conventional PFM specimens. Such finding is explained by the absence of a sharp metal-ceramic interface with an oxide layer that could suffer from the degradations processes previously described. Along with it, the reduced cracks generated during fatigue tests (Figure 8.5) and the flawless ceramic produced by hot pressing technique are considered the main cause for such finding.

5. Conclusions

From the results of this study, the following conclusions can be drawn for the materials tested:

- 1- The metal-ceramic shear bond strength values of the new functionally graded (FGMR) restorations were significantly ($p < 0.05$) higher than those of conventional porcelain fused to metal (PFM) restorations ($\geq 130\%$), irrespective of the fatigue testing conditions.
- 2- The metal-ceramic shear bond strength of PFM and FGMR specimens decreased significantly ($p < 0.05$) after thermal and mechanical cycling (12000 thermal cycles and 100000 mechanical cycles). The bond strength reduction was 43% in the case of PFM specimens (from 109 ± 29 MPa to 63 ± 28 MPa) and only 11% in the case of FGMR specimens (from 255 ± 29 MPa to 226 ± 15 MPa).

6. References

Anusavice KJ. Phillips' science of dental materials. 11th ed. Philadelphia:W.B. Saunders, 2006.

Anusavice KJ, Dehoff PH, Fairhurst CW. Comparative evaluation of ceramic-metal bond tests using finite element stress analysis. *J Dent Res*, 1980; 59: 608-613.

Akova T, Ucar Y, Tukay A, Balkaya MC, Brantley WA. Comparison of the bond strength of laser-sintered and cast base metal dental alloys to porcelain. *Dent Mater*, 2008; 24: 1400-1404.

Atta OM, Smith BGN, Brown D. Bond strengths of three chemical adhesive cements adhered to a nickel–chromium alloy for direct bonded retainers. *J Prosthet Dent*, 1990; 63: 137-143.

Craig RG, Powers JM. Restorative dental materials. 11th ed. Mosby, 2002, pp.480-492.

Crim GA, Mattingly SL. Evaluation of two methods for assessing marginal leakage. *J Prosthet Dent*, 1981; 45: 160-163.

de Melo RM, Travassos AC, Neisser MP. Shear bond strengths of a ceramic system to alternative alloys. *J Prosthet Dent*, 2005; 93: 64-69.

Dlouhy I, Boccaccini AR. Preparation, microstructure and mechanical properties of metal-particulate/glass-matrix composites. *Comp Sci Tech*, 1996; 56: 1415-1424.

Donovan TE, Swift EJJr. Porcelain-Fused-to-Metal (PFM) Alternatives. *J Comp*, 2009; 1: 4-6.

dos Santos JG, Fonseca RG, Adabo LG, Cruz CAS. Shear bond strength of metal-ceramic repair systems. *J Prosthet Dent*, 2006; 96(3): 165-173.

Eliasson A, Arnelund CF, Johansson A. A clinical evaluation of cobalt-chromium metal ceramic fixed partial dentures and crowns: A three-to seven-year retrospective study. *J Prosthet Dent*, 2007; 98, 6-16.

Elsaka SE, Hamouda IM, Elewady YA, Abouelatta OB, Swain MV. Effect of chromium interlayer on the shear bond strength between porcelain and pure titanium. *Dent Mater*, 2010a; 26: 793-798.

Elsaka SE, Hamouda IM, Elewady YA, Abouelatta OB, Swain MV. Influence of chromium interlayer on the adhesion of porcelain to machined titanium as determined by the strain energy release rate. *J Dent*, 2010b; 38(8): 648-654.

Fischer J, Zbären C, Stawarczyk B, Hämmerle CHF. The effect of thermal cycling on metal-ceramic bond strength. *J Dent*, 2009; 37: 549-553.

Fusayama T, Katayoi T, Nomoto S. Corrosion of gold and amalgam placed in contact with each other. *J Dent Res*, 1963; 42: 1183-1197.

Gasik M, Kawasaki A, Kang Y. Optimization of FGM TBC and their thermal cycling stability. *Mater Sci For*, 2005; 492: 9-14.

Gale MS, Darvell BW. Thermal cycling procedures for laboratory testing of dental restorations. *J Dent*, 1999; 27: 89-99.

Hammad IA, Talic YF. Designs of bond strength tests for metal-ceramic complexes: Review of the literature. *J Prosthet Dent*, 1996; 75: 602-608.

Hamouda IM, El-Waseffy NA, Hasan AM, El-Falal AA. Evaluation of an experimental dental porcelain. *J Mech Behav Biomed Mater*, 2010; 3: 610-618.

Henriques B, Soares D, Silva F. Optimization of bond strength between gold alloy and porcelain through a composite interlayer obtained by powder metallurgy. *Mater Sci Eng A*, 2011a; 528: 1415-1420.

Henriques B, Soares D, Silva F. Shear bond strength of a Hot Pressed Au-Pd-Pt alloy-porcelain dental composite. *J Mech Behav Biomed Mater*, 2011b; 4(8), 1718-1726.

Huang M, Wang R, Thompson V, Rekow D. Bioinspired design of dental multilayers. *J Mater Sci: Mater Med*, 2007; 18: 57-64.

Jörn D, Waddell JN, Swain MV. The influence of opaque application methods on the bond strength and final shade of PFM restorations. *J Dent*, 2010; 38: 143-149.

Leibrock A, Degenhart M, Behr M, Rosentritt M, Handel G. In vitro study of the effect of thermo and load-cycling on the bond strength of porcelain repair system. *J Oral Rehab*, 1999; 26: 130-137.

Lorenzoni FC, Martins LM, Silva NRFA, Coelho PG, Guess PC, Bonfante EA, Thompson VP, Bonfante G. Fatigue life and failure modes of crowns systems with a modified framework design. *J Dent*, 2010; 38: 626-634.

Morgan MJ, James DF, Pilliar RM. Fractures of the fixture component of an osseointegrated implant. *Int J Oral Maxillofac Imp*, 1993; 8: 409-414.

Napankangas R, Salonen-Kemppi MA, Raustia AM. Longevity of fixed metal ceramic bridge prostheses: a clinical follow-up study. *J Oral Rehab*, 2002; 29: 140-145.

Nikaido T, Kunzelmann KH, Chen H, Ogata M, Harada N, Yamaguchi S, Cox CF, Hickel R, Tagami J. Evaluation of thermal cycling and mechanical loading on bond strength of a self-etching primer system to dentin. *Dent Mat*, 2002; 18: 269-275.

Nobil 4000 - Alloy Data. [Online] [Cited: November, 2012.] http://www.nobilmetal.it/public/products_attach/st_nobil_4000.pdf

Oyafuso DK, Özcan M, Bottino MA, Itinoche MK. Influence of thermal and mechanical cycling on the flexural strength of ceramics with titanium or gold alloy frameworks. *Dent Mat*, 2008; 24: 351-356.

Pjetursson BE, Tan K, Lang NP, Brägger U, Egger M, Zwahlen M. A systematic review of the survival and complication rates of fixed partial dentures after an observation period of at least 5 years. *Clin Oral Impl Res*, 2004; 15: 654-666.

Pröbster L, Maiwald U, Weber H. Three-point bending strength of ceramics fused to cast titanium. *Europ J Oral Sci*, 1996; 104: 313-319.

Rees JS, Jacobsen PH, Koliniotou-Kubia E. The current status of composite materials and adhesive systems. Part 4. Some clinically related research. *Rest Dent*, 1990; 6(3): 4-8.

Rizkalla AS, Jones DW. Indentation fracture toughness and dynamic elastic moduli for commercial feldspathic dental porcelain materials. *Dent Mat*, 2004; 20: 198-206.

Rosentritt M, Behr M, Scharnagel P, Handel G, Kolbeck C. The influence of the resilient support of abutment teeth on the fracture resistance of all-ceramic fixed dental prostheses: An in vitro study. *Int J Prosthodont*, 2011; 24: 465 – 468.

Rosentritt M, Behr M, van der Zel JM, Feilzer AJ. Approach for valuating the influence of laboratory simulation. *Dent Mater*, 2009; 25: 348-352.

Salazar MSM, Pereira SMB, Ccahuana VZ, Passos SP, Vanderlei AD, Pavanelli CA, Bottino MA. Shear bond strength between metal alloy and a ceramic system, submitted to different thermocycling immersion times. *Acta Ontolog Latinoam*, 2007; 20(2): 97-102.

Sartori R, Corrêa CB, Fernandes FRB, Marcantonio E, Vaz LG. Mechanical properties of dental implants submitted to fluoride ions action. *Rev Odont*, 2007; 36(4): 317-322.

Scherrer SS, Wiskott AHW, Coto-Hunziker V, Belser UC. Monotonic flexure and fatigue strength of composites for provisional and definitive restorations. *J Prosthet Dent*, 2003; 89: 579-588.

Shimoe S, Tanoue N, Yanagida H, Atsuta M, Koizumi H, Matsumura H. Comparative strength of metal–ceramic and metal–composite bonds after extended thermocycling. *J Oral Rehab*, 2004; 31: 689-694.

Souza JCM, Nascimento RM, Martinelli AE. Characterization of dental-ceramic interfaces immersed in artificial saliva after substructural mechanical metallization with titanium. *Surf Coat Tech*, 2010; 205: 787–792.

Suresh S, Mortensen A. *Fundamentals of functionally graded materials*. London: Maney publishing, 1998.

Suresh S. Graded materials for resistance to contact deformation and damage. *Science*, 2001; 292: 2447-2451.

Tróia MG, Henriques GEP, Nóbilo MAA, Mesquita MF. The effect of thermal cycling on the bond strength of low-fusing porcelain to commercially pure titanium and titanium-aluminium-vanadium alloy. *Dent Mat*, 2003; 19: 790-796.

Upadhyay D, Panchal MA, Dubey RS, Srivastava VK. Corrosion of alloys used in dentistry: A review. *Mat Sci Eng A*, 2006; 432(1-2): 1-11.

Van Noort R. *Introduction to Dental Materials*. 3rded. Elsevier, 2007.

Vásquez V, Özcan M, Nishioka R, Souza R, Mesquita A, Pavanelli C. Mechanical and Thermal Cycling Effects on the flexural of glass Ceramics Fused to Titanium. *Dent Mat J*, 2008; 1(27): 7-15.

Vásquez VZC, Özcan M, Kimpara ET. Evaluation of interface characterization and adhesion of glass ceramics to commercially pure titanium and gold alloys after thermal- and mechanical-loading. *Dent Mater*, 2009; 25: 221–31.

Vichi A, Louca C, Corciolani G, Ferrari M. Color related to ceramic and zirconia restorations: A review. *Dent Mater*, 2011; 27: 97-108.

Wagner WC, Asgar K, Bigelow WC, Flinn RA. Effect of interfacial variables on metal-porcelain bonding. *J Biomater Res*, 1993; 27: 531-537.

Walter M, Reppel PD, Böning K, Freesmeyer WB. Six year follow-up of titanium and high-gold porcelain-fused-to-metal fixed partial dentures. *J Oral Rehab*, 1999; 26: 91-96.

Wu Y, Moser JB, Jameson LM, Malone WFP. The effect of oxidation heat treatment on porcelain bond strength in selected base metal alloys. *J Prosthet Dent*, 1991; 66: 439-444.

Zarone F, Russo S, Sorrentino R. From porcelain-fused-to-metal to zirconia: Clinical and experimental considerations. *Dent Mater*, 2011; 27: 83-96.

Chapter 9

Fabrication of functionally graded metal-ceramic crowns

In this chapter is presented the experimental procedure for the fabrication functionally graded metal-ceramic crowns. The aim is to demonstrate that the production of this new type of restorations can be performed using the standard technology yet employed in the fabrication of conventional metal-ceramic restorations. The functionally graded restorations were produced using the hot pressing system of Ivoclar® (IPS Line® PoM – Press on Metal). The details of the process and the analysis are presented ahead.

It is important to point out that a patent on the “Method of making functionally graded metal-ceramic dental restorations” has been submitted (Pending patent nº 106226). Additionally, it is also planned the development of a fully automated CAD-CAM equipment for the production of these new types of restorations. The application of the composite interlayer(s) and the porcelain build-up on the metal framework, as well as their sintering step, will be controlled by computer and thus performed in a completely automatic fashion. Conversely to current hot pressing systems, which requires an investment step (see below), this new system is designed to work with hot isostatic pressing (HIP). This will avoid the investment of the restoration and will turn the restorations’ manufacturing process much more easy and fast, and with improved accuracy.

9.1. Fabrication of functionally graded metal-ceramic crowns

1. Casting and preparation of the metal copings

The fabrication of the restoration started with the preparation of the master model (Figure 9.1) and the casting of the metal copings by the lost-wax process. The dental copings were made of CoCrMo alloy and were casted using an electric arc furnace (Degumat 2033, Degussa, Germany). Afterwards they were sandblasted with alumina particles (110 μ m) at a pressure of 3bar.

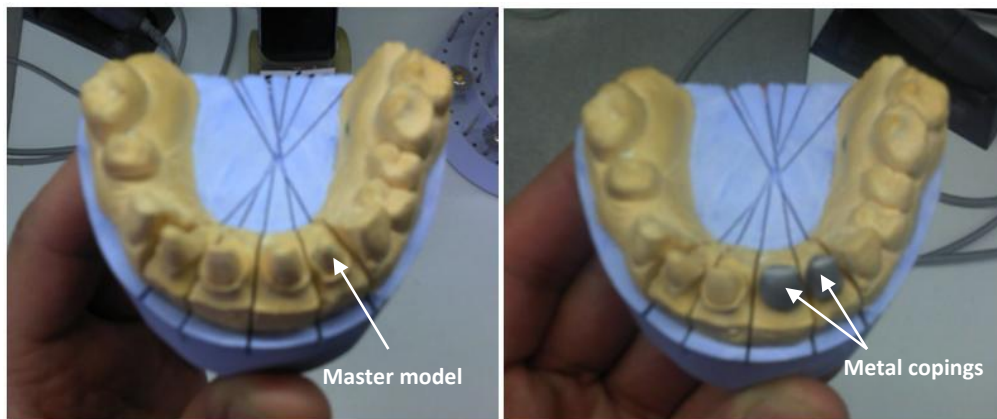


Figure 9.1. Master model and metal copings.

2. Application of the metal/ceramic composite interlayer

The composite interlayer comprised a mixture of 50% metal (CoCrMo alloy powder) and 50% porcelain (Ceramco3 Opaque powder) (%vol.). The mixture conditions were the same as described in Chapter 8. The powder mixture was mixed with water (mixing ratio of 2:1, in weight) and applied with a brush to the metal coping (Figure 9.2). The coping was then placed in the furnace for the composite sintering according to the porcelain firing cycle. Afterwards, two opaque layers were applied over the sintered composite interlayer.



Figure 9.2. Application of the metal-ceramic composite interlayer with a brush.

3. Wax Up and Sprueing

The complete restoration was waxed (Figure 9.3) and the sprues were attached to the most voluminous part of the crown.

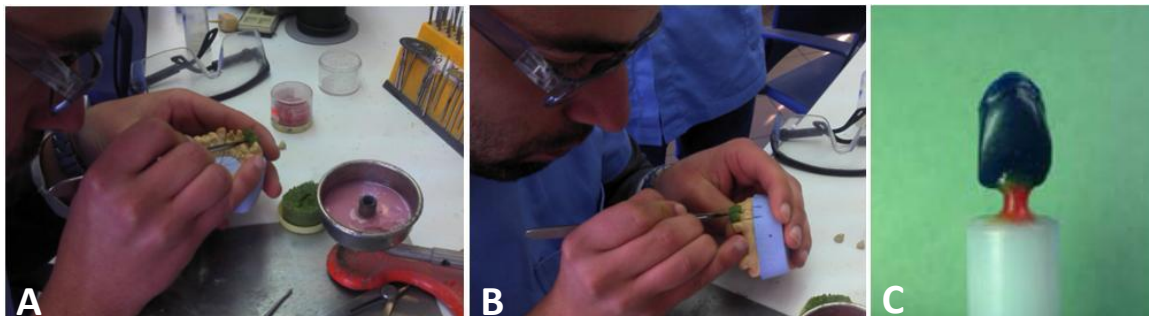


Figure 9.3. A and B - Wax-up on the metal coping; C – waxed restoration on attached to the plunger with a sprue.

4. Investment

The waxed restoration was placed in the silicon ring and was invested with an investment recommended for press over metal (Figure 9.4). Investing was done

following manufacturer's instructions (Table 9.1) (IPS_in_Line, 2010). The mould was vibrated during the process to prevent possible air bubbles.



Figure 9.4. Investing the restoration with IPS PressVEST.

Table 9.1. Investment materials mixing ratio.

	100g investment ring
IPS PressVEST	13 ml liquid + 9 ml dist. water

5. Burn out

The investment was burned out in an oven (Figure 9.5) following the investment manufacturer's instructions (Table 9.2) (IPS_in_Line, 2010).

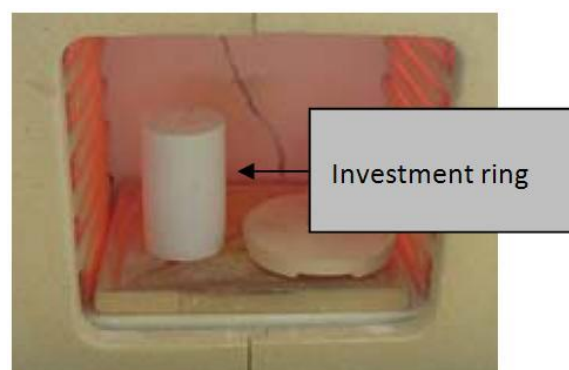


Figure 9.5. Investment ring in the heating oven towards the rear wall, tipped with the opening facing down. The IPS InLine PoM ceramic ingot and the IPS plunger were not preheated.

Table 9.2. Manufacturer's instructions of the burnout cycle of the IPS Press Vest (IPS_in_Line, 2010).

Setting time	min. 60 min
Preheating furnace temperature	Start room temperature heat up to 850°C at 5°C/min
Positioning of the investment ring in the furnace	Towards the rear wall, tipped with the opening facing down
IPS InLine PoM ceramic ingot	No preheating
IPS AloX plunger	No preheating
Holding time at final temperature 850°C	90 min

6. Pressing

The investment ring was removed from the burn out and placed into the pressing furnace (Programat EP5000, Ivoclar, Liechtenstein). The ceramic ingot (glass-ceramic, IPS inLine PoM, Ivoclar, Liechtenstein) and the plunger were placed in the investment ring and the pressing cycle started (see Figure 9.6 and Table 9.3).

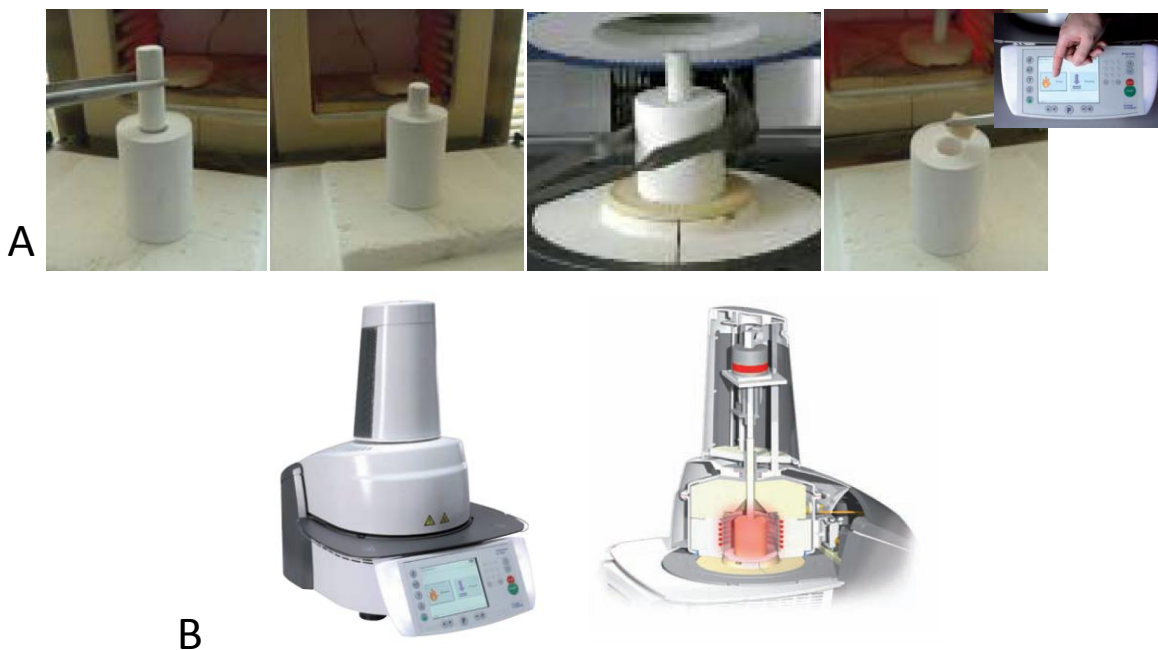


Figure 9.6. A - Insertion of the IPS InLine PoM ingot and the IPS AloX Plunger into the hot investment ring. Placing of the hot and completed investment ring in the centre of the hot press furnace and starting the program. B - Programat EP5000 press furnace.

Table 9.3. Firing parameters of ceramic for furnace Programat EP 5000 (IPS_in_Line, 2010).

t °C/min	T °C	H min (100g)	V ₁ °C	V ₂ °C
60	940	10	500	940

t:heating rate; T: set temperature; H: holding temperature; V₁: vacuum start; V₂:vacuum stop

7. Divesting

Once the pressing was complete, the investment ring was allowed to cool down to room temperature. The investment ring was cut using a disc and the two pieces were separated using a metal spatula. The investment was removed from the restoration using a sandblasting process of fine grain aluminum oxide of 110 microns (Figure 9.7).

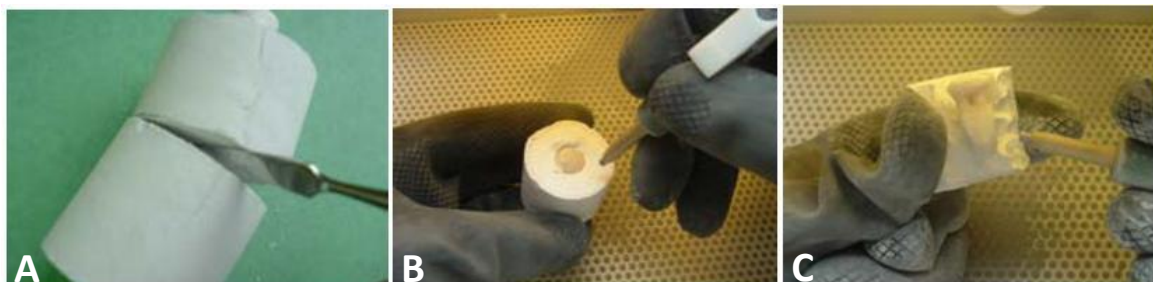


Figure 9.7. A- Separation of the investment ring using a separating disk and a spatula; B and C- Removing the restoration from the investment using alumina sandblasting.

8. Cut off sprues and finishing

The sprue was cut off with a diamond disk. Then, the excess porcelain was removed with a stone and the finishing operation proceeded with a diamond disk at low speed over the surface of the restoration.



Figure 9.8. Separation of the sprue using a diamond disk.

9. Glazing

To finalize the preparation of the restoration a final glaze was applied.



Figure 9.9. Application of the glaze material using a brush.

Figure 9.10 presents the finalized functionally graded restorations fitted to the master model. A good aesthetic and accurate fitting was achieved by this process.

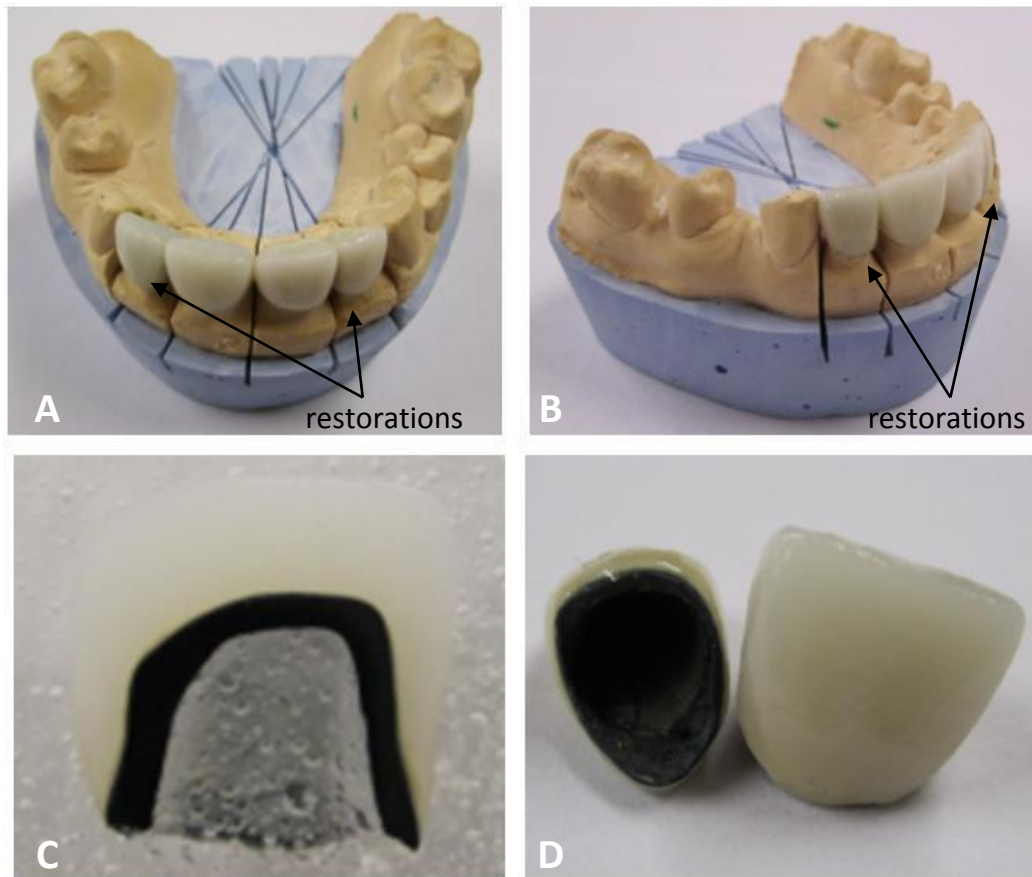


Figure 9.10. **A** and **B**: Final aspect of functionally graded metal-ceramic restorations fitted to the master model. **C**: Cross section of the restoration; **D**: Close view of the restoration with inside metallic structure and outside aesthetic ceramic.

The cross section of the functionally graded restoration is presented in Figure 9.11. The metal-interlayer-ceramic region was analyzed by the means of optical microscopy in several locations. It was observed a good adhesion between the interlayer and the metal, and between the interlayer and the opaque ceramic. The interlayer exhibited residual porosity though. The residual porosity can be mitigated, if not avoided, using less liquid in the preparation of the metal/ceramic composite mixture. The thickness of the interlayer was not uniform all over the crown due to the application method, i.e. by brush. The new machine designed for the manufacturing of functionally graded restorations should be able to control precisely the thickness of the interlayer.

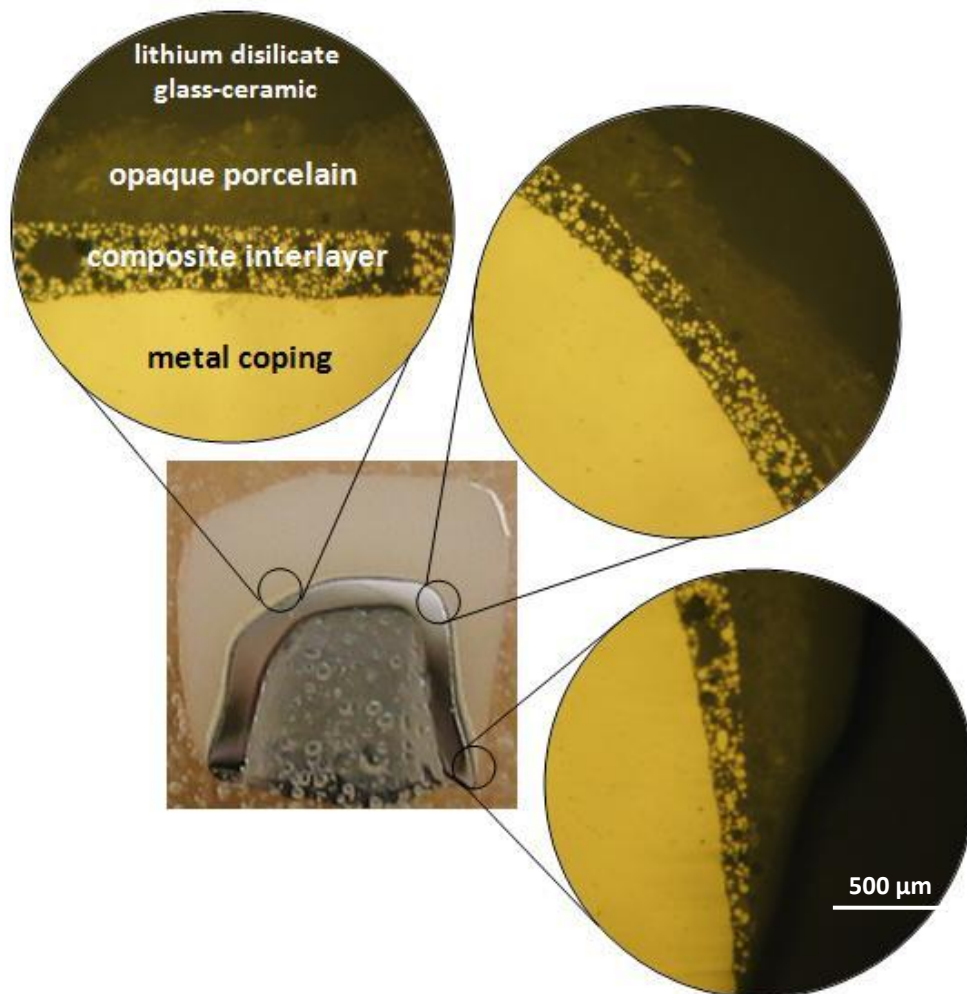


Figure 9.11. Cross section of a functionally graded restoration obtained by hot pressing. The micrographs show the metal-interlayer-ceramic transition zone in several locations of the restoration.

9.2. References

IPS_in_Line_instructions for use, 2010

<http://www.ivoclarvivadent.com/en/all/products/metal-ceramics/ips-inline-system/ips-inline-pom>

Chapter 10

General discussion

In order to conceive strong and long lasting metal-ceramic dental restorations, it is critical to understand the underlying mechanisms that rule the metal-ceramic adhesion. This should create a platform from where the optimization of the existing systems and techniques, and the development of new ones could be performed. Accordingly, this thesis is devoted to the study of conventional and non-conventional systems in metal-ceramic dental restorations. In this thesis was studied the influence of several processing variables on the adhesion between metal and ceramic, namely: the hot pressing effect; the type of metal substructure; and the preoxidation heat treatment. Moreover, this thesis concerns with the development of new functionally graded metal-ceramic dental restorations. Next, a general discussion about each of these topics is presented, focusing on the main highlights of each theme. For detailed reading please refer to the corresponding sections of this thesis.

10.1. Hot pressing effect and surface treatment

One of the aims of this thesis was to study the influence of hot pressing technique on the metal-ceramic bond strength. The hot pressing technique was assessed for two

types of metal alloys and for two types of surface treatments. The alloys used in this study were a high-gold alloy (Au-Pt-Pd) and a base metal alloy (Co-Cr-Mo-Si). The surface treatments were polished surfaces and roughened surfaces.

The hot pressed metal-ceramic specimens revealed higher bond strength than those found in conventional porcelain fused to metal specimens (see Figure 2.3 and Figure 6.3). The metal substrates with rough surface also exhibited higher bond strength values than those with polished surface, for the same processing conditions, i.e. hot pressed and PFM (see Figure 2.3 and Figure 6.3).

The hot pressing technique is regarded for better adhesion between metal and porcelain. The enhanced adhesion provided by the hot pressing technique was explained by the flawless interfaces that are produced through this technique. The enforced contact between the two materials imposed by the external pressure helps to prevent the formation of processing defects often found in PFM restorations, namely the undesired cracks and pores that jeopardize the performance of the interface (Figure 2.7a and Figure 6.6a-d). The full contact between metal and ceramic also contributes to the formation of better chemical bonds.

Roughness also showed to enhance metal-ceramic bond strength. The reasons behind this finding are related with the higher surface area and with the surface asperities of rough surfaces. The high surface area of rough surfaces improves the chemical bonding (Wagner et al., 1993) whereas the surface asperities are regarded for metal-ceramic interlocking, which enables mechanical retention of the porcelain (Wagner et al., 1993).

This study showed that the combination of surface roughness with the hot pressing technique yielded metal-ceramic systems with the highest metal-ceramic bond strength and with a significant lower variability in the results (see Figure 2.3 and Figure 6.3). Accordingly, the production of more reliable dental restorations with greater reproducibility can be expected using this process.

The hot pressing technique also showed to impart better mechanical properties to the ceramic. The fracture strength of conventional vacuum sintered porcelain and hot pressed porcelain was assessed in this study by the means of a shear test. Results

showed significantly higher cohesive strength of the hot pressed porcelain when compared to vacuum sintered porcelain (Figure 6.4). This finding was explained by the absence of flaws within the ceramic and by an increased presence of uniformly distributed leucite phase (Drummond et al., 2000; Kelly, 1997).

10.2. Cast vs. hot pressed metal substructures

In this thesis was studied and compared the cast and hot pressed CoCrMo alloy for dental substructures in terms of microstructure, hardness, electrochemical behavior and metal-ceramic adhesion.

The microstructure of hot pressed substrates was different from that seen in cast substrates. Cast substrates presented a typical dendritic microstructure whereas a globular microstructure was found in hot pressed substrates (Figure 5.2). Dendrites were of a Co rich phase and the interdendritic regions were Cr and Mo rich phases (Table 5.3). Sigma (σ) phase was detected in the interdendritic regions of cast substrates, exhibiting an elongated shape. This phase (σ) was also found in hot pressed substrates but with a globular shape and in less extent. The porosity found in cast and hot pressed substrates were less than 1%.

Hot pressed substrates showed significantly higher hardness than cast substrates (Figure 5.3). The finer microstructure of the former specimens can explain such hardness increase relative to the latter substrates (Figure 5.2). Additionally, the microstructure of cast specimens might also have influence on the hardness. According to Matković et al. (2004), interdendritic regions exhibits significantly lower hardness than dendritic ones. Hence, since the dendritic region corresponds only to ~37% of the microstructure of cast substrates, it means that most of their microstructure is composed by the soft phase. The high hardness of dental alloys may impact the ability to finish/polish the alloy clinically. Therefore, a subsequent heat treatment of hot pressed substrates might be required.

The electrochemical tests performed in this thesis confirmed the excellent corrosion resistance that is a characteristic of CoCr alloys. Nevertheless, the hot pressed substrates exhibited better corrosion resistance than that of cast substrates, namely in terms of open circuit potential (OCP), corrosion potential (E_{corr}) and current densities (i_{corr}) after polarization tests (Table 5.4). The OCP curve showed that cast substrates have more tendency for corrosion when compared to hot pressed specimens (Figure 5.7). The corrosion potential and the anodic polarization curves indicated that both cast and hot pressed specimens are in the passive state (Figure 5.7). This is a feature exhibited by materials with high resistance to corrosion and consists in the formation of a thin oxide layer on the metal's surface which inhibits the transportation of oxygen and metallic ions (Huang et al., 2002). However, the corrosion current densities found in cast specimens were greater than those found in hot pressed substrates (Table 5.4). Since both types of substrates are full dense compacts (>99% of density) the different corrosion behavior was originated by the different microstructure (Matković et al., 2004). According to Matković et al. (2004) findings, the dendritic phase has fcc structure and is a noble phase, whereas interdendritic regions has hcp structure and is regarded to be a less noble phase. Hence, the presence of significantly greater amount of noble phase in hot pressed specimens (83%) relative to cast specimens (37%) might explain the difference in the electrochemical behavior.

The metal-ceramic bond strength tests performed in this study did not found significant differences between cast and hot pressed substrates. The same findings were reported elsewhere (Akova et al., 2008). The failure type was the same for both types of specimens. No statistically relevant correlation could be established between the failure type and the bond strength.

This study has demonstrated the applicability of powder processing in the dental prosthetics. The hot pressed CoCrMo alloy substructures have shown superior mechanical and electromechanical properties when compared to those obtained by casting technique. Moreover, the hot pressed substructures proved to produce metal-ceramic bonds with, at least, the same characteristics of those found in cast specimens. Therefore, hot pressed substructures arise as an alternative to cast

substructures for the production of metallic substructures for metal-ceramic dental restorations.

10.3. Influence of preoxidation heat treatment

The influence of preoxidation heat treatment on the metal-ceramic bond strength was assessed in this thesis. The materials used were a base metal alloy (CoCrMo dental alloy) and dental porcelain. Porcelain was bonded to metal substrates with three types of surface treatments: non-preoxidized; preoxidized; and preoxidized followed by fine grinding to remove the oxide in excess on the metal surface. Porcelain did not show adhesion to preoxidized metal substrates. The reason was that the oxide layer did not show adhesion to its metal. On contrary, porcelain did bond to the other metal substrates, namely non-preoxidized and preoxidized/ground. However, porcelain showed significantly higher adhesion to non-preoxidized substrates than to preoxidized/ground substrates. The lower metal-ceramic bond strength results exhibited by preoxidized/ground substrates were explained by the remnants of oxide layer that remained on the metal surface after grinding and by the greater oxide thickness found at the metal-ceramic interface of these specimens (~75% thicker than that of non-preoxidized specimens). The oxides of CoCr alloys are known to exhibit poor adherence to its metal (Mackert et al., 1984), especially with thick oxide layers (Rokni and Baradaran, 2007).

The bond strength tests were performed using metal substrates with plane surfaces (fine ground). The aim was to assess the adhesion through chemical bonding without considering the effect of the mechanical retention provided by a rough surface.

Nevertheless, the sandblasting treatment is often performed in the preparation of metal substructures prior to porcelain veneering aimed at removing the oxides in excess after preoxidation heat treatment and also to impart roughness to the metal surface for porcelain retention. Because the sandblasting treatment plays an important role in the metal-ceramic adhesion, it was performed a complementary analysis to an

alumina-blasted CoCrMo alloy substrate previously oxidized. Along with the surface roughening, the alumina-blasting also introduced considerable cold work into the metal surface (surface hardness increased 84%). A surface contamination by alumina particles was also detected after the alumina-blasting surface treatment (Figure 4.8b). Wagner et al., 1993 suggested that alumina can have a positive effect on the metal-ceramic bond strength. Therefore, alumina-blasting can be regarded for a dual-effect surface treatment, which results in mechanical and chemical surface modifications: 1) surface roughening and hardening through cold work; and 2) alumina embed on the metal's surface, respectively. Additionally, the increase of surface area after sandblasting treatment also accounts for the improvement of the adherence between metal and ceramic (Wagner et al., 1993).

10.4. Bio-inspired FGM restorations

This thesis deals with the development of new metal-ceramic functionally graded restorations following a bio-inspired approach. The FGM concept applied to metal-ceramic dental restorations has never been studied and is for the first time introduced in this thesis. The study comprised two major steps: first, several metal/ceramic composite interlayers were experimentally evaluated as graded transitions between metal and ceramic, and their influence on the metal-ceramic bond strength was assessed. From this study it was possible to experimentally identify the interlayer composition that maximized the adhesion between metal and ceramic. The next step was to compare the performance of the new FGM restorations to conventional PFM ones, under fatigue conditions simulating those found in oral cavity.

10.4.1. Evaluation of m/c composite interlayers for graded metal-ceramic systems

The presence of several metal/ceramic composites (20%M; 40%M; 60%M; 80%M), acting as graded transition between metal and ceramic, was evaluated in terms of

their influence on the global performance of the metal-ceramic interface, and particularly on the adhesion strength between metal and ceramic. Bond strength results were compared with those obtained in conventional metal-ceramic sharp transitions.

All specimens with graded metal-ceramic transitions revealed higher bond strength means than those with metal-ceramic sharp transitions (Figure 7.3). The interlayer composition that showed to maximize metal-ceramic bond strength was the 40%M interlayer (Figure 7.3). The improvement found with 40%M interlayer relative to conventional PFM sharp transition exceeded 130%. The bond strength results plotted against the interlayers' composition (Figure 7.3) showed an upward trend until the composition of 40%M, inflecting at this point and exhibiting a downward trend for increasing metal contents in the composite, namely 60%M and 80%M. The 40%M composition showed a right balance of the metal particles in the composite, yielding the best bond strength results. This was explained by the bonding of metal particles of the interlayer to the metal substrate and by some bridging effects (see Figure 7.4) between metal particles as well, thus improving the mechanical retention between the interlayer and the metal substrate (Figure 7.4). This rationale also supports the results of 20%M interlayer, where the amount of metal particles was insufficient to create the same reinforcing mechanisms as shown in 40%M interlayer. The problem reported with the 60%M and 80%M interlayers was related with a high content of metal particles, which enabled from one side, an improvement in the bond strength between the interlayer and the metal substrate but, on the other side, a weakening of the bond between the interlayer and the ceramic, in the same proportion (Figure 7.4).

Concerning the role of metallic particles in the 40%M composite interlayer, they also acted as a reinforcing phase, mainly due to its higher elastic modulus relative to the ceramic matrix (Figure 7.9). The incorporation of a ductile, metallic, secondary phase in glass and glass-ceramics matrix, thus forming a composite, is regarded for an improvement in the latter's mechanical properties, in particular the fracture resistance (Dlouhy and Boccaccini, 1996). The fracture toughness of the composite interlayer,

relative to plain porcelain, was then increased by exploiting the plastic deformation of the ductile phase provided by the metal particles (Figure 7.8).

10.4.2. Evaluation of functionally graded metal-ceramic systems under fatigue conditions

This thesis also deals with the performance of the new metal-ceramic graded restorations under fatigue conditions. Therefore, it was evaluated the effect of fatigue conditions on the bond strength of these new functionally graded restorations and compared to the conventional PFM sharp transitions, under the same circumstances. It is important to consider fatigue conditions when performing in-vitro studies involving restorative dental materials (Scherrer et al., 2003) since the dental restorations are clinically subjected to thermal and mechanical cyclic stresses originated by the daily feeding routines (Pröbster et al., 1006). The graded specimens comprised a 50M composite interlayer at the metal-ceramic interface. Regarding the fatigue tests, they encompassed thermal cycling followed by mechanical cycling tests (Table 8.5).

As expected, specimens with graded metal-ceramic transition exhibited significantly higher bond strength results than conventional PFM sharp transition specimens (Figure 8.3). Results have shown that fatigue conditions significantly affected the bond strength between metal and ceramic (Table 8.6). However, the same fatigue testing conditions affected differently the two types of specimens, FGM and PFM. Bond strength data measured after the most severe fatigue testing conditions showed a bond strength loss of 43% for the conventional PFM specimens and only 11% for the new graded metal-ceramic system, when compared to the initial bond strength values (Figure 8.3). Hence, the bond strength improvement of the graded specimens over the conventional PFM ones rose from 140%, measured before fatigue tests, to 210% after fatigue tests.

The enhanced performance of the new graded metal-ceramic systems relative to PFM sharp transition systems under thermal and mechanical fatigue conditions was

explained by the significant reduction in the properties mismatch (e.g. CTE, Young's modulus, hardness, etc.) at the metal-ceramic interface that was observed in FGM specimens (Figure 8.6A). The reduction in the coefficient of thermal expansion (CTE) mismatch and in the Young's modulus mismatch through the use of a graded metal-ceramic interface (Figures 8.10a and 8.10b) are regarded for lower elastic deformations occurring at the metal-ceramic interface due to thermal and mechanical stresses, respectively.

The micrographs of metal-ceramic interfaces taken after fatigue tests (Figure 8.4) showed different damage extensions, especially within the ceramic, for the two types of specimens. The damage extension, namely crack formations, was higher in PFM specimens. Unlike what was observed in PFM specimens, where cracks propagated freely throughout the ceramic and the interface, in the new functionally graded specimens the metallic particles of the interlayer acted as crack stoppers (Figure 8.4D), retaining the crack propagation. This feature was considered to contribute to the enhanced performance exhibited by FGM systems under fatigue conditions.

The analysis of the surface fracture of PFM specimens subjected to fatigue tests revealed traces of liquid penetration, namely artificial saliva, through the interface during the tests, which seemed to accelerate the interface degradation. The cause for this phenomenon was attributed to the corrosion of the oxide layer at the interface (Fischer et al., 2009) and to the liquid penetration through the interconnected cracks.

10.5. References

Akova T, Ucar Y, Tukay A, Balkaya MC, Brantley WA. Comparison of the bond strength of laser-Hot Pressed and Cast base metal dental alloys to porcelain. *Dent Mater*, 2008; 24:1400-1404.

Dlouhy I, Boccaccini AR. Preparation, microstructure and mechanical properties of metal-particulate/glass-matrix composites. *Comp Sci Tech*, 1996; 56:1415-1424.

Drummond JL, King TJ, Bapna MS, Koperski RD. Mechanical property evaluation of pressable restorative ceramics. *Dent Mater*, 2000; 16: 226-233.

Fischer J, Zbären C, Stawarczyk B, Hämmerle CHF. The effect of thermal cycling on metal-ceramic bond strength. *J Dent*, 2009; 37: 549-553.

Huang HH. Effect of chemical composition on the corrosion behavior of Ni-Cr-Mo dental Casting alloys. *J Biomed Mater Res*, 2002; 60: 458-465.

JR Kelly. Ceramics in restorative and prosthetic dentistry. *Annu Rev Mater Sci*, 1997; 27:443-36.

Mackert JR, Parry EE, Hashinger DT, Fairhurst CW. Measurement of oxide adherence to PFM alloys. *J Dent Res*, 1984; 63(11):1335-1340.

Matković T, Matković P, Malina J. Effects of Ni and Mo on the microstructure and some other properties of Co–Cr dental alloys. *J Alloys Comp*, 2004; 366: 293–297.

Pröbster L, Maiwald U, Weber H. Three-point bending strength of ceramics fused to cast titanium. *Euro J Oral Sci*, 1996; 104: 313-319.

Rokni SR, Baradaran H. The effect of oxide layer thickness on the bond strength of porcelain to Ni-Cr alloy. *J Mashhad Dental School*, 2007; 31:17-21.

Scherrer SS, Wiskott AHW, Coto-Hunziker V, Belser UC. Monotonic flexure and fatigue strength of composites for provisional and definitive restorations. *J Prosth Dent*, 2003; 89: 579-588.

Wagner WC, Asgar K, Bigelow WC, Flinn RA. Effect of interfacial variables on metal-porcelain bonding. *J Biomed Mater Res*, 1993; 27: 531-537.

Main conclusions and future perspectives

The following conclusions can be withdrawn from this thesis:

Hot pressing effect

- Hot pressing technique can significantly improve the metal-ceramic bond strength;
- Hot pressing technique significantly improves the porcelain's fracture strength;
- The hot pressing technique together with the metal surface roughness result in improved metal-ceramic bond strength and low variability in results;

Cast vs. hot pressed metal substructures

- Hot pressed and cast metal substrates presents different microstructure and constituents volume fractions;
- Hot pressed substrates showed significantly higher hardness than cast substrates;
- Hot pressed substrates exhibited greater corrosion resistance than cast substrates;
- The metal-ceramic bond strength was not affected by the type of metal substrate, cast or hot pressed.

Influence of preoxidation and sandblasting

- Preoxidation heat treatment showed to decrease the bond strength between CoCrMoSi alloy and porcelain. Therefore, it must be avoided when using the same conditions of this study;
- Grit-blasting treatments do not completely remove the oxide layer formed on metal surface during preoxidation heat treatment. Part of the oxide layer is embedded in the asperities of the deformed surface;

-
- Alumina-blasting produces a chemical modification of the metal surface as it gets contaminated by the alumina particles;
 - Alumina-blasting produce both a mechanical and a chemical effect on metal's surface, converging in two complementary effects of metal-ceramic bond strength enhancement;

Bio-inspired FGM restorations

- The new functionally graded metal-ceramic dental systems showed significantly higher bond strength than that exhibited by conventional sharp transition between metal and ceramic;
- Improvements in bond strength, when using graded metal-ceramic transitions, can be of 140% relative to conventional sharp transitions;
- The new functionally graded metal-ceramic dental-systems performs significantly better than traditional systems even under in-vitro fatigue test conditions (thermal and mechanical cycling);

The findings of this study provide the following future research opportunities:

- In-vitro testing of the new functionally graded dental restorations applied to real geometries, such as crowns and fixed partial dentures, including shipping tests and fatigue tests in artificial saliva;
- In-vivo testing of the new FGM restorations.
- Development of an equipment capable of producing the new functionally graded dental restorations in an automatically fashion;

Others

- Evaluation of hot pressing technique using other dental base materials, including titanium and titanium alloys and their compatible ceramic veneers;
- Further evaluation of the exact materials limited to this study with other established metal-ceramic bond tests (such as the Schwickerath crack initiation test - the ISO standard, for instance);
- Evaluation of the hot pressing processing parameters on the mechanical and electrochemical properties of hot pressed dental alloys compacts;
- Comparison of the electrochemical behavior of a metal-ceramic interface obtained by the hot pressing technique and by the conventional porcelain-fused-to-metal technique;
- Characterization of the mechanical and thermal properties of metal/ceramic homogeneous composites with different volume fractions for different pairs of dental materials in order to allow subsequent FGM modeling;
- Optimization in terms of bonding strength of functionally graded dental restorations;
- Electrochemical evaluation of graded metal-ceramic interfaces;

- Study of the influence of the powders size on the mechanical and electrochemical properties of metal/ceramic homogeneous composites;
- Assessing the influence of the metal/ceramic composite interlayer on the metal-ceramic bond strength;
- Evaluation of the interlayers size on the metal-ceramic bond strength;